

LUNAR ORBITER III

MISSION SYSTEM PERFORMANCE

Prepared for the
NATIONAL AERONAUTICS AND SPACE ADMINISTRATION

Langley Research Center

by

THE **BOEING** COMPANY

Distribution of this report is provided in the interest of information exchange. Responsibility for the contents resides in the author or organization that prepared it.

Contract No. NAS1-3800
August 11, 1967

BOEING DOCUMENT NO. D2-100753-3

FACILITY FORM 602

N67-37275
(ACCESSION NUMBER)

175
(PAGES)

CR-66461
(NASA CR OR TMX OR AD NUMBER)

(THRU)

(COPIES)

(CATEGORY)

CONTENTS

	Page
1.0 Launch Operations	1
1.1 Spacecraft Processing	1
1.1.1 Hanger "S"	1
1.1.2 Explosive Safe Area	6
1.1.3 Launch Pad 13	7
1.2 Launch Conduct	7
1.2.1 Launch Criteria	7
1.2.2 Countdown and Launch	8
1.2.3 Weather	10
1.2.4 Tracking Coverage	10
1.2.5 Telemetry Coverage	12
1.3 Launch Vehicle Performance	12
1.3.1 Atlas Performance	21
1.3.2 Agena Performance	21
2.0 Flight Operations	22
2.1 Flight Plan and Conduct	22
2.1.1 Flight Plan	22
2.1.2 Flight Conduct	23
2.1.2.1 Flight Profile	23
2.1.2.2 Nominal Mission	31
2.1.2.3 Photo Data Acquisition	32
2.2 Flight Control	33
2.2.1 Mission Control	33
2.2.2 Spacecraft Control	33
2.2.2.1 Command Programming	33
2.2.3 Flight Path Control	35
2.2.3.1 Countdown, Launch, and Acquisition	37
2.2.3.2 Injection Through Midcourse	38
2.2.3.3 Midcourse Through Deboost	43
2.2.3.4 Initial Ellipse	48
2.2.3.5 Photo Ellipse	55
3.0 Spacecraft Performance	67
3.1 Photo Subsystem Performance	69
3.1.1 Thermal Control	69
3.1.2 Camera Film Advances	79
3.1.3 Processor Operation and Readout Film Handling	79
3.1.3.1 Processor Operation	79
3.1.3.2 Readout Film Handling	90
3.1.4 Photo, Data Analysis	90
3.1.4.1 White-Level Variation	90
3.1.4.2 Video Analysis Reports	91
3.1.4.3 White-Level Variation Plots	92
3.1.4.4 Analysis of Data	92

CONTENTS (Continued)

	Page
3.1.5 Processing Variations Across the Spacecraft Film	99
3.1.6 Problem Analysis	99
3.2 Communications Subsystem Performance	103
3.2.1 Launch Through Cislunar Injection	103
3.2.2 Cislunar to Lunar Injection	103
3.2.3 Lunar Injection Through Final Readout	105
3.2.3.1 Telemetry Link	105
3.2.3.2 Video Link	105
3.2.4 Component Performance	105
3.2.4.1 Transponder	105
3.2.4.2 Signal Conditioner	108
3.2.4.3 High- and Low-Gain Antennas	108
3.2.4.4 Traveling-Wave-Tube Amplifier	111
3.2.4.5 Multiplexer Encoder	111
3.2.4.6 Command Decoder	111
3.2.4.7 Modulation Selector	111
3.2.5 Computer Program Performance	112
3.2.5.1 TRBL Program	112
3.2.5.2 SGNL Program	114
3.3 Power Subsystem Performance	114
3.3.1 Launch to Sun Acquisition	114
3.3.2 Cislunar Through Lunar Injection	114
3.3.3 Initial Ellipse Through Orbit Transfer	115
3.3.4 Photo Ellipse Through Photo Taking	116
3.3.5 Final Readout	117
3.3.6 Component Performance	118
3.3.6.1 Solar Array	118
3.3.6.2 Battery	120
3.3.6.3 Charge Controller	120
3.3.6.4 Shunt Regulator	120
3.4 Attitude Control Subsystem Performance	120
3.4.1 Cislunar Coast	122
3.4.2 ΔV Maneuvers	122
3.4.3 Photo Maneuvers	122
3.4.4 Readout	123
3.4.5 Component Performance	125
3.4.5.1 Canopus Star Tracker	125
3.4.5.2 Sun Sensors	125
3.4.5.3 Closed-Loop Electronics	126
3.4.5.4 Reaction Control System	126
3.4.5.5 Thrust Vectors Control System	127
3.4.5.6 Inertial Reference Unit	127
3.4.5.7 Flight Programmer and Switching Assembly	127
3.4.6 Nitrogen Consumption	127

CONTENTS (Continued)

	Page
3.4.7 Problem Areas	129
3.4.7.1 Thermal Problem	130
3.4.7.2 Tracker Glint Problem	130
3.5 Velocity Control Subsystem Performance	130
3.5.1 ESA Spacecraft Fueling Operations	131
3.5.2 Launch and General Mission Events Through Midcourse Maneuver ..	131
3.5.3 Lunar-Orbit Injection Through Final Readout	132
3.5.4 Subsystem Time-History Data	132
3.5.5 Maneuver Performance	135
3.6 Structures and Mechanisms	138
3.6.1 Launch Vibration Environment	138
3.6.2 Deployment and Squib Actuation	138
3.6.3 Camera Thermal Door	138
3.6.6.4 Thermal Control	138
3.6.4.1 Battery Temperature Variation	155
3.6.4.2 Lower TWTA Temperatures	155
3.6.4.3 Thermal Problems	155
3.6.4.4 EMD Thermal Coating Degradation	155
3.6.5 Thermal-Design Differences Between Mission II and III	158
4.0 Ground Data System Performance	159
4.1 Space Flight Operations Facility	159
4.1.1 Computer and Communications Complex	159
4.1.2 SFOF Software	159
4.1.2.1 System Software	160
4.1.2.2 SPAC Software	160
4.1.3 FPAC Software System Performance	160
4.1.3.1 Flight Path Control Programs	160
4.1.3.2 Orbit Determination Programs	161
4.1.4 Ground Reconstruction Equipment (GRE)	161
4.2 Ground Communications System	161
4.3 Deep Space Stations	162
5.0 Lunar Environmental Data	164
5.1 Radiation Data	164
5.2 Micrometeoroid Data	164
Summary of Lunar Orbiter II Anomalies	165

ILLUSTRATIONS

Figure	Title	Page
1-1:	Lunar Orbiter Uprange Radar Coverage	11
1-2:	Tracking Coverage	13
1-3:	Ground Tracking for February 5, 1967	15
1-4:	Telemetry Coverage	16
1-5:	Lunar Orbiter Space Vehicle	18
1-6:	Lunar Orbiter Spacecraft	19
1-7:	Launch Vehicle	20
2-1:	Early Orbit Determination Results	38
2-2:	Effect of Midcourse Time on ΔV Required	40
2-3:	Effect of Time of Arrival on Midcourse ΔV Requirement	41
2-4:	Pre-Midcourse Encounter Parameter Summary	43
2-5:	Midcourse Geometry	44
2-6:	Midcourse Doppler Shift	45
2-7:	Deboost Doppler Shift	47
2-8:	Orbital Geometry at Deboost	49
2-9:	Initial-Ellipse Conic Elements History	51
2-10:	Transfer Doppler Shift	52
2-11:	Orbital Geometry at Transfer	54
2-12:	Perilune Altitude vs Longitude	56
2-13:	Photo Orbit Traces for Primary Targets	57
2-14:	Predicted Primary Photo Altitudes based on Transfer Design	58
2-15:	Perilune Altitude vs Time	60
2-16:	Inclination vs Time	61
2-17:	Argument of Perilune History	61
2-18:	Inertial-Node Longitude History	62
2-19:	Predicted Primary Photo Altitudes Based on Real-Time EVAL Runs	65
2-20:	Perilune Altitude vs Longitude of Descending Node	66
3-1:	Photo Subsystem Cislunar Temperatures	80

ILLUSTRATIONS

Figure	Title	Page
3-2:	Photo Subsystem Cislunar Temperatures	81
3-3:	Photo Subsystem Cislunar Temperatures	82
3-4:	Photo Subsystem Sunrise Temperatures	83
3-5:	Photo Subsystem Sunrise Temperatures	84
3-6:	Photo Subsystem Sunrise Temperatures	85
3-7:	Photo Subsystem Sunset Temperatures	86
3-8:	Photo Subsystem Sunset Temperatures	87
3-9:	Photo Subsystem Sunset Temperatures	88
3-10:	Camera Film Advances	89
3-11:	H&D Curve for SO-243	89
3-12:	White-Level Densities—Readout Sequence 010	91
3-13:	White-Level Densities—Readout Sequence 098	93
3-14:	White-Level Densities—Readout Sequence 087	94
3-15:	White-Level Densities—Readout Sequence 105	95
3-16:	White-Level Densities—Readout Sequence 070	96
3-17:	White-Level Densities—Readout Sequence 007	97
3-18:	White-Level Densities—Readout Sequence 095	98
3-19:	Variation of Densities Along Framelets	100
3-20:	GRE Film Density vs Spacecraft Density	101
3-21:	Communications Subsystem Block Diagram	104
3-22:	Typical Mode 3 Received Signal Strengths during Lunar Orbit	106
3-23:	Transponder Temperature—RF Power and EMD Temperature	107
3-24:	Transponder AGC Data	110
3-25:	Priority Readout—Site III P-5B	113
3-26:	Array Current and Temperature vs Time	115
3-27:	Array Current and Temperature vs Time	116
3-28:	Array Current and Temperature vs Time	117
3-29:	Array Current and Temperature vs Time	119

ILLUSTRATIONS

Figure	Title	Page
3-30:	Solar-Array Degradation	119
3-31:	Spacecraft Battery Depth of Discharge	121
3-32:	Attitude Control System Nitrogen Usage	128
3-33:	Velocity Control System Available Nitrogen History	133
3-34:	Velocity Control System Pressure-Time Histories	134
3-35:	Velocity Control System Temperature-Time Histories	135
3-36:	Velocity Control System Orbit Injection Maneuver—System Pressures and Temperatures	136
3-37:	Velocity Control System Orbit Injection Maneuver—System Dynamics	137
3-38:	Spacecraft Vibration—Peak Longitudinal Response (214X)	139
3-39:	Spacecraft Vibration—Peak Lateral Response (210Z)	140
3-40:	Random Response at Liftoff—Longitudinal Pickup (214X)	141
3-41:	Random Response at Liftoff—Lateral Pickup (210Z)	142
3-42:	Random Response at Transonic Longitudinal Pickup (214X)	143
3-43:	Random Response at Transonic Lateral Pickup (210Z)	144
3-44:	BECO Longitudinal Vibration (214X)	145
3-45:	BECO Lateral Vibration (210Z)	146
3-46:	SECO Longitudinal Vibration (214X)	147
3-47:	SECO Lateral Vibration (210Z)	148
3-48:	Longitudinal Vibration (214X)—Agena First Ignition	149
3-49:	Lateral Vibration (210Z)—Agena First Ignition	150
3-50:	Longitudinal Vibration (214X)—Agena First Cutoff	151
3-51:	Lateral Vibration (210Z)—Agena First Cutoff	152
3-52:	Longitudinal Vibration (214X)—Agena Second Ignition	153
3-53:	Lateral Vibration (210Z)—Agena Second Ignition	154
3-54:	Spacecraft Battery Temperature Difference	156
3-55:	Spacecrafts 5 and 6 Solar Absorptivity History	157

TABLES

	Title	Page
1-1	Spacecraft retests	2
1-2	Spacecraft Special Tests	2
1-3	Summary of Differences from Standard Flight Spacecraft	4
1-4	Explosive Safe Area Tests	6
1-5	Launch Area Tests	7
1-6	Spacecraft Prelaunch Milestones	8
1.7	Ascent Trajectory Event Times	17
2-1	Significant Event Summary	24
2-2	Photographic Site Location	25
2-3	Core Map Actual Photographic Activity	26
2-4	Film Budget Actual	28
2-5	Mission Launch Period and Windows	31
2-6	Trajectory Sequence of Events	36
2-7	Powered Flight Trajectory Events	37
2-8	Pre-Midcourse Orbit Determination Encounter Parameter Summary	39
2-9	Orbit Determinations Used for Photo Site Command Conferences	59
2-10	Frame Exposure Summary	63
2-11	Harmonic Model vs Site	64
3-1	Key Events	68
3-2	Photo Data Summary	70
3-3	Transponder Power Discontinuities	109
3-4	Spacecraft Load Currents	118
3-5	Attitude Control Subsystem Data During Photo Operations	124
3-6	Velocity Control Subsystem Maneuver Performance	131
3-7	Propellant and Nitrogen Servicing Summary Velocity Control Subsystem	131
3-8	Engine Valve Temperature Maximum Conduction	137
3-9	Gimbal Actuator Position	138
3-10	Spacecraft TWTA Temperatures	156
4-1	Lunar Orbiter SPAC Program Execution	160
4-2	Communications Down Time—(%)	162
5-1	Radiation Data-Record Mission III	164

LUNAR ORBITER III FINAL REPORT

MISSION SYSTEM PERFORMANCE

1.0 LAUNCH OPERATIONS

The Launch Operations Plan (LOP), Lockheed Missiles and Space Company Document LMSC-A751901C, dated March 31, 1967, provided the primary planning for overall space vehicle program direction through the lunar preinjection phase of the Lunar Orbiter III flight. This document served as the basis for directing the activities required to achieve and evaluate flight objectives, launch criteria and constraints, and implementation of preflight tests, checkouts, and launch of the space vehicle.

The same basic launch operations plan was used for the Mission III launch as was used during the first two missions. A description of the launch operation organization and supporting launch/postlaunch tracking and communication facilities is contained in the Lunar Orbiter Mission I Final Report, Section 3.3.1, "Launch Operation Plan" and 3.3.2, "Launch Base Facilities."

1.1 SPACECRAFT PROCESSING

Spacecraft 6 arrived at Cape Kennedy on August 26, 1966, to serve as backup for the Mission II flight article, Spacecraft 5. Upon arrival, it was moved to Hangar "S" to initiate processing of the spacecraft for the backup function per Boeing Document D2-100406-2, Volume II. This spacecraft was accepted by NASA on October 18, 1966. After the November launch of Mission II, Spacecraft 6 was placed in storage until needed for Mission III. Spacecraft 7 arrived at Cape Kennedy on November 21, 1966 to be prepared for use as a backup unit for Mission III.

1.1.1 Hangar "S"

On January 2, 1967, the spacecraft was removed from storage and retested per D2-100717-1 at Hangar "S," as indicated in Table 1-1. In addition, Table 1-2 lists the special tests performed. These groups of tests were performed to ascertain that all subsystems were still satisfactory, and to test those subsystems modified as a result of Mission I and II experience. Refer to Table 1-3 for a summary of differences from Lunar Orbiter I, designated the standard flight spacecraft.

The following discrepancies were disclosed during retest.

- The accelerometer in the IRU Serial No. 110 failed during component level tests in Seattle, so IRU Serial No. 113 was installed in the spacecraft.
- The TWTA Serial No. 23 was replaced due to suspect test history.
- A damaged micrometeoroid detector was replaced.
- The Canopus star tracker was removed for a special engineering test on the baffles.
- A bent solar panel actuator arm was found. The actuator was replaced.
- The film-advance motor in the photo subsystem was replaced due to erratic film-advance behavior.

All retests and special tests were satisfactorily concluded.

Table 1-1: SPACECRAFT RETESTS

PARAGRAPH	TEST TITLE
6.1	Spacecraft-Hangar "S" DSIF-71 Checkout
6.2	Spacecraft Alignment Verification
6.5	Pre-"Power On" Check
6.6	Initial Test Setup
6.7	Initial Conditions/Readiness Test
6.9	Radiation Dosage Scintillation Counter FCO
6.10	Attitude Control Functional Test
6.12	Volocity Control Subsystem Test
6.13	Power Subsystem Performance
6.14	High-Gain-Antenna Position Control, Camera Thermal Door Operation, and Antenna Deployment
6.17	Solar Panel Test and Low-Gain-Antenna Alignment
6.20	Photo Subsystem FCO
6.21	Photo Subsystem Removal
6.23	Equipment Mounting Deck Reflectance Test
6.25	Camera Telephoto Shutter Test

Note: Test paragraphs referred to in this table are part of Boeing Document D2-100717-1, Spacecraft Retest Procedures—ETR—Lunar Orbiter.

Table 1-2: SPACECRAFT SPECIAL TESTS

PARAGRAPH	TEST TITLE
6.8.10	Ranging, Mode II, and RF Probe
6.24.1	Command Time Delay
6.10.1.A	Plug (P254) Verification Test
6.10.4.6	Voltage Calibration of Star Tracker Test Set (Serial No. 2) and Canopus Star Tracker (Serial No. 11G2)
6.2.4.7	Transponder Modulation Index Test
6.13.1	Transistor Panel and Power Resistor Test
6.24.2	Plugs (P475 and P461) Verification Test
6.24.3	Verify Correct Operation of ACS Portion of Countdown Procedure
6.24.4	Plug (P372) Verification Test

Table 1-2: SPACECRAFT SPECIAL TESTS (Continued)

PARAGRAPH	TEST TITLE
6.24.5..6..9	Solar Panel Illumination Test
6.24.11	EMD Paint Coupon Test
6.24.12	Plugs (P251, P254, and P354) Verification Test
6.24.13	Photo Subsystem (P/S No. 6) V/H Test
6.10.4	Canopus Star Tracker (Serial No.09G2) Performance Verification
6.20.4.6	Verify Ranging with DSIF-71
6.24.14	Programmer Memory Core Verification Test
6.24.16	Photo Subsystem (P/S No. 5) Spacecraft V/H Test
6.20	Photo Subsystem (P/S No. 5) FCO
6.2.3	Photo Subsystem (P/S No. 5) Alignment Verification
6.14.5	Low-Gain-Antenna (Serial No. 009) Deployment Test
6.17	Solar Panel Tests and Low-Gain- Antenna Alignment
D2-100457-1 Sec. 3,7, and 14	Photo Subsystem (P/S No. 5) Performance and Focus Measurement Tests
D2-100717-1 Para. 6.26.1	Canopus Star Tracker 9G2 Star Map Output Voltage Verification
D2-100717-1 Para. 6.26.2	Transponder "Tap" Test and DSIF-71 Reference Frequency Test
D2-100717-1 Para. 6.26.3, 6.26.4, 6.26.5, 6.26.6	RF Investigative and Ranging Tests
<p>Note: Test paragraphs noted in this table are part of Boeing Document D2-100406-2, Volume II, <u>Spacecraft "6" Test Procedures—ETR—Lunar Orbiter</u> unless otherwise noted.</p>	

Table 1-3: SUMMARY OF DIFFERENCES FROM STANDARD FLIGHT SPACECRAFT

SUBSYSTEMS	PART NUMBER *		REMARKS
	Lunar Orbiter I	Lunar Orbiter III	
PHOTO SUBSYSTEM	1200-100	1200-100	Reference Eastman Kodak Photo Subsystem No. 5 preshipment Data Package 2-1572-02-2907 dated Oct. 22, 1966, for configuration differences from P/s 4 and 5. Incorporated a 0.21 ± 0.02 neutral-density filter to the 80-mm lens per ECM-LO-I-0571
STRUCTURES AND MECHANISMS			
Thermal Coating Coupon Installation	—	25-55218-1	Incorporated ECM LO-I-0567 Thermal Coating Coupons
Paint Coupons	25-51848-1	25-51848-4	Incorporated ECM LO-I-0558 EMD overcoating - changed types of coupons
Equipment Mounting Deck	No Part Number Change		Incorporated ECM LO-I-0558 EMD overcoating
Low-Gain Antenna Microswitch	No Part Number Change		Incorporated ECM LO-I-0562 provide safety lock on low-gain antenna microswitch
ATTITUDE CONTROL SUBSYSTEM			
IRU Inertial Reference Unit	1512469-905 (10-70053-1)	1512469-903 (10-70053-1)	Incorporated ECM LO-I-0544 elimination of noise spikes in IRU, RIM - incorporated a capacitor in the IRU Incorporated ECM LO-I-0515 IRU Gyroscope Backup Program - changed supplier of gyroscope

Table 1-3: SUMMARY OF DIFFERENCES FROM STANDARD FLIGHT SPACECRAFT

SUBSYSTEMS	PART NUMBER *		REMARKS
	Lunar Orbiter I	Lunar Orbiter III	
COMMUNICATION SUBSYSTEM			
Command Decoder Address Plugs	1726659-501	1726659-503	Each spacecraft has a "one of a kind" address plug
Low-Gain Antenna	25-50937-11	25-50937-12	Incorporated ECM LO-I-0557 stray-light test—painted antenna with non-reflective paint
POWER SUBSYSTEM			
Solar Panels	No Part Number Change		Incorporated ECM LO-I-0557 stray-light test
Power Transistor Panel	No Part Number Change		Incorporated ECM-LO-I-0542 replacement and rework of transistor assembly
* The part numbers noted under the Part Number column are part number differences if a difference exists.			

1.1.2 Explosive Safe Area

On January 14, 1967, the spacecraft was moved to the Explosive Safe Area (ESA) for flight fueling and final testing. A listing of tests performed at the ESA is shown in Table 1-4. After performance of the regulator and leak check, the fuel, oxidizer, and nitrogen were loaded during January 16 to 18.

After the DSIF-71 test without shroud on January 23, the thermal barrier was installed. However, during final checks on the barrier it was discovered that Micromete-

roid Detector MT-717 was punctured. The decision was made to launch the spacecraft without replacing the detector. Following installation of the spacecraft shroud (launch vehicle nose cone), the DSIF test with shroud and Agena adapter was conducted without incident on January 25. The encapsulated spacecraft was then transported to Pad 13 for mating with the launch vehicle.

During ESA operations, considerable difficulties were encountered from erratic operation of the facility crane.

Table 1-4: EXPLOSIVE SAFE AREA TESTS

PARAGRAPH	TEST TITLE
6.1.1.2	Photo Subsystem Launch Preparation
6.1.3	Spacecraft Regulator and Leak Test
6.1.4	Propellant Servicing
6.1.5	Nitrogen Servicing
6.1.6	Photo Subsystem Installation and Alignment
6.1.7	Weight and Balance Verification
6.1.8	Battery Verification
6.1.9	Camera Thermal Door Verification
6.1.10	Spacecraft Operational Check with DSIF-71
6.1.11	Ordnance Check and Hookup
6.1.12	Agena Adapter Installation
6.1.13	Thermal Barrier Installation
6.1.14	Nose Fairing Installation
6.1.15	Spacecraft Operational Check with DSIF-71 through Shroud and Agena Adapter
6.2	Transport Spacecraft to Pad 13

NOTE: Test paragraphs referred to in this table are part of Boeing Document D2-100406-2, Volume III, Spacecraft "6" Test Procedure-ETR-Lunar Orbiter.

1.1.3 Launch Pad 13

After successful completion of the spacecraft-Agena matchmate on the launch pad, tests were conducted to verify impedance and interface compatibility. Table 1-5 lists scheduled and unscheduled spacecraft tests conducted in the launch area.

When an attempt was made to apply power to the spacecraft, no indication of spacecraft power was evident. Investigation disclosed that a shorting bar on the chart recorder, which was used to record bus voltage and current, was shorting out the ground power supply. As a precautionary measure, the ground power supply was replaced with a spare. Ground power was then applied to the spacecraft, and the pad checkout completed satisfactorily. Upon completion of these tests

the spacecraft was ready for simulated launch.

1.2 LAUNCH CONDUCT

The launch plan, activities, facilities, and participating organizations were similar to those for Missions I and II. Specific information may be obtained from Section 3.3, "Launch Operations," of the Mission I final report.

1.2.1 Launch Criteria

Launch criteria and space vehicle preparation were governed by the Launch Operations Plan, LMSC/A751901A. Although Spacecraft 6 had been tested and used as a backup to Spacecraft 5 for Mission II, it was necessary to retest it for Mission III in accordance

Table 1-5: LAUNCH AREA TESTS

DOCUMENT NUMBER	TEST TITLE
D2-100406-2, Volume IV	Spacecraft to Adapter and Agena Matchmate
D2-100626-3, Volumes I and V	Lunar Orbiter Spacecraft Third Flight Spacecraft Initial Pad Tests
D2-100626-3, Volumes II and V	Lunar Orbiter Spacecraft Third Flight Spacecraft Operational Readiness Test*
D2-100626-3, Volumes III and V	Lunar Orbiter Spacecraft Third Flight Spacecraft Simulated Launch
Not Recorded	Transponder Threshold Test**
Not Recorded	Power Supply Transient Test**

* Performed as a part of the simulated launch

** Trouble isolation tests conducted on the launch pad to identify anomalies which occurred during the scheduled tests

with the requirement of Section 5.0 of Boeing Document D2-100111-3, Spacecraft Test Specification - Eastern Test Range - Lunar Orbiter.

Significant milestones described in Table 1-6 were satisfactorily completed by Spacecraft 6 in preparation for launch.

1.2.2 Countdown and Launch

The spacecraft did not participate in the joint flight acceptance composite test (J-FACT) on January 27, 1967 for Mission III. During the test, an Agena voltage-controlled oscillator (VCO) 1461717-135 failed, a faulty Agena helium sphere temperature transducer was discovered, and a broken wire in the AGE cable to the squib simulator circuitry was disclosed. The VCO and the transducer were replaced and the wire was repaired after the test. The test started at T-230 minutes and concluded satisfactorily at a plus count of 2167 seconds. All objectives were met.

The simulated launch test was conducted

January 31, 1967. The spacecraft count was picked up at T-520 minutes at 10:50 GMT. After power was applied to the spacecraft and the rf link established between the spacecraft and DSIF-71 at T-420 minutes, there was a noticeable variation of as much as 15 db below normal in the "up" link rf power to the spacecraft. This situation continued until approximately T-28 minutes in the count, when the signal suddenly increased approximately 8 db and the operation was normal through the plus count.

At T-60, a spacecraft internal power check was initiated. At T-55, an attempt was made to reapply ground power, with no results. It was found that the ground power supply had failed. Subsequent investigation revealed that the failed power supply was an unmodified version of the standard power supply in use. The spare ground power supply replaced the failed unit. During the changeover and subsequent ground power turn-on, power transi-

Table 1-6: SPACECRAFT PRELAUNCH MILESTONES

COMPLETION DATE	EVENT
January 2, 1967	Spacecraft removed from storage
January 3, 1967	Photo subsystem arrived at ETR
January 14, 1967	Spacecraft moved to explosive safe area
January 18, 1967	Spacecraft fueling
January 21, 1967	Photo subsystem installed in spacecraft
January 23, 1967	DSIF-71 checks without the shroud
January 23, 1967	Spacecraft matchmated to Agena adapter
January 25, 1967	Shroud installation
January 25, 1967	Spacecraft checkout with DSIF (Shroud on)
January 26, 1967	Spacecraft matchmated to Agena
January 31, 1967	Simulated launch
February 4, 1967	Final countdown and launch commenced

ents were observed and a photo subsystem film advance was noted. After determination was made that no damage had been done to the photo subsystem, the count was resumed and the test continued through the plus count without further incident. This problem caused 73 minutes of unplanned hold time during the simulated countdown.

The following minor problems were encountered.

- Readouts by the Agena beacon indicated a signal strength 2 db below downrange requirements. The beacon was later removed and a bench power reading confirmed satisfactory signal strength.
- An interlock circuit "program open loop" light was observed. Investigation revealed that the door covering the manual constant setting switches was open. Closing the door corrected the situation.
- A switch malfunctioned in the automatic checkout sequence circuit of the track checkout equipment panel. Installing a spare panel corrected the problem.
- An intermittent flashing of the track transmitter confidence circuit light was traced to the automatic frequency control circuit. This was corrected by adjusting the confidence circuitry tolerance.
- During Lox tanking of the Atlas booster, oscillations of the Lox boiloff system yielded vibrations on the spacecraft EMO of approximately 7 g's peak to peak at a frequency of approximately 23 Hz.

Tests were conducted with the spacecraft van after the simulated launch test to investigate the rf level variations. These tests showed no anomalies in the spacecraft transponder. Checks were also made in the pad

complex wiring, at which time the rf switch that directs the rf to the DSIF-71, the van, and DSIF-71-van was suspected and replaced. This switch was bench tested and indicated no problems. Further investigation resulted in a request to boresight the 10-foot parabolic antenna on the complex with DSIF-71, after which a gain in signal of 10 db was noted.

On February 1, an rf verification test was conducted on the spacecraft with satisfactory results.

On February 2, a test was conducted on the spacecraft to exercise the external power supply and repeat that portion of the spacecraft countdown internal power checks where the trouble had been experienced on the simulated launch test. Ground power supply problems were again encountered when returning to ground power after the internal power checks. The spacecraft simulator was brought to the complex and connected to the complex wiring at the Agena-spacecraft interface. When the power supply was turned on the first two times, similar problems were experienced, and trouble shooting continued with the spacecraft simulator. The launch attempt scheduled for February 3, 1967 was cancelled and processing of the backup spacecraft, Lunar Orbiter Serial Number 7, was initiated.

Trouble shooting continued on February 3. After initial duplication of the power supply problem with the spacecraft simulator, 20 further attempts failed to reproduce this problem. The power supply remote control panel on the blockhouse console was replaced. A test was run on the spacecraft simulator and the spacecraft was put through that portion of the test where all the problems had been encountered. These tests were completely successful and the launch was rescheduled for the following day. Prior to turning power on the spacecraft, it was

discovered that the Agena umbilical pull-away connector was not properly cocked. The umbilical was disconnected from the vehicle, recocked, and reconnected.

The spacecraft count was picked up at T-520 minutes. After power was supplied to the spacecraft at T-420 minutes, there was some fluctuation in rf signal between the spacecraft and DSIF-71. Prior to T-315 minutes, when the traveling-wave-tube amplifier (TWTA) was checked, a requirement for the TWTA to be above 45°F was imposed. Spacecraft air conditioning was dumped and the nitrogen purge was started to meet this requirement. At cooling air shutdown, variations in rf signal were noticed. The air conditioning was cycled on and off with corresponding variations in rf signal. The TWTA was finally checked successfully at about T-250 minutes, causing the rf silent period at T-255 minutes to be delayed for approximately 5 minutes. From this point, a normal spacecraft countdown was conducted to lift-off. Primary spacecraft air conditioning was lost at about T-30 minutes and a switchover to the backup system was accomplished without incident.

1.2.3 Weather

Weather during the launch operation was favorable. Upper wind shears were within acceptable limits. At liftoff, the following weather parameters were recorded.

Temperature 54.3°F
Relative Humidity 94%
Visibility 10 miles
Dew Point 53°F
Surface Winds Calm
Clouds Clear Skies
Sea-Level Atmospheric
Pressure 29.970 inches of Mercury

1.2.4 Tracking Coverage

The Air Force Eastern Test Range (AFETR), Deep Space Network (DSN), and Manned Space Flight Network (MSFN) are the elements of the Tracking and Data System (TDS) that together support the tracking and telemetry requirements for the Lunar Orbiter III launch.

Tracking during the launch phase consisted of C-band tracking of the launch vehicle and reception of VHF and S-band telemetry from the launch vehicle and spacecraft, respectively. Figure 1-1 shows AFETR and MSFN uprange coverage for any launch day.

Tracking data provided to AFETR during the launch phase established (1) the Agena orbit and the normalcy of spacecraft cis-lunar injection in real time, and (2) launch vehicle performance evaluation. This was done by first tracking the Agena stage and then, after separation, both the spacecraft and Agena. Since the separation velocity was small, tracking of the Agena stage both prior to and subsequent to separation was valuable in determining an early spacecraft trajectory.

Other elements of the TDS received the tracking data to prepare acquisition and prediction data for the Deep Space Stations (DSS). Prediction data based upon actual launch vehicle performance was used during initial acquisition by all stations. The tracking data supplied by the uprange AFETR and MSFN radars were processed by the real-time computer system (RTCS) at the AFETR, and station predictions were generated in real time for the AFETR, MSFN, and DSS farther downrange. The AFETR forwarded the tracking data directly to Goddard Space Flight Center (GSFC) so the GSFC could generate prediction data for the MSFN stations. These data were also relayed to the Space Flight Operations Fa-

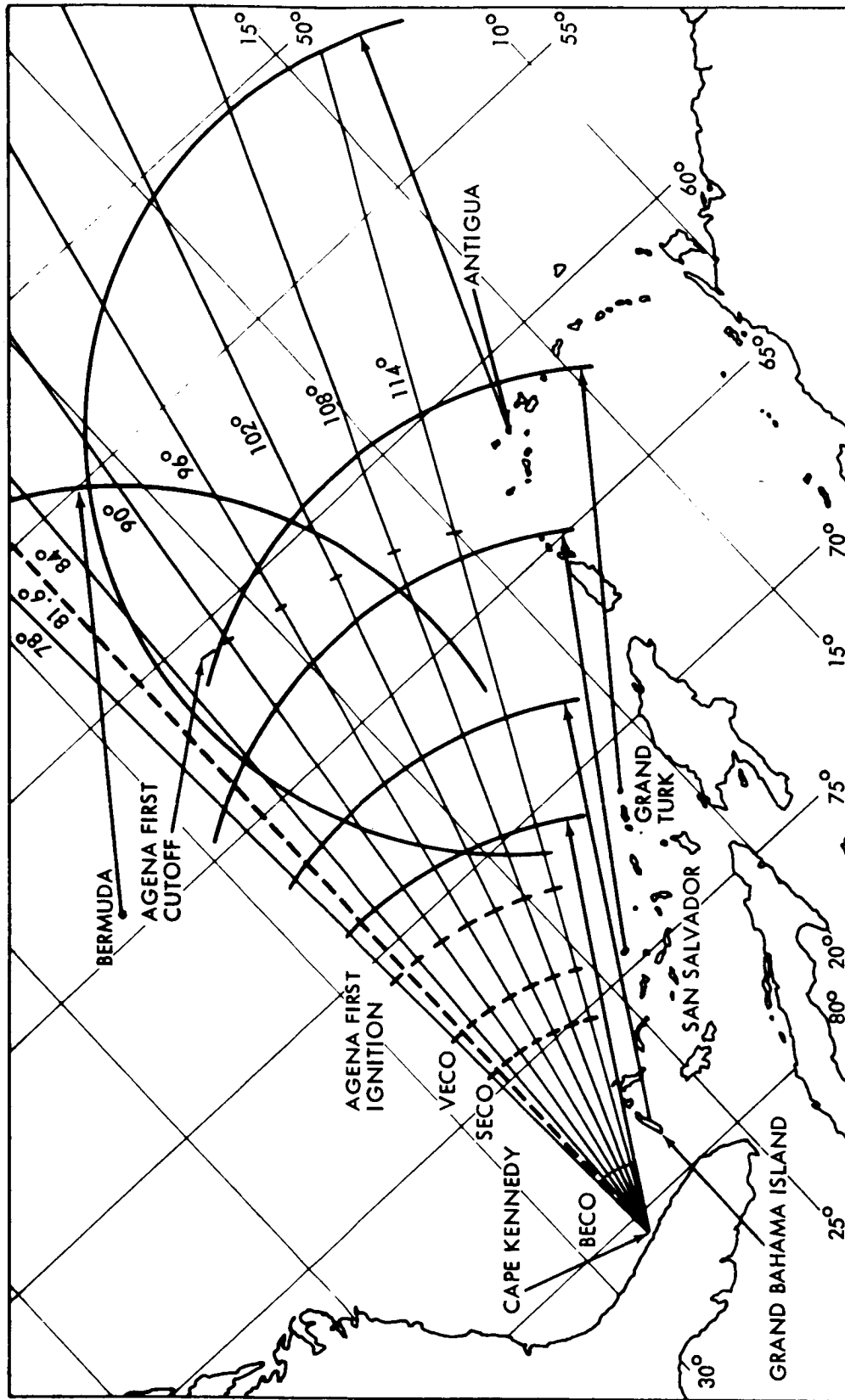


Figure 1-1: Lunar Orbiter Uprange Radar Coverage

cility (SFOF) for use with DSS data in calculating the spacecraft trajectory. The MSFN transmitted Bermuda and Carnarvon tracking data to the AFETR. The AFETR retransmitted their raw tracking data and that of the MSFN stations to the SFOF in near-real time.

Tracking coverage for various portions of the near-Earth phase of the launch trajectory is shown in Figure 1-2.

The ability to satisfy the near-Earth phase tracking and telemetry requirements was strongly dependent upon trajectory characteristics and TDS facilities during that phase. The most dominant trajectory characteristic was the variable location of the cis-lunar orbit injection point. With the injection taking place uprange—i.e., in the Atlantic Ocean—the support problems were quite different than for an injection far downrange in the Indian Ocean as experienced during Mission I. An Earth map with injection loci for the February launch period is presented in Figure 1-3. The injection point for the launch of February 5, 1967, on an azimuth of 81.6 degrees, was near the western edge of Africa in the Atlantic Ocean.

1.2.5 Telemetry Coverage

Elements of the TDS received and recorded spacecraft and launch vehicle telemetry during the near-Earth phase of the mission (see Figure 1-4). Spacecraft telemetry was received and recorded via the Agena S-band and VHF links.

The Kennedy Space Center (KSC) telemetry station supported all vehicle checkout and the launch on both vehicle links. Local signals were used until T+435 seconds, at which time Agena data was switched to the submarine cable signal from Antigua. All vehicle events through first burn of the Agena were recorded and reported in real time.

In addition, the Canary Island MSFN station relayed the velocity meter information to the KCS. All second-burn events were also recorded in real time. The various AFETR second-burn relays were not needed on the launch azimuth that was flown.

1.3 LAUNCH VEHICLE PERFORMANCE

The first stage of the launch vehicle was an SLV-3 (Atlas), Serial Number 5803. All SLV-3 flight objectives were satisfied.

Position charts indicated the vehicle flight to be low and left from liftoff until approximately T + 240 seconds when the vehicle approached nominal. It remained near nominal throughout the powered flight. The performance of all Atlas systems was satisfactory. Atlas-Agena separation was properly accomplished, and good telemetry data was obtained for Atlas systems analysis.

The second stage of the launch vehicle was an Agena-D, Serial Number 6632. Agena performance was satisfactory throughout the flight. A velocity meter cutoff terminated Agena first and second burns. First burn was approximately 1.2 seconds longer than nominal; second burn was 0.4 second longer than nominal. Agena telemetry yielded the expected responses, with the exception of longitudinal acceleration measurement A-9, which indicated the wrong polarity prior to launch.

Significant ascent trajectory events and times in seconds relative to initial vehicle 2-inch motion are covered in Table 1-7.

The configuration of the Atlas-Agena launch vehicle for Mission III was identical to the Lunar Orbiter Mission I and Mission II launch vehicles except that new light weight engine boots were employed on the Atlas. Performance of the boots apparently was satisfactory since thrust section temperatures

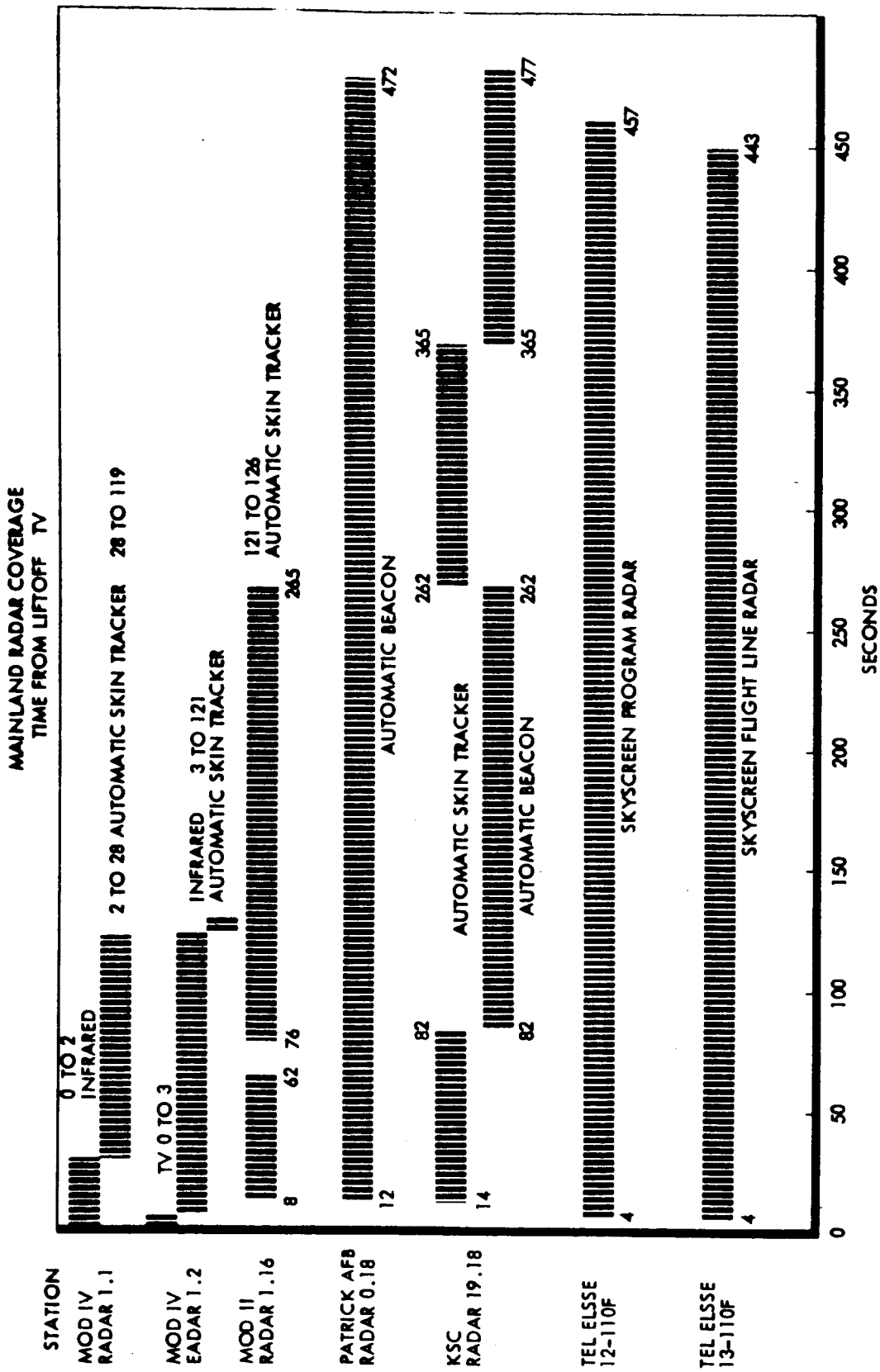


Figure 1-2: Tracking Coverage

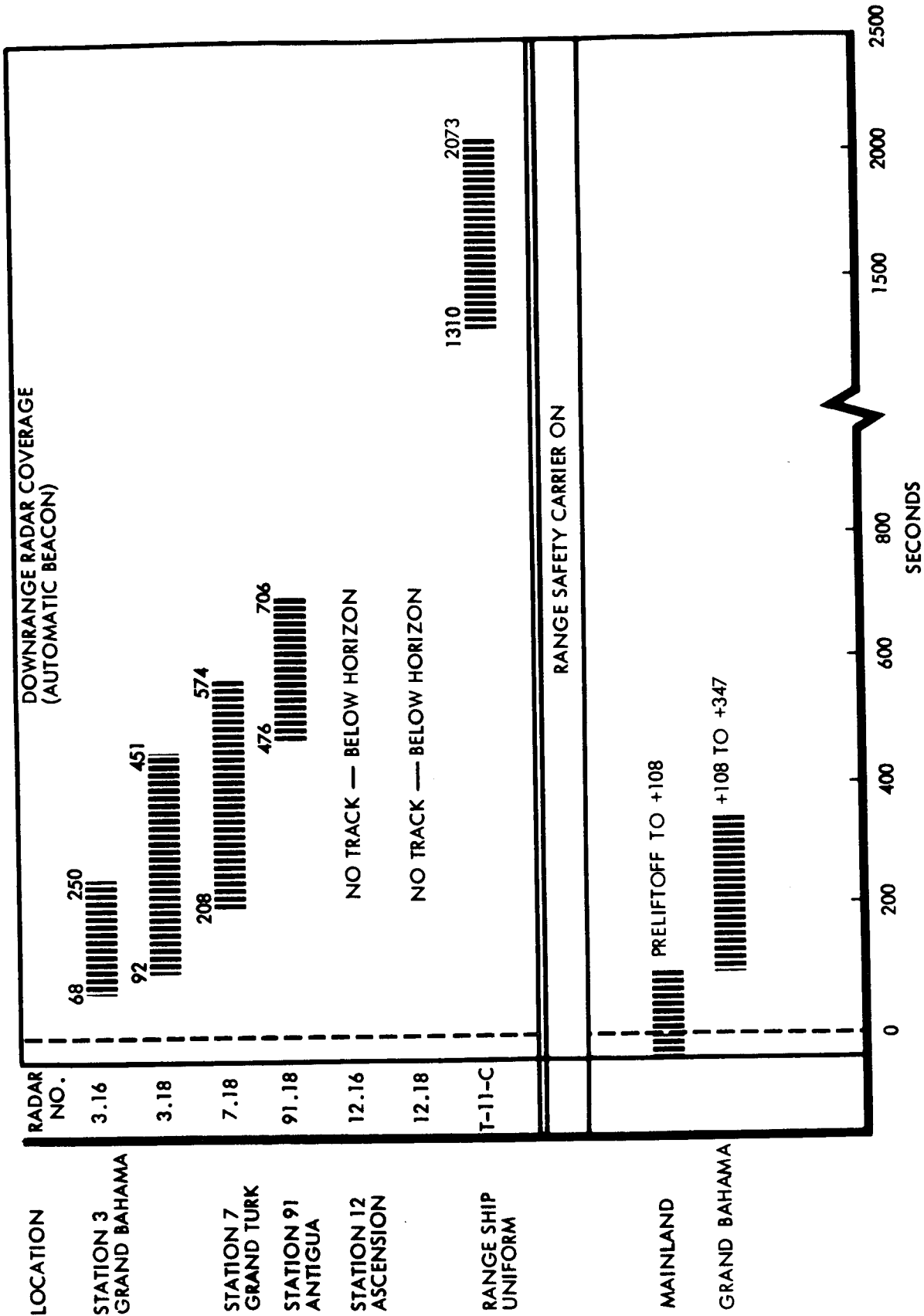


Figure 1-2: Tracking Coverage (Continued)

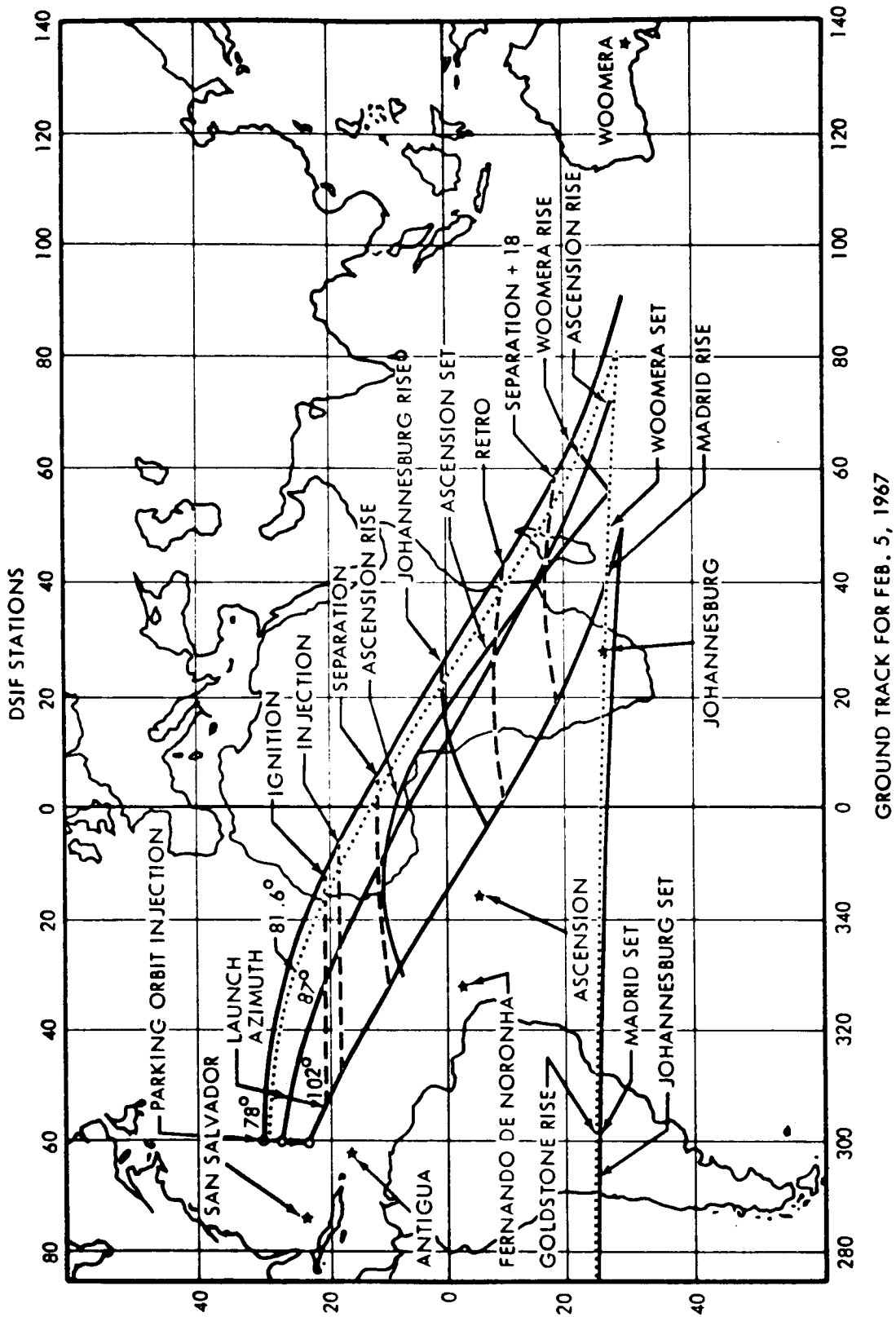


Figure 1-3: Ground Tracking for February 5, 1967

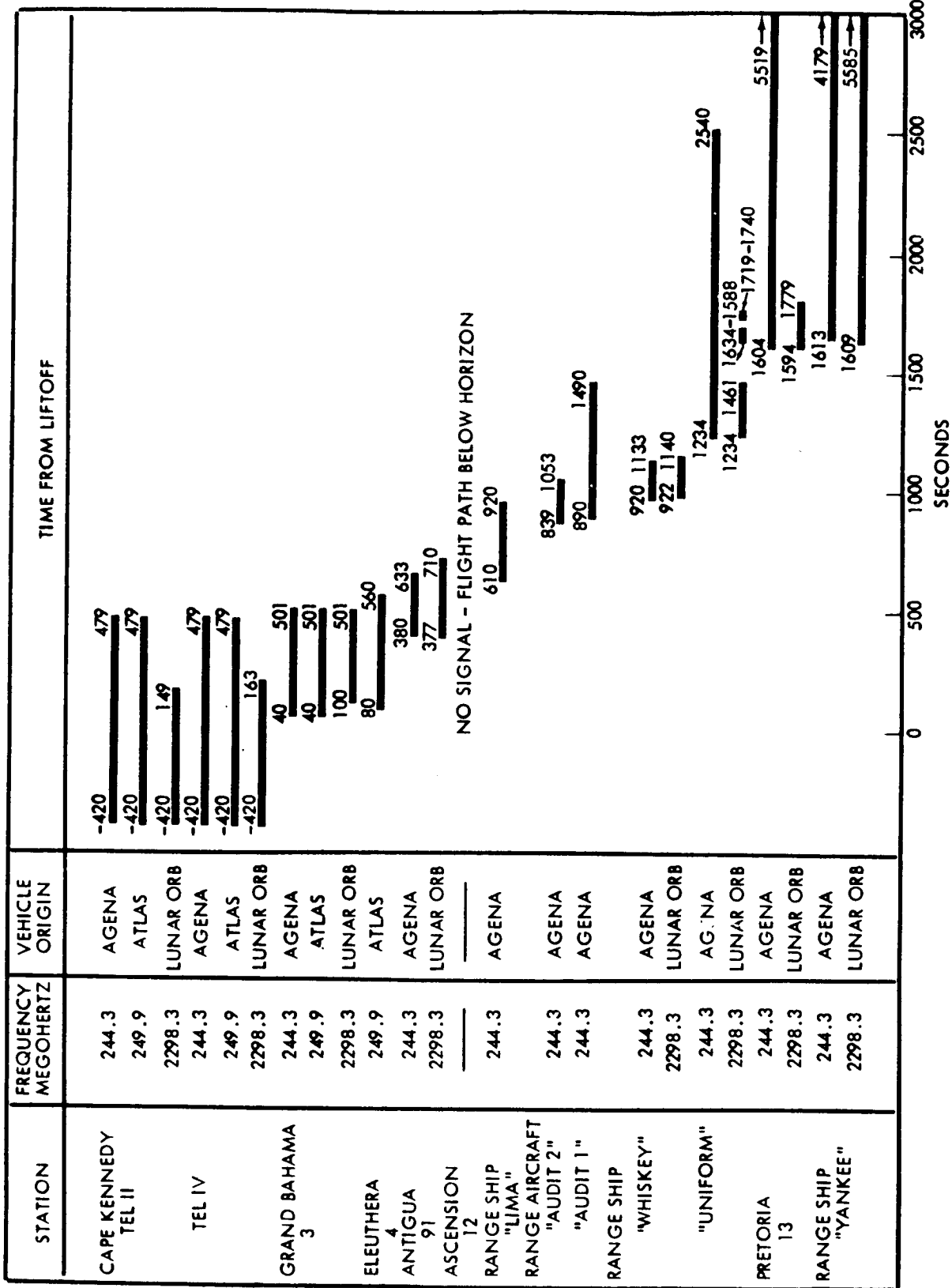


Figure 1-4: Telemetry Coverage

Table 1-7: ASCENT TRAJECTORY EVENT TIMES

EVENT	TIMES (+ SEC)	
	NOMINAL	ACTUAL
Liftoff (2-inch motion)	0117:01.120 GMT	
BECO	129.9	129.78
Jettison Booster	132.9	132.99
Start Agena Auxiliary Timer	270.21	270.48
SECO	288.3	288.02
Start Primary Sequence Timer	293.88	297.36*
VECO	308.7	309.21
Jettison Nose Shroud	311.0	311.43
Atlas-Agena Separation	312.0	313.57
Agena First-Burn Ignition (90% pc)	368.03	371.64
Agena First-Burn Cutoff**	522.807	527.38
Stop Primary Sequence Timer	578.5	—
Restart Primary Sequence Timer	1090.21	1090.49
Agena Second-Burn Ignition (90% pc)	1105.36	1105.65
Agena Secon-Burn Cutoff***	1193.73	1194.37
Spacecraft-Agena Separation	1358.21	1358.55
Agena Yaw Maneuver	1361.21	1361.46
Stop Yaw Maneuver	1421.21	1421.46
Fire Agena Retro Rocket	1958.21	1958.55
Retro Rocket Burnout		1974.99

* Primary sequence timer started 3.48 seconds late

** First-burn duration: nominal, 154.7 seconds; actual, 155.9 seconds

*** Second-burn duration: nominal, 88.4 seconds; actual, 88.8 seconds

appeared nominal throughout flight. Details of the Atlas-Agena configuration are presented in the Mission I final report (Boeing Document D2-100727-1, Volume I), and in the

Lunar Orbiter C Launch Report (Lockheed Document LMSC 274220). The general space vehicle system configuration is shown in Figures 1-5, 1-6, and 1-7.

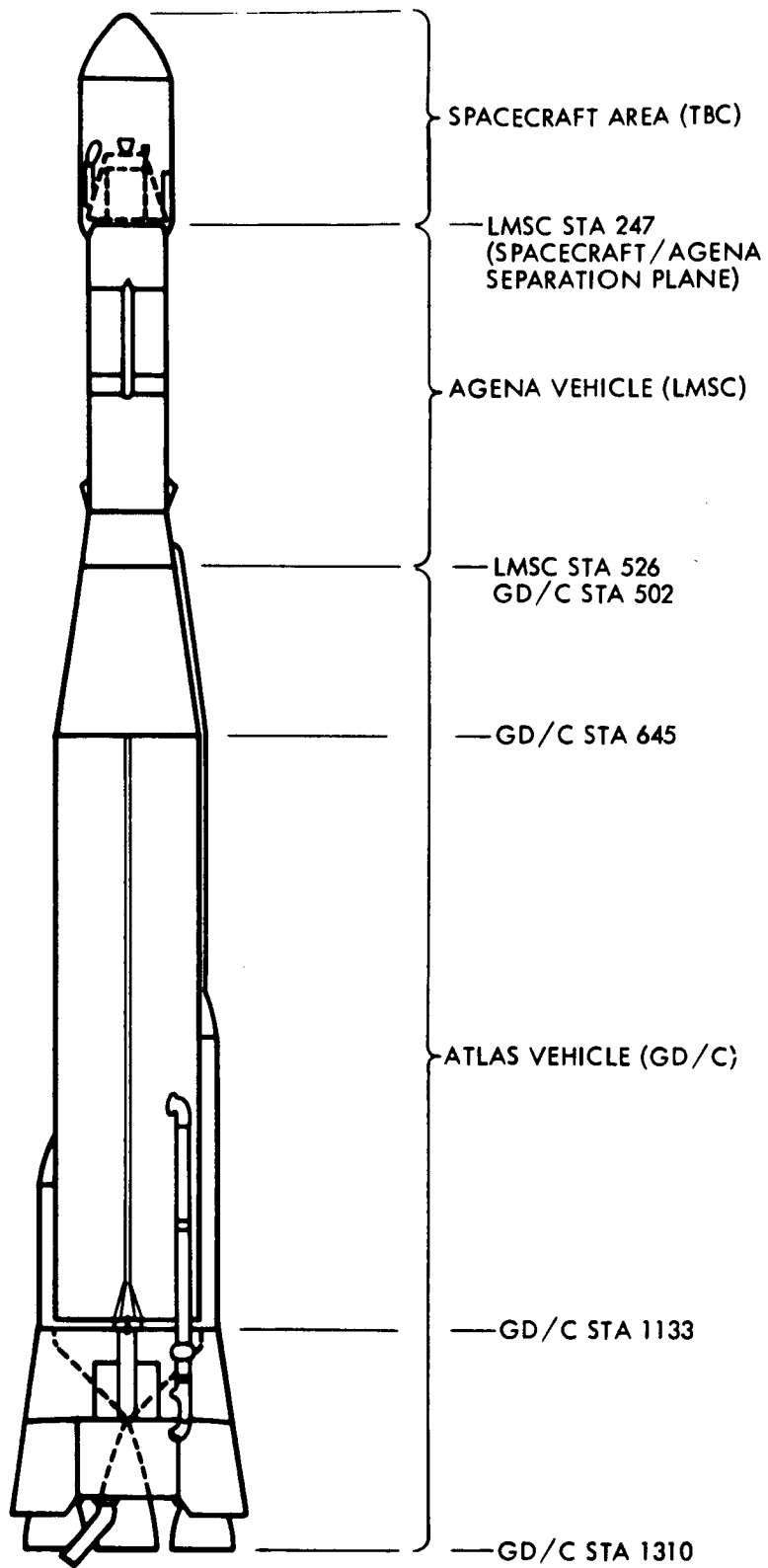
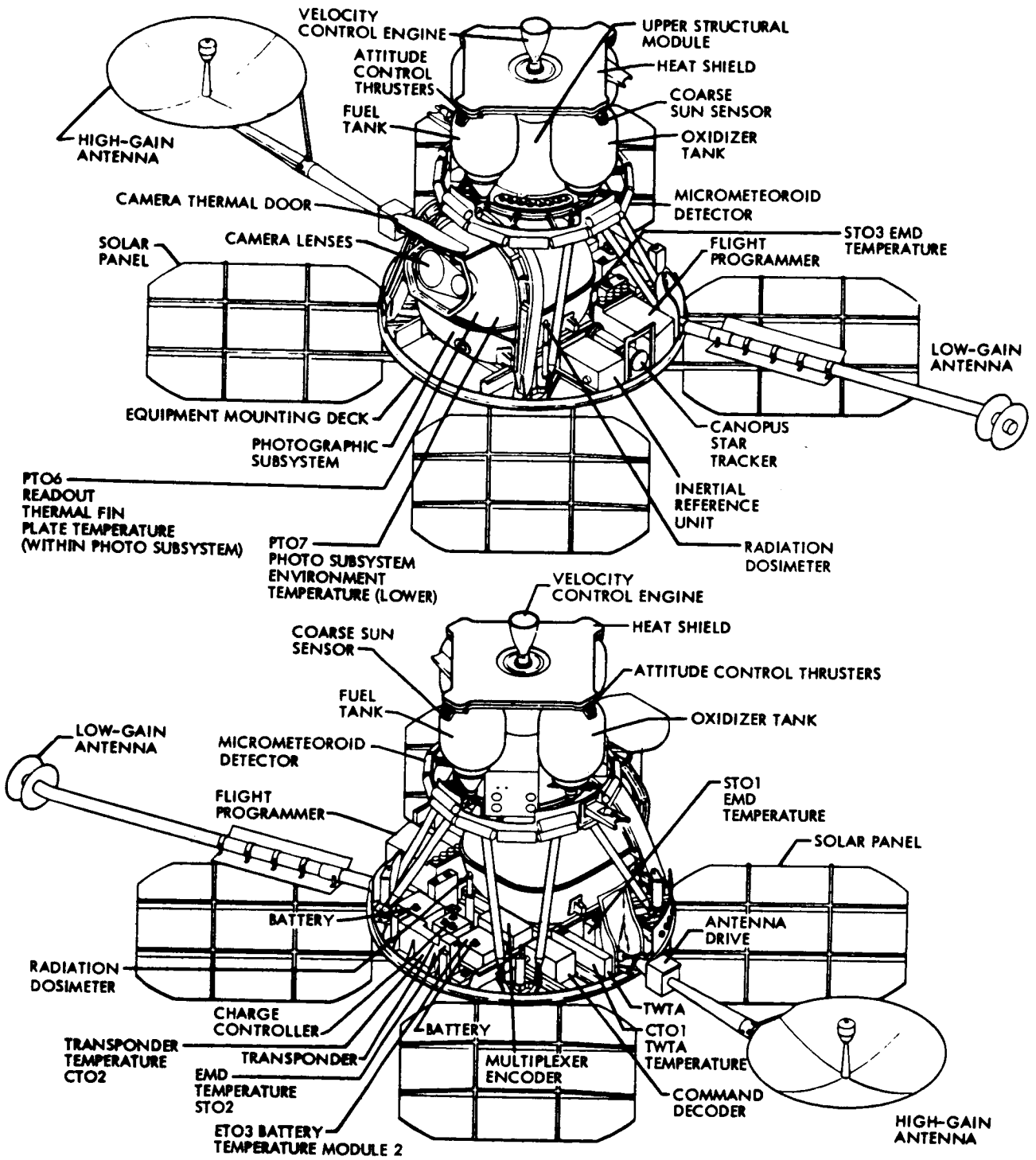


Figure 1-5: Lunar Orbiter Space Vehicle



NOTE: SHOWN WITH THERMAL BARRIER REMOVED

Figure 1-6: Lunar Orbiter Spacecraft

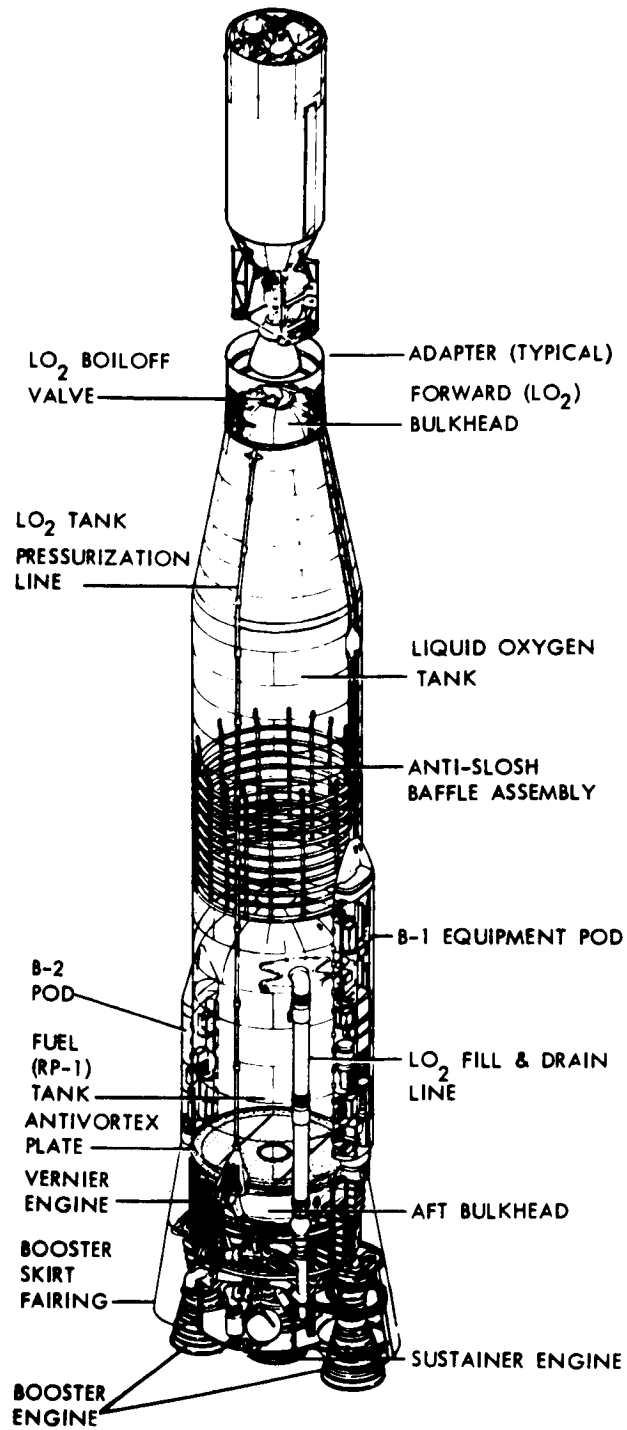


Figure 1-7: Launch Vehicle

1.3.1 Atlas Performance

The Atlas launch vehicle, Serial Number 5803, had three primary objectives and one secondary objective in support of Lunar Orbiter Mission III. The primary goals were:

- Place the upper stage into proper coast ellipse:
- Initiate or relay commands properly for separation of upperstage vehicle and start the Agena primary timer;
- Relay commands to the Atlas-Agena interface to jettison the shroud and start the secondary timer of the launch vehicle.

The secondary objective was determination of Atlas performance by using telemetry data.

All objectives were successfully achieved.

1.3.2 Agena Performance

The second-stage Agena vehicle, Serial Number 6632, had two primary objectives and one secondary objective in support of Lunar Orbiter Mission III. The primary goals were:

- Inject the spacecraft into a lunar-coincident transfer (cislunar) trajectory

within prescribed orbit dispersions ;

- Perform Agena attitude and retro-maneuvers following Agena-spacecraft separation to ensure that the Agena would not, to the specified probabilities, intercept the spacecraft, pass within 20 degrees of the center of the Canopus tracker field of view, or impact the Moon.

The secondary aim of the Agena vehicle was to provide tracking and telemetry data for evaluation of Agena performance.

All objectives were satisfied. Evaluation of orbital data of the Agena after retro maneuver indicate that the Agena arrived in the lunar vicinity approximately 6 hours after the spacecraft and was approximately 17,000 km beyond lunar capture. Based on available data, the Agena vehicle is now in a long lifetime Earth orbit with apogee of 428,662 km and perigee of 24,611 km.

A detailed technical description of flight parameters is contained in Document LMSC/A858188, Lunar Orbiter C Agena Vehicle 6632 Flight Performance Analysis Report, prepared by Space System Division of the Lockheed Missiles and Space Company.

2.0 FLIGHT OPERATIONS

This section describes Lunar Orbiter Mission III flight operations from liftoff at Cape Kennedy, Florida, at 01:17 GMT on February 5, 1967 through the completion of final readout during Orbit 154 at 07:17 GMT on March 3, 1967. Included are a comparison of the flight plan with the actual mission, a discussion of the operational controls used to control the spacecraft trajectory and performance, and descriptions of airborne and ground systems performance.

Mission III from liftoff until Orbits 149 and 150 on March 2, 1967 was nominal and closely followed the flight plan. An anomaly in the photo subsystem during the readout sequence during Orbits 149 and 150 prevented the completion of readout of all of the exposed film; however, approximately 75 per cent of all film was read out.

The Flight Operations organization remained essentially unchanged from that used in Mission II. A high return of experienced personnel provided the basis for manning this organization.

Operational techniques developed in Missions I and II were used in conducting Mission III. Although some modifications to these techniques may be required prior to Mission IV, the techniques required little modification prior to or during Mission III.

2.1 FLIGHT PLAN AND CONDUCT

This section describes the Lunar Orbiter Mission III flight plan and summarizes the nominal mission design. Flight conduct is discussed, identifying conditions encountered in flight which necessitated deviations from the planned nominal mission. An outline of the control techniques that were implemented for mission control, spacecraft control, and flight path control is also included.

2.1.1 Flight Plan

The flight plan for Lunar Orbiter Mission III was in major respects parallel to Missions I and II, due to the similarity of target distribution on the lunar surface. The Mission III flight plan was predicated on a nominal mission design, designated P-9A.

The P-9A mission launch was planned for 0 hours, 22 minutes, 09.0 seconds GMT on February 3, 1967 at a launch azimuth of 78 degrees. A 90-hour cislunar trajectory was planned with midcourse corrections at 28 hours and 70 hours from launch. The mission design included a mandatory first midcourse correction, rather than an optional correction as in earlier missions. A plane change of 13.04 degrees at injection was required.

Approximately 6 days waiting time was allowed from initial orbit injection until orbit transfer. An additional 2 days was allowed from orbit transfer before photography of the first photo site. Forty-four sites were selected for photography. Twelve potential Apollo sites distributed within the area of interest ($\pm 5^\circ$ latitude and $\pm 45^\circ$ longitude) on the lunar surface were designated as primary sites (IIIP-1, IIIP-2, etc.). Thirty-two additional sites were designated as secondary sites (IIS-1, IIS-2, etc.).

The photography plan required exposures to be made during nearly every orbit from initiation through completion of photography. A total of 212 exposures was planned (211 exposures were used).

Priority readout was scheduled on virtually every orbit between photo sites. Readout scheduling provided for transmission of higher priority exposures during this period. Subsequent to completion of photography, an 11-day period was allocated for complete

readout of the proposed 212 frames, thereby dictating a total mission duration of 32 days. A summary of planned activities occurring after injection is provided by Table 2-1.

2.1.2 Flight Conduct

Few significant flight plan deviations were required in the conduct of this mission. Minor changes to prelaunch planning were made as required to optimize the mission in real time as a function of actual flight profile.

Additional details regarding flight parameters and spacecraft performance will be included in later sections. Times of significant mission events are summarized in Table 2-1.

2.1.2.1 Flight Profile

Liftoff was delayed 1 day by a ground power supply failure at the Eastern Test Range. This failure resulted in an inadvertent one-frame film advance in the photo subsystem due to a power transient. This single-frame advance did not bring the leader-to-film splice under tension; the only impact was the necessity for a ten-frame, rather than 11-frame, initial film advance to position the film for photography. The flight proceeded nominally through the cislunar and initial orbit phases and no significant flight plan deviations were required prior to initiation of photography.

Site photography was performed as planned, with the exception of numerous minor changes to site locations and one secondary-site deletion for technical causes. Reasons for the majority of site changes were to ensure coverage of specific areas such as the Surveyor I landing area, and to optimize photo data acquisition in real time. Site coordinates were changed for 13 of 20 prime-site photo orbits, and one additional photo pass was added. These changes were for Sites IIIP-2b, -4, -5a, -5b, -7a, -9a, -9b, -9c, -11,

-12a, -12b.1, -12b.2, and -12c. Secondary-site coordinates or photographic procedure changes were required for 10 of 33 photo passes, including two deletions and one addition. Affected sites were IIIS-2, -4, -8, -12, -14, -21.5, -20, -23, -25, and -32. Photographic site location as actually photographed is provided by Table 2-2. Also, it was determined that use of the V/H sensor was inadvisable on certain secondary targets. These changes necessitated revisions to both core map loading and the film budget plan, as well as abbreviated reaction time for computations of spacecraft attitude and camera-on times. Experience levels of operations personnel allowed incorporation of these changes to the relatively complex photographic plan to be met on a time scale, which could have proven infeasible in earlier missions. Revised core map loading and film budget plans are included for additional detail as Tables 2-3 and -4.

Priority readout was initiated at every opportunity during the photographic phase of the mission. During these readouts, the first spacecraft anomaly was observed—some framelets were repeatedly reread when the 0.1-inch film advance became erratic. It was determined that this "hangup" condition was correctable by temporary termination of readout.

As empirical evidence indicated some degree of predictability of hangup, a partially successful preventive procedure was developed for final readout: schedule readout termination after each 19 inches of film readout. In this way, it was frequently possible to avoid this abnormal subsystem operation. The phenomenon continued throughout priority readout until the operations team was directed to delete the final secondary site, IIIS-32, and perform an early Bimat cut.

Table 2-1: SIGNIFICANT EVENT SUMMARY

Time		Event
Planned	Actual	
36:01:17:00	36:01:17:01.1	Liftoff
36:01:19:10.6	36:01:19:09.9	Booster Engine Cutoff
36:01:19:13.0	36:01:19:13.1	Booster Jettison
36:01:21:50.3	36:01:21:49.1	Atlas Sustainer Cutoff
36:01:22:10.5	36:01:22:10.3	Atlas Vernier Cutoff
36:01:22:12.6	36:01:22:12.5	Shroud Separation
36:01:22:14.5	36:01:22:14.7	Atlas-Agena Separation
36:01:23:07.7	36:01:23:12.7	Agena First Ignition (90% Pc)
36:01:25:43.9	36:01:25:48.5	Parking Orbit Injection
36:01:35:26.5	36:01:35:26.8	Agena Second Ignition (90% Pc)
36:01:36:54.8	36:01:36:55.5	Cislunar Injection
36:01:39:39.4	36:01:39:39.7	Spacecraft Separation
	36:01:41:30.4	Deployment Start
	36:01:50:00.0	Sun Acquisition Start
	36:12:03:30	Canopus Acquisition
	36:17:05:00	Bleed Propellant Lines
	37:14:43:42.4	Start attitude maneuver for midcourse correction
	37:15:00:00.0	Engine ignition— ΔV 5.11 M/S (16.7 f/s) Engine burn time 4.4 seconds
	37:15:08:05.4	Complete reverse attitude maneuver
	39:21:38:38	Start attitude maneuver for lunar injection
	39:21:54:19.0	Engine ignition— ΔV 704.3 M/S (2310.1 f/s) Engine burn time 542.5 seconds
	39:22:11:07.3	Complete reverse attitude maneuver
	43:18:00:52	Start attitude maneuver for orbit transfer
	43:18:13:26.6	Engine ignition— ΔV 50.7 M/S (168.3 f/s) Engine burn time 33.7 seconds
	45:18:18:00	Read out test film
	46:10:00:40.6	Start site photography
	54:06:36:41.6	Cut Bimat Start final readout
	54:09:34:00.0	Photo Subsystem Anomaly

Table 2-2 PHOTOGRAPHIC SITE LOCATION

PRIMARY SITES							NOTES
Orbit	Site No	Longitude	Latitude	Frame	Direction Code (See Notes)	Remarks Code	
44	IIP-1	35 15' E	2 55' N	16 Fast	a.	A.	
45	P-2a	42 25' E	0 50' S	8 Fast	b.	A.	
46	P-2b	42 41' E	0 55' S	4 Fast	g.	A.	
50	P-3	20 15' E	3 20' N	4 Slow	b.	A.	
51	P-4	27 27' E	0 37' N	8 Fast	b.	A.	
52	P-5a	24 31' E	0 27' N	8 Fast	g.	A.	
53	P-5b	24 31' E	0 27' N	8 Fast	b.	A.	
54	P-6	21 30' E	0 20' N	4 Slow	b.	A.	
64	P-7a	1 17' W	1 02' N	8 Fast	g.	A.	
65	P-7b	1 20' W	0 55' N	8 Fast	b.	A.	
77	P-8	19 50' W	0 50' S	8 Fast	a.	A.	
80	P-9a	23 11' W	3 09' S	8 Fast	g.	A.	
81	P-9b	23 11' W	3 09' S	8 Fast	j.	A.	
82	P-9c	23 11' W	3 09' S	8 Fast	b.	A.	
86	P-10	42 00' W	1 45' N	8 Fast	g.	A.	
89	P-11	36 56' W	3 17' S	8 Fast	b.	A.	
90	P-12b 2	See Direction Code		4 Fast	m.	A.	
91	P-12a	43 52' W	2 23' S	16 Fast	b.	A.	
92	P-12b 1	See Direction Code		4 Fast	n.	A.	
93	P-12c	See Direction Code		8 Fast	k.	A.	
SECONDARY SITES							NOTES
Orbit	Site No.	Longitude	Latitude	Frame	Direction Code (see Notes)	Remarks Code	
44	IIS-1	47 10' E	1 50' S	4 Fast	h.	D.	
47	S-2	~104 E		1	l.	D.	
48	S-3	38 45' E	4 30' S	1	e.	D.	
49	S-4	24 31' E	0 27' N	1	f.	C.	
55	S-5	24 12' E	0 35' S	1	e.	D.	
56	S-6	6 20' E	7 45' N	1	e.	D.	
57	S-7	6 50' E	3 40' N	4 Slow	a.	D.	
58	S-8	26 25' E	11 20' S	1	d.	D.	
59	S-9	17 35' E	1 25' S	1	e.	D.	
61	S-10	13 30' E	1 30' S	4 Slow	b.	B.	
62	S-11	1 20' W	0 55' N	1	f.	C.	
—	S-12	Deleted					
63	S-13	0 30' W	5 00' N	1	e.	D.	
66	S-14	9 00' W	5 00' N	1	c.	B.	
67	S-15	5 30' W	0 40' N	4 Slow	b.	D.	
69	S-16	5 40' W	0 20' S	1	b.	D.	
70	S-17	4 05' E	4 45' S	4 Slow	b.	B.	
71	S-18	8 02' W	1 50' S	4 Fast	e.	D.	
72	S-19	3 40' W	3 20' S	4 Slow	b.	B.	
74	S-21	20 00' W	0 30' S	1	f.	C.	
74	S-21.5	~126 E		1	o.	D.	
75	S-22	22 05' W	1 10' N	1	b.	B.	
76	S-20	27 45' W	7 40' N	1	c.	D.	
78	S-23	17 14' W	3 31' S	4 Slow	o.	D.	
79	S-24	23 15' W	3 05' S	1	f.	C.	
83	S-25	42 00' W	1 45' N	1	f.	C.	
84	S-26	37 50' W	8 10' N	1	e.	D.	
87	S-27	37 10' W	3 30' S	1	f.	C.	
88	S-28	43 55' W	2 20' S	1	f.	C.	
94	S-29	60 33' W	5 00' S	1	e.	D.	
96	S-30	64 35' W	7 00' N	1	c.	D.	
97	S-31	67 00' W	1 50' N	1	a.	D.	

Direction Code

a. Taken vertical on orbit which passes nearest to site. Coordinates may not be within telephoto coverage.

b. Camera pointed at site from nearest orbit -- using cross track tilt if necessary.

c. Oblique photo looking North

d. Oblique photo looking South

e. Oblique photo looking normal to orbit.

f. Oblique photo looking westerly

g. Telephoto convergent, stereo using cross track tilt to point camera at site.

h. Using same attitude as site IIP-1.

i. 5% telephoto sidelap with equal cross track tilt from each orbit.

j. 10 to 15% telephoto sidelap with P-9c

k. Convergent stereo overlap with first 8 frames of 16 frames from site IIP-12a.

l. Wide angle field of view contains S/C shadow.

m. 25% telephoto sidelap with frame numbers, 10, 11, 12 and 13 of Site IIP-12a 16 frame sequence using cross track tilt as required.

n. 25% telephoto sidelap with frame numbers 10.5, 11.5, 12.5, 13.5 and 14.5 of Site IIP-12a 16 frame sequence using cross track tilt as required.

o. Oblique looking south. Take at 20° from IM terminator using roll maneuver only.

Remarks Code

A. Provide additional data now needed to select Surveyor sites in support of Apollo and other candidate sites for first Apollo mission.

B. Provide data necessary to screen other candidate landing sites for Surveyor.

C. Provide oblique views of promising Apollo landing sites.

D. Provide data of scientific interest.

General

● Orbit numbers have been adjusted from P9A to agree with Mission III.

Table 2-3 CORE MAP ACTUAL PHOTOGRAPHIC ACTIVITY

CORE MAP	ORBIT LOADED	ORBITS INVOLVED*	PHOTO SITES	CAMERA MODE	V/H MODE	CARRYOVER FROM PREVIOUS MAP
15	42	43 44	Film Advance P-1,S-1#	(10 frames) F16, F4	On	
16**	44	45	P-2a	F8	On	P-1, S-1
17**	45	46	P-2b	F4	On	P-2a
18	46	47 48	S-2 S-3	S1 S1	Off Off	P-2b
19	48	49 50	S-4 P-3	S1 S4	Off On	S-3
20	50	51 52	P-4 P-5a	F8 F8	On On	P-3
21	52	53 54	P-5b P-6	F8 S4	On On	P-5a
22	54	55 56	S-5 S-6	S1 S1	On On	P-6
22 Update	55	56	Store S-6 Camera and V/H modes			
23	56	57 58	S-7 S-8	S4 S1	On Off	S-6
23 Update	57	58	S-8	V/H Mode		
24	58	59 60	S-9 —	S1	On	S-8
25	60	61 62	S-10 S-11	S4 S1	On Off	—
26	62	63 64	S-13 P-7a	S1 F8	Off On	S-11
27	64	65 66	P-7b S-14	F8 S1	On On	P-7a
28	66	67 68	S-15 —	S4	On	S-14
29	68	69 70	S-16 S-17	S1 S4	On On	—
30	70##	71	S-18	F4	On	S-17

* To Sunrise of the following Orbit

** Data for both maps to be presented at same preliminary and final command conferences.

No attitude change between P-1 and S-1

Part of Map may have to be loaded on following orbit

Table 2-3 CORE MAP ACTUAL PHOTOGRAPHIC ACTIVITY (Continued)

CORE MAP	ORBIT LOADED	ORBITS INVOLVED*	PHOTO SITES	CAMERA MODE	V/H MODE	CARRYOVER FROM PREVIOUS MAP
30		72 73	S-19 —	S4	On	
31	73	74 75	S-21, S-21.5 S-22	S1, S1 S1	Off, Off On	—
32	75	76 77	S-20 P-8	S1 F8	Off On	S-22
32 Update	76	77	Store P-8 Camera Mode			
33	77	78 79	S-23 S-24	S4 S1	On Off	P-8
33 Update	78	79	Store S-24 Camera and V/H Modes			
34	79	80 81	P-9a P-9b	F8 F8	On On	S-24
35	81	82 83	P-9c S-25	F8 S1	On Off	P-9b
36	83	84 85	S-26 —	S1	Off	S-25
37	85	86 87	P-10 S-27	F8 S1	On Off	—
38	87	88 89	S-28 P-11	S1 F8	Off On	S-27
39	89	90 91	P-12b.2 P-12a	F4 F16	On On	P-11
39 Update	90	91	Store P-12a camera mode			
40	91	92 93	P-12b.1 P-12c	F4 F8	On On	P-12a
40 Update	92	93	Store P-12c camera mode			
41	93	94 95	S-29 —	S1	Off	P-12c
42	95	96 97	S-30 S-31	S1 S1	Off On	—
43	97	98 99	Readout and bimat cut in this Map			

* To Sunrise of the following orbit

Table 2-4 FILM BUDGET ACTUAL

SITE NUMBER	ORBIT NUMBER	EVENT (FRAMES)			TOTAL FRAMES ACCUMULATED			EXPOSED	FRAME NUMBERS			ORBIT NUMBER OF READOUT
		TAKE	PROCESS	READOUT	READOUT	EXTRA IN STORAGE LOOPER	BIMAT THRU PROCESSOR		RESULTING READOUT SEQUENCES			
									TELE - PHOTO	WIDE ANGLE & TIME CODE	TELE - PHOTO	
	43	10	10				2	-6 to 4				
P-1 S-1	44	16;4	19			1	21	5-20 21-24	20% 7	5	20% 6	45
P-2a	45	8	4			5	25	25-32	20% 11	9	50% 10	46
P-2b	46	4	2			7	27	33-36	20% 13	11	40% 12	47
S-2	47	1	2			6	29	37	20% 15	13	40% 14	48
S-3	48	1	2			5	31	38	—	15	50% 16	49
S-4	49	1	2			4	33	39	—	17	50% 18	50
P-3	50	4	2			6	35	40-43	—	19	40% 20	51
P-4	51	8	6			8	41	44-51	—	25	40% 26	52
P-5a	52	8	6			10	47	52-59	—	31	30% 32	53
P-5b	53	8	2			16	49	60-67	—	33	30% 34	54
P-6	54	4	2.44			18	51	68-71	60% 37	20% 35	—	55
S-5	55	1	3			16	54	72	60% 40	38	—	56
S-6	56	1	2			15	56	73	60% 42	40	—	57
S-7	57	4	2			17	58	74-77	60% 44	50% 42	—	58
S-8	58	1	2			16	60	78	60% 46	90% 44	—	59
S-9	59	1	6			11	66	79	60% 52	50	—	60
—	60	—	2			9	68	—	60% 54	52	10% 53	61

NOTES (BY ORBIT NUMBER)

43 Six frames of Estar leader and four frames of S0243 film are advanced through camera but not exposed. Ten frames of film leader are "processed" with eight frames of dry and two frames of wet Bimat.

54 Process 2.44 frames to shift processing stop line index. From this Orbit on, there will be 0.44 frames less in the storage looper and 0.44 frames more Bimat thru Processor than indicated in the tables.

Table 2-4 FILM BUDGET ACTUAL (Continued)

SITE NUMBER	ORBIT NUMBER	EVENT (FRAMES)			TOTAL FRAMES ACCUMULATED			EXPOSED	FRAME NUMBERS			ORBIT NUMBER OF READOUT
		TAKE	PROCESS	READOUT	READOUT	EXTRA IN STORAGE LOOPER	BIMAT THRU PROCESSOR		RESULTING READOUT SEQUENCES			
									TELE - PHOTO	WIDE ANGLE & TIME CODE	TELE - PHOTO	
S-10	61	4	6			7	74	80-83	60% 60	58	20% 59	62
S-11	62	1	2			6	76	84	60% 62	60	30% 61	63
S-13	63	1	3			4	79	85	60% 65	63	30% 64	64
P-7a	64	8	3			9	82	86-93	60% 68	66	40% 67	65
P-7b	65	8	2			15	84	94-101	60% 70	68	40% 69	66
S-14	66	1	2			14	86	102	60% 72	70	40% 71	67
S-15	67	4	3			15	89	103-106	60% 75	73	40% 74	68
—	68	—	5			10	94	—	50% 80	78	50% 79	69
S-16	69	1	3			8	97	107	50% 83	81	50% 82	70
S-17	70	4	4			8	101	108-111	50% 87	85	50% 86	71
S-18	71	4	2			10	103	112-115	50% 89	87	50% 88	72
S-19	72	4	5			9	108	116-119	50% 94	92	50% 93	73
—	73	—	2			7	110	—	50% 96	94	50% 95	74
S-21 S-21.5	74	1;1	2			7	112	120-121	50% 98	96	50% 97	75
S-22	75	1	2			6	114	122	50% 100	98	50% 99	76
S-20	76	1	2			5	116	123	50% 102	100	50% 101	77
P-8	77	8	2			11	118	124-131	50% 104	102	50% 103	78
S-23	78	4	7			8	125	132-135	50% 111	109	50% 110	79

Table 2-4 FILM BUDGET ACTUAL (Continued)

SITE NUMBER	ORBIT NUMBER	EVENT (FRAMES)			TOTAL FRAMES ACCUMULATED			EXPOSED	FRAME NUMBERS			ORBIT NUMBER OF READOUT
		TAKE	PROCESS	READOUT	READOUT	EXTRIN STORAGE LOOPER	BIMAT THRU PROCESSOR		RESULTING READOUT SEQUENCES			
									TELE - PHOTO	WIDE ANGLE & TIME CODE	TELE - PHOTO	
S-24	79	1	4			5	129	136	50% 115	113	50% 114	80
P-9a	80	8	4			9	133	137-144	50% 119	117	50% 118	81
P-9b	81	8	5			12	138	145-152	50% 124	122	50% 123	82
P-9c	82	8	2			18	140	153-160	50% 126	124	50% 125	83
S-25	83	1	5			14	145	161	50% 131	129	50% 130	84
S-26	84	1	6			9	151	162	50% 137	135	50% 136	85
—	85	—	2			7	153	—	50% 139	137	50% 138	86
P-10	86	8	6			9	159	163-170	50% 145	143	50% 144	87
S-27	87	1	3			7	162	171	50% 148	146	50% 147	88
S-28	88	1	4			4	166	172	50% 152	150	50% 151	89
P-11	89	8	3			9	169	173-180	50% 155	153	50% 154	90
P-12b.2	90	4	9			4	178	181-184	50% 164	162	50% 163	91
P-12a	91	16	4			16	182	185-200	50% 168	166	50% 167	92
P-12b.1	92	4	8			12	190	201-204	50% 176	174	50% 175	93
P-12c	93	8	5			15	195	205-212	50% 181	179	50% 180	94
S-29	94	1	2			14	197	213	50% 183	181	50% 182	95
—	95	—	5			9	202	—	50% 188	186	50% 187	96
S-30	96	1	4			6	206	214	50% 192	190	50% 191	97
S-30	96	1	3			7	205	214	50% 191	189	50% 190	97
S-31	97	1	2			6	207	215				
BIMAT CUT												

Table 2-5: MISSION LAUNCH PERIOD AND WINDOWS

LAUNCH DATE (GMT)	LAUNCH ASIMUTH RANGE	LAUNCH WINDOW (GMT)	LAUNCH WINDOW (hrs, Min)
February 2-3, 1967	(degrees)	Begin End	1 45
4	73.7- 82.8	23:31* - 01:16	1 47
5	76.5- 87.2	00:25 - 02:12	1 56
6	80.2- 94.1	01:11 - 03:07	2 10
7	84.5- 103.2	01:52 - 04:02	2 04
8	92.5-114.0	02:54 - 04:58	2 34
	90.0-114.0	02:33 - 05:07	

NOTES:

1. For the first 5 days in the period, launches at times earlier than those indicated (more northerly launch azimuths) may be possible if transit time is adjusted at midcourse to satisfy the arrival time constraint.
2. AFETR tracking and telemetry coverage commitments are not included. Consideration of this constraint may cause further reduction in the launch windows.

* P-9A Mission Window

On completion of Bimat cut, final readout was initiated. During this phase, in which the hangup preventive procedure was employed, only isolated incidents of the film advance anomaly were observed.

Final readout progressed normally until Orbit 149. Upon attempting initiation of readout at this time, an anomalous cessation of readout electronics operation was observed. Simultaneously, telemetry indicated the occurrence of nonstandard logic states within the photo subsystem, accompanied by abnormal power loading and thermal conditions. Corrective commands were transmitted as indicated by real-time analysis of available data, and readout was re-initiated. Readout capability was found operational, but it was subsequently found that film ad-

vance from the readout looper to the supply reel was not operable. Readout of additional film was therefore limited to the four-frame capacity of the readout looper. Numerous experiments were run attempting to regain the film advance capability, but the anomaly persisted. The primary mission was then terminated with readout of spacecraft film approximately 75% complete.

*2.1.2.2 Nominal Mission
Trajectory and Orbit Parameters*

For planning purposes, a nominal mission was designed based on a specific launch time within one of the six windows of the launch period of February 2 through 11, 1967. All launch windows within the period are summarized in Table 2-5. Significant trajectory

and orbit data parameters for the P-9A mission plan follow.

Launch

Launch Date and Time: Day 34 (Feb. 3), 1967; 00:22:09 GMT

Launch Azimuth: 78 degrees

Earth Parking Orbit Coast Time: 6 minutes, 45.0 seconds

Cislunar Trajectory

Injection Time: Day 34 (Feb. 3), 1967; 00:39:01 GMT

Injection Location: 25.11° N; 24.32° W

Transit Time: 91.954 hours

Lunar Arrival

Date and Time of Closest Approach: Day 37 (Feb. 6), 1967; 20:36:14 GMT

Inclination of Approach Hyperbola: 19.33 degrees

Perilune Altitude of Approach Hyperbola: 862 km

Lunar Orbit Injection

Injection Time: Day 37 (Feb. 6), 1967; 20:25:31

Lunar Location of Injection: 18.96° N; 43.26° E

Altitude of Injection Point: 1057 km

Plane Change: 13.04 degrees

ΔV : 811.0 meters per second

Initial Ellipse

Apolune Altitude: 1850 km

Perilune Altitude: 200 km

Inclination: 21.00 degrees

Period: 3 hours, 37 minutes, 13 seconds

Longitude of Ascending Node at Injection: 20.25° W

Argument of Perilune at Injection: 174.49 degrees

Longitude of Sun at Injection: 144.74° W

Orbit Transfer

Transfer Date and Time: Day 43 (Feb. 12), 1967; 16:32:43 GMT

Lunar Location of Transfer: 0.76° S; 101.41° W

Altitude of Transfer Point: 1838 km

ΔV : 26.10 meters per second

Final Ellipse

Apolune Altitude: 1838 km

Perilune Altitude: 59 km

Inclination: 21.00 degrees

Period: 3 hours, 28 minutes, 15 seconds

Longitude of Ascending Node at Transfer: 99.43° W

Argument of Perilune at Transfer: 177.93 degrees

Longitude of Sun at Transfer: 144.08° E

2.1.2.3 Photo Data Acquisition

All photos were scheduled subsequent to orbit transfer with the V/H sensor on. In the majority of cases the primary sites were scheduled to be photographed using the fast repetition rate, with multiple sequences of 4, 8, or 16 frames. Often a primary target consisted of sequences exposed on two or three consecutive orbits. For secondary sites either one or four frames were scheduled. With one exception, a three-axis spacecraft maneuver was required for each site. The location of primary and secondary sites ensured that at least one exposure would be made in any 8-hour period. This precludes the possibility of improper film advance distances which might otherwise result from the film assuming the shape of system rollers and thereby inhibiting the proper operation of friction drive mechanisms. The photographic plan also included an 11-frame film advance just prior to photography of the first site, to advance the leader-to-film splice from the supply reel to the takeup reel. Provisions were also made to minimize the time the film splice was under tension.

Processing was planned in accordance with previously established operating constraints. To avoid processing degradation resulting from Bimat dryout, at least two frames of processing were scheduled for every orbit

(catastrophic failure could result from failure to process at least two frames every 15 hours). Processing was limited to the period beginning 5 minutes after sunrise and ending 5 minutes before sunset. Since the length of processing periods dictated which exposures were available for priority readout, processing periods were scheduled to permit readout of high-priority photos.

Priority readout was planned for almost every orbit from initiation of photography through completion of processing. In addition to previously established readout constraints contingent on temperatures, signal strength, and power levels, new constraints were established on TWTA operation as a result of analysis of Mission II TWTA failure. Approximately 11 days were allocated for final readout of all spacecraft film subsequent to Bimat cut.

2.2 FLIGHT CONTROL

2.2.1 Mission Control

Mission control activities are those required to integrate such operational areas as SPAC, FPAC, DSS, and data systems into a functional unit to successfully meet flight plan objectives.

Mission control procedures and personnel for Mission III were in major respects similar to those of Mission II.

The on-line direction of mission operations was performed by the assistant space flight operations director (ASFOD). The position was staffed in a dual capacity (ACE-2, DEUCE-2) during all mission operation periods (except for the final readout phase, when only the ACE-2 position was manned). The major problem area encountered was the difficulty in maintaining close liaison with such areas as SPAC at critical periods. This condition will be alleviated prior to Mission IV by procedural changes.

The command coordinator position was occupied by experienced personnel and no significant difficulties were encountered.

Mission event coordinator activities were performed similarly to Mission II in an efficient, trouble-free manner. Close adherence to the flight plan precluded extensive revisions to the sequence of events document (SEAL). A total of 21 issues was made throughout the mission. The DSS sequence of events underwent minor changes prior to Mission III to improve the teletype scripts and reduce transmission time. No problems were encountered.

2.2.2 Spacecraft Control

The following paragraphs describe the command programming and photography controls that were established to meet the requirements of the flight plan (reference Section 2.1). Procedural changes subsequent to Mission II were minimal due to the similarity of Mission III to earlier flights, and consisted primarily of improvements and refinements to proven methods as a result of flight experience. The organizational structure remained unchanged. This section discusses personnel activities involved in the implementation of these controls, and includes recommendations for increased effectiveness in future missions.

2.2.2.1 Command Programming

Summary—As of 15:30 GMT on March 2, a total of 3615 commands had been prepared, transmitted to Lunar Orbiter III, and properly executed by the flight programmer. Procedures used in command preparation were the same as those followed in Mission II. In general, command activity proceeded smoothly and on schedule. However, an improper sequence of commands did result in loss of the time code on Site IIIP-1 photos.

Pre-mission Activity—A core map plan defining the contents of each core map and the loading schedule during photography was prepared for overall coordination of command activity.

Countdown and Mode 2 commands for Mission III had been prepared and sent to the appropriate stations during the final readout phase of Mission II. Launch plan commands were sent to DSS-71 during Mission III training.

Mission Activity—Command preparation was conducted in essentially the same way as during Mission II, with two command programmers per team. A conference room for their uninterrupted use resulted in better coordination of efforts and greater flexibility in dividing tasks among the programmers.

An improper sequence of commands resulted in loss of time code data on Site IIP-1 photos. The sequence for Sites IIP-1 and IIS-1 photography was revised by SPAC directive to replace the stored-program command with a real-time command to change the shutter speed between those sites. There was an interval of 3 minutes, 38.8 seconds between the camera-on times of IIP-1 and IIS-1. Allowing about 45 seconds for IIP-1 photography and 52 seconds of V/H sensor operation prior to IIS-1, there remained about 2 minutes in which to execute the real-time shutter speed change. To provide the 2-minute transmission window, two "wait time" commands immediately after the first "camera-on" command were replaced by a "compare time" command. This decision was made without recognition that a "wait time" was necessary to obtain the time code. With the targets so close together it was, in fact, not feasible to implement a real-time shutter speed change.

Some operational problems were encountered during Mission III:

- Too many methods of command direction;
- Sending commands to the DSS only after the final command conference;
- Delaying the start of final command conferences until FPAC was ready to present a command update;
- Scheduling of real-time command activity during flight programmer loading transmission windows.

The first problem caused a moderate amount of confusion in command preparation. There were too many kinds of directives (mission directives, operations directives, and SPAC directives) and they were too frequently allowed to substitute for a command preparation directive. Some of these directives were received too late to permit adequate study of the impact of the directive or of the command preparation requirements. The loss of the IIP-1 time code discussed above was a consequence of this tardiness.

The latter three problems unnecessarily jeopardized the transmission of commands in a timely manner. As soon as the command programmer has informed the SPAC director that he is ready to support the final command conference, the assistant SFOD should authorize sending the commands to the DSS. This avoids a delay in initiating command transmission to the spacecraft after the commands are approved and also obviates the possibility of a computer failure preventing the commands from getting to the DSS.

During the L.O. III mission, the final command conference was delayed several times because FPAC had announced that a com-

mand update was forthcoming. As a result, the command transmission windows were frequently cut into. The conference should always start no later than the scheduled time so that command transmission is not held up. Real-time command activity for attitude reference updating was scheduled during command transmission windows. In two instances, the start of transmission of a map was delayed until completion of the attitude updating. Once, this resulted in the transmission window closing before the complete map had been transmitted. As a result, the command sequence had to be reprogrammed, the command generation program rerun, and a new transmission window scheduled. Real-time command activity at such times should be avoided. In future missions, attitude updating will be scheduled in the mission sequence of events whenever possible.

Photo Control—For data on photographic control during Mission III refer to Volume II of this document.

2.2.3 Flight Path Control

From launch through completion of photographic readout, maintaining control of the spacecraft trajectory (or flight path) is the responsibility of Flight Path Analysis and Command (FPAC). Responsibility for control of the mission from pre-launch checkout through about launch plus 6 hours belongs to the DSN FPAC. After the spacecraft has been acquired and is supplying good tracking data to the SFOF (about launch plus 6 hours), the DSN FPAC team is relieved by the project FPAC team. At this point the project FPAC team assumes the responsibility for flight path control for the remainder of the mission. Within both teams the tracking data analysis function is carried out by JPL analyst. A description of the two FPAC teams is contained in the Mission I final report, Boeing Document D2-100727-1.

Flight path control by the FPAC team entails execution of the following functions.

- 1) Tracking Data Analysis—(1) Monitoring and passing judgment on the quality of the incoming radar tracking data (doppler and range). This raw tracking data is the sole link between the spacecraft and FPAC, and is the basis for determination of the current position and velocity of the vehicle. (2) The preparation of tracking predicts to support the DSS in spacecraft tracking.
- 2) Orbit Determination—A process of finding a trajectory that best “fits” the tracking data. This includes the tasks of editing the raw tracking data into a form acceptable to the orbit determination computer program (ODP), and subsequent operation of this program to obtain that trajectory best fitting the data—usually a lengthy task that consumes large blocks of computer time.
- 3) Flight Path Control—When the orbit determination process yields a trajectory, the flight path control function is initiated to determine the need for a corrective maneuver or the design of a planned maneuver. Thus, this function is principally one of guidance, control, and prediction.

FPAC executes these functions to design maneuvers that will best achieve the objectives of the nominal flight plan that is furnished to FPAC by the mission design group and provides the criteria, ground rules, and constraints that must be observed in any maneuver design. The computer programs, or FPAC software system, used for maneuver designs is identical to that used during Mission I, with the exception of some internal modifications to individual programs. A description of the FPAC software system is contained in the Mission I final report, Boeing Document D2-100727-1.

From a trajectory point of view, the mission can be subdivided into the following phases.

- 1) Countdown, Launch, and Acquisition Phase—Covers the period from FPAC entry into the countdown through DSN acquisition of the spacecraft and subsequent handover from DSN FPAC team to Project FPAC team.
- 2) Injection through Midcourse—From completion of the second Agena burn through completion of the midcourse maneuver. This phase overlaps the acquisition portion of the previous phase.

- 3) Midcourse through Deboost—From end of midcourse burn through completion of the deboost maneuver.
- 4) Initial Ellipse—From end of deboost burn through the transfer maneuver.
- 5) Photo Ellipse—From end of transfer burn through completion of photo readout.

Table 2-6 lists the principal FPAC events and their times of occurrence (GMT) within these phases. The orbit determination and flight path control functions executed in these phases will be discussed in the following subsections.

Table 2-6: TRAJECTORY SEQUENCE OF EVENTS

<u>Launch and Acquisition</u>		at Feb. 6, 15:00	
Feb. 4, 14:00	FPAC begins prelaunch checkout of software system.	Feb. 6, 15:00	Start midcourse burn.
Feb. 5, 01:17	Launch	<u>Midcourse through Deboost</u>	
Feb. 5, 01:25	Agena first burn complete. Start 578-sec coast.	Feb. 7, 04:20	Determined second midcourse not required.
Feb. 5, 01:36	Agena second burn complete. Cislunar injection.	Feb. 8, 07:30	Completed design of deboost maneuver.
Feb. 5, 02:35	First DSS-41 two-way doppler data.	Feb. 8, 21:54	Start injection burn.
Feb. 5, 04:35	DSN FPAC hands over control to Project FPAC.	<u>Initial Ellipse</u>	
<u>Injection through Midcourse</u>		Feb. 8, 23:15	Obtained first post-deboost orbit determination (OD No. 4102).
Feb. 5, 06:15	Calculated 3.8 m/sec midcourse for execution at cislunar injection plus 20 hours, 5.4 m/sec at plus 40 hours.	Feb. 12, 16:00	Completed design of transfer maneuver.
Feb. 5, 10:30	Selected midcourse maneuver time of Feb. 6, 15:00	Feb. 12, 18:13	Start transfer burn.
Feb. 6, 05:45	Calculated 5.11 m/sec midcourse for execution	<u>Photo Ellipse</u>	
		Feb. 12, 22:00	Obtained first posttransfer orbit determination (OD No. 5302).
		Feb. 15, 10:01	Start of photography.
		Feb. 23, 02:11	End of photography.
		Mar. 3, 07:17	Termination of readout.

NOTE: All times are in GMT.

2.2.3.1 Countdown, Launch, and Acquisition

Project FPAC entered the countdown procedure at launch minus 5 (T-5) hours on February 4, 1967. Check cases of the project FPAC user programs were run on both computer strings. These were completed at T-4 hours on the project (Y) and DSN (X) strings. No problems were encountered on either string.

Frequency reports from ETR (DSS-71) were received on schedule and frequency parameters were supplied to the real-time computer system (RTCS) for DSIF predicts. All liftoff predicts programs (PRDL) cases were run as required.

Launch occurred on Feb. 5 at 01:17:01:12 GMT at a launch azimuth of 80.8 degrees. Table 2-7 lists the major powered-flight

events ("Mark events") from liftoff through completion of Agena retro.

The early orbit determination results obtained by project FPAC, DSN FPAC, and the RTCS of AFETR, all projected to lunar encounter, are shown in Figure 2-1.

Three hours after liftoff, spacecraft acquisition was verified. FPAC control was then handed over to the project by the DSN.

DSIF stations used for tracking during Mission III were:

STATION IDENTIFICATION	
Goldstone (ECHO)	DSS-12
Woomera	DSS-41
Johannesburg	DSS-51
Madrid	DSS-62

Table 2-7: POWERED-FLIGHT TRAJECTORY EVENTS

<u>Mark</u>	<u>Event</u>	<u>Actual Time (GMT)</u>
0	Liftoff	Feb. 5, 01:17:01.12
1	Atlas Booster Engine Cutoff (BECO)	01:19:10.83
2	Atlas Booster Engine Jettison	01:19:13.70
3	Start Agena Secondary Timer	01:21:31.68
4	Atlas Sustainer Engine Cutoff (SECO)	01:21:49.80
5	Start Agena Primary Timer	01:21:58.48
6	Atlas Vernier Engine Cutoff (VECO)	01:22:10.48
7	Shroud Separation	01:22:12.58
8	Atlas-Agena Separation	01:22:14.68
9	Agena First Ignition	01:23:12.76
10	Agena Shutdown (Parking Orbit Injection)	01:25:48.55
11	Agena Second Ignition	01:35:26.80
12	Agena Second Shutdown (Cislunar Injection)	01:36:55.50
13	Agena-Spacecraft Separation	01:39:39.67
14	Begin Agena Yaw	01:39:42.6
15	End Agena Yaw	01:40:42.6
16	Agena Retro Rocket Fire	01:55:39.7

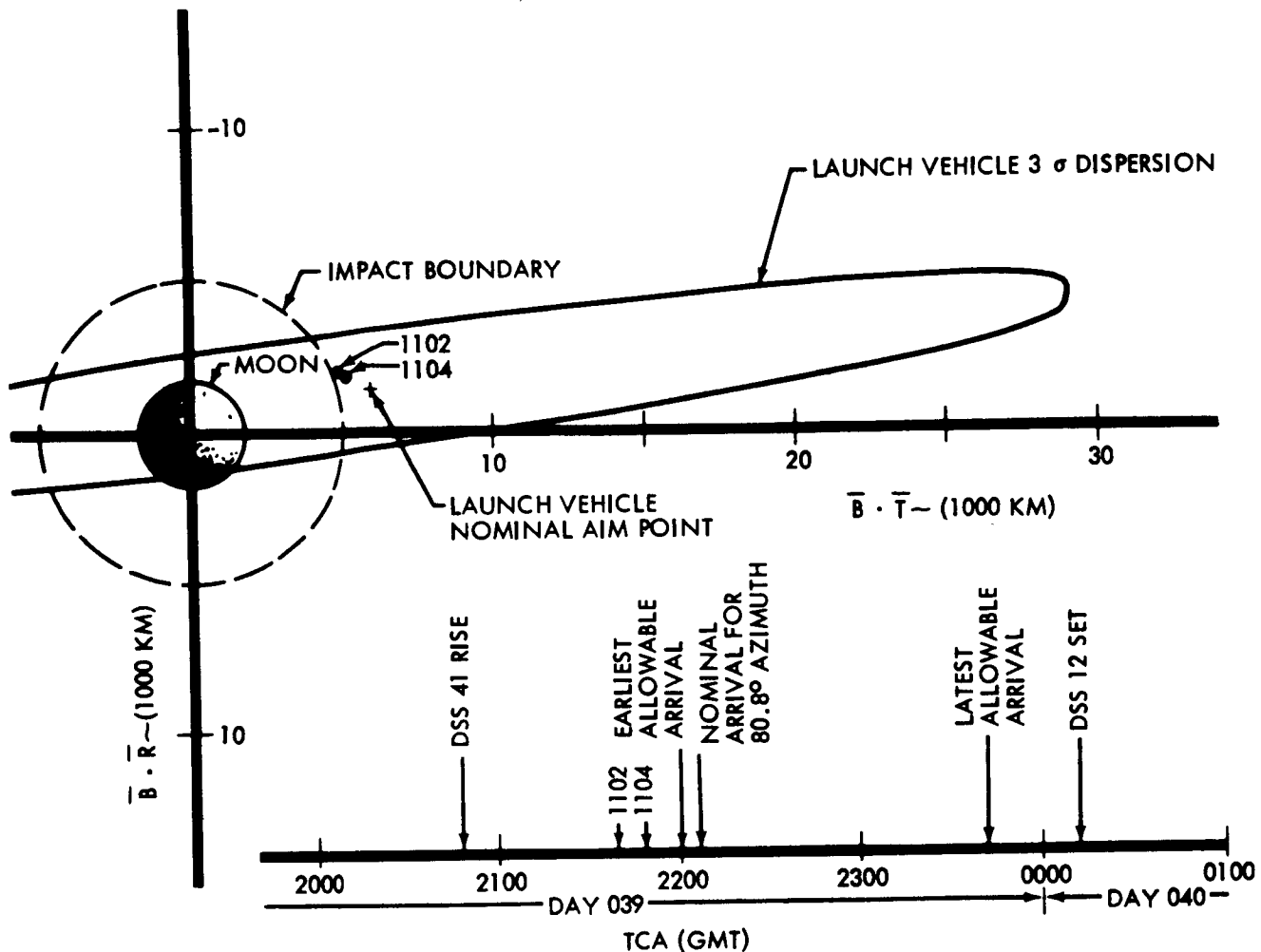


Figure 2-1: Early Orbit Determination Results

2.2.3.2 Injection through Midcourse

Events during the injection through midcourse phase of the mission followed the premission plan. No anomalies were encountered.

Orbit Determination—Table 2-8 shows the chronological sequence of the lunar encounter parameters obtained from the six project orbit determinations performed before midcourse. Final design of the midcourse maneuver used OD 1216, which was based on 24.5 hours of two-way lock doppler data from DSS -12, -41, -51, and -62. The fit of the doppler

data to the orbit solution was excellent. Range unit data was available during this data span but was used only as a check and was not included in the data fit. Range unit residuals were on the order of 200 meters. (Appendix B, Volume VI of this document contains the inflight orbit determination results.)

Midcourse Design and Execution—Within 2 hours after cislunar injection, projected lunar encounter parameters (see Figure 2-1) indicated that the second Agena burn had resulted in a trajectory well within the mid-

**Table 2-8: PRE-MIDCOURSE ORBIT DETERMINATION
ENCOUNTER PARAMETER SUMMARY**

<u>Orbit Solution</u>	<u>B.T (km)</u>	<u>B.R (km)</u>	<u>Time of Closest Approach (GMT)</u>
1102*	4864.7	-1937.3	Feb. 8, 21:39:01
1104**	5108.4	-1885.3	21:47:52
XX06	This number was skipped		
1208	5068.	-1813.0	21:46:40
1210	5074.	-1809.0	21:46:49.6
1312	5048.3	-1768.5	21:47:03.8
1114	5075.2	-1813.1	21:46:53
1115	5075.4	-1795.2	21:46:54.2
1216	5076.8	-1801.0	21:46:53.9
1218	5076.5	-1803.8	21:46:54.3
Nominal Aimpoint	5590.	-2460.0	22:06:00

* This very early solution was based on only 20 minutes of DSS-51 tracking.

** This early solution was based on 1.67 hours of DSIF tracking; subsequent solutions used longer tracking arcs.

course capability of the spacecraft. It also became apparent that although a midcourse maneuver would be required, midcourse execution time would not be critical and an early midcourse would not be necessary.

The criteria used in designing the midcourse maneuver were:

- 1) Delay the maneuver as long as practicable to minimize the effect of midcourse execution errors on lunar encounter conditions;
- 2) Perform the first midcourse maneuver at least 50 hours before orbit injection to allow time for a second midcourse;

- 3) Minimize the ΔV required for lunar ellipse injection (deboost), transfer, and midcourse with a maneuver at the selected midcourse time.

OD 1208, based on 2.5 hours of tracking data, became available within 5 hours after cis-lunar injection. This OD solution was used for a study of midcourse execution time, correcting both the time of flight to the nominal encounter time (February 8, 22:06:00GMT), and the miss parameter ($\bar{B.T}$ and $\bar{B.R}$) to those computed in the midcourse targeting program. Figure 2-2 shows the results of this study. The midcourse maneuver could easily

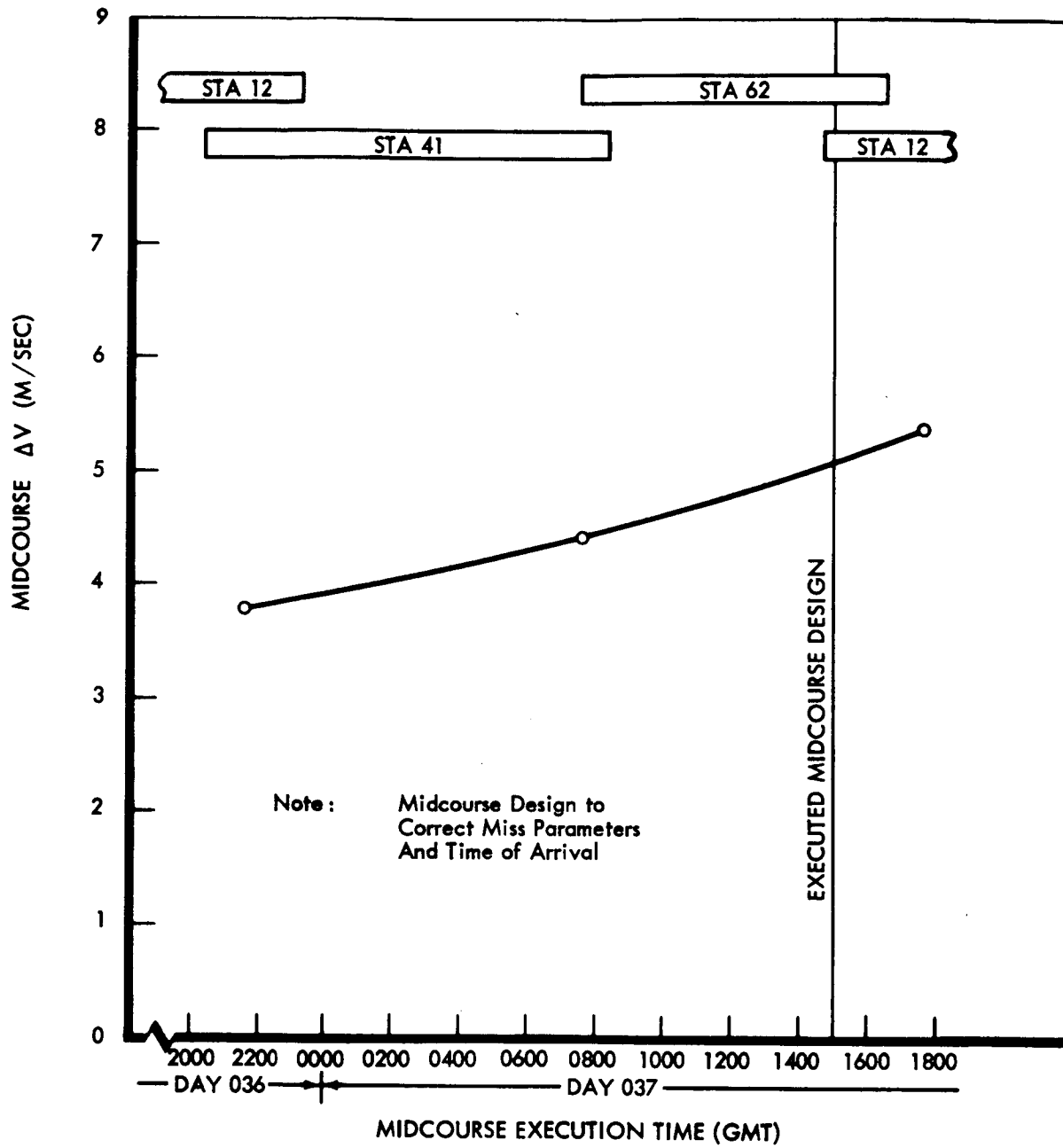


Figure 2-2: Effect of Midcourse Time on ΔV Required

be delayed until 40 hours after cislunar injection without requiring excessive ΔV for the maneuver.

Optimization of deboost, transfer, and midcourse ΔV is done automatically by the FPAC software programs for a given midcourse

execution time and specified lunar encounter time. By varying the arrival time for a selected midcourse execution time, it is possible to minimize the total ΔV for midcourse, deboost, and transfer. The results of this analysis are shown in Figure 2-3 for a midcourse

Note: Based on a Midcourse Maneuver at Day 037 1500 GMT 1967

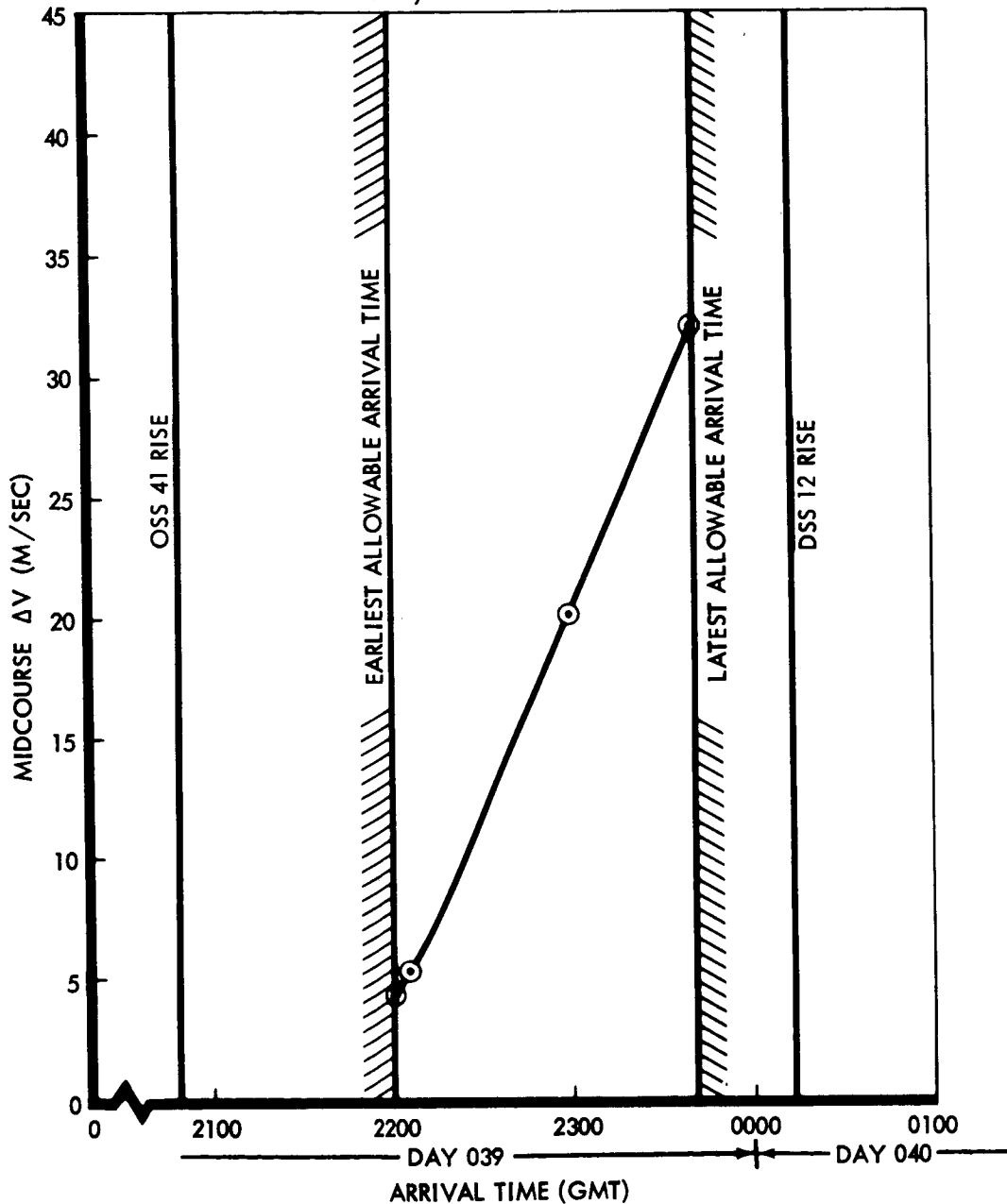


Figure 2-3: Effect of Time of Arrival on Midcourse ΔV Requirement

executed at approximately 37.5 hours after cislunar injection. The minimum ΔV in this case is obtained by correcting the arrival time to the earliest allowable time. On the basis of the data contained in Figures 2-2 and 2-3, it was decided to correct the time of arrival to the nominal arrival time with a first midcourse maneuver executed approximately 37.5 hours after cislunar injection. The execution time, February 6, 15:00 GMT, was chosen on the basis of desirable two-station viewing during and after the burn. DSS-12 viewing began 18 minutes before engine ignition to overlap with DSS-62.

A backup first midcourse maneuver for February 6, 21:00 GMT, was also designed but was not needed.

The midcourse maneuver specified by FPAC was:

sunline roll = 39.94 degrees
pitch = 123.39 degrees
 ΔV = 5.11 m/sec.
ignition time = February 6, 15:00:00 GMT

This attitude maneuver was selected from 12 possible two-axis maneuvers on the basis of (1) maintaining Sun lock as long as possible, (2) viewing DSS line-of-sight vector not passing through any antenna null regions, and (3) minimizing total angular rotation. OD 1216 was used for the midcourse final design.

Midcourse targeting resulted in the following set of encounter parameters. The preflight nominal and pre-midcourse values are also given. These data are presented graphically in Figure 2-4.

Figure 2-5 shows Earth-Moon-spacecraft geometry at the time of the midcourse maneuver, and direction of the desired velocity change. Engine ignition occurred at February 6, 15:00:00 GMT and the engine burned for 4.3 seconds, resulting in a doppler shift of 55 cps. The doppler data observed during the burn indicated a nominal burn as shown in Figure 2-6.

ENCOUNTER PARAMETERS			
	Nominal (Preflight Design)	Pre-Midcourse (Actual)	Post-Midcourse (Maneuver Design)
$\overline{B.T}$ (Km)	5590.	5077.	5604.6
$\overline{B.R}$ (Km)	-2460.	-1801.	-2465.2
TCA (GMT)	Feb. 8, 22:06:00	Feb. 8, 21:46:53.9	Feb. 8, 22:06:00
V (km/sec)	0.8204	0.8227	0.8188

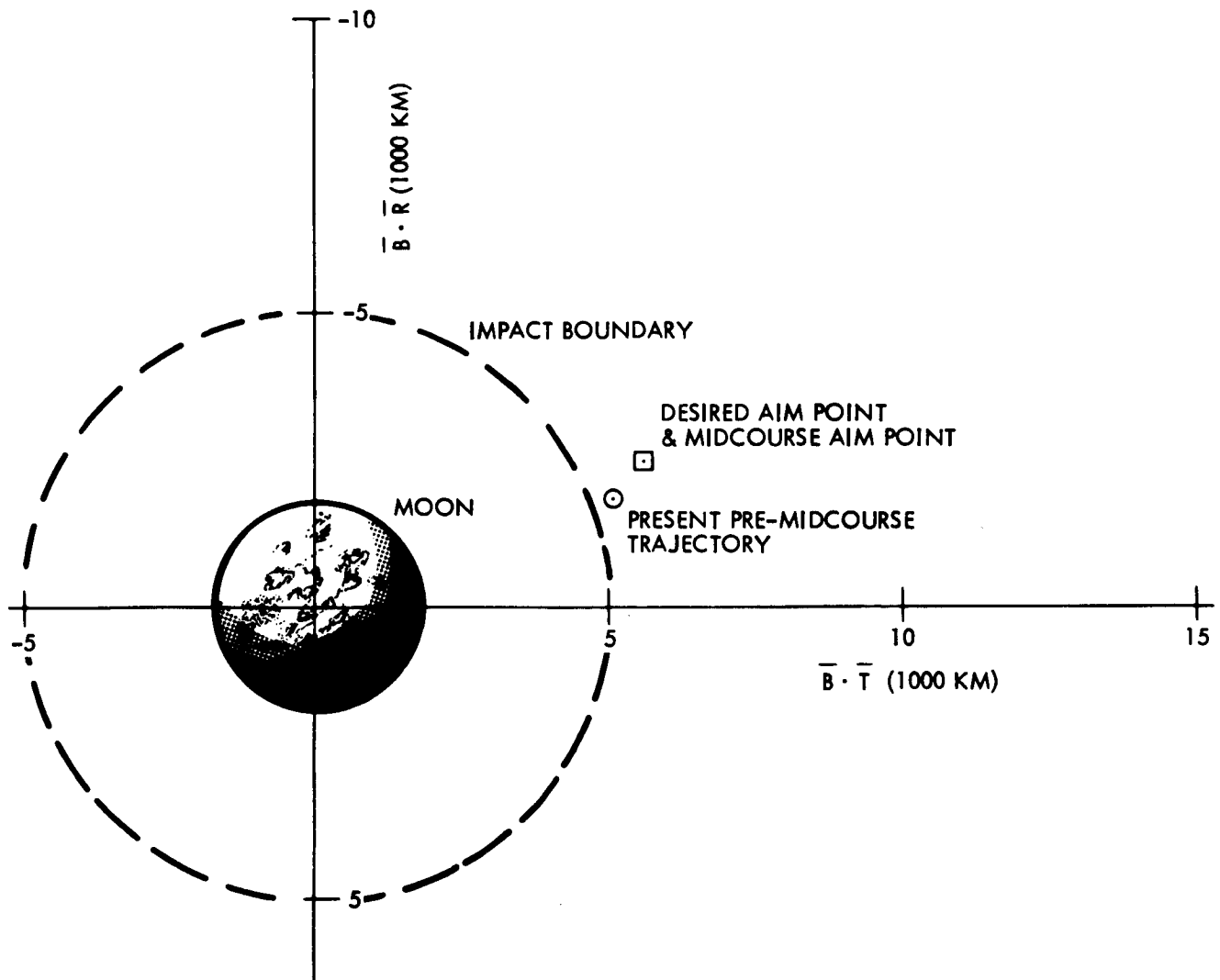
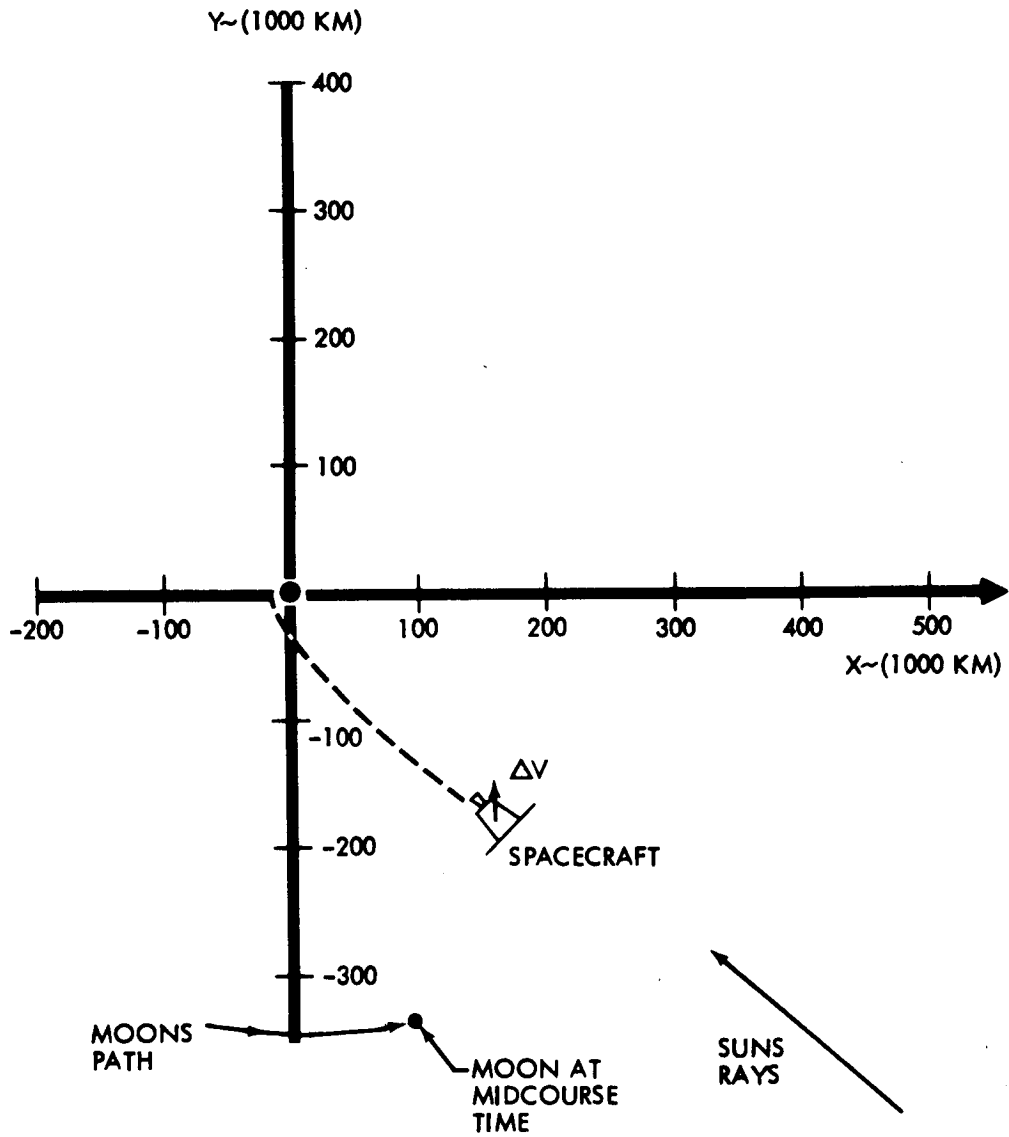


Figure 2-4: Pre-Midcourse Encounter Parameter Summary

2.2.3.3 Midcourse through Deboost

Orbit Determination—The first orbit determination after the midcourse maneuver (OD 2102) was not started until 8 hours after midcourse correction because the trajectory curvature was so small in this region that meaningful determinations of spacecraft position are difficult to obtain earlier. This determination (OD 2102) predicted encounter perilune altitude and closest approach time

within 7.6 km and 1.1 sec of the best estimates. (Best-estimate trajectory was subsequently achieved using 10.5 hours of two-way doppler data prior to the deboost maneuver, OD 2125). Table 2-8 shows the early orbit determination prediction, the best estimate of the actual encounter conditions, the midcourse-designed encounter conditions, and the estimate used for the final deboost maneuver calculation.



PROJECTION IN EARTH EQUATOR
 MIDCOURSE TIME: FEB. 6, 15:00:00 (GMT)

Figure 2-5: Midcourse Geometry

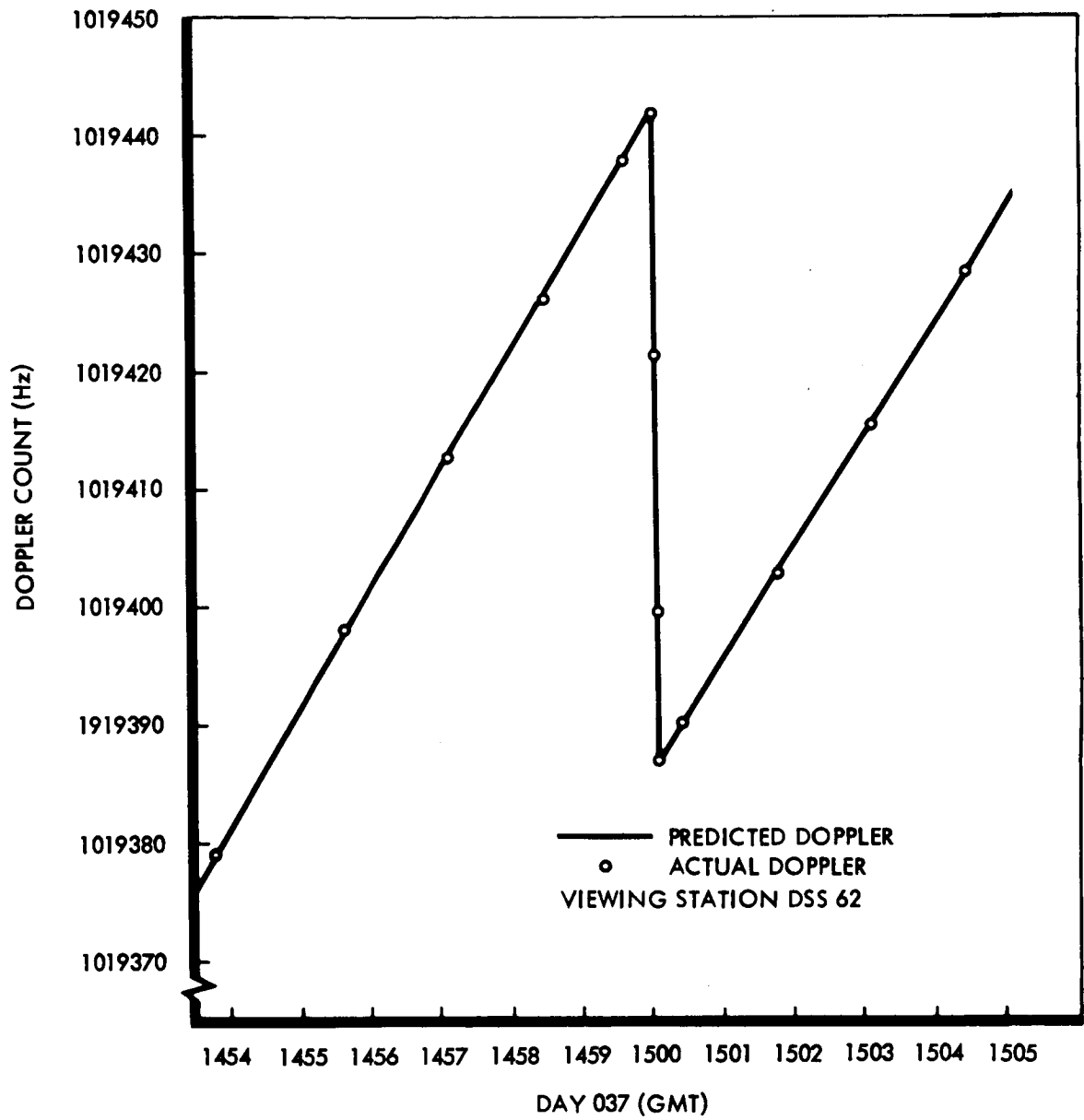


Figure 2-6: Midcourse Doppler Shift

ENCOUNTER CONDITIONS

Elements	Midcourse Designed	1st OD (OD 2102)	Final Deboost Calculation (OD 2212)	Best Estimate (OD 2125)
Perilune Altitude (km)	2224.7	2237.1	2237.3	2229.5
Time of Closest Approach 39:22:06 GMT	00.0	05.7	22.2	04.6
$\bar{B} \cdot \bar{T}$ (km)	5604.6	5620.3	5618.9	5607.1
$\bar{B} \cdot \bar{R}$ (km)	2465.2	-2477.2	-2482.4	-2478.7
\bar{B} (km)	6122.8	6142.0	6149.2	6130.5

The above table shows that the orbit determination used for the deboost maneuver calculation (OD 2212) predicted perilune altitude 7.8 km too large and time of closest approach 17.6 seconds too late. These errors are on the order of 10σ compared to expect uncertainties. Examination of the other real-time orbit determinations indicates that this orbit determination is competitive with regard to perilune altitude error but the time of closest-approach error was significantly larger than for the other determinations.

OD 2212 was chosen over the other determinations available at the time for the following reasons:

- 1) The determination fit the 37 hours of two-way doppler data after midcourse very well.
- 2) This determination predicted a value of $\bar{B} \cdot \bar{T}$ that was consistent with the previous determinations.

There were two factors that introduced some uncertainty into the choice of this determination:

- 1) The range unit residuals were on the order of 4 km.

- 2) The time of closest approach changed from the neighborhood of 22:06:06 to 22:06:22.6.

The range residuals mentioned above deserve some discussion. A serious effort was made during this mission phase to use the range unit data generated by DSN, including it as a data type in the orbit determination fits on a weighted equivalent basis with the two-way doppler data. In the early determinations (up to midcourse +24 hours), this technique was fairly successful. A very good fit on the ranging data could be obtained and an acceptable fit on the doppler data was obtained. However, as more data was added, particularly with the amount of data included in the OD 2212 determination (37 hours), the fit of the doppler and ranging data deteriorated markedly. It was decided at that point not to use the range data in the fit but to rely exclusively on the two-way doppler. This was the philosophy followed in OD 2212. Operational procedures have been modified to preclude this problem in the future.

Several hours before the deboost maneuver, a set of engine-burn doppler predicts was

computed. This computation used the deboost maneuver orbit determination and the predicted nominal orbit conditions after the engine burn. These predicted doppler data were plotted in the region of the burn. The actual doppler shift data were plotted on the same curve during the maneuver from the incoming raw TTY data, Figure 2-7.

Deboost Design and Execution—The deboost maneuver was executed February 8 at 21:54:19 GMT and concluded the cislunar cruise portion of Mission III by injecting the spacecraft into the initial lunar ellipse.

OD 2212, based on 37 hours of tracking data, was used for the design of the deboost maneuver. The design philosophy was to guide the spacecraft from its approach hyperbola into an ellipse such that the ellipse inclination and apolune altitude resulted in the preflight nominal values. Attention was also given to holding the remaining ellipse parameters—ascending node longitude (Ω), argument of perilune (ω), and perilune altitude (h_p)—as close to nominal as possible. The Boeing C-2 lunar harmonics were used during the deboost maneuver design.

The elements of the designed initial ellipse

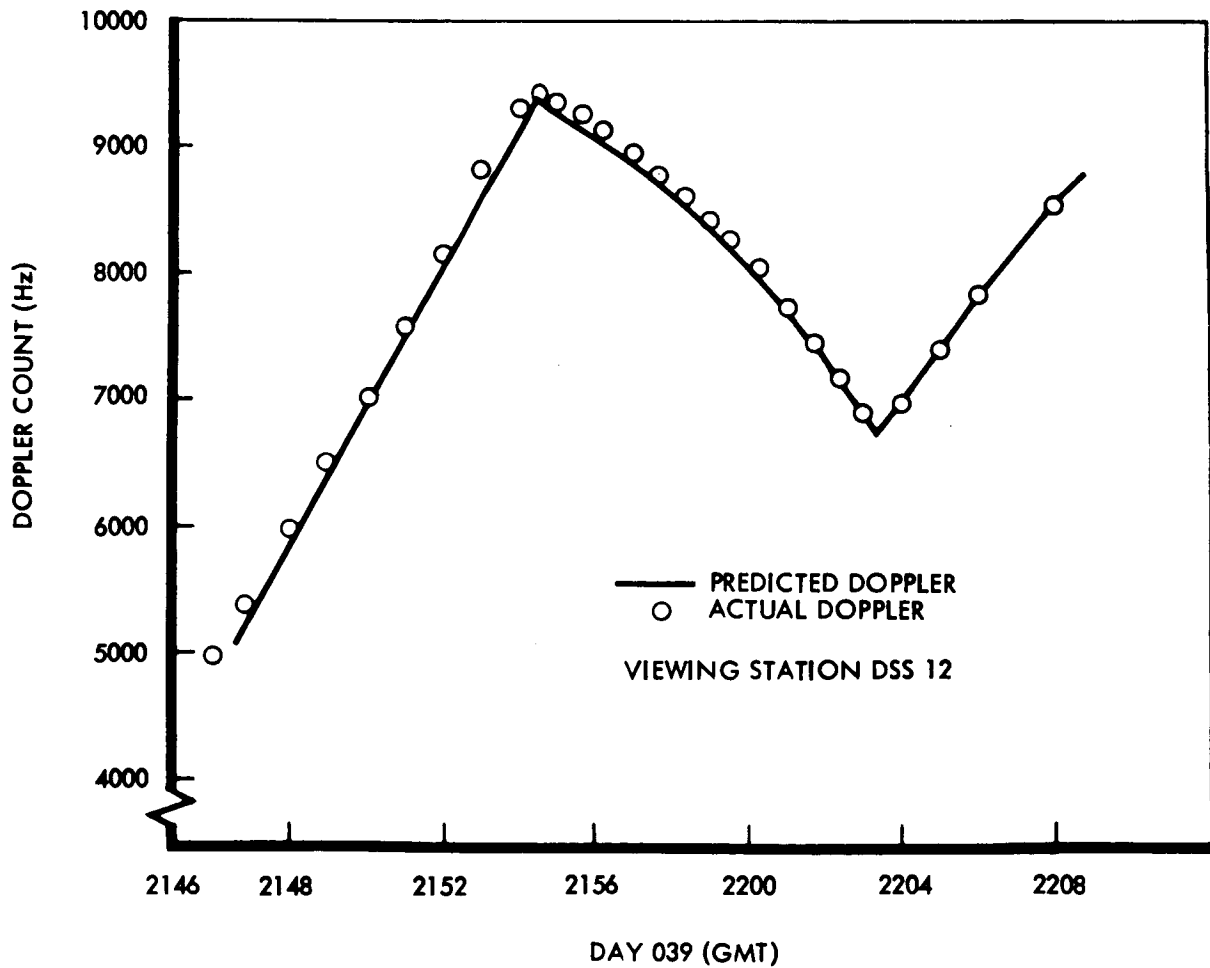


Figure 2-7: Deboost Doppler Shift

and the preflight nominal values are given below:

<u>Element</u>	<u>Design</u>	<u>Nominal</u>
h_a (km)	1849.97	1850.00
h_p (km)	213.38	200.00
i (deg)	21.05	21.00
ω (deg)	176.22	176.22
Ω (deg)	311.70	311.16
Time 2/8/67	22:03:19.6	22:39:7.2

The engine ignition was designed to occur at Feb. 8, 21:54:19 GMT. The required maneuver was:

roll	30.88 degrees
pitch	-125.88 degrees
Δv	704.3 m/sec

The attitude maneuver was selected from the 12 possible two-axis maneuvers on the basis of (1) maintaining Sun lock as long as possible, (2) DSS vector not passing through any antenna null regions, and (3) minimum total rotation angle.

A series of fly-by maneuvers was also designed to be used in the event of engine failure at deboost. These maneuvers consisted of an initial three-axis attitude maneuver to point the camera axis along the local vertical at a time when the Moon fills the wide-angle camera frame, about 70 minutes after the intended deboost. Then five consecutive pitch maneuvers followed with the exposure of seven frames, the last of which was to occur when the Moon filled the narrow dimension of the telephoto frame, at about 9 to 10 hours. Finally, a three-axis maneuver would be performed to expose a photo of the Earth and the Moon at 9 to 10 hours after the intended deboost. At least 45 minutes was allowed between the time to start deboost and the time

at which the fly-by sequence would have had to be initiated. This would have allowed a maximum length of time to attempt to ignite the engine, had a problem been encountered.

The deboost attitude maneuver was completed 10 minutes before engine ignition. The actual engine burn occurred at Feb. 8, 21:54:19.0 GMT and the burn lasted for 542.5 seconds, producing a doppler shift of 2725 cps. See Figure 2-7 for a plot of the doppler data during the deboost maneuver.

The geometry at maneuver time is shown in Figure 2-8. At Feb. 8, 20:51 GMT, Station 41 rose to begin the two-station view period with Station 12. Engine ignition occurred 63 minutes later. View of the spacecraft from DSS-12 and -41 was occulted by the Moon 21 minutes after thrust termination.

Inspection of the early initial-ellipse orbit determinations indicated that the orbital elements resulting after the burn were not exactly those predicted in the deboost design. The differences were greater than had been witnessed in Missions I and II.

2.2.3.4 Initial Ellipse

Orbit Determination—Immediately following doppler shift monitoring during the deboost maneuver, incoming tracking data was logged and edited in preparation for a quick determination of first-orbit elements. The objective was to ensure that the stations would promptly reacquire the spacecraft when it emerged from behind the Moon. It was necessary to determine the new orbit, calculate a set of DSS doppler predicts based on this determination, and send these predicts to the station before first emergence of the spacecraft. The first orbit determination (4102) was accomplished at deboost + 40 minutes using about 20 minutes of two-station view. This determination, coupled with the

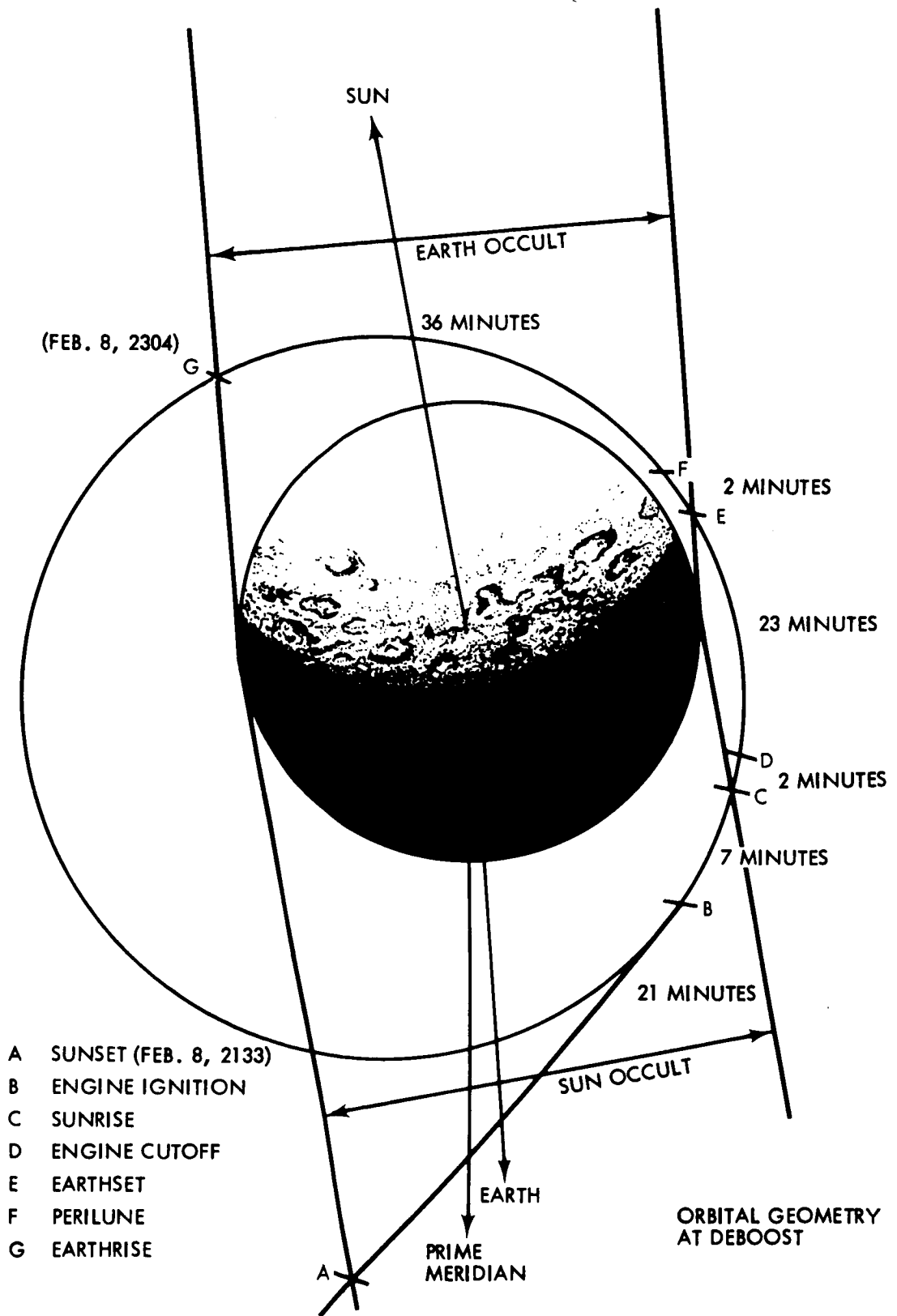


Figure 2-8: Orbital Geometry at Deboost

near-nominal deboost doppler shift, gave an indication that the deboost was near nominal. Station predicts based on this determination were computed by the DSN but were not sent to the stations because they agreed within 100 of the nominal predicts. A comparison of the designed post-deboost orbital elements, the best estimate of these elements (OD 4312), and the first orbit determination results (OD 4102) is shown in the following table.

Orbital Elements	Deboost Design	First OD Results (OD 4102)	Best Estimate (OD 4312)
Perilune Altitude	213.38	210.76	210.26
Apolune Altitude	1849.97	1803.93	1802.1
Inclination	21.05	20.99	20.94
Longitude of Asc. Node	311.70	311.07	310.33
Argument of Perilune	176.22	176.99	177.3

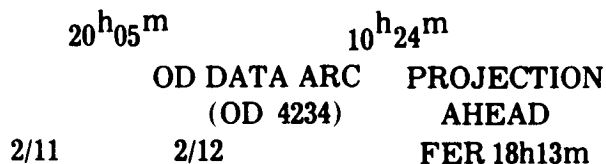
No difficulties were encountered in the initial orbit determination.

Orbit determination activities during the 4 days from deboost to transfer consisted of routine updating of the spacecraft state vector and support of the orbit transfer maneuver design. A complete set of lunar gravitational harmonics was not evaluated in Mission III as it was during this phase in Mission I. The procedure that was followed used the LRC 9/4/66 lunar harmonics as a basic harmonic set and "tailored" these harmonics to the particular lunar gravitational field being experienced by solving for the eight higher order tesseral harmonics C32, C33, C43, C44, S32, S33, S43, and S44. This procedure gave a good fit on the data and produced consistent values of orbital elements. Plots of the orbital elements determined during this phase are shown in Figure 2-9. The orbit

determination reports detailing the solutions are presented in Appendix B, Volume VI of this document.

Ranging unit data were not used in the fitting process at any time during this mission phase but the range unit residuals were consistently displayed as an indicator of orbit determination quality. The maximum value of these residuals was approximately 200 meters, which was within the accuracy of the lunar ephemeris used.

The orbit determination used for the transfer calculation (OD 4234) used 14.3 hours of two-way lock doppler tracking data from DSS-12, -41, and -62. The placement of the data relative to the transfer time is shown in the following figure.



This determination put the transfer calculations on a firm footing because the projection to transfer was shorter than the data arc used. This situation provides a good orbit determination basis for performing a maneuver calculation. Further details of this determination are given in Appendix B.

Several hours before the transfer maneuver, a set of engine-burn doppler predicts was computed. This computation used the latest orbit determination results and the predicted nominal orbit conditions after the engine burn. These predicted doppler data were then plotted in the region of the burn. The actual doppler shift data were plotted on the same curve during the maneuver from the incoming raw TTY data. The resulting curve (Figure 2-10) showed that the expected doppler shift was obtained, giving a quick indication that the maneuver was nominal.

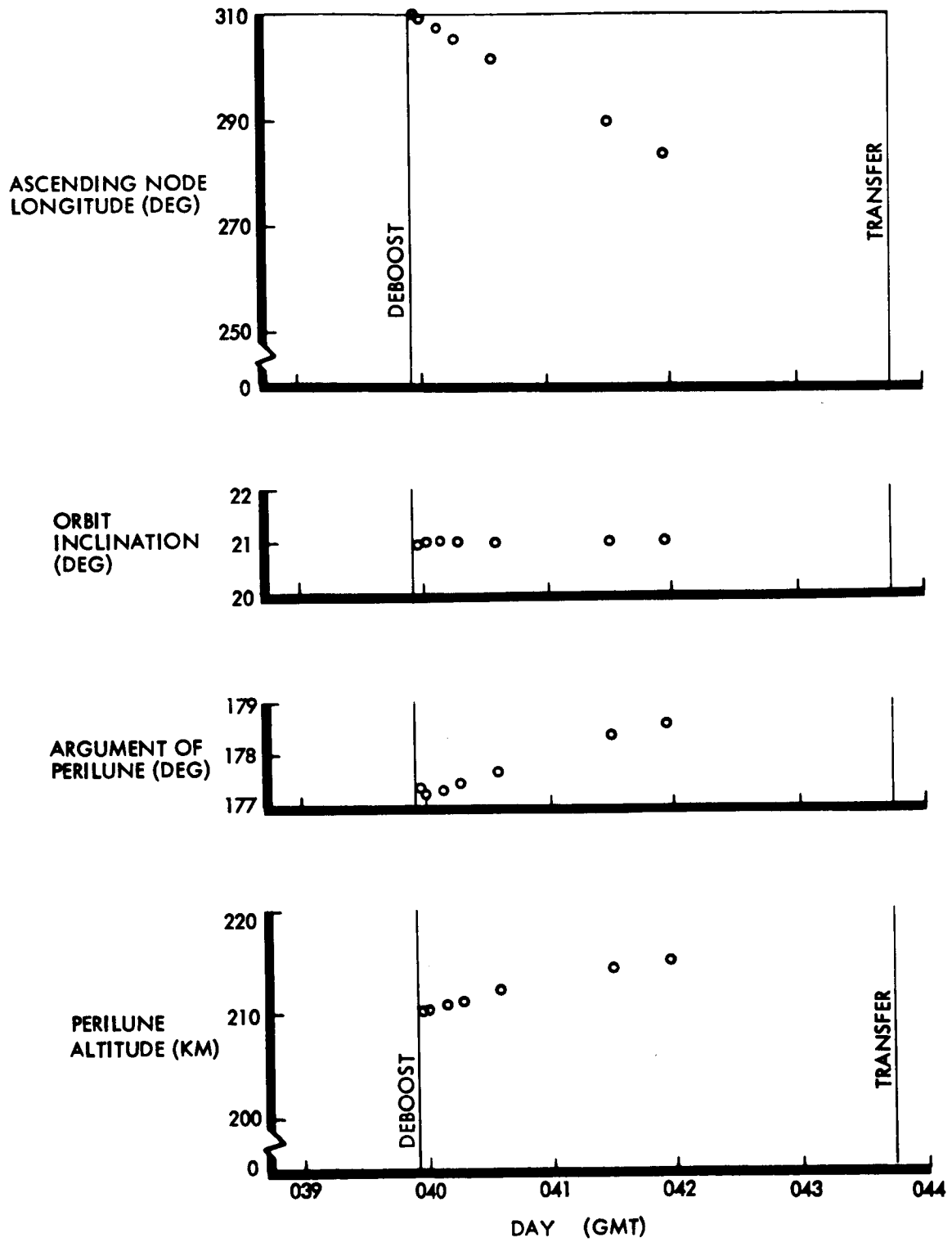


Figure 2-9: Initial Ellipse Conic Elements History

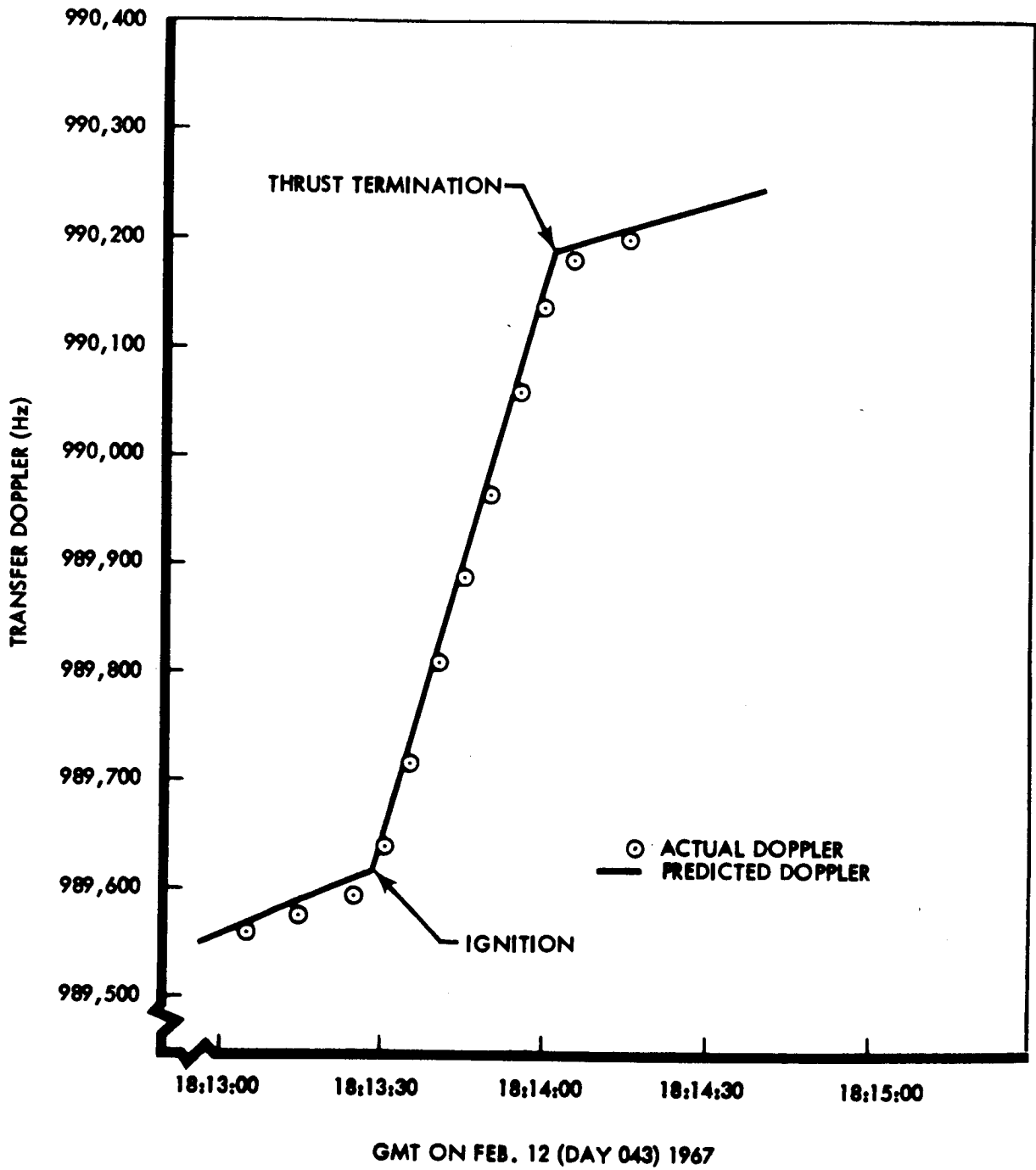


Figure 2-10: Transfer Doppler Shift

Transfer Design and Execution—The primary task of the flight path control group during the initial-ellipse phase of Mission III was the design of an appropriate transfer maneuver. The transfer from initial to photo ellipse was executed on February 12, 1967, at 18:13:26.6 GMT and resulted in a photo ellipse nearly identical to the designed ellipse. This event concluded nearly 4 days in initial orbit and initiated the principal phase of the mission: photograph 12 potential Apollo landing sites.

The design of the transfer maneuver was based on the following round rules.

- 1) Minimum perilune altitude of 48.0 km;
- 2) Illumination angles between 60 and 80 degrees at primary targets;
- 3) Transfer at least 24 hours prior to first photo;
- 4) A minimum of 30 minutes between end of Earth occultation and start of engine burn.

A set of lunar harmonic coefficients generated by NASA-Langley, designated LRC 9/4/66 harmonics, was modified by the orbit determination group and used during the transfer design. The maneuver design was based on a state vector from Orbit Determination Solution 4234.

Orbit 26 of the initial ellipse was selected for the transfer, allowing between 18 and 19 orbit revolutions from transfer to first photo.

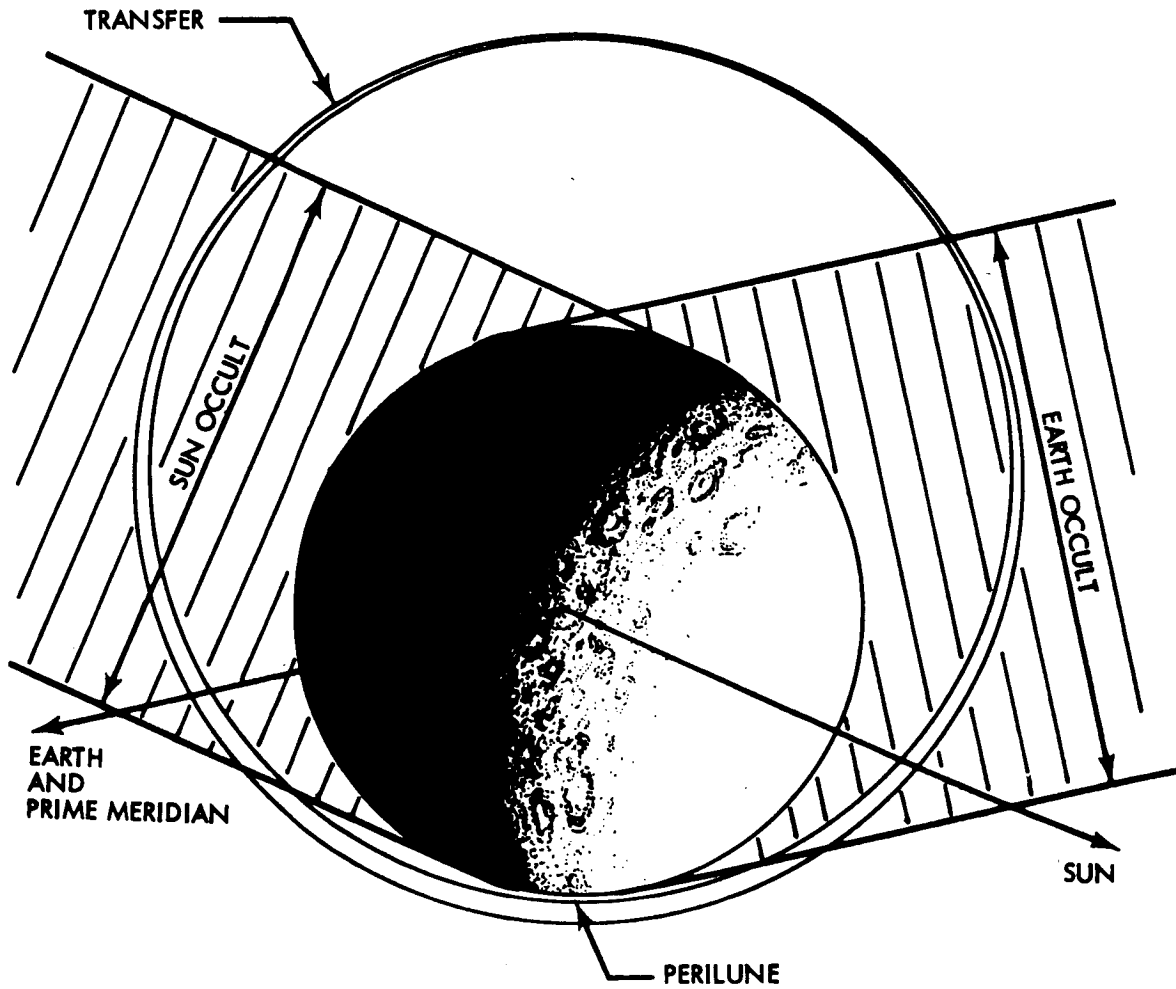
As a precaution, a backup maneuver was also designed. This maneuver was to be executed only in the event that the prime transfer maneuver could not be performed. The backup maneuver would have been executed two orbit revolutions later than the prime transfer.

The transfer maneuver was designed by targeting to the three parameters: (1) perilune radius (R_p); (2) latitude of perilune (μ); and (3) longitude of the ascending node (Ω). To reduce the computer time required for the search program, the desired values of the targeting parameters were specified at the first perilune following the transfer maneuver. The desired perilune radius, 1792.87 km, was selected to satisfy the minimum perilune altitude constraint of 48 km approximately midway through the photo activity. The desired perilune latitude, 0.596 degree, centers the perilune trace properly with respect to the photo sites. The desired longitude of the ascending node, 257.93 degrees, optimizes the lighting angle of the photo targets. By choosing the transfer true anomaly of 206 degrees, the apolune radius was held at the nominal value and orbit inclination changed only slightly. The time of the maneuver satisfied the tracking time constraint and the required ΔV , 50.73 m/sec, was well below the budgeted 302.0 m/sec. The attitude maneuvers required to perform this transfer were:

sunline roll	51.74 degrees
pitch	19.86 degrees

Selection of this attitude maneuver sequence was based on maintaining Sun lock as long as possible and compliance with antenna constraints with a minimum of angular rotation.

The orbital geometry at the time of transfer is shown in figure 2-11. The predicted conic elements at the first perilune after the transfer maneuver, Orbit 26, are given below with the desired nominal values from premission design.



ORBITAL GEOMETRY
 AT TRANSFER
 Feb. 12, 1813 GMT
 1967

Figure 2-11: Orbital Geometry at Transfer

Element	Pretransfer Prediction	Preflight Nominal	
Apolune radius	3584.46 km	3578.14 km	
Perilune radius	1792.93 km	1792.87 km	
Inclination	20.87 deg.	21.05 deg.	Selenographic-of-date coordinates
Argument of perilune	178.33 deg.	178.34 deg.	
Longitude of ascending node	257.93 deg.	257.93 deg.	

All elements above are given for February 12, 19:29:07.933 GMT.

The predicted conic elements before and after the impulsive transfer maneuver are given below to indicate the change in each caused by the maneuver. All elements are given for February 12, 18:13:43.286 GMT.

Element	Pretransfer	Posttransfer	
Ra (km)	3533.35	3584.53	
Rp (km)	1954.17	1792.87	
i (deg)	20.94	20.87	Selenographic-of-date coordinates
ω (deg)	179.58	178.30	
Ω (deg)	258.74	258.64	

Prior to acceptance of this final transfer maneuver design, various alternative sets of search parameters were investigated: Rp, Ω , ω ; Rp, μ , i ; Rp, i , λ ; Rp, a, i ; Rp, period, Ω . In each case, some conic element was allowed to deviate to satisfy the search parameters. No other set of search parameters gave results as satisfactory as the set used in the final design, Rp, μ , Ω .

Predicted results of the transfer design are shown graphically in the figures which follow. Figure 2-12 shows the perilune altitude (referred to the nominal lunar radius of 1738.09 km) as a function of descending-node longitude in the area of photo activity. Figure 2-13 is a plot of the primary photo orbit traces and includes the targeted perilune trace. Figure 2-14 indicates the spacecraft altitude above the nominal lunar radius at photo time for

each of the primary targets, as well as the lighting incidence angle for each primary photo event.

2.2.3.5 Photo Ellipse

The photo ellipse phase of Mission III extended from transfer burn termination through photo readout termination.

The principal FPAC tasks in this phase included:

- 1) A high-quality orbit determination prior to each primary photo event, which was the basis for design of camera pointing maneuvers and camera-on times.
- 2) Design of secondary-site photo maneuvers on a noninterference basis with primary photo activity.
- 3) Trajectory predictions, including sun rise and set times and Earth occultation periods.

Orbit Determination—Immediately after monitoring the transfer maneuver doppler shift, tracking data were logged and edited in preparation for the first orbit determination after the burn. This calculation used 1.33 hours of two-station view doppler data; by T+100 minutes, the calculation was complete and the results reported. This calculation—together with the excellent agreement observed between the predicted and actual doppler shift during the burn—indicated that a nominal maneuver had occurred. The following table shows the designed post-transfer conditions, the first estimate of these conditions obtained at T+100 minutes (OD 5302), and a more definitive estimate (OD 5106) obtained at T+7.5 hours.

Elements	Designed Post-transfer Conditions	First Estimate (OD 5302)	Best Estimate (OD 5106)
hp (km)	54.84	54.92	54.85
ha (km)	1846.37	1847.15	1847.35
(deg.)	20.87	20.86	20.91
(deg.)	257.93	258.75	257.86
(deg.)	178.33	178.12	178.88

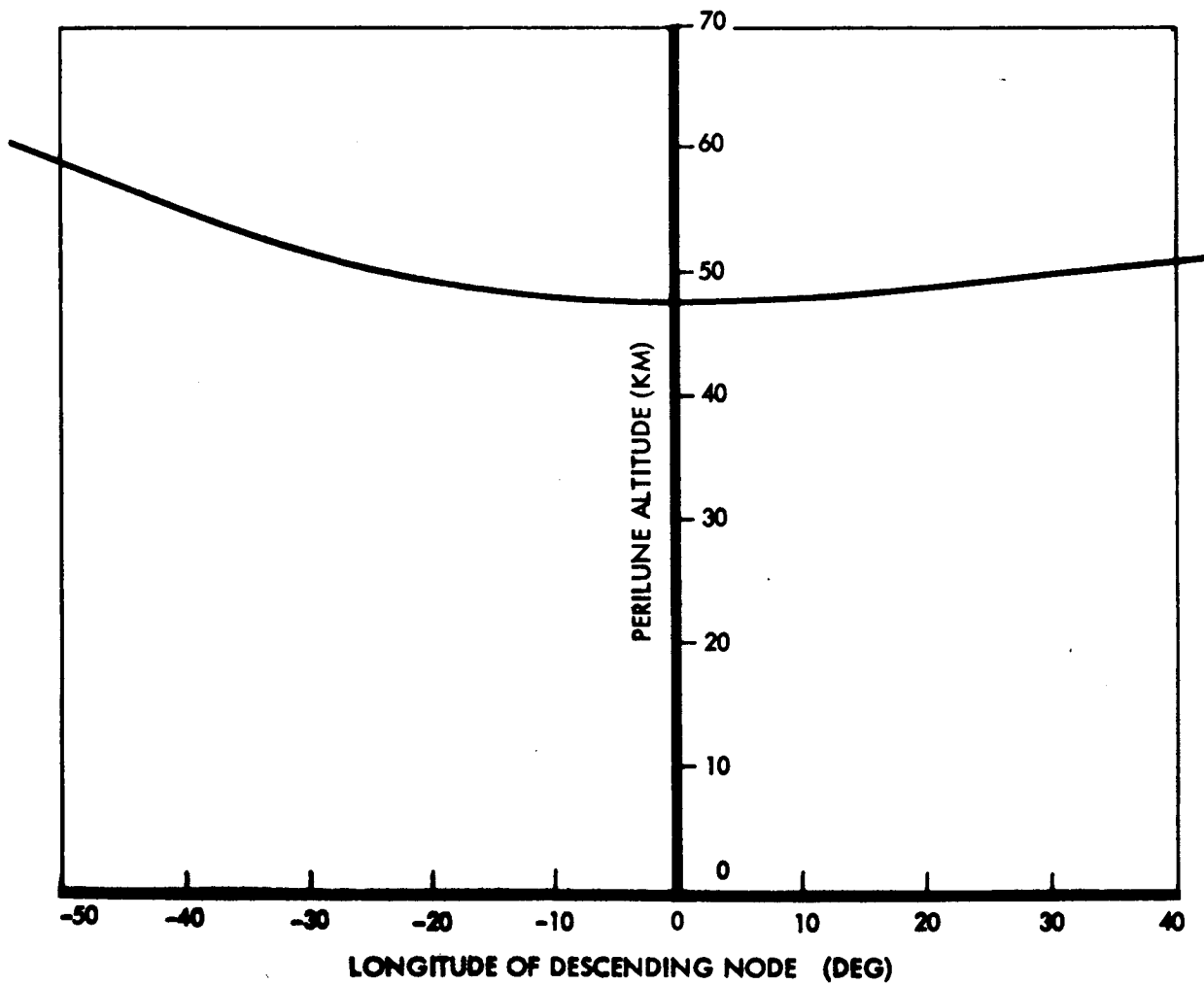


Figure 2-12: Perilune Altitude vs Longitude

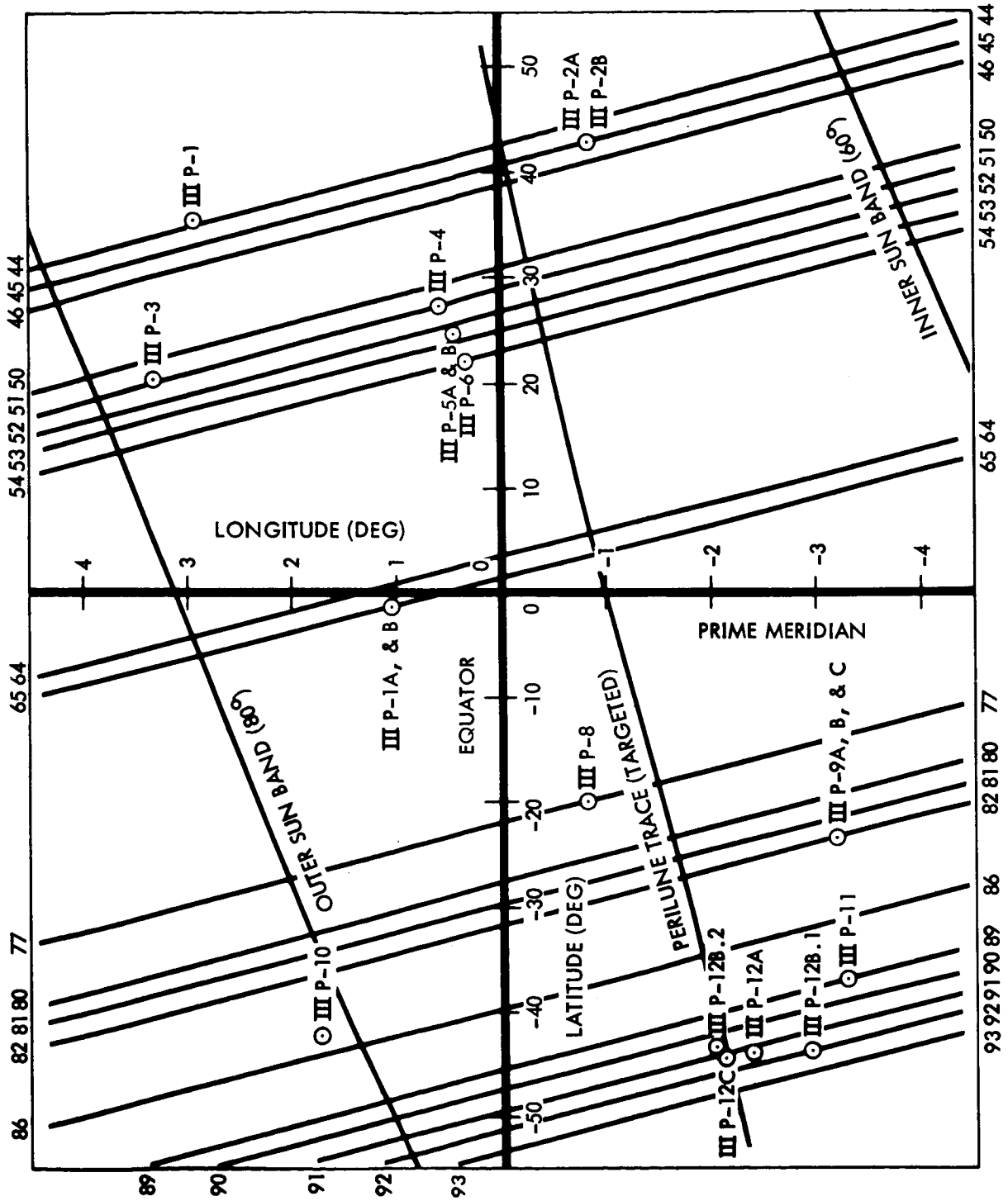


Figure 2-13: Photo Orbit Traces for Primary Targets

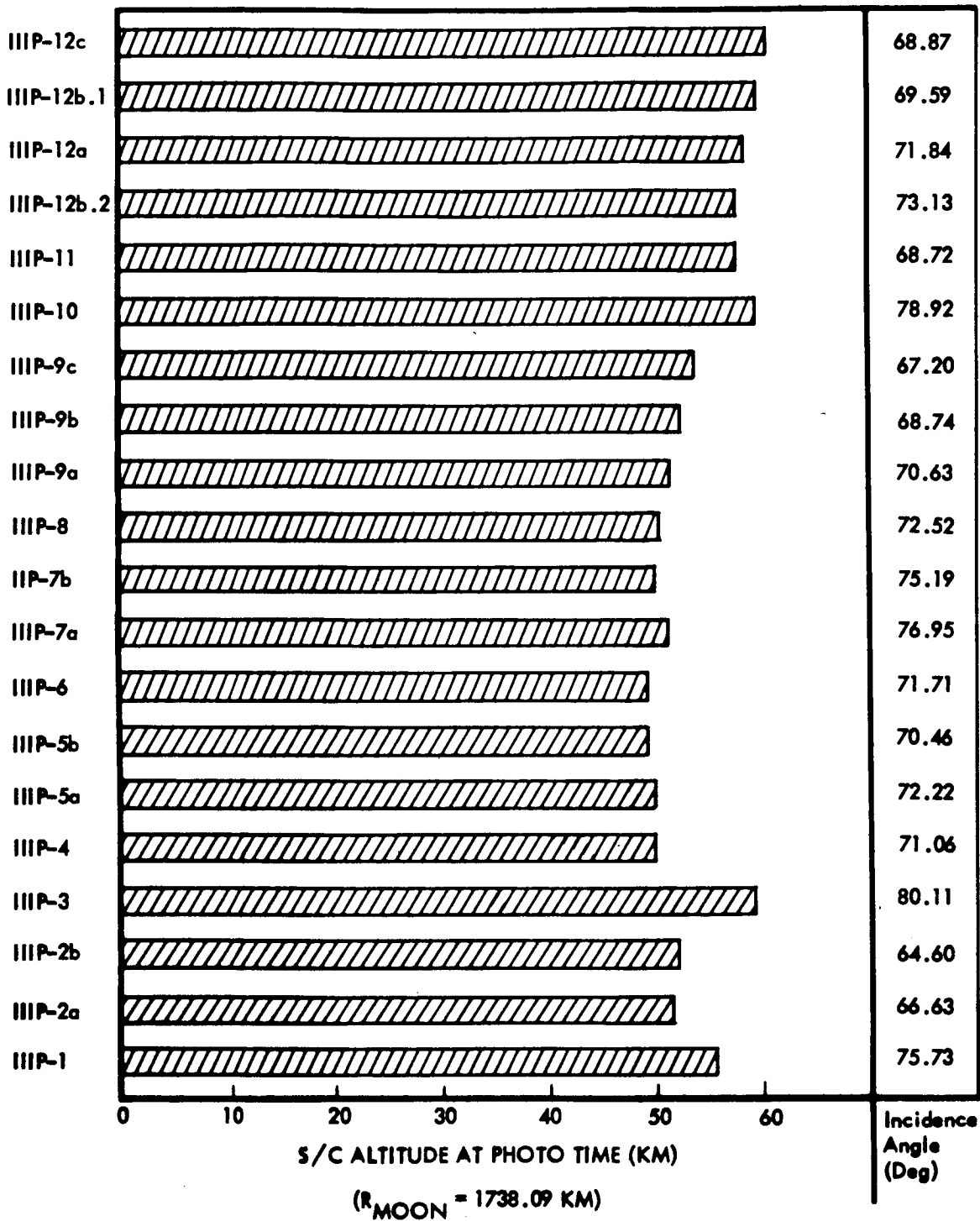


Figure 2-14: Predicted Primary Photo Altitudes based on Transfer Design

No difficulties were encountered in the initial orbit determination and no backup orbit determination procedures were necessary. Plots of orbital elements obtained during this phase are shown in Figure 2-15 through 2-18.

This mission phase was the most active of all the phases. A total of 50 orbit determinations were made before Bimat cut; 30 of these were used to directly support command conferences. Table 2-9 shows the orbit determination runs used to support command conferences for each photo event. Details of each of these orbit determinations may be found in Appendix B, Volume VI of this document.

Photo Design—In Mission III, all photo activity occurred during the second or photo ellipse. There were 156 frames exposed for primary photo sites and 55 frames exposed for secondary sites.

Volume II of this document contains a detailed listing of photo information, including actual camera-on times and spacecraft attitude maneuvers. A summary of frames exposed is given in Table 2-10.

The orbit determination procedures used during this phase were similar to those used in initial ellipse. That is, a basic set of lunar harmonic coefficients (LRC 11/11/66 set) was tailored to the particular gravitational field being experienced by solving for eight of the higher order coefficients (C32, C42, C33, C43, S32, S42, S33, S43). This procedure produced good fits to the tracking data, no divergence problems were encountered, and the resultant orbital elements were consistent. The data arc used was four orbits in length. Perilune data was used in the fit and the doppler data oscillations near perilune observed previously in Missions I and II were again present. No ranging data were included in

Table 2-9:
ORBIT DETERMINATIONS USED FOR
PHOTO SITE COMMAND CONFERENCES

Photo Site Number	Orbit Determination Number	
	PCC*	FCC**
IIIP-1, S-1	5114	5320
P-2a, P-2b	5320	5124
S-2, S-3	5124	5126
S-4, P-3	5126	5228
P-4, P-5a	5228	5332
P-5b, P-6	5332	5134
S-5, S-6	5134, 5236	5238
S-7, S-8	5238	5340
S-9	5340	5144
S-10, S-11	5342	5146
S-13, P-7a	5146	5248
P-7b, S-14	5248	5352
S-15	5352	5356
S-16, S-17	5356	5158-A
S-18, S-19	5158-A	5260
S-21, S-21.5, S-22	5260	5364
S-20, P-8	5364	5168
S-23, S-24	5168	5272
P-9a, P-9b	5272	5005
P-9c, S-25	5005	5176
S-26	5176	5278
P-10, S-27	5278	5380
S-28, P-11	5380	5382
P-12b.2, P-12a	5382	5284
P-12b.1, P-12c	5284	5286
S-29	5286	5388
S-30, S-31	5388	5192

* PCC — Preliminary Command Conference

**FCC — Final Command Conference

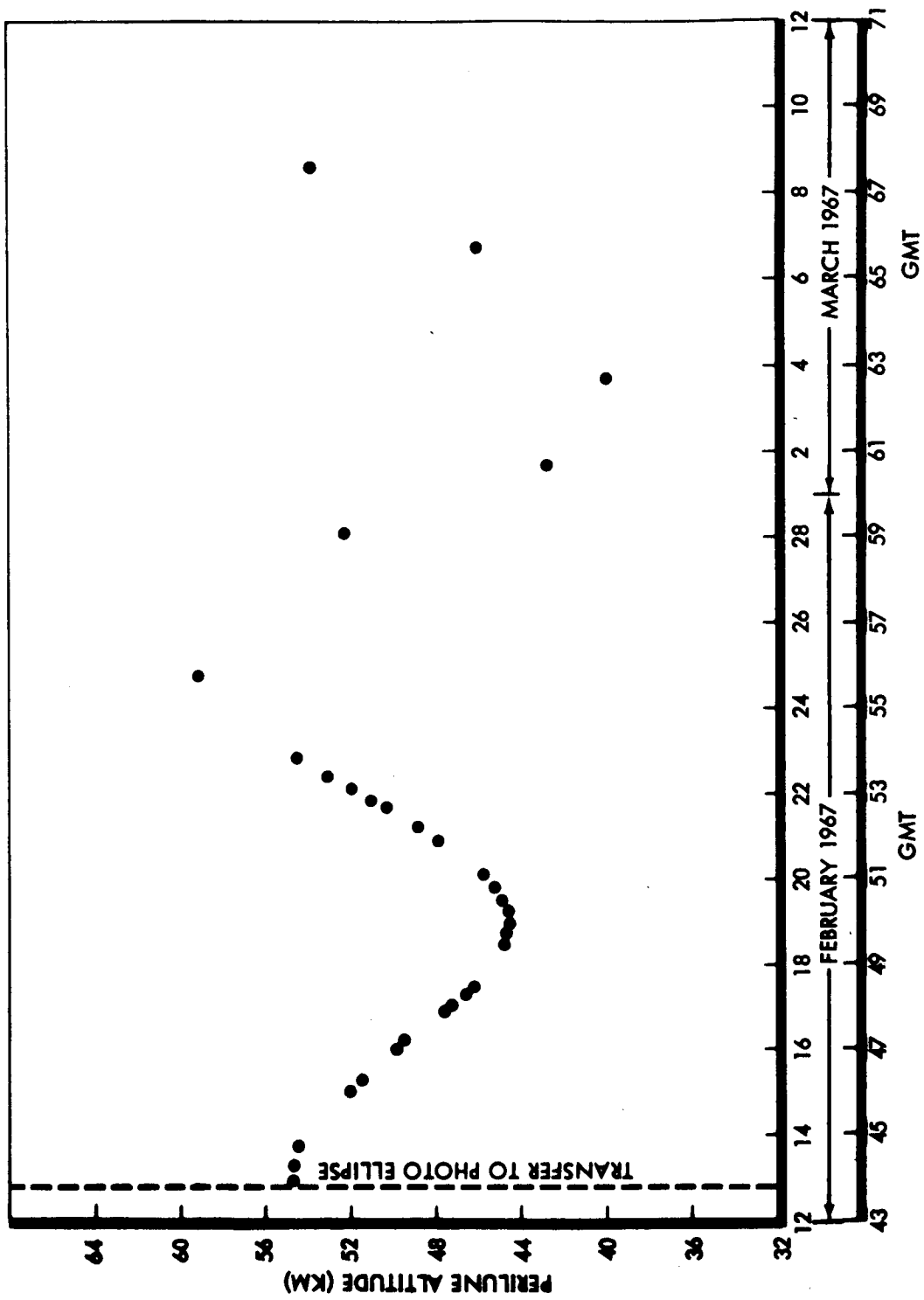


Figure 2-15: Perilune Altitude vs Time

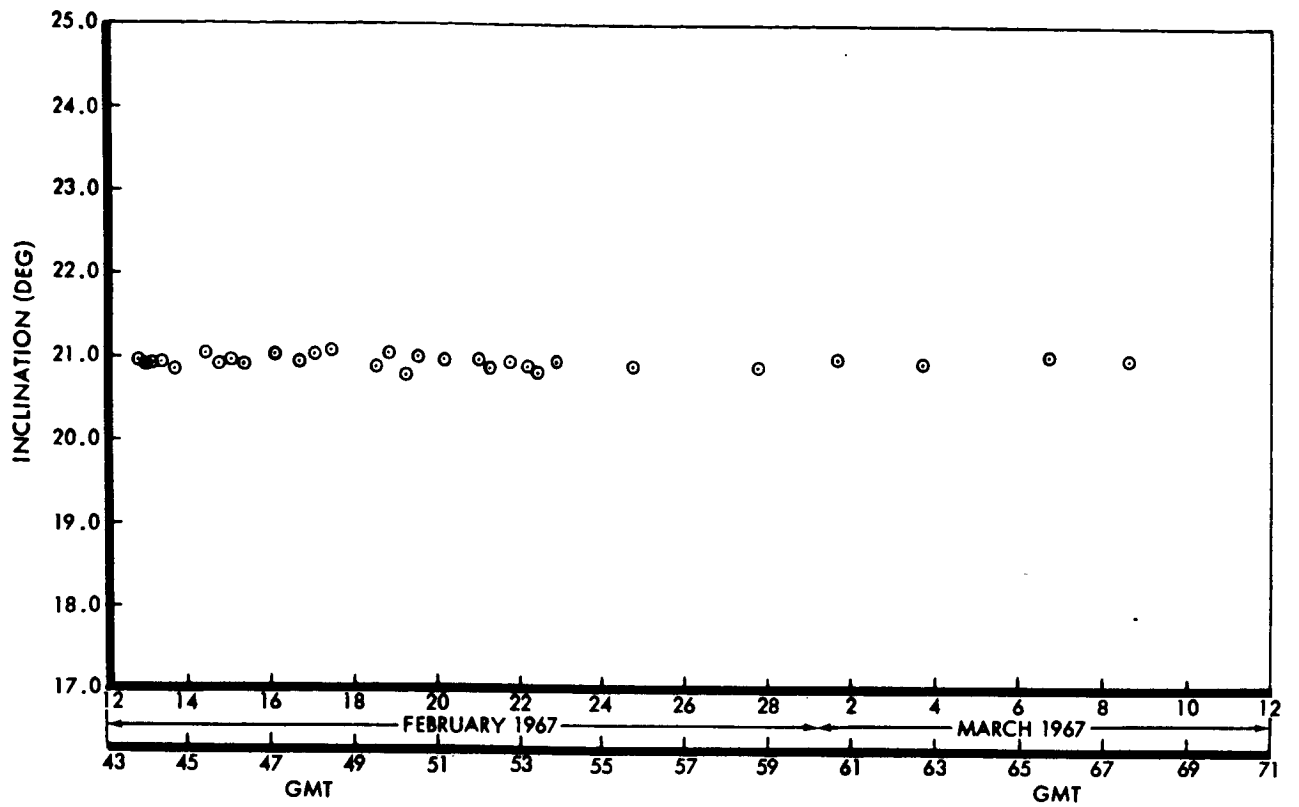


Figure 2-16: Inclination vs Time

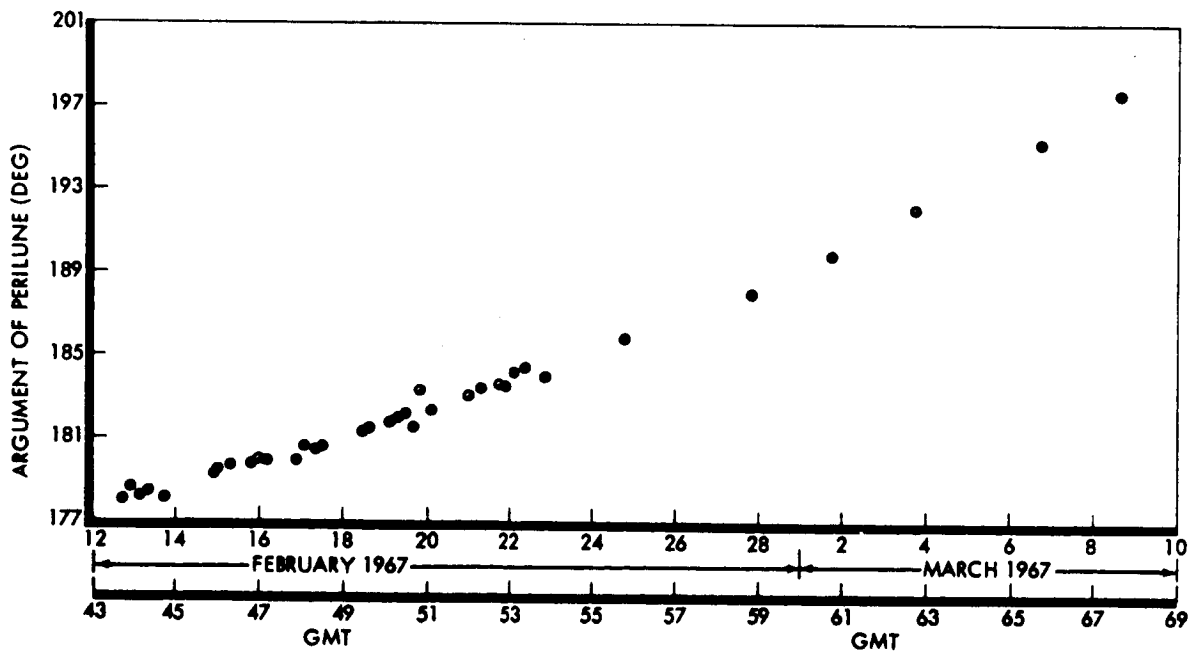


Figure 2-17: Argument of Perilune History

INERTIAL NODE LONGITUDE HISTORY
 NODE LONGITUDE @ $T_0 = 257.86$ DEG.

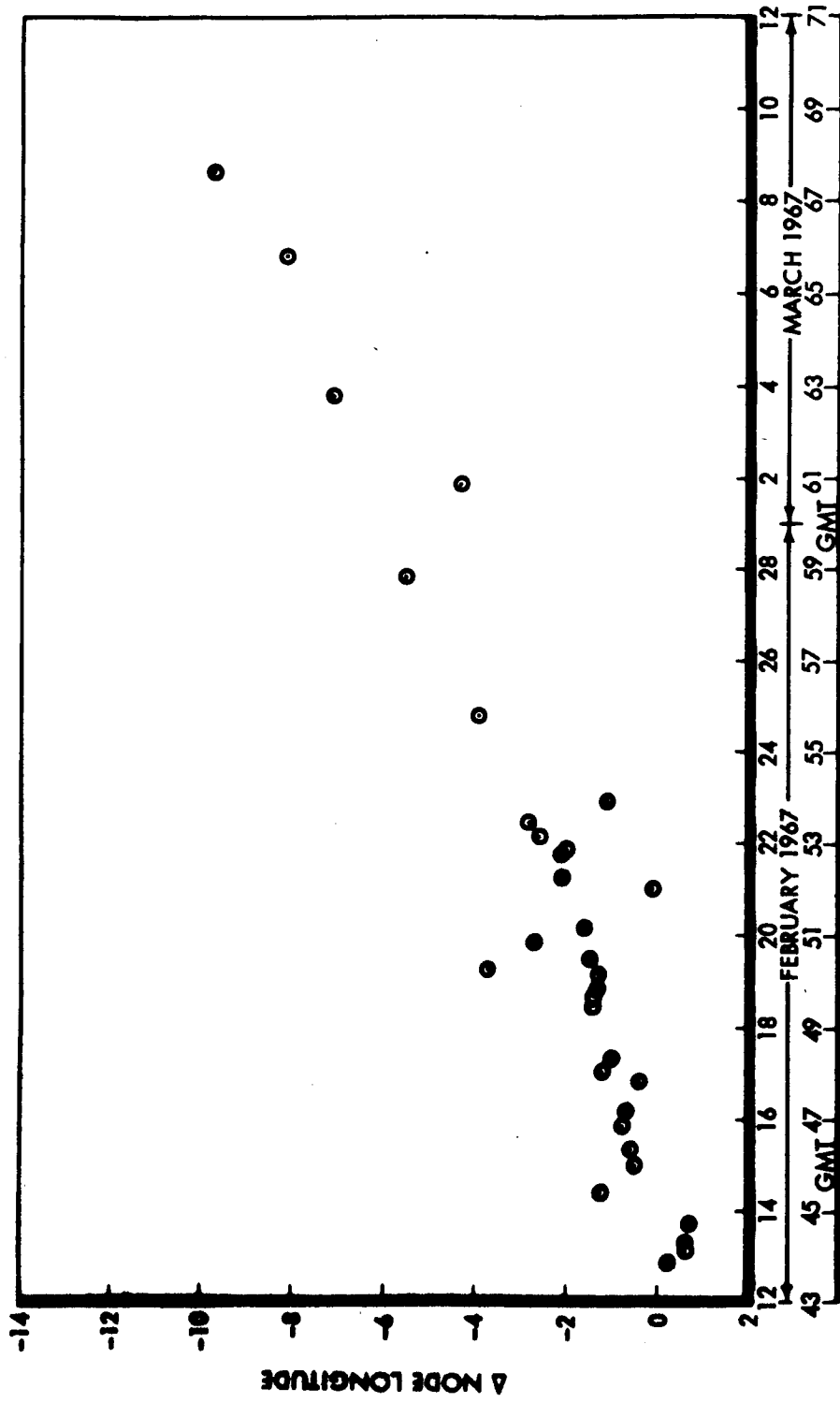


Figure 2-18: Inertial-Node Longitude History

Table 2-10: FRAME EXPOSURE SUMMARY

Frame Numbers	Photo Site	Orbit Number	Frame Numbers	Photo Site	Orbit Number
5 through 20	IIIP-1	44	112 through 115	IIIS-18	71
21 through 24	IIIS-1	44	116 through 119	IIIS-19	72
25 through 32	IIIP-2a	45	120	IIIS-21	74
33 through 36	IIIP-2b	46	121	IIIS-21.5	74
37	IIIS-2	47	122	IIIS-22	75
38	IIIS-3	48	123	IIIS-20	76
39	IIIS-4	49	124 through 131	IIIP-8	77
40 through 43	IIIP-3	50	132 through 135	IIIS-23	78
44 through 51	IIIP-4	51	136	IIIS-24	79
52 through 59	IIIP-5a	52	137 through 144	IIIP-9a	80
60 through 67	IIIP-5b	53	145 through 152	IIIP-9b	81
68 through 71	IIIP-6	54	153 through 160	IIIP-9c	82
72	IIIS-5	55	161	IIIS-25	83
73	IIIS-6	56	162	IIIS-26	84
74 through 77	IIIS-7	57	163 through 170	IIIP-10	86
78	IIIS-8	58	171	IIIS-27	87
79	IIIS-9	59	172	IIIS-28	88
80 through 83	IIIS-10	61	173 through 180	IIIP-11	89
84	IIIS-11	62	181 through 184	IIIP-12b.2	90
85	IIIS-13	63	185 through 200	IIIP-12a	91
86 through 93	IIIP-7a	64	201 through 204	IIIP-12b.1	92
94 through 101	IIIP-7b	65	205 through 212	IIIP-12c	93
102	IIIS-14	66	213	IIIS-29	94
103 through 106	IIIS-15	67	214	IIIS-30	96
107	IIIS-16	69	215	IIIS-31	97
108 through 111	IIIS-17	70			

the fits because none was taken after photography started. Orbit determinations were done for both the preliminary and final command conferences. In most cases, recalculation of the camera-on times and maneuver angles with the new state vectors caused significant changes to these quantities. Appendix B contained in Volume VI of this document, includes a tabulation of the maneuver angle and camera-on-time changes associated with updated orbit determinations. A summary of the data arc lengths and prediction intervals for each photo site may also be found in Appendix B.

The DSIF procedure of using the backup

receiver during photo readout sequences again proved successful.

Although tracking data obtained during photo readout were two to ten times more noisy and had more frequent blunder points caused by photo readout interference, they were nevertheless useable data. Data were sampled at 20-second intervals during these periods--instead of the normal 60-second rate--and then compressed to 60-second intervals by the editing programs. This procedure resulted in a smoother data stream for orbit determination use. The presence of blunder points inherent in this phase required that the tracking data be processed care-

fully, which increased computation time by about 20%.

The lunar harmonics used for the design of each photo maneuver were either those designated LRC 11/11/66 or LRC 11/11/66 harmonics modified by the various orbit determination solutions. The modified LRC 11/11 harmonics were assigned numbers identical to the orbit determination solution with which they were associated.

Table 2-11 shows the harmonic model used for the final design of attitude maneuvers and timing for each photo site.

To minimize the timing error in the camera-on times, the state vectors were updated, using ODPL, to within a few minutes of the expected camera-on times. Thus, the mean element trajectory program was used over only a short span of time. After the design of each photo maneuver, the camera-on time

and attitude maneuvers were checked using the program EVAL with the integrating trajectory option.

All photos exposed during Mission III occurred on the preflight design orbit numbers. It was not necessary to make real-time adjustments to the photo orbit numbers.

Figure 2-19 shows the spacecraft altitude (based on a mean lunar radius of 1738.09 km) at photo time for each primary photo event. Also given are sunlight incidence angles. These data were extracted from the individual real-time photo maneuver designs. Figure 2-20 shows perilune altitude (above the mean lunar radius) as a function of descending-node longitude, as predicted during transfer maneuver design as well as from real-time photo maneuver designs. The difference between the two curves indicates that the modified LRC 9/4/66 harmonics used in the transfer design did not represent the perilune history perfectly.

Table 2-11 HARMONIC MODEL VS SITE

SITE NUMBERS	HARMONIC MODEL
III P-1, S-1	5320
P-2a, P-2b, S-2, S-3, S-4, P-3	5114
P-4, P-5a, P-5b, P-6, S-5, S-6	5001
S-7, S-8, S-9, S-10, S-11, S-13, P-7a, P-7b	5002
S-14	5003
S-15, S-16, S-17	LRC 11/11/66
S-18, S-19	5260
S-21, S-21.5, S-22	5362
S-20, P-8	5168
S-23, S-24	5272
P-9a, P-9b	5005
P-9c, S-25	5176
S-26	5278
P-10, S-27	5380
S-28, P-11	5382
P-12b.2, P-12a	5284
P-12b.1, P-12c	5286
S-29	5388
S-30, S-31	5192

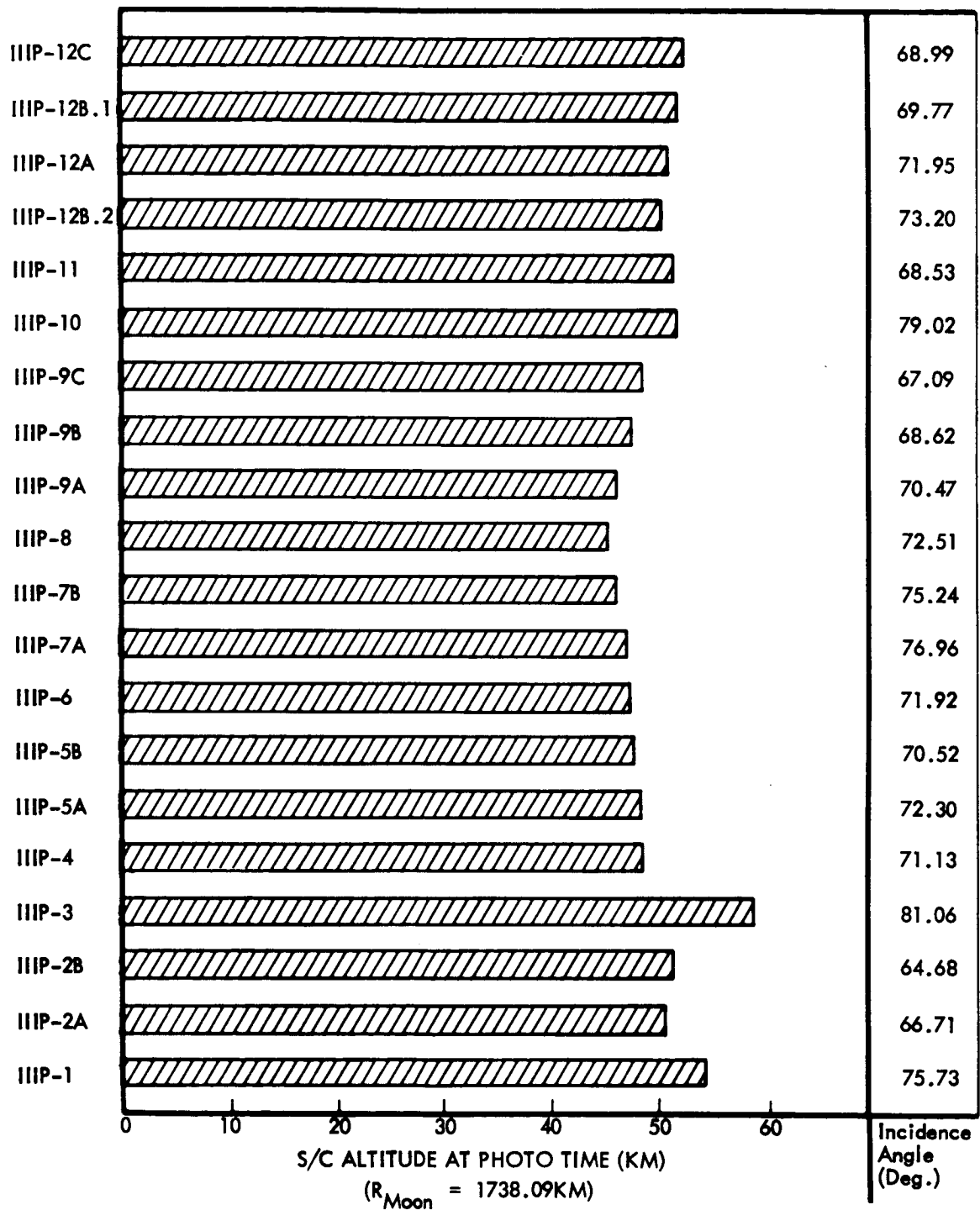


Figure 2-19: Predicted Primary Photo Altitudes Based on Real-Time EVAL Runs

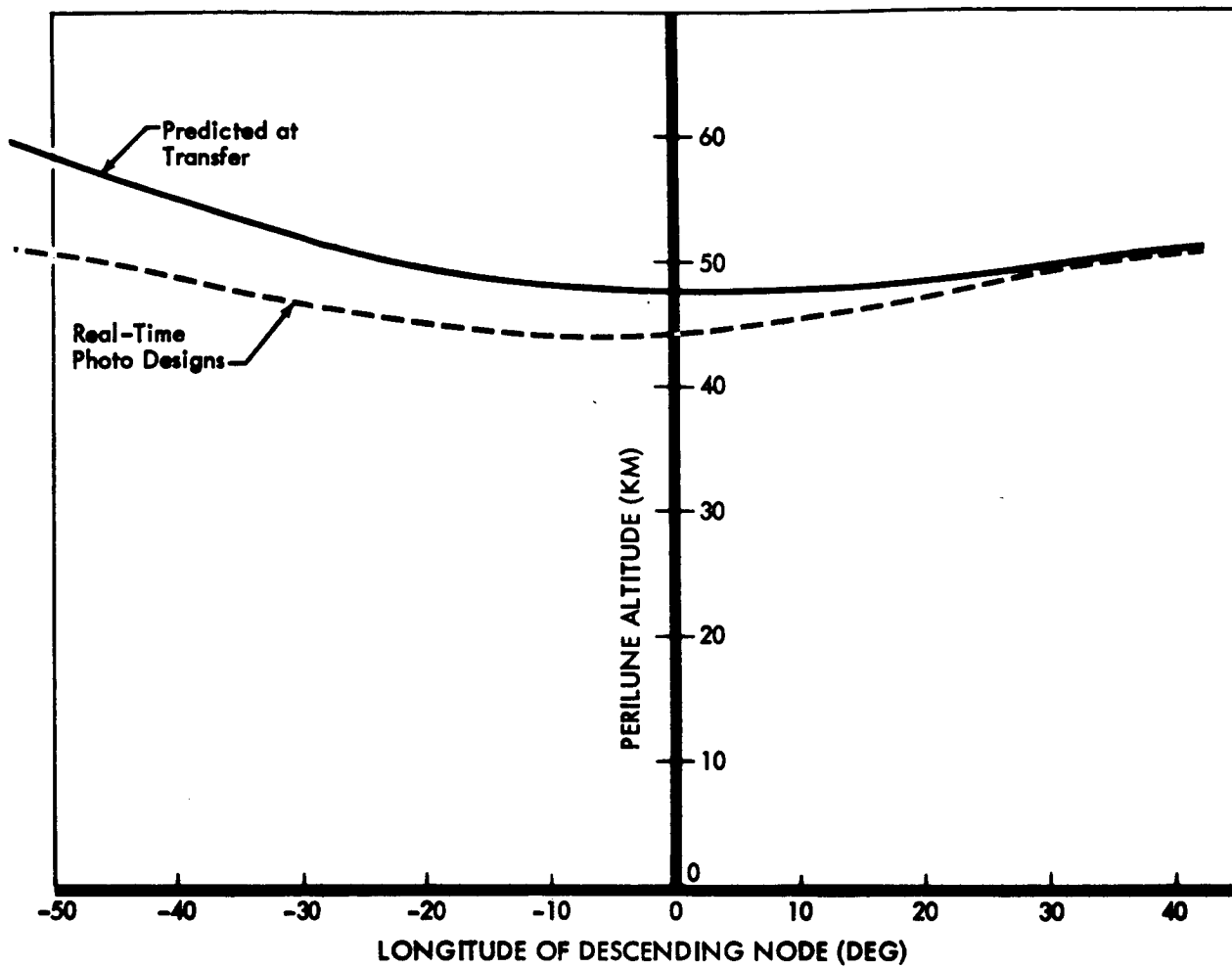


Figure 2-20: Perilune Altitude vs Longitude of Descending Node

3.0 SPACECRAFT PERFORMANCE

The performance of the individual subsystems aboard Lunar Orbiter III is summarized in this section. A brief description of each subsystem is also presented. For more detailed configuration and functional information on each subsystem, consult the Mission I final report, Boeing Document D2-100727-3, Volume III, Mission Operational Performance. The key events of the primary mission are tabulated in Table 3-1.

Launch through Cislunar Injection—Launch vehicle liftoff occurred at 01:17:01.120 GMT on Day 36 (February 5, 1967). The first and second-stage boosters performed as programmed and Lunar Orbiter III was injected into the cislunar trajectory at the end of the Agena second burn approximately 20 minutes after liftoff. Separation from the Agena followed approximately 3 minutes later.

Cislunar Injection through Lunar Injection—DSS-51 (Johannesburg) acquired the vehicle in one-way lock 29.1 minutes after launch. Approximately 1.6 minutes later DSS-51 acquired two-way lock and remained in contact for 6.5 hours. DSS-41 (Woomera) acquired the spacecraft in three-way lock at 50.5 minutes after launch on the basis of two good data frames at 56 minutes after liftoff, antenna and solar panel deployment and Sun acquisition were verified. Handover from DSS-51 to DSS-41 occurred 73 minutes after launch with no difficulties encountered.

A star map maneuver was initiated 10 hours 35 minutes after liftoff and Canopus was located successfully. The propellant line bleed and propellant squib valve firing events were conducted successfully at approximately 16 hours after liftoff to prepare the velocity control subsystem for the midcourse correction maneuver. The spacecraft was then pitched 36 degrees off Sun to reduce

overheating and minimize thermal paint degradation.

The midcourse maneuver was successfully accomplished 37 hours 43 minutes after launch with a velocity change of 5.09 meters per second. The spacecraft was returned to its 36-degree off-Sun attitude until the orbit injection maneuver.

Injection of the spacecraft into lunar orbit was performed at 92 hours 37 minutes after liftoff. The velocity control rocket engine operated for 542.5 seconds, producing a velocity change of 704.3 meters per second, as programmed. The spacecraft achieved an initial orbit with an apolune of 1802.1 km, a perilune of 200.2 km, and an orbital inclination of 20.94 degrees to the lunar equator.

Initial Ellipse through Transfer into Photo Ellipse—After three orbits on-Sun the spacecraft was pitched 28 degrees off-Sun to improve the thermal balance. The Sun was reacquired during Orbit 22 in preparation for the transfer maneuver to the final orbit.

During Orbit 26, 185 hours after launch, the transfer maneuver was performed, placing the spacecraft in a final orbit with an apolune of 1847.35 km, a perilune of 54.85 km, and an inclination of 20.94 degrees.

Photo Ellipse through Photo Taking—To verify photo subsystem operation, the Goldstone film was read out by DSS-12 and -62 during Orbit 39 and by DSS-12 and -41 during Orbit 42. First photos were taken during Orbit 44, followed shortly by the first priority readout.

Site photography progressed normally. However, during Orbit 67 priority readout, an intermittent film advance hangup problem

Table 3-1: KEY EVENTS

GMT				Event
Day	Hour	Min	Sec	
036	01	17	01.120	Liftoff
(2-5-67)	01	36	55.5	Cislunar Injection
	01	39	39.7	Spacecraft-Agena Separation
	01	41	30	Antenna Deployment (Predicted)
	01	41	56	Solar Panel Deployment (Predicted)
	01	46	10	DSS-51 One-way R.F. Lock
	01	47	43	DSS-51 Two-way R.F. Lock
	02	07	02	DSS-41 Three-way R.F. Lock
	02	35	02	DSS-41 Two-way R.F. Lock
				Sun Presence (time unknown)
		11	52	Canopus Acquisition
		17	08	Bleed Propellant Lines
	17	20	31	Propellant Squib Valve Actuation
037	15	00	00	Ignition—Midcourse Maneuver, $\Delta V = 5.09$ mps, Burntime 4.3 sec.
(2-6-67)				
039	21	54	19.0	Ignition—Lunar Orbit Injection, $\Delta V = 704.3$ mps, Burntime 542.5 sec.
(2-8-67)				
043	18	13	26.6	Ignition—Orbit transfer maneuver, $\Delta V = 50.7$ mps, Burntime 33.7 sec.
(2-12-66)				
046	10	00	38	First photographic exposure, Site P-1 (Orbit 44)
(2-15-67)				
046	11	56	28	Start first Priority Readout, Site P-1 (Orbit 45)
(2-15-67)				
054	02	11	22	Last Photographic Exposure Site S-31 (Orbit 97)
(2-23-67)				
054	06	36	42	Bimat cut (Orbit 98)
054	09	35	56	Start Final Readout (Orbit 99)
061	15	45	33	Readout Drive Anomaly (Orbit 149)
(3-2-67)				
062	07	17	12	End Readout (Orbit 153-154)
(3-3-67)				

was encountered. Methods were developed to alleviate this problem and the last photo, Site S-31, was taken during Orbit 97. Two hundred eleven photos were taken of 51 sites during the photo period. Bimat was cut during Orbit 98, 437 hours after launch. A total of 36.48 photos was received during priority readout.

Final Readout—Final readout was initiated 3 hours after Bimat cut during Orbit 99 and progressed normally through Orbit 148, averaging 2.7 frames per orbit. In Orbit 149, an anomaly within the photo subsystem caused the logic to change state and film readout did not start when commanded. Further attempts to start readout using nor-

mal commands resulted in inadvertent operation of the film advance motor, causing it to stall and subsequently burn out. After this failure film could not be advanced and readout was terminated after receipt of the four photos stored in the storage loopers. A total of 132 photos were read out of the 211 photos taken. Of this total, 20.97 photos had been transmitted during priority readout.

3.1 PHOTO SUBSYSTEM PERFORMANCE

The photo subsystem is designed to photograph the lunar surface, process the exposed film, scan the processed film with a flying-spot scanner, and provide video signals to the communications subsystem for transmission to Earth.

The Mission III photo subsystem was equipped with a 0.21 neutral-density filter in front of the 80-mm lens. The resultant 80-mm lens transmissivity was 59%. The 610-mm lens transmissivity was 65%. NASA provided shutter speed calibration data. The following values were used for operational purposes.

CAMERA	610-mm LENS	80-mm LENS
1/25	35.7 milliseconds	Nominal
1/50	18.7 milliseconds	Nominal
1/100	9.2 milliseconds	Nominal

Photo subsystem performance was generally satisfactory from launch through the Orbit 149 anomaly. Real-time analysis indicated photo quality better than that of Missions I and II. Measured exposures were good within limitations imposed by the mission plan. A difference between the measured and predicted spacecraft film densities is not attributed to any system malfunction. This subject is discussed under "Photography Control" (Volume II of this document). The neutral-density filter in the wide-angle cam-

era equalized the two cameras satisfactorily. The observed density differences were less than 0.1, except for marginal-exposure situations. See Volume II of this document for Mission III film densities.

The photo video chain performed normally until Orbit 149. White-level variations were somewhat smaller than those encountered during Mission II, probably because the Bimat temperature was maintained at a lower level during Mission III.

No detailed analysis of V/H sensor performance was attempted, due to the large cross-track tilts used for many of the prime photo sites. However, telemetry observations of V/H ratio, during the mission, generally fell within 3% of the predicted values. A deviation of this size is within combined telemetry and sensor tolerances, and had no effect on photographic quality.

Film handling within the photo subsystem was not as good as in preceding missions. The processing rate was nominal; however, the camera film advance showed some small effects of film set. There was no mission degradation resulting from the few abnormal film advances. The readout looper hangups are discussed in more detail under "Readout Film Handling." The hangups, which occurred throughout the mission, may have reduced the total amount of data retrieved from the spacecraft, but had no effect on photo quality.

Photo operations are summarized in Table 3-2.

3.1.1 Thermal Control

Thermal control of the photo subsystem during Mission III may be discussed in three phases of the mission.

- Countdown and cislunar phase;
- Orbit cruise phase;
- Final photo readout phase

Table 3-2: PHOTO DATA SUMMARY

FRAME	PHOTO		SHUT- TER SPEED	PROC ORBIT INDEX	R/O SEQ T	R/O SEQ WA	R/O ORBIT	EDGE WA NOS	TC FRMLT	EDGE TELE NOS	S/C TIME	EXPOSURE GMT	.
	SITE	ORBIT											
1													
2													
3				(-2.28)									2
4				44									
5	P1	44	1/25			3/100%	45	708 677	676		None		1
6					3/30%		45						1
7													1
8													1
9						4/99%	46	201					1
10					4/72%		46			196			1
11						5/100%	47	491 462	460	450			1
12					5/45%		47						1
13					5/23%	6/100%	47/8	753 724	723	483			1
14					6/46%		48			721			1.3
15					6/12%	7/100%	48/9	012 986	985	756			1
16				(16.30)	7/50%		49			985			1
17				45	7/13%	8/100%	49/0	278 250	248	018			1
18					8/27%		50			241			1
19					8/10%	9/100%	50/1	541 512	510	281			1
20				(20.05)	9/31%		50			508			1
21	S1	44	1/50	46	9/11%		51			543			
22				(22.20)									
23				47									
24				(24.19)									
25	P2A	45	1/50	48		10/100%	52	327 299	297		00421.4	46:13:32:03.58	
R/O SEQ	FRAMELETS		R/O SEQ	FRAMELETS		*COMMENTS:							
001	949/842					1. No time recorded on S/C film for Frames 1-20.							
002	726/841					2. Processing started in Goldstone header.							
003	708/843					3. Bimat defect 719-713.							
004	330/134					P1--22.4% T, 43.7% WA							
005	300/414					S1--11% T							
006	708/876					P2A 100% WA							
007	081/986					P 74.2% T 77.3% WA							
008	201/313					S 60% T 59% WA							
009	584/477												
010	333/273												

Table 3-2: PHOTODATA SUMMARY (Continued)

FRAME	PHOTO		SHUT- TER SPEED	PROC ORBIT INDEX	R/O SEQ T	R/O SEQ WA	R/O ORBIT	EDGE WA NOS	TC FRMLT	EDGE TELE NOS	S/C TIME	EXPOSURE GMT	*
	SITE	ORBIT											
26	P2A	45	1/50	(26.58)	10/21%		52			294			2
27				49	10/1%		52			331			2
28				(28.55)									
29				50									
30				(30.50)									
31				51		11/100%	53	115 088	085		69435.1	46:13:32:17.28	
32					11/18%		53		215	082			
33	P2B	46	1/50		11/9%	12/100%	53/4	375 347	345	116	81972.2	46:17:01:14.37	
34					12/5%		54			344			
35					12/21%		54			380			
36				(36.54)									
37	S2	47	1/100	52	13/59%		55						
38	S3	48	1/100										
39	S4	49	1/100										
40	P3	50	1/25		14/62%		56						
41													
42				(42.56)	15/72%		57						1,
43				53									
44	P4	51	1/50	(44.58)	16/72%		58						
45				54									
46				(47.02)	17/85%		59						
47				55									
48				(50.02)									
49													
50				56	18/1%		60	605					
R/O SEQ	FRAMELETS		R/O SEQ	FRAMELETS		*COMMENTS: 1. PSL at 363 at 42.56 2. GRE 08 Fan Failure caused kine line to be obscured by mask. Replay of FR900 tape satisfactory.							
010	332/273												
011	125/082												
012	401/330												
013	719/680												
014	123/081												
015	382/310												
016	645/873												
017	911/838												
018	687/805												

Table 3-2: PHOTO DATA SUMMARY (Continued)

FRAME	PHOTO		SHUT- TER SPEED	PROC ORBIT INDEX	R/O SEQ T	R/O SEQ WA	R/O ORBIT	EDGE WA NOS	TC FRMLT	EDGE TELE NOS	S/C TIME	EXPOSURE GMT	.
	SITE	ORBIT											
51	P4	51	1/50	(52.01)									
52	PSA	52	1/50	57	18/88%		60			609			4
53				(54.03)		19/1%	61	968	967		52079.5	47:13:50:39.29	
54				58	19/92%		61			966			3,
55													
56				(56.02)									
57				59									
58						20/80%	62	654					
59													
60	PSB	53	1/50		20/82%	21/100%	63/3	917 889	887	657			1,
61													
62				(62.03)	21/71%		63			920			2,
63				60		22/100%	64	310 281	279		64624.7	47:17:19:44.48	8,
64				(64.06)	22/2%		64			278			8,
65				61	22/78%		64						8,
66						23/100%	65	703 675	673		64631.4	47:17:19:51.18	
67					23/6%					671			
68	P6	54	1/50		23/81%	24/100%	65/6	966 938	937	706	77110.9	47:20:47:50.67	
69				(69.06)	24/17%		66			932			
70				62	24/72%	25/50%	66/7	228		969			5,
71				(71.87)									7,
72	S-5	56	1/25	63	25/74%		67			231			6,
73	S-6	56	1/25				68	621					10,
74	S-7	57	1/25	(74.88)									
75				64	26/80%	26/80%	68			623			9,
R/O SEQ	FRAMELETS	R/O SEQ	FRAMELETS	*COMMENTS:									
018	087/086			1. Bubbles throughout TP frame.									
019	088/074			2. PSL at 62.06.									
020	728/089			3. PSL at 54.04									
021	091/087			4. PSL at 52.01									
022	391/376			5. PSL at 69.87									
023	787/088			6. Er. ratio R/O Advancement, #289 scanned 18 times 14 times #281 on Seq. 26.									
024	041/015			7. PSL at 71.88									
025	202/213			8. gain step 8, Seq. 23.									
026	702/086			9. Erratic R/O advancement, #088, scanned 21 1/2 times, # scanned times on Seq. 68.									
7				10. PSL at 74.88.									
5				P4: 0% PSA 22.5% T, 10% WA PSB 26.8% T, 37.5% WA P6 48% T, 37% WA S6 80% WA S7 80% T									

Table 3-2: PHOTO DATA SUMMARY (Continued)

FRAME	PHOTO		SHUT- TER SPEED	PROC ORBIT INDEX	R/O SEQ T	R/O SEQ WA	R/O ORBIT	EDGE WA NOS	TC FRMLT	EDGE TELE NOS	S/C TIME	EXPOSURE GMT	
	SITE	ORBIT											
76	S-7	57	1/25	64									
77	↓	↓	↓	(77.90)									
78	S-8	58	1/100	65		109/100%	153	277 248	247		22530.1	48:10:45:47.47	
79	S-9	59	1/100	(79.90)	76% 109/10	109/100%	153/4	408 378	377	245	34918.1	48:14:12:15.49	
80	S-10	61	1/50	66	27/109		69/153	537 508	508	374 278	59926.3	48:21:09:3.69	1,
81				(81.90)	109	108/9 28/106/7	70	668 639	638	505 409	59934.2	48:21:09:11.59	
82					28/106/8	105	70/148	800 772	771	637 541	59942.2	48:21:09:19.59	2,
83				67	107 28/1056	105	70/148	932 903	902	769 672	59950.3	48:21:09:27.69	
84	S-11	62	1/100	(84.90)	105	105	148	064 035	033	901 804	72296.9	49:00:35:14.28	
85	S-13	63	1/25		105	104	147/8	193 165	164	031 935	84767.5	49:04:03:04.86	
86	P-7A	64	1/25		104/5	104	147/8	325 296	295	162 066	97312.2	49:07:32:09.51	
87				68	29/104	30/103/4	71/2	456 427	426	292 197	97314.5	49:07:32:11.87	3,
88					30/104	103	72/146	589 557	558	426 329	97316.8	49:07:32:14.17	
89				(89.90)	30/103	103	72/146	718 690	689	555 459	97319.0	49:07:32:16.37	
90				69	103	103/2	146/4	850 821	821	687 591	97321.5	49:07:32:18.87	
91					103	102	146/4	981 952	950	818 727	97323.4	49:07:32:20.77	
92				(92.90)	102	31/101/2	73/144	112 083	083	948 852	97325.8	49:07:32:23.17	
93				70	102	101	144/5	243 214	214	080 964	97328.0	49:07:32:25.37	
94	P-7B	65	1/25		31/101	32/101	73/4/144	374 346	345	212 115	4995.4	49:11:01:10.37	4,
95					101	100	143	503 475	474	340 244	4997.4	49:11:01:12.37	
96				(96.90)	32/100	33/100	74/5/143	637 608	607	474 377	4999.4	49:11:01:14.37	
97				71	33/100	99	75/142/3	768 739	738	605 509	5001.5	49:11:01:16.47	5,
98				(98.90)	33/99/100	34/98	75/6/142	899 871	871	735 639	5003.5	49:11:01:18.47	
99				72	34/99	99	76/142	029 000	000	866 770	5005.5	49:11:01:20.47	
100					34/99	35/98	76/7/141	161 133	131	998 902	5007.6	49:11:01:22.57	
R/O SEQ	FRAMELETS	R/O SEQ	FRAMELETS	*COMMENTS:									
027	335/307	98	463/091	1. R/O Sequence 27 erratic, #307 repeated 22 times.									
028	747/622	99	090/733	2. R/O Sequence 28 erratic, #622 repeated 6 times.									
029	278/203	100	732/358	3. R/O sequence 29 erratic, #262 repeated 13 times, #246 repeated 8 times.									
030	530/373	101	357/087	4. R/O Sequence 31 erratic, #175 repeated 14 times.									
031	177/091	102	086/823	5. Birnat pull off 97.85.									
032	448/386	103	831/481	6. R/O seq. 110, #169 repeated 43 times.									
033	708/576	104	480/094										
034	972/842	105	098/730										
035	234/108	106	738/888										
		107	736/849										
		108	648/436										
		109	433/169										
		110	169										
				5B 100% WA 58-76% T, 100% WA									

Table 3-2: PHOTO DATA SUMMARY (Continued)

FRAME	PHOTO		SHUT- TER SPEED	PROC ORBIT INDEX	R/O SEQ T	R/O SEQ WA	R/O ORBIT	EDGE WA NOS	TC FRMLT	EDGE TELE NOS	S/C TIME	EXPOSURE GMT	
	SITE	ORBIT											
101	P-7B	65	1/25	72	35/98	98	77/141	292 284	263	129 033	5009.6	49:11:01:24.57	
102	S-14	66	1/25		35/98	36/98	77/8	423 395	393	280 164	17407.6	49:14:28:02.57	
103	S-15	67	1/25	(103.86)	98	97	140/1	554 525	524	391 295	30005.7	49:17:58:00.67	
104				73	36/97	97	78/140	685 657	655	522 426	30014.2	49:17:58:09.17	
105				(105.86)	97	96/5	139/40	818 788	787	655 558	30022.7	49:17:58:17.67	
106				74	97	96	139	947 918	917	784 688	30031.2	49:17:58:26.17	
107	S-16	69	1/50	(107.86)	96	96	139	079 054	050	916 820	55101.0	50:00:56:15.96	4
108	S-17	70	1/50	75	96	95	138/9	209 181	180	047 949	67796.7	50:04:22:53.68	
109				(109.86)	95/6	37/95	79/138/9	339 311	310	176 080	67807.6	50:04:28:02.58	
110				76	37/95	95	79/138	471 443	442	308 212	67816.7	50:04:28:11.68	
111				(111.86)	37/95	94	79/137	804 575	573	440 344	67825.9	50:04:28:20.88	
112	S-18	71	1/50	77	94/5	94	137/8	735 706	705	572 475	80149.6	50:07:55:44.59	
113				(113.86)	94	38/93/4	80/136/7	864 835	834	701 605	80152.0	50:07:53:46.98	
114				78	38/94	93	80/136/7	995 967	966	832 737	80154.4	50:07:53:49.38	
115					38/93	93	80/136	128 099	098	965 868	80156.8	50:07:53:51.78	
116	S-19	72	1/50		93	92	135/136	260 231	230	087 000	92753.9	50:11:23:48.87	3
117					92/93	39/92	81/135/6	390 360	359	225 129	92762.1	50:11:23:57.07	
118					39/92	92	135	520 491	490	356 261	92770.4	50:11:24:05.37	
119					39/92	91	81/134/5	651 623	621	488 382	92778.9	50:11:24:13.87	2
120	S-21	74	1/50	(120.86)	91/92	91	134/135	783 756	752	639 523	12782.0	50:18:18:34.57	
121	S-21.5	74	1/50	79	91	91	134	909 883	880	747 651	16587.7	50:19:22:00.26	
122	S-22	75	1/25		91	40/90	133/134	043 016	013	881 785	25224.4	50:21:45:56.97	
123	S-20	76	1/25		40/90/.1	90	82/133/4	174 146	145	012 912	37664.6	51:01:13:17.5	1.
124	P-8	77	1/25	(124.86)	40/90	89/90	82/132/3	306 277	276	143 047	50339.7	51:04:44:32.26	
125				80	90	89	132/3	437 408	407	274 178	50341.7	51:04:44:34.26	
R/O SEQ	FRAMELETS		R/O SEQ	FRAMELETS		*COMMENTS:							
035	234/ 106		088	068/ 283		1. Frame smeared in direction of flight.							
036	494/ 413		090	282/ 928		2. Framelet 397 scanned 7 times.							
037	411/ 399		091	937/ 546		3. Framelet 076 scanned 19 times.							
038	947/ 817		092	884/ 194		4. #064 scanned 6 times, #886 scanned 12 times.							
039	473/ 346		093	195/ 846									
040	189/ 978		094	844/ 480									
			095	449/ 138									
			096	131/ 818									
			097	818/ 464									
			098	485/ 091									

Table 3-2: PHOTO DATA SUMMARY (Continued)

FRAME	PHOTO		SHUT- TER SPEED	PROC ORBIT INDEX	R/O SEQ T	R/O SEQ WA	R/O ORBIT	EDGE WA NOS	TC FRMIT	EDGE TELE NOS	S/C TIME	EXPOSURE GMT	
	SITE	ORBIT											
126	P-8	77	1/25	80	41/89	89	83/132	568 540	539	406 310	50343.7	51:04:44:36.26	1,
127					89	88	131	700 671	670	537 440	50345.7	51:04:44:38.26	
128				(128.86)	88/89	88	131/132	832 801	800	669 572	50347.8	51:04:44:40.36	
129				81	88	88	131	961 932	931	796 702	50349.8	51:04:44:42.36	
130					88	87	130	093 065	064	930 834	50351.8	51:04:44:44.36	
131	S-23	78	1/50		42/87/8	87	84/130	225 196	195	062 966	50353.8	51:04:44:46.36	
132					87	87	130	355 328	326	193 097	62926.3	51:08:14:20.27	
133				(133.86)	87	86	129/0	486 457	457	323 227	62936.1	51:08:14:29.67	
134				82	86/7	86	129/0	618 590	589	456 359	62946.0	51:08:14:38.57	
135	S-24	79	1/100	(135.86)	86	85	128/9	749 721	720	586 490	62956.0	51:08:14:48.57	7,
136	P-9A	80	1/50	83	85/6	85	128/9	881 853	851	718 622	75429.8	51:11:42:42.36	6,
137					43/85	44/84/5	85/6/127	011 981	980	847 751	87918.1	51:15:10:50.68	2,
138					85	84	127/8	142 113	112	979 883	87920.7	51:15:10:53.28	
139					44/84	84	86/127	247 246	244	111 015	87923.4	51:15:10:55.98	
140				(140.86)	84	83	126/7	405 377	375	245 146	87926.1	51:15:10:58.68	5
141				84	83/84	83	126/7	536 507	506	373 277	87928.7	51:15:11:01.28	3
142					83	83	126	667 637	636	503 407	87931.4	51:15:11:03.98	
143					83	45/82	87/126/5	799 770	769	635 539	87934.0	51:15:11:06.58	
144					45/83/2	82	87/126/5	929 901	900	766 671	87936.7	51:15:11:09.28	
145	P-9B	81	1/25		45/82	82	87/125	061 032	031	898 802	100459.5	51:18:39:52.06	4
146				(146.86)	82	46/81	88/124/5	190 161	160	027 930	100461.7	51:18:39:54.28	
147				85	46/81/2	81	88/124/5	324 295	294	160 065	100463.8	51:18:39:56.36	
148				(148.86)	46/81	80	88/123/4	455 426	425	292 195	100466.0	51:18:39:58.56	
149				86	80/81	80	123/124	585 557	556	422 326	100468.1	51:18:40:00.66	
150					80	47/80	89/123	716 688	686	553 457	100470.3	51:18:40:02.86	
R/O SEQ	FRAMELETS	R/O SEQ	FRAMELETS	*COMMENTS:									
041	390/362	080	775/411	1. R/O Sequence 41 erratic, #362 scanned 35 times.									
042	021/962	081	410/065	2. R/O Sequence 43 erratic, #808 scanned 30 times.									
043	819/808	082	064/707	3. R/O Sequence 83, #535 scanned 11 times.									
044	081/985	083	706/363	4. R/O Sequence 82, #876 scanned 10 times.									
045	898/730	084	381/999	5. R/O Sequence, #192 scanned 11 times.									
046	381/140	085	998/697	6. R/O Sequence 085, R/O stopped at #885, #884 scanned 14 times (137.84).									
047	740/658	086	888/383	7. R/O Sequence 088, R/O stopped at 135.06, #408 scanned 10 times, PSL at 135.83.									
		087	361/024										
		088	024/080										

Table 3-2: PHOTO DATA SUMMARY (Continued)

FRAME	PHOTO		SHUT- TER SPEED	PROC ORBIT INDEX	R/O SEQ T	R/O SEQ WA	R/O ORBIT	EDGE WA NOS	TC FRMLT	EDGE TELE NOS	S/C TIME	EXPOSURE GMT	
	SITE	ORBIT											
151	P9B	81	1/25	86	47	79	89/122	848 819	818	685 588	100472.4	51:18:40:4.96	
152					47/79	79	89/122	979 950	948	816 719	100474.6	51:18:40:07.16	
153	P9C	82	1/25		79	48/79	90/122	110 061	060	946 850	8135.8	51:22:08:45.97	
154				(154.86)	79	78	121/2	240 211	210	981 077	8138.0	51:22:08:48.17	
155				87	48/78/9	78	90/121/2	373 344	343	210 113	8140.2	51:22:08:50.37	
156					78	77/8	120/1	502 474	472	337 243	8142.4	51:22:08:52.57	6.
157				(157.86)	78	77	120/1	634 607	605	471 375	8144.6	51:22:08:54.77	5.
158				88	77	77	120	765 736	735	602 506	8146.8	51:22:08:56.97	4.
159					77	76	119/20	897 868	867	734 637	8149.0	51:22:08:59.17	4.
160					76/7	76	119/20	027 999	996	865 766	8151.2	51:22:09:01.37	
161	S-25	83	1/50	(161.86)	76	76	119	158 130	128	995 899	20427.7	52:01:33:37.87	
162	S-26	84	1/25	89	76	49/76/5	91/119/8	290 257	256	123 029	32931.2	52:05:02:01.35	
163	P-10	86	1/25		49/76/5	75	91/119/8	420 392	390	258 161	57971.4	52:11:59:21.58	
164				(164.86)	49/75	74	91/117/8	552 523	522	392 292	57973.9	52:11:59:24.06	
165				90	75	74/5	117/8	683 655	654	520 424	57976.3	52:11:59:26.48	3
166					74	50/74	92/117	813 785	784	651 553	57978.8	52:11:59:28.96	
167					50/74	73	92/116/7	945 917	916	783 686	57981.2	52:11:59:31.38	
168					50/73/74	73	92/116	076 049	047	913 816	57983.6	52:11:59:33.78	
169					73	73	116	207 178	177	044 948	56986.0	52:11:59:36.18	
170					73	72	115/116	388 310	309	175 079	57988.5	52:11:59:38.68	
171	S-27	87	1/100		72/73	72	115/116	470 443	441	306 211	70672.2	52:15:31:02.39	
172	S-28	88	1/100		72	72	115	601 572	567	434 337	83102.4	52:18:58:12.57	
173	P-11	89	1/25	(173.86)	72	71	115/114	732 704	703	569 473	95688.7	52:22:27:58.87	
174				91	72/71	51/71	93/115/4	863 834	833	700 604	95691.0	52:22:28:01.17	1
175					51/71	71	93/114	996 967	966	833 737	95693.4	52:22:28:03.57	2.
R/O SEQ	FRAMELETS	R/O SEQ	FRAMELETS	*COMMENTS:									
047	740/655	071	000/650	1. R/O Sequence 51 erratic, short scan advances; #803 scanned 6 times.									
048	180/090	072	640/264	2. Sequence 71, hangup 813 scanned 13 times.									
049	356/229	073	263/878	3. Sequence 74, hangup 678 scanned 13 times.									
050	883/766	074	877/523	4. R/O Sequence 77, #699 scanned 11 times, #578 scanned 12 times.									
061	925/808	075	822/179	5. PSL at 157.81 (#491).									
		076	178/817	6. R/O stopped during 078 at #307, 156.49.									
		077	816/488										
		078	491/137										

Table 3-2: PHOTO DATA SUMMARY (Continued)

FRAME	PHOTO		SHUT- TER SPEED	PROC ORBIT INDEX	R/O SEQ T	R/O SEQ WA	R/O ORBIT	EDGE WA NOS	TC FRMLT	EDGE TELE NOS	S/C TIME	EXPOSURE GMT	*
	SITE	ORBIT											
176	P-11	89	1/25	91	51/71	70	93	125 096	095	962 866	95695.7	52:22:28:5.87	1,
177				(177.86)	70	70	113	257 228	227	094 998	95698.0	52:22:28:8.17	
178				92	70	69/70	112	387 358	356	223 127	95700.4	52:22:28:10.67	
179					70	69	112	518 489	488	355 259	95702.8	52:22:28:12.97	
180					69	69	112	650 621	620	487 391	95705.1	52:22:28:15.27	
181	P12B2	90	1/25		52/68/9	69	94/111/2	781 753	752	619 522	3266.4	53:01:55:14.15	2,
182					69	68	111/2	910 882	881	747 651	3268.8	53:01:55:16.55	6,
183					53/68	68	95/111	044 015	014	881 785	3271.2	53:01:55:18.95	3,6
184					68	67	110/1	175 146	145	010 916	3273.6	53:01:55:21.35	6,
185	P-12A	91	1/25	(185.86)	67/8	67	110/1	306 277	276	143 047	15785.3	53:05:23:53.06	6,
186				93	67	67	110	436 407	406	273 177	15787.7	53:05:23:55.46	
187					67	66	109/10	569 540	539	706 316	15790.1	53:05:23:57.86	
188					54/66/7	66	96/109/10	699 670	667	536 439	15792.5	53:05:24:00.26	4,
189					66	65/6	108/9	830 801	800	667 570	15794.8	53:05:24:02.56	
190				(190.86)	66	65	108/9	960 931	930	707 701	15797.2	53:05:24:04.96	
191				94	55/65/6	65	97/108/9	091 063	062	929 831	15799.6	53:05:24:07.36	5,
192				(192.86)	65	65	108	224 195	194	060 964	15802.0	53:05:24:09.76	
193				95	65	64/5	107/8	354 325	323	191 095	15804.4	53:05:24:12.16	
194					64	64	107	485 456	456	322 226	15806.8	53:05:24:14.56	
195					64	64	107	617 588	588	454 358	15809.2	53:05:24:16.96	
196					64	63	106/7	747 720	717	595 488	15811.6	53:05:24:19.36	
197				(197.86)	63/4	63	106/7	879 850	849	716 620	15813.9	53:05:24:21.66	
198				96	63	63	106	010 981	980	841 751	15816.3	53:05:24:24.06	
199						62	105	141 113	111	979 882	15818.7	53:05:24:26.46	
200				200.86	62/3	62	105	273 244	243	109 013	15821.1	53:05:24:28.86	
R/O SEQ	FRAMELETS	R/O SEQ	FRAMELETS	*COMMENTS:									
051	925/803	066	889/484	1. R/O Seq. 51 erratic, #803 scanned 6 times.									
052	506/505	067	433/088	2. R/O Seq. 52 erratic: #565 scanned 13 + 24 times,									
053	640/622	068	068/758	3. R/O Seq. 53 erratic, #822 scanned 10 + 24 times.									
064	479/487	069	737/381	4. R/O Seq. 54 erratic: #457 scanned 6 times.									
066	678/677	070	389/801	5. R/O Seq. 55 erratic.									
068	419/888	071	888/888	6. R/O Seq. 68 erratic, #898 repeated 18 times, #883 repeat- ed 9 times, #848 repeated 11 times, R/O terminated and restarted.									
069	684/677												
064	678/388												
066	387/891												

Table 3-2: PHOTO DATA SUMMARY (Continued)

FRAME	PHOTO		SHUT- TER SPEED	PROC ORBIT INDEX	R/O SEQ T	R/O SEQ WA	R/O ORBIT	EDGE WA NOS	TC FRMLT	EDGE TELE NOS	S/C TIME	EXPOSURE GMT	
	SITE	ORBIT											
201	P12B1	92	1/25	(200.86)	62	62	105	403 375	373	241 144	28344.6	53:08:53:12.36	
202				97	62	61	104 / 5	534 505	504	371 274	28346.7	53:08:53:14.66	
203					61/2	61	104/5	666 638	637	504 407	28349.3	53:08:53:17.06	
204					61	60/1	103/4	796 767	766	633 537	28351.7	53:08:53:19.46	
205	P-12C	93	1/25	(205.87)	61	60	103	928 900	899	765 689	40654.5	53:12:21:42.28	
206				98	60	60	103	058 031	028	884 798	40657.3	53:12:21:45.06	
207					60		103	192 162	161	028 932	40660.1	53:12:21:47.88	
208					59/60	59	102/3	321 292	291	158 061	40662.9	53:12:21:51.68	
209					59	58/9	101/2	453 424	423	290 194	40665.8	53:12:21:53.58	
210					59	58	101/2	584 554	553	420 323	40668.6	53:12:21:56.38	
211					58	58	101	714 686	685	552 455	40671.4	53:12:21:59.18	
212					58	57	100/1	846 817	816	686 587	40674.3	53:12:22:02.07	
213	S-29	94	1/50		57/8	57	100/1	976 947	946	814 718	53168.7	53:15:46:56.47	
214	S-30	96	1/25		57	56	99/100	108 079	078	945 847	78136.4	53:22:43:04.17	
215	S-31	97	1/25		56/7	56	99/100	236 206	207	074 979	90636.1	54:02:11:23.89	
216	FILM ADVANCE	98			56		99						
217					56		99						
218													
219				(219.27)									
220				(BIMAT) CLEAR									
221													
222													
223													
224													
227													
R/O SEQ	FRAMELETS	R/O SEQ	FRAMELETS	*COMMENTS:									
056	285/030												
057	029/804												
058	809/488												
060	448/110												
069	188/773												
081	772/420												
082	419/055												

Prior to the cislunar phase, the photo subsystem thermal environment was controlled as required during prelaunch pad testing. At 035:17:18:36 the photo subsystem heaters were uninhibited. At 035:19:40:41, the heaters were inhibited and remained in that state throughout the cislunar phase. During cislunar, the photo subsystem thermal environment was basically slaved to the equipment mounting deck temperatures. Spacecraft pitch angles were selected to keep the spacecraft and consequently the photo subsystem temperatures at acceptable levels. Average Bimat temperature during this phase was maintained at a very acceptable 48°F level.

Just prior to orbit injection, the heater inhibit was removed (at 039:20:40:00) to provide the photo subsystem with a source of heat during the injection night period and the following orbital night periods. At this point solar eclipse was on and, consequently, only the night heaters were active. This thermal control method, along with desirable pitch angles, provided the photo subsystem with an acceptable and stable thermal environment. During this phase, Bimat temperatures averaged about 63°F.

Seven orbits prior to Site I photos, normal cycling of the day and night photo subsystem heaters was initiated (at 045:09:29:22). It was done at this time to thermally stabilize all photo subsystem components in anticipation of site photos. This cycling of the heaters was continued throughout the remainder of the mission and provided acceptable thermal control. The thermal history of the system is presented in Figures 3-1 through -9.

3.1.2 CAMERA FILM ADVANCES

The average camera film advance for Mission III was 11.70 inches or 130 ± 1 edge numbers as reported in the data package for PS-5. The edge numbers reported in the readout

analysis logs are listed in Table 3-1. Data on the film advances are plotted in Figure 3-10 for Frames 80 through 215. The plot shows that film advance through the camera was quite accurate and that any errors were due to film set and not mechanical encoder errors since the errors are a short advance followed by a long advance on the first or second advances. There was an anomalous film advance with no "camera on" command during operational readiness test ORT-1 prior to the final countdown; this advance was attributed to a ground power fluctuation. The first film advance to place live film in position for exposure was planned to be an 11-frame advance but this was changed to 10 frames due to the inadvertent pre-countdown advance. Since readout is incomplete up to Frame 79, the data is not plotted for those frames, but no errors other than film set errors were detected. Camera film handling was satisfactory during Mission III.

3.1.3 Processor Operation and Readout Film Handling

3.1.3.1 Processor Operation

The average processor rate for Mission III was 2.42 inches per minute, well inside the 2.40 ± 0.10 inches-per-minute specified rate. At least two frames were processed each orbit to minimize Bimat dryout effects.

Data from the prelaunch film loading was used for the H & D curve for the flight film during the mission. The analysis conducted by the video engineers and data supplied later from Eastman Kodak, has resulted in H & D curve is shown in Figure 3-11. Several interesting characteristics of this curve may be noted from its shape. Gamma is about 0.99 over the dynamic range that could be read out by the photo subsystem. There is a long "toe" on the curve and Bimat processing variations were less noticeable than on prior missions. Focus and gain changes during readout were not required as often as on

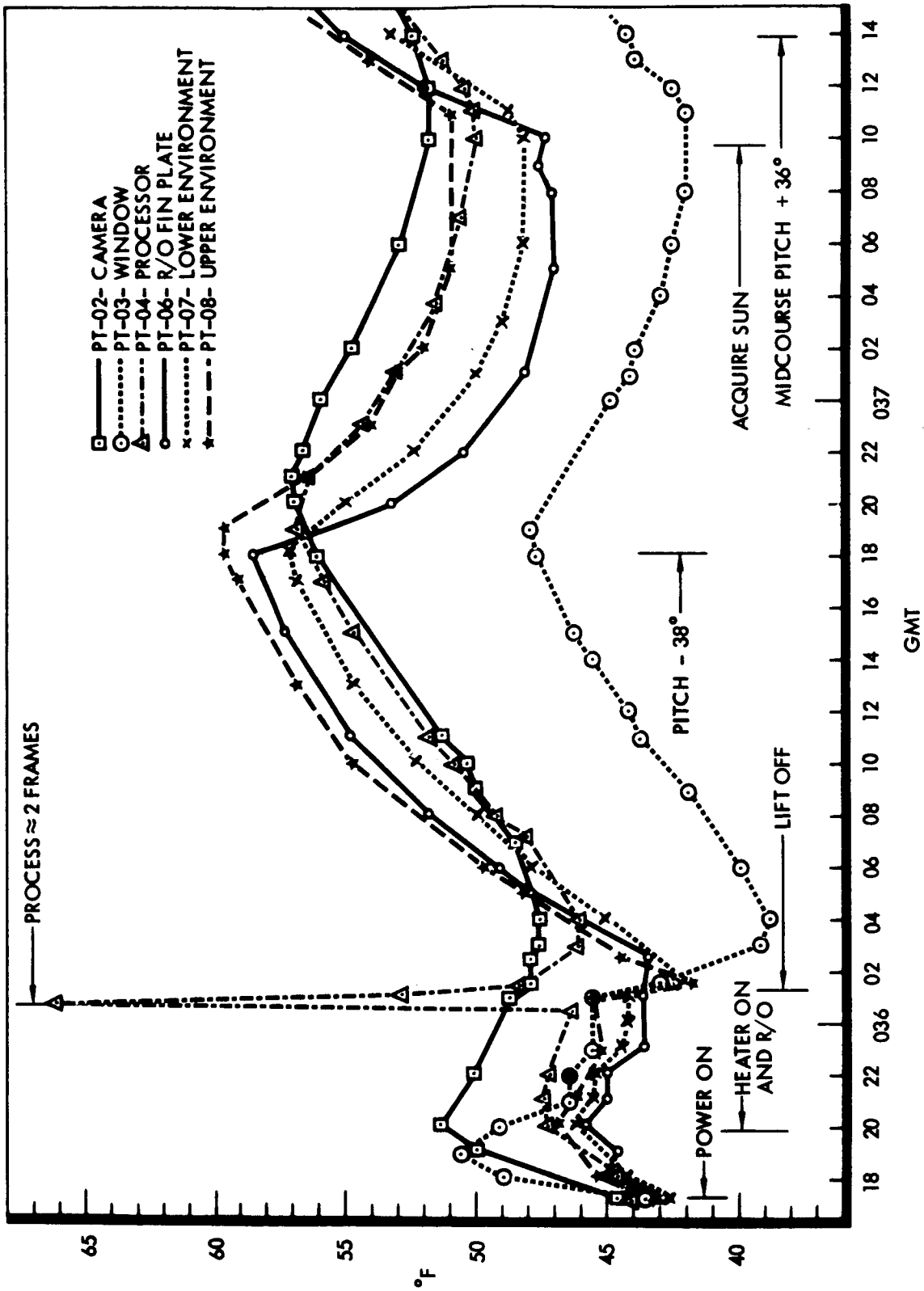


Figure 3-1: Photo Subsystem Cislunar Temperatures

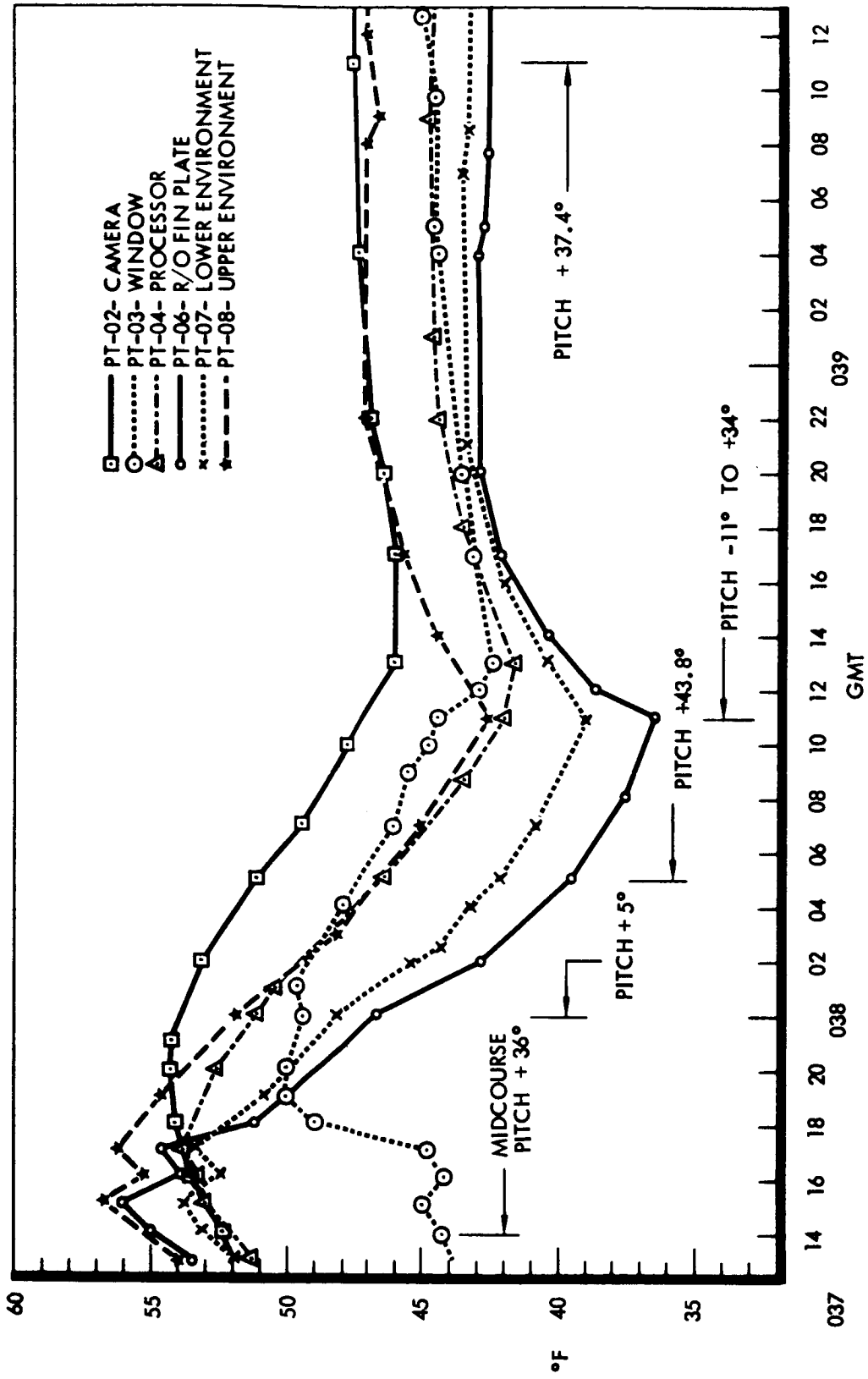


Figure 3-2: Photo Subsystem Cislunar Temperatures

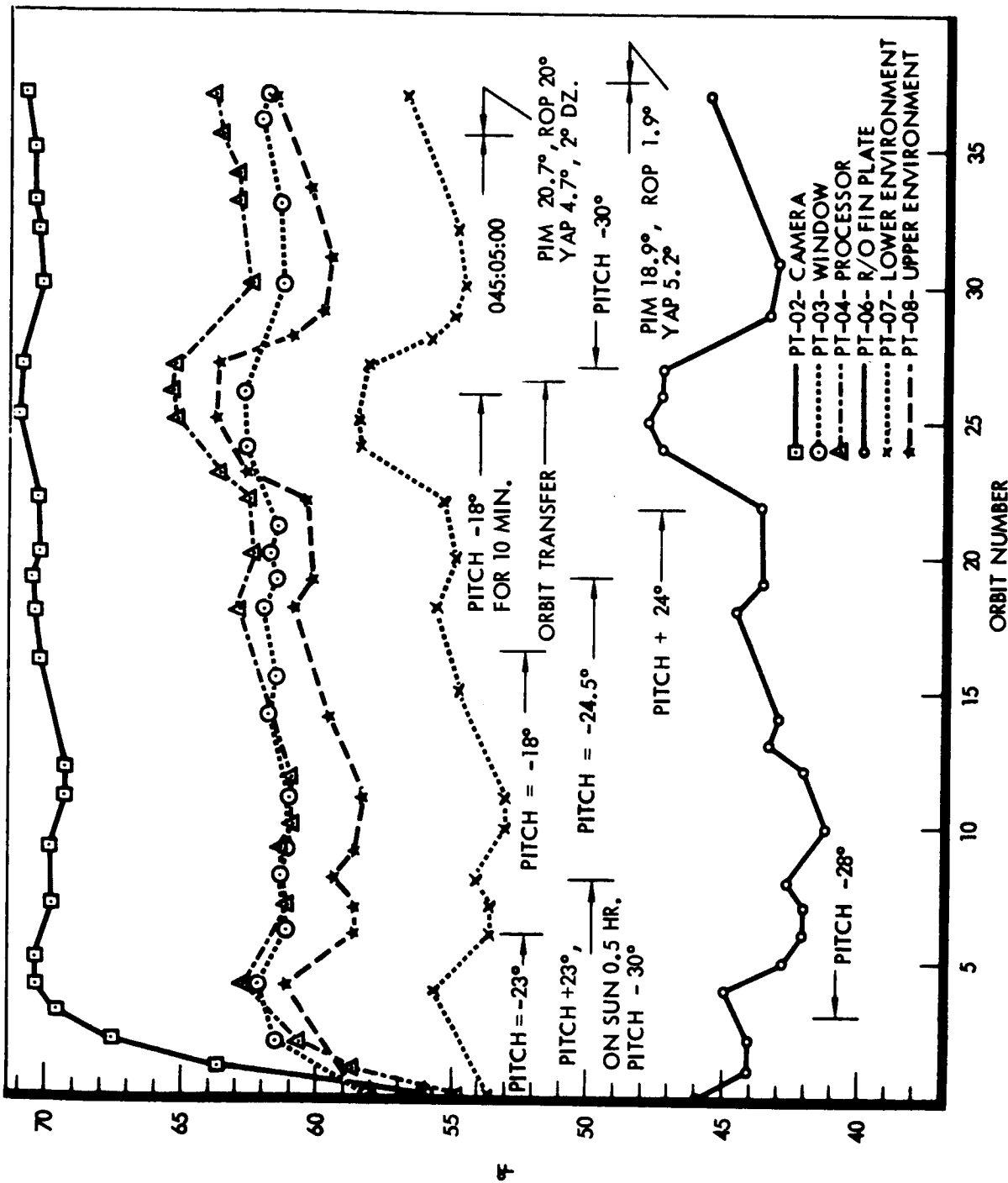


Figure 3-4: Photo Subsystem Sunrise Temperatures

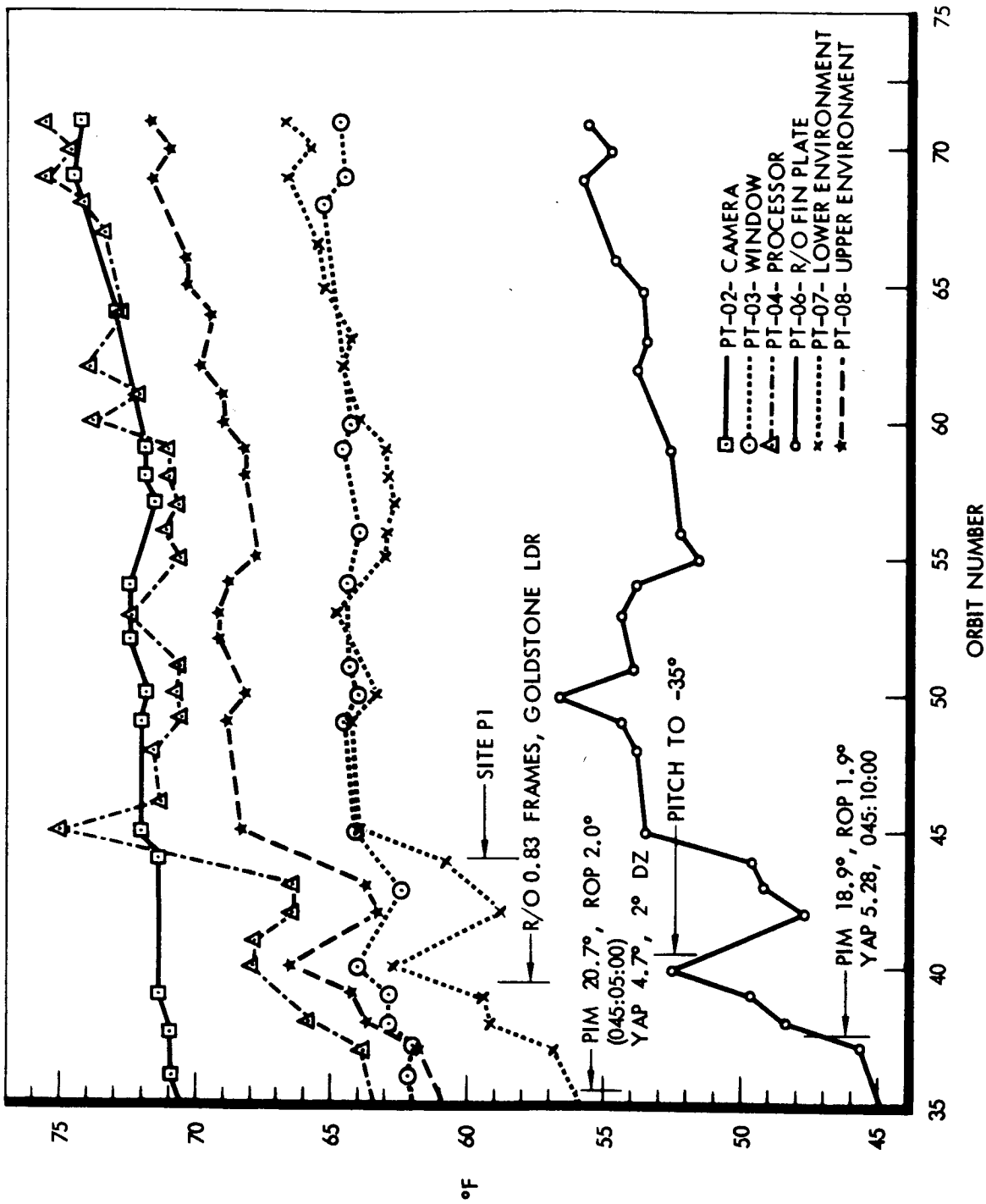


Figure 3-5: Photo Subsystem Sunrise Temperatures

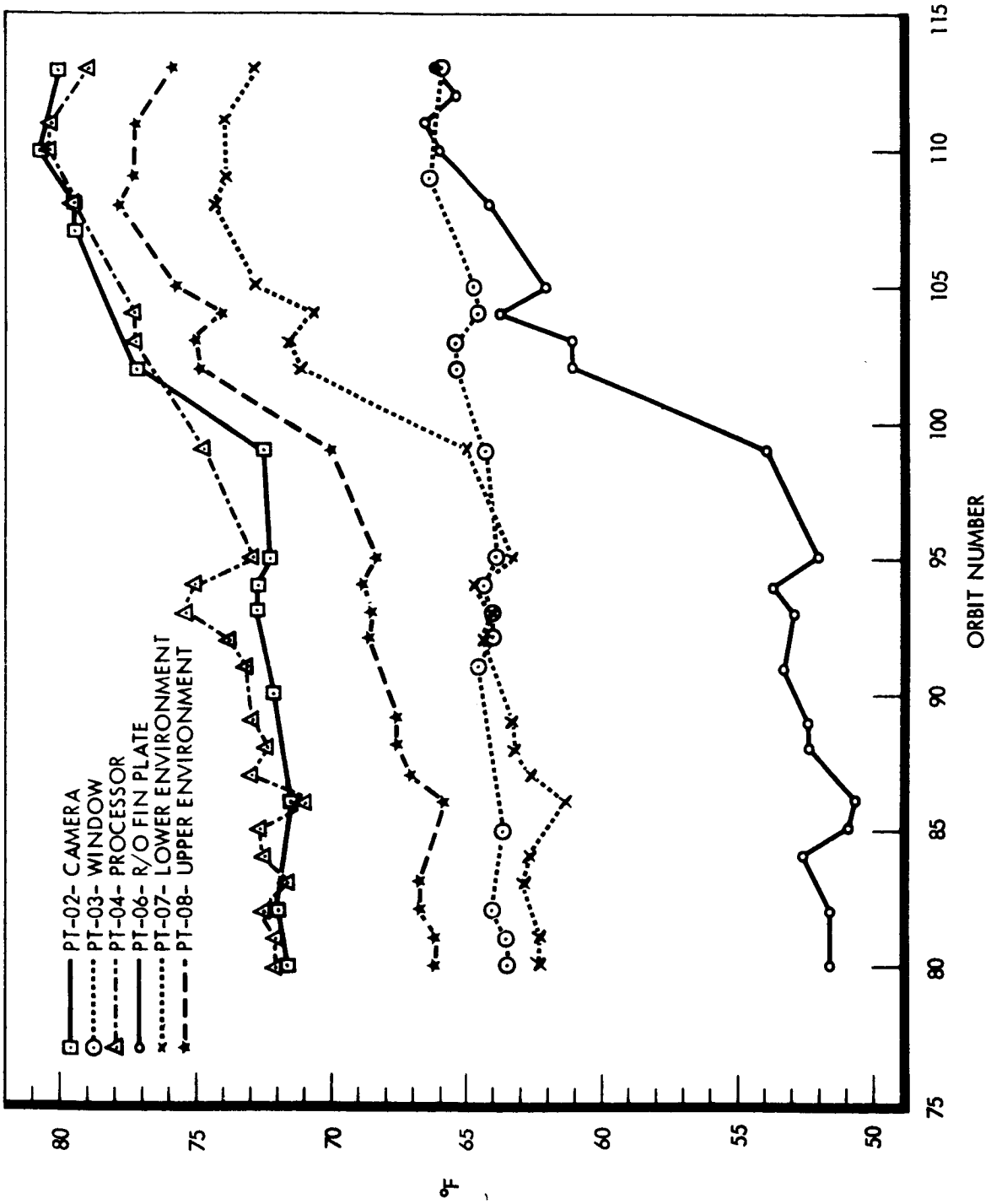


Figure 3-6: Photo Subsystem Sunrise Temperatures

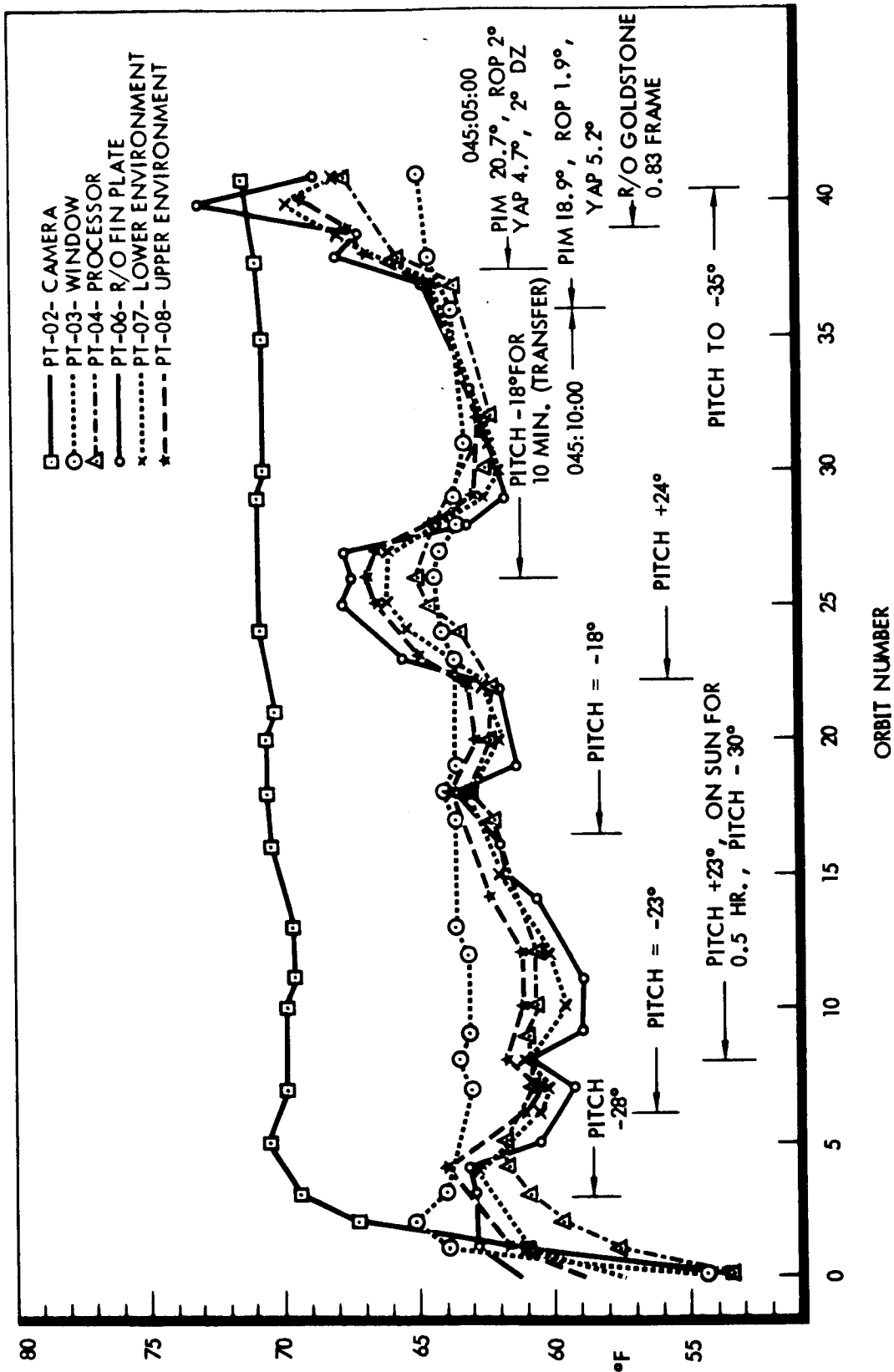


Figure 3-7: Photo Subsystem Sunset Temperatures

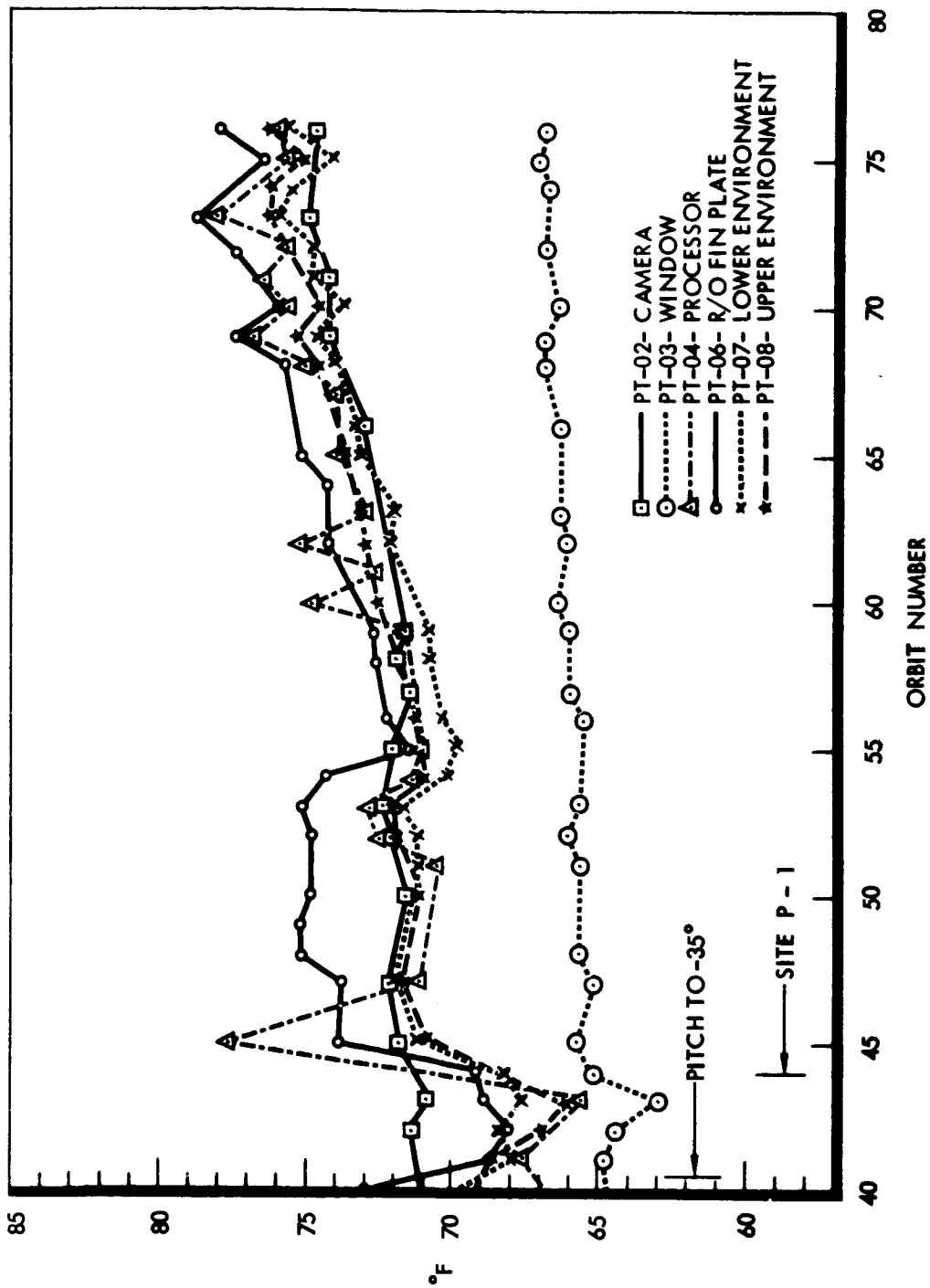


Figure 3-8: Photo Subsystem Sunset Temperatures

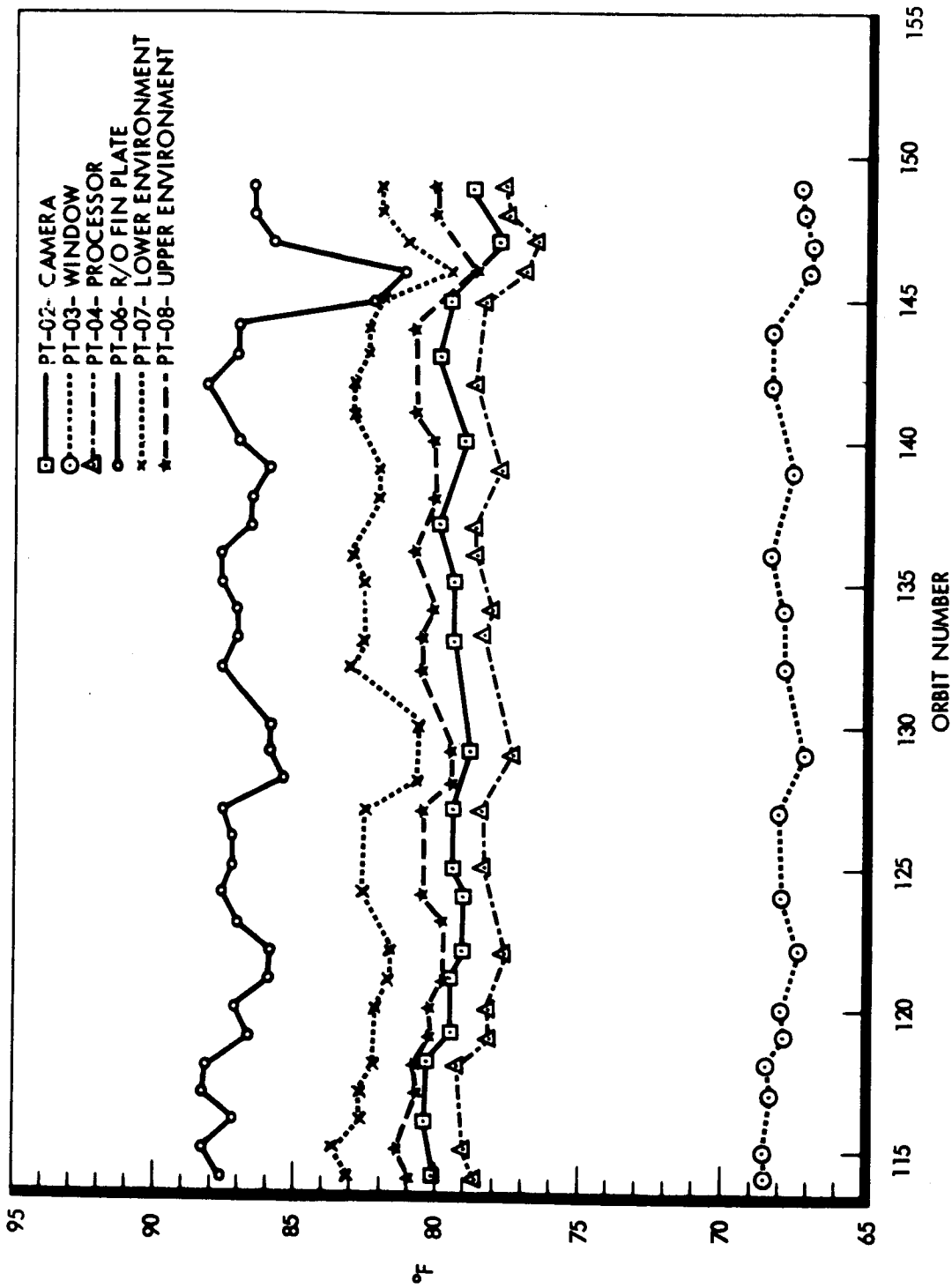


Figure 3-9: Photo Subsystem Sunset Temperatures

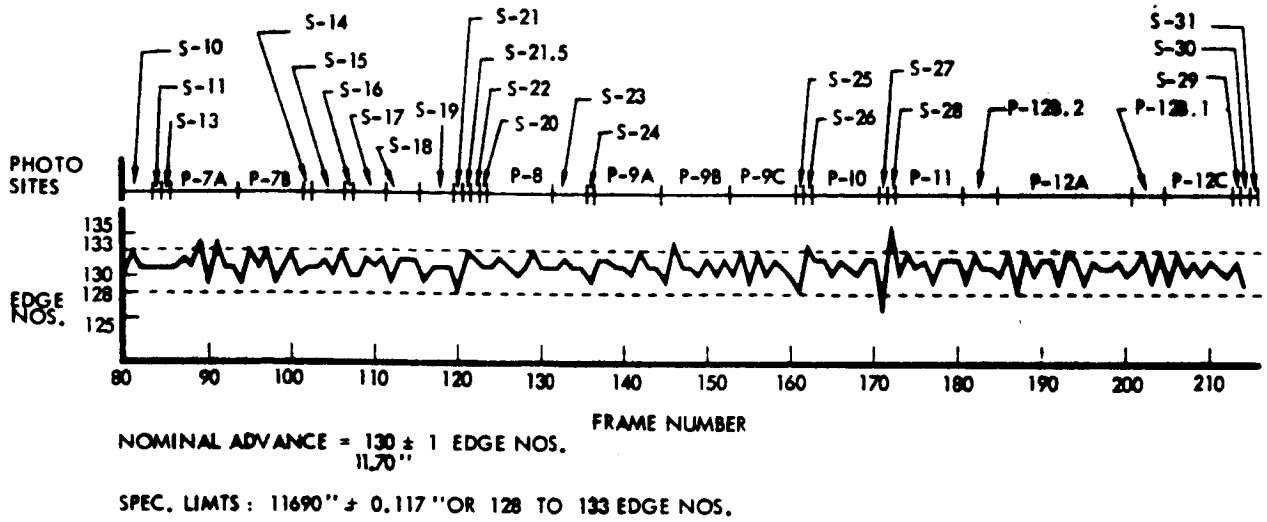


Figure 3-10: Camera Film Advances

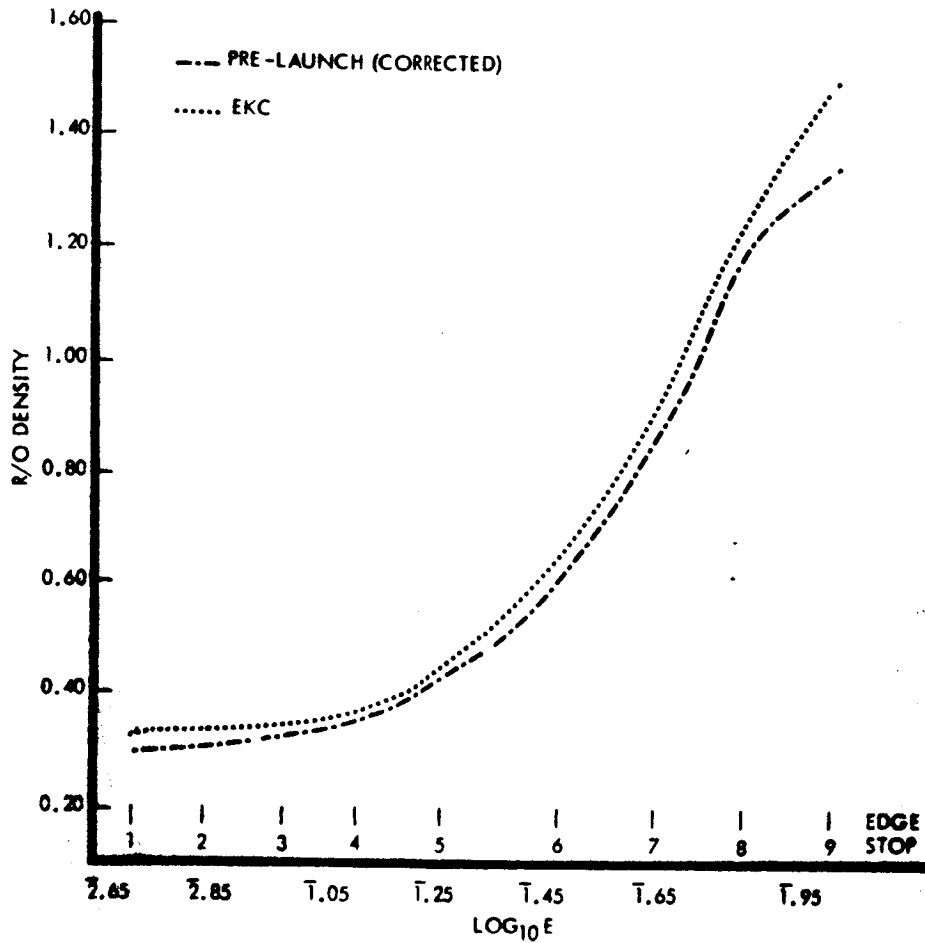


Figure 3-11: H&D Curve for SO-243

previous missions. Also, this is the first mission in which the Bimat life was not exceeded. After Orbit 54 the processing schedule was maintained to place the stop lines in the wide-angle subframes.

Some film advance irregularities were observed in the readout looper during processing when the loopers were emptied during the countdown, and during the first processing period of the mission. This was attributed to the lack of friction on the leader in passing through the system. After SO-243 film entered the system, readout looper and take-up looper operation was normal during the remainder of Mission III. Bimat cut was performed normally. The last three attempts at priority readout were completely unsuccessful.

3.1.3.2 Readout Film Handling

Priority readout was conducted normally as scheduled in the flight operations plan until Readout Sequence 25 in Orbit 68. At that time telemetry indicated that normal film advance was interrupted. Postmission analysis and photo subsystem testing indicated that film movement was being obstructed by one of the readout looper mounting screws. The following plan was developed by the operations team to continue with readout.

- 1) Transmit "R/O electronics on" command after four telemetry frames showing no film advance.
- 2) Execute the command after 10 telemetry frames showing no film advance.
- 3) Wait 10 minutes, transmit and execute the "R/O drive on" command.

This procedure was used successfully until Orbit 98 when three attempts at priority readout were made with no film advance. Due to this condition and the possible consequences if further readout were tried, Bimat was cut

one orbit sooner than planned, canceling the last secondary photo site. The mission continued into the final readout mode with no abnormality until Readout Sequence 68 when again the film advance stoppage occurred. The flight operations team developed a second plan to continue readout by emptying the readout looper when telemetry indicated 19 inches of film in the looper or when stoppage occurred. Final readout continued in this manner, averaging 2.7 frames per orbit, until the anomaly discussed earlier in this section occurred. The plans developed to overcome the film advance problem were completely successful in that there was no loss of data directly attributable to this problem.

3.1.4 Photo Data Analysis

3.1.4.1 White-Level Variation

For purposes of this discussion, "white level" is defined as the GRE video output level as observed on an oscilloscope when the OMS is in the "focus stop" position. This position is a controlled-density area of approximately 0.30 readout density, provided the spacecraft film has been properly processed. A density of 0.30 will produce a white level of 5.0 volts. A density greater than 0.3 will produce a white level of less than 5.0 volts. The focus stop position, therefore, is used to measure spacecraft photo video chain (PVC) gain provided the spacecraft film at this point is believed to have been processed properly. To determine these spacecraft film areas of proper processing, periodic white-level reports were given verbally to the photo data analyst or were included in the video analysis reports. These reports confirmed the significant variations between the processing stop line (PSL) and the Bimat pull-off line (BPO). Therefore, no gain changes were to be made while scanning in this area. These areas could be reasonably predicted because the PSL is in this area. These areas could be reasonably

located at the processor index. The processor indices are tabulated in the film status log and are reproduced in the photo data summary (Table 3-2).

The processor index is defined as that point where the fresh Bimat and the undeveloped spacecraft film initially come into contact. It is manifested on the spacecraft film by a straight line across the frame about one-fourth of a framelet in width. The actual location of a processor stop line is uncertain, however, until it is actually read out along with a frame edge. This did not occur until Readout Sequence 018. Therefore, the processor indices up to this time were not precisely known. This accounted for the im-

proper gain increase command sent at the start of Readout Sequence 010 (Figure 3-12), resulting in abnormally high spacecraft gain.

The BPO is not tabulated but can be considered to be about one frame pair (i.e., a telephoto and a wide-angle pair) in ahead of the PSL. It is caused by the Bimat obliquely leaving the Bimat supply reel and, therefore, is manifested on the spacecraft film by an oblique line, highly curved at one end, crossing about seven framelets.

3.1.4.2 Video Analysis Reports

The video analysis reports prepared by the video engineers include the measured white level at specific points

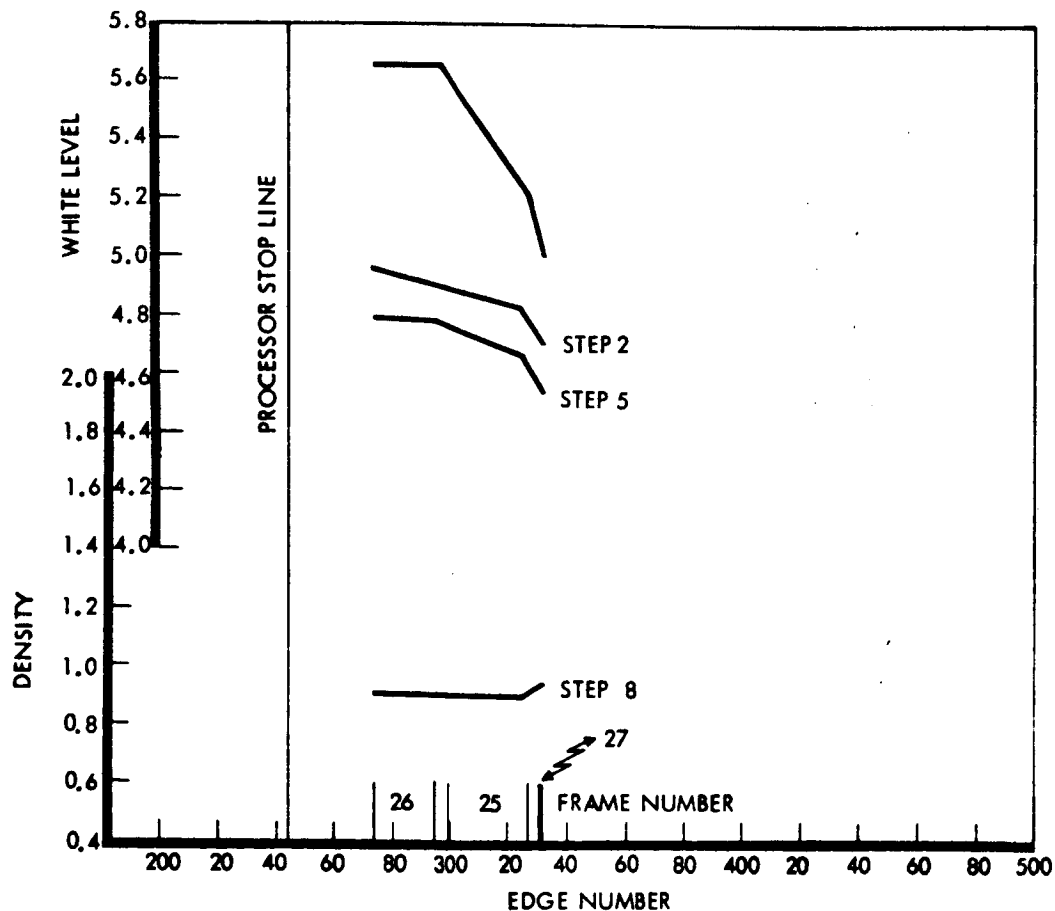


Figure 3-12: White-Level Densities—Readout Sequence 010

and certain measured GRE densities. The procedure for reporting the video analysis reports is covered in Section 10 of the Tracking Instruction Manual, Volume III.

Essentially, reports are made at the time of observation of the spaces between the telephoto and the wide-angle frames, and at 10 and 20 minutes into the telephoto frame. The measured GRE densities are edge data Steps 2, 5, and 8. During priority readouts, video analysis reports were made for each readout. During final readout, video analysis reports were made for selected readouts only, usually one readout per station view period

3.1.4.3 White-Level Variation Plots

The data from the video analysis reports are plotted on the white-level variation plots. Selected plots are included in this section for analysis.

Several of the plots also show edge data step densities from the readout analysis logs and density variations along the center of a framelet. The edge data steps are shown as data with the appropriate step number. The density variations are plotted using the left-hand density scale and an outline of a framelet. A discussion of these density variations is covered further in a section below.

3.1.4.4 Analysis of Data

Several phenomena should be observed on the white-level variation plots. First, there is a variation for almost every readout, even when processing effects are felt to be insignificant (Figures 3-13 and 3-14). Much of this variation is believed to be caused by the limited precision available in acquiring the data: the video engineer must take the reading from an oscilloscope of a rapidly changing pattern. The white level is reported only to the nearest 0.1 volt. Steps 2, 5, and 8, however,

follow the white level report very closely. The scale, therefore, used to plot the variation tends to exaggerate the variations.

Secondly, there is a significant variation that starts just before the PSL (Figures 3-15, -16, -17, and -18). Typically, the white level increases as the PSL is approached, decreases shortly afterwards to a minimum between the PSL and the BPO, and rises as the BPO is approached, then tends to level off.

Thirdly, the minimum white level appears to be a function of the interval of processing the total Bimat age. For example, the first few frames processed, Readout Sequence 007, Figure 3-17, were processed by Bimat in which the interval of processing was long, whereas for the last few frames processed the minimum white level is less. It is assumed that dryout is more pronounced in the outside layers of the Bimat than in the inner layers. As the Bimat ages, all of the Bimat is dryer and the additional dryout in the area between the processor index and the Bimat supply reel pull-off is less

Bimat effects are caused by the following. The Bimat imbibant is better retained while the Bimat is on its supply reel than when it is in the diffusion channel between the Bimat pull-off and the processor index. The Bimat in this region tends to dry out. Although the Bimat process is supposed to go to completion, more than likely only the developing action does as it is accomplished very quickly. The fixing action, however, has a much longer time requirement (hence the long time on the processing drum) and film that is not entirely fixed will exhibit a greater density than completely fixed film. This greater density in the spacecraft film accounts for the decrease in white level.

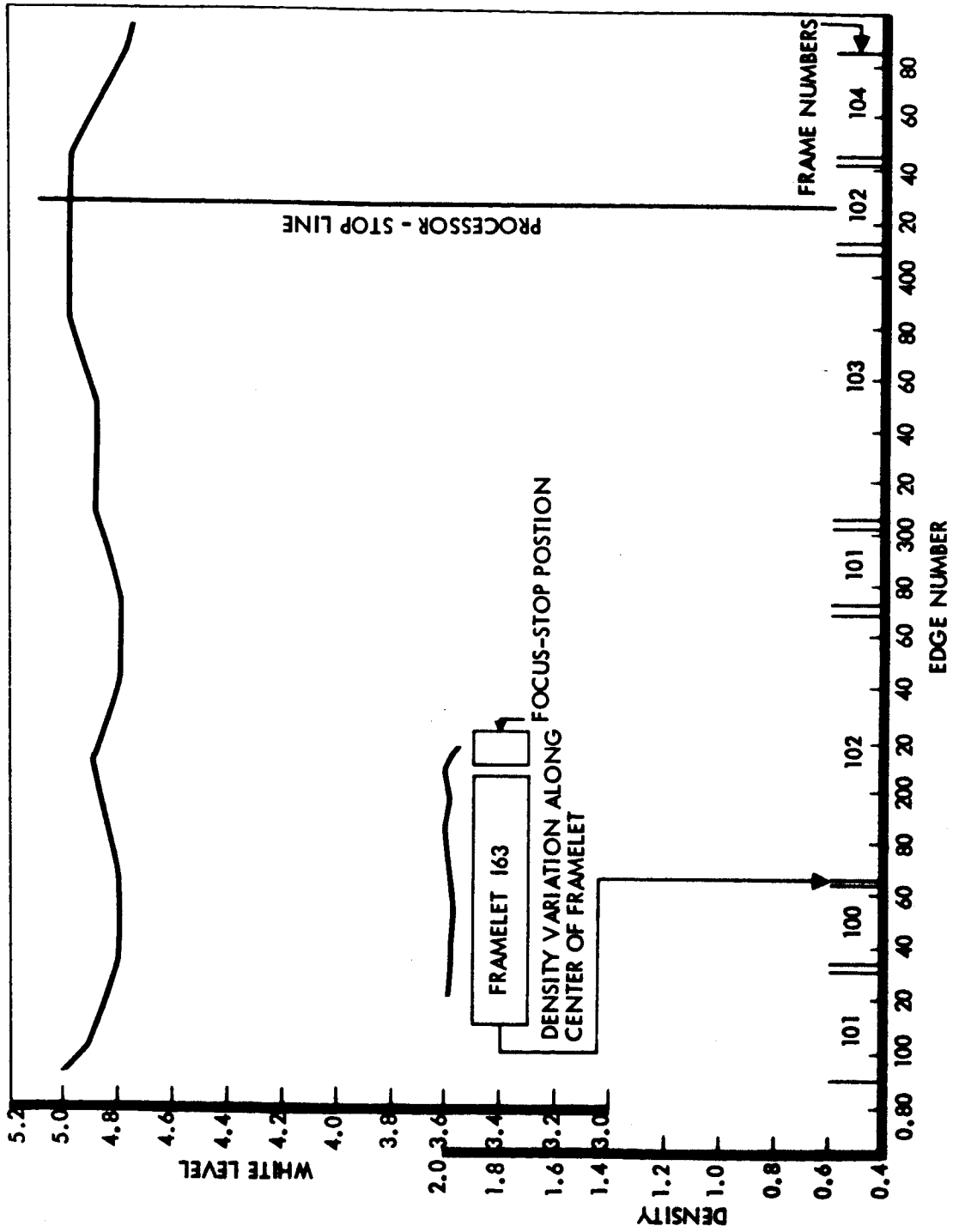


Figure 3-13: White-Level Densities—Readout Sequence 098

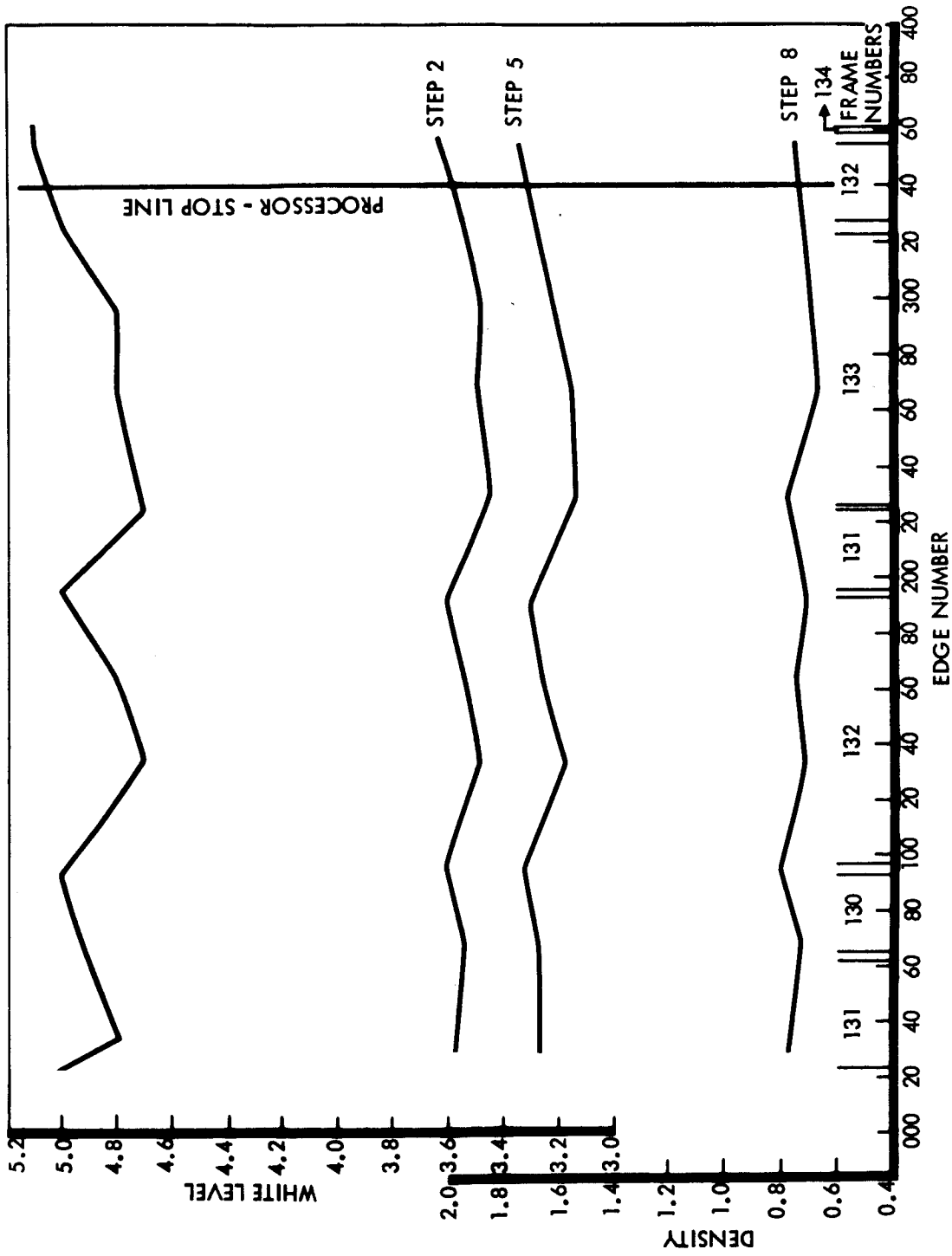


Figure 3-14: White-Level Densities—Readout Sequence 087

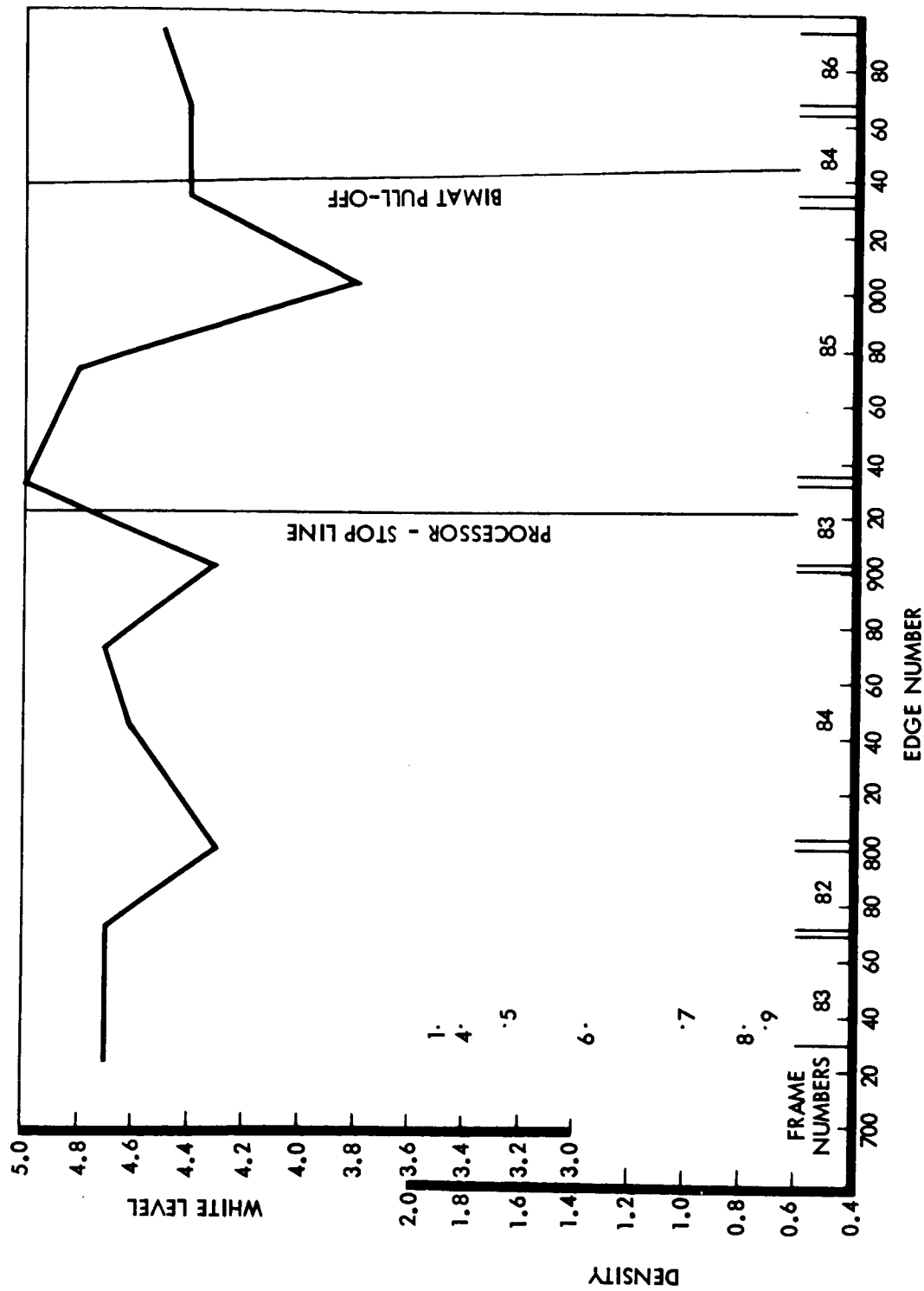


Figure 3-15: White-Level Densities—Readout Sequence 105

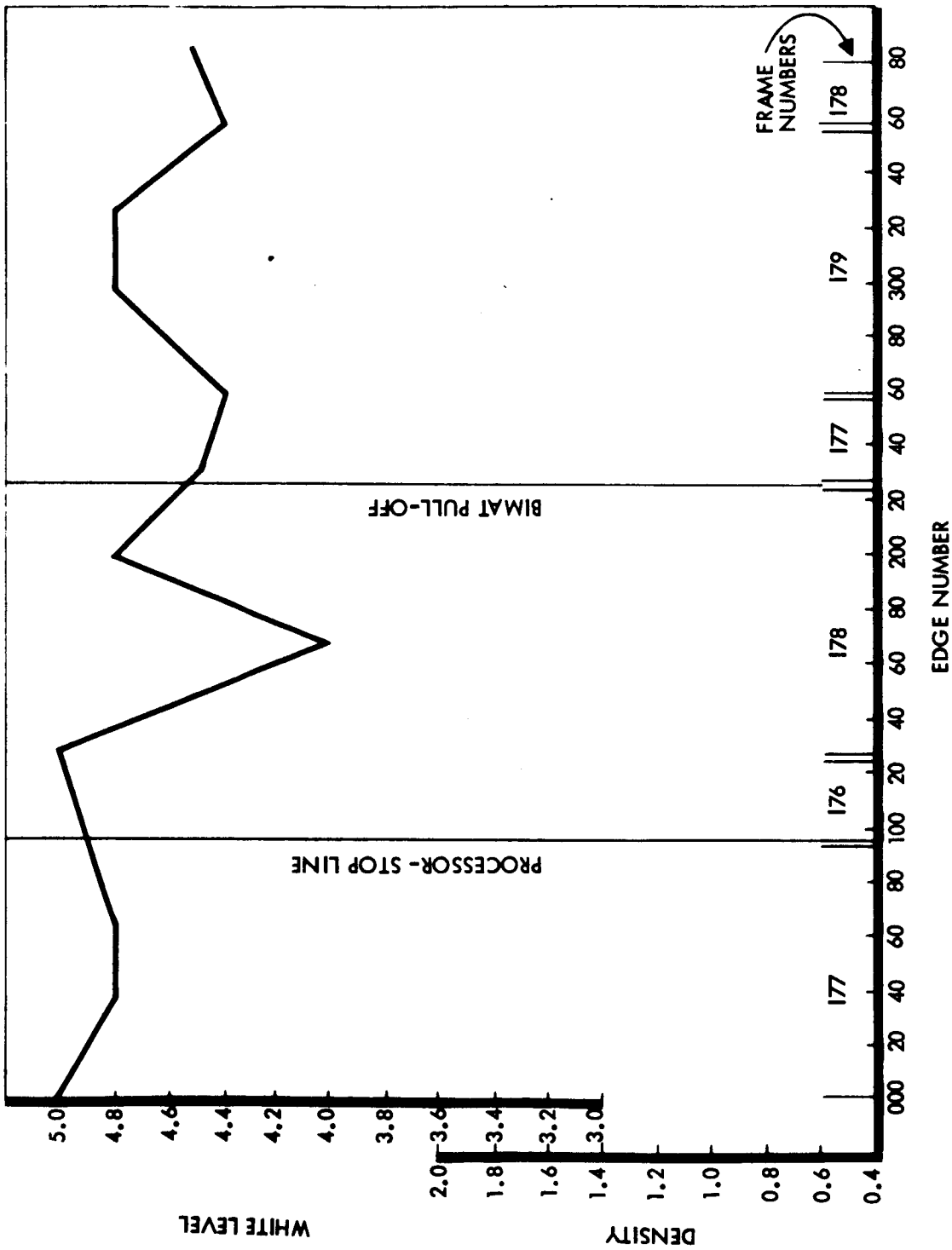


Figure 3-16: White-Level Densities—Readout Sequence 070

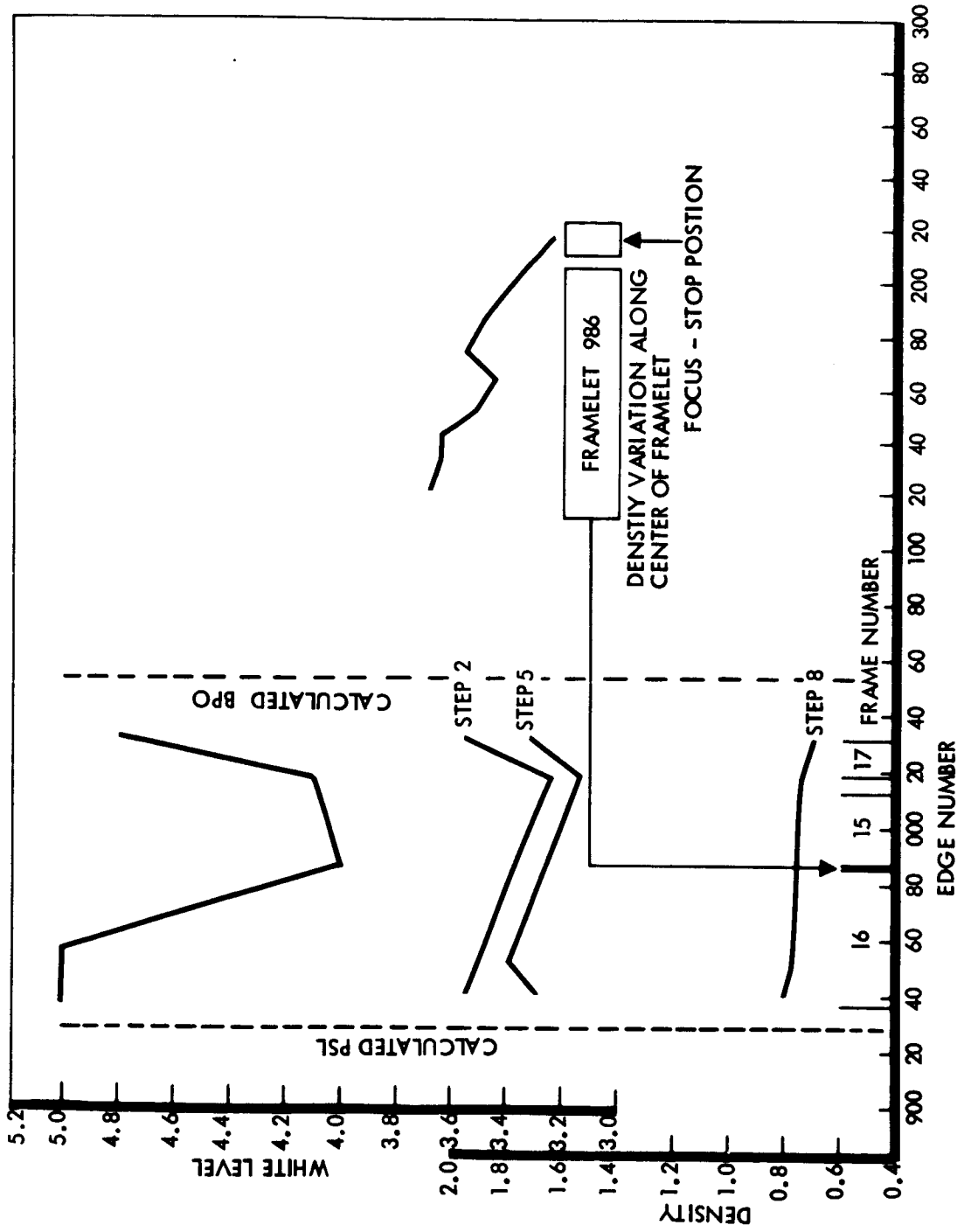


Figure 3-17: White-Level Densities—Readout Sequence 007

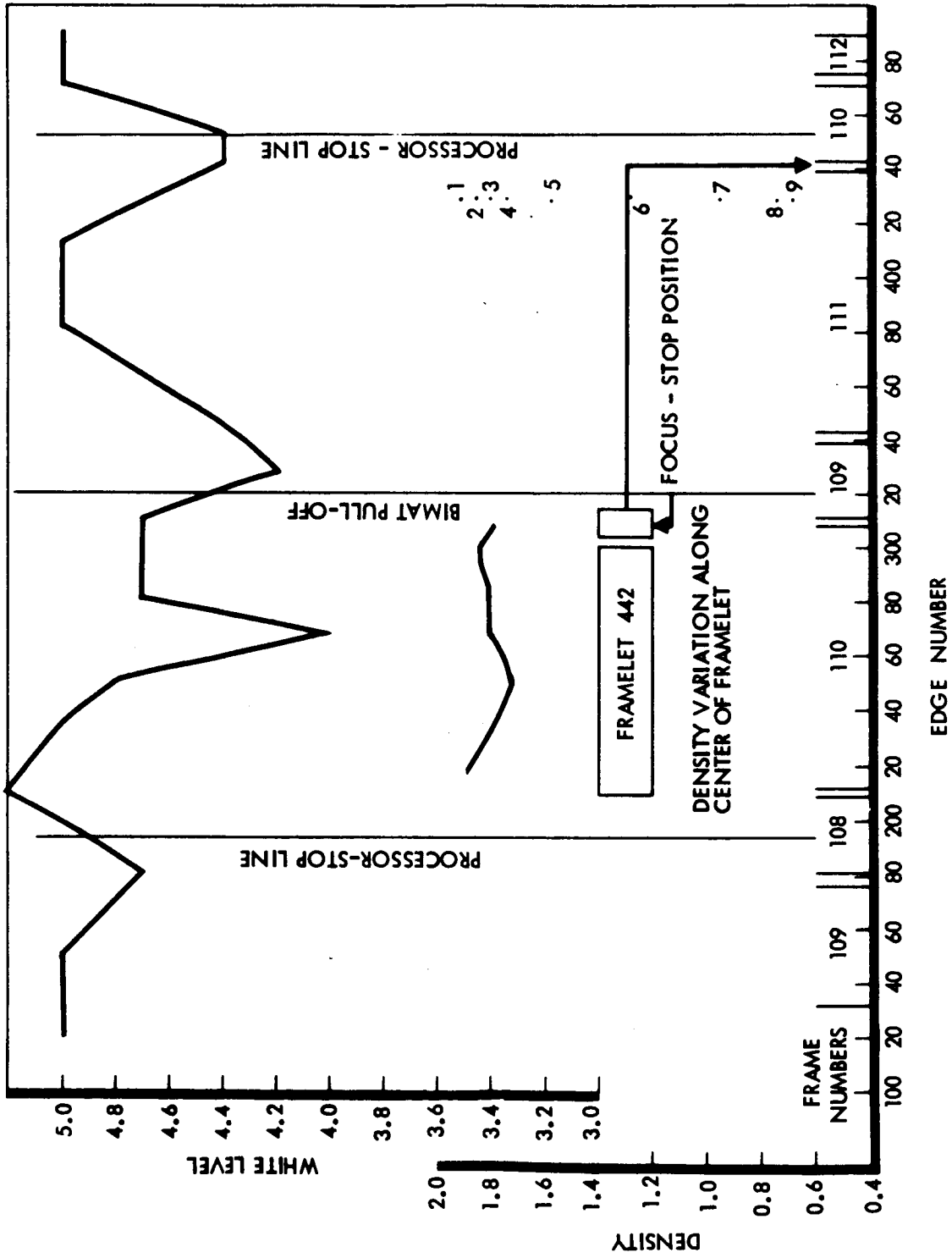


Figure 3-18: White-Level Densities—Readout Sequence 095

In relation to readout and processing the phenomena discussed above are not defects. Rather, they are variations which must be expected when temperature-dependent photo processing is carried out in a less than ideal environment. This data is presented as a guide to future photo subsystem operations. None of the data indicates performance quality below the standards required for the mission.

3.1.5 Processing Variations Across the Spacecraft Film

Although white-level measurements indicate processing variations along the edge of a frame, there is no evidence obtainable in real time to indicate processing variations across the frame. Therefore, density measurements were made on six framelets from six GRE rolls: three framelets represent Bimat dryout areas, and three represent areas where Bimat dryout does not appear significant. The ten density measurements were made in the center of the framelet to reduce the effect of the density variation caused by the W pattern of the video signal.

The framelets that were chosen were those with no exposure: those between a telephoto and a wide angle and those between a wide angle and a telephoto which also have a time code exposure. The white-level plots for Readout Sequences 004, 007, 077, 083, 095, and 098 demonstrate GRE density variation along the selected framelet and the framelet location. Figure 3-19 shows the GRE densities converted to spacecraft film densities (Readout density) using the "measured" curve shown in Figure 3-20.

The upper set of curves represents variations in densities where the white-level reading indicates Bimat dryout, while the lower set of curves represents the smaller density variations in an area where Bimat dryout

would appear to be insignificant.

Several conclusions may be drawn from the data. First, there appears to be more density variation where Bimat dryout is expected. Second, the density of "focus stop" position is considerably different than those further into the framelet and is in the right direction and magnitude to decrease the white level. Third, although the data are quite limited, it does indicate trends and more data should be accumulated. Fourth, readings to determine proper exposure of the spacecraft film should be restricted to those framelets in which Bimat dryout is not expected to be significant. Fifth, the focus stop density further confirms that gain adjustments should only be made in areas of proper Bimat processing.

3.1.6 PS Problem Analysis

At 15:12:42 during Orbit 149, "readout electronics on" was commanded. The following telemetry frame (15:13:034) indicated the command was verified by the PS and that the readout electronics were coming on normally. PEO6, the photo multiplier supply voltage value, was -1828 volts—the same as in previous readouts—and PEO3 indicated a normal line scan tube (LST) cathode current of 17.62 microamps. The LST high-voltage supply which is delayed by 30 seconds had not come on at this time. The next telemetry frame (15:13:26.5) indicated readout electronics had turned off with all video telemetry channels going to their preturn-on readings. The video engineer at DSIF-41 noted that the high-voltage supply had come on 4 to 5 seconds prior to loss of video. During this same telemetry frame (15:13:26.5), the following changes were noted: PC-12, command verification for focus and video gain commands, went from a "1" to "0", and PB05, platen count, changed from "20" to "19".

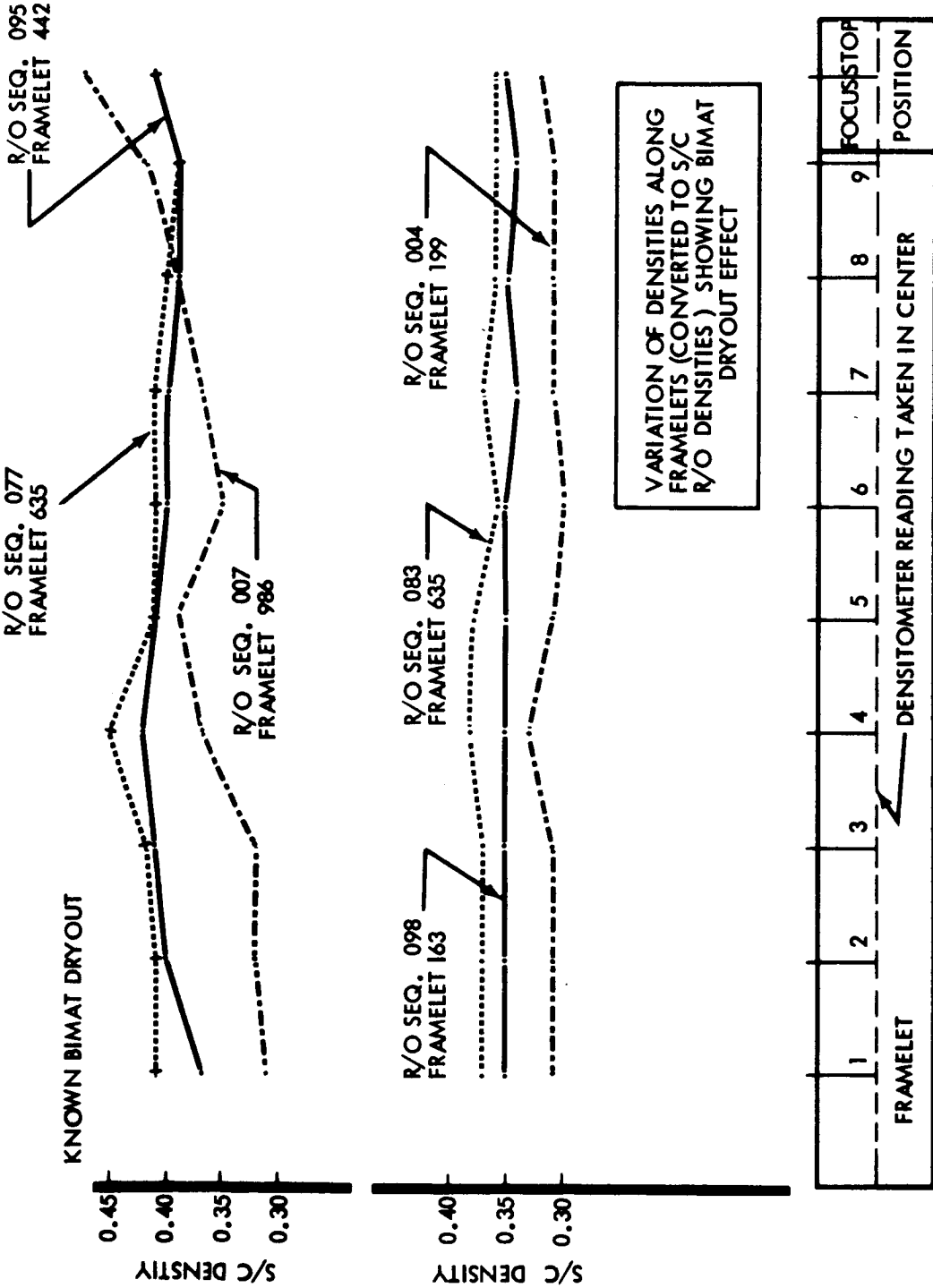


Figure 3-19: Variation of Densities Along Framelets

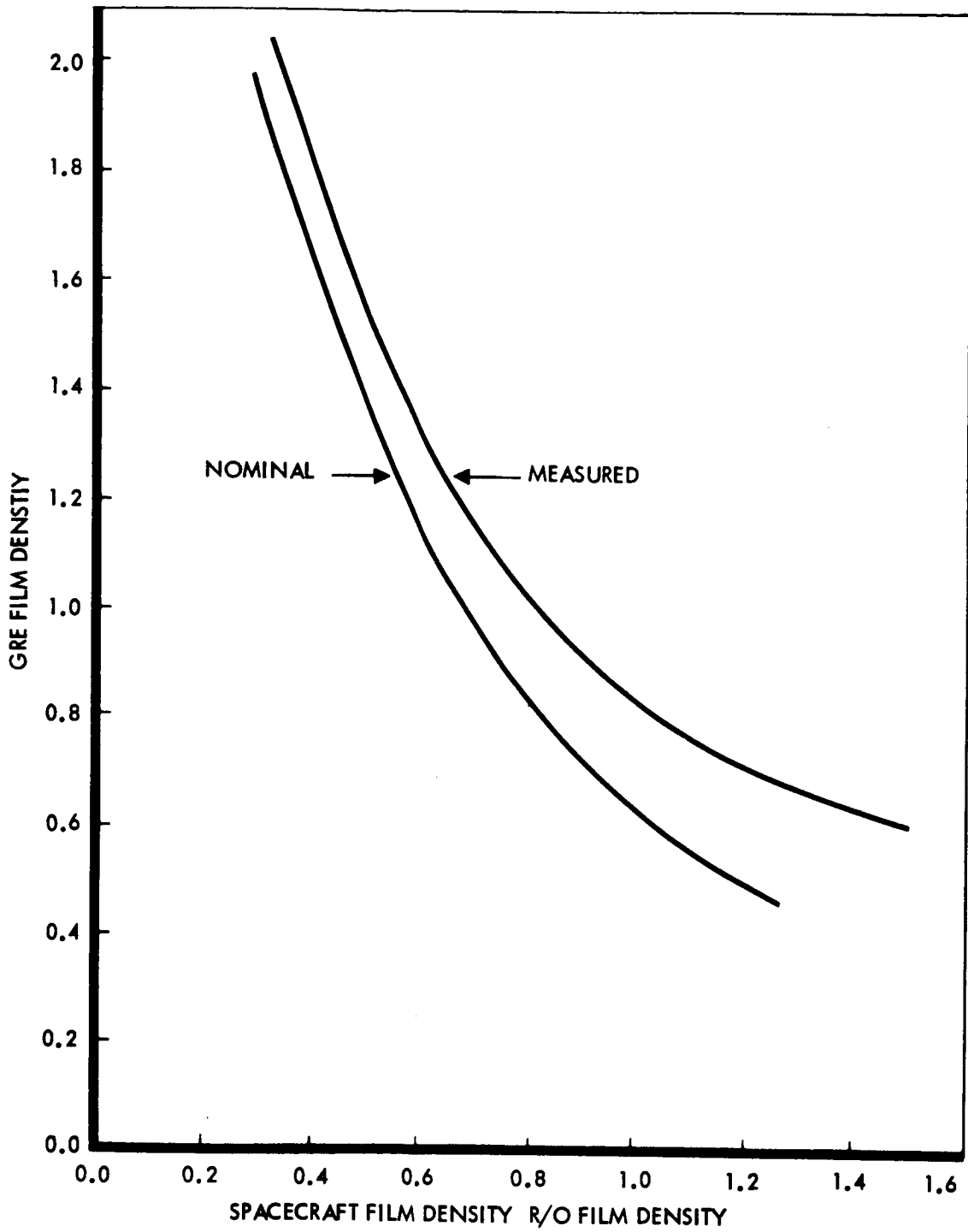


Figure 3-20: GRE Film Density vs Spacecraft Density

At 15:18:04, "R/O electronics on" was executed and had no effect. This was the first indication that the PS logic had changed state in some manner. At 15:35:45 "solar eclipse off" was executed. At this time a 2-amp increase in load current occurred, which is an abnormal amount.

Readout electronics was then commanded on and came on normally at 15:39:10. The first "R/O drive on" command occurred at 15:40:40. The following commands were then required to optimize the video signal: five video gain increases and one focus increase. This indicates that both the focus and gain counters had returned to their preset condition, which is Step 8 for focus and Step 4 for gain. Before the counters were reset, the gain was at Step 7 and focus at Step 10. After optimization on this readout, gain was at Step 9 and focus was at Step 9. Readout proceeded normally with normal film movement into the readout looper. At about 16:08, a 1.2-amp decrease in load current was noted. Heater power was then commanded off and on with no change in load current because the PS heaters are inhibited during readout. At 16:47:23, "R/O drive off" was executed. Following telemetry frames indicated that film was not moving out of the readout looper. Readout electronics was turned on again at 16:51:36. The second "R/O drive on" command was executed at 16:53:57 and readout again proceeded normally. At 16:58:37, "R/O drive off" was executed and again the film did not move out of the readout looper. At this point it was decided to use the turn-on sequence recommended in the PS reference handbook for turn-on in the "Bimat clear" mode. The following sequence of "solar eclipse on," set single frame rate, "camera on," "solar eclipse off," and "camera on" were executed beginning at 17:24:20. Following the second "camera-on" command, one frame of film should have been advanced;

however, telemetry indicated there was no film advance and the shutter counter, instead of indicating a single count, kept cycling until "V/H sensor off" command was executed at 17:40:30, which turned off the camera memory. At this time the readout looper emptied normally as the film was pulled back onto the takeup reel by the takeup motor. "Solar eclipse on" was then executed at 17:45:51.

From the telemetry data it is concluded that a power dropout or transient from some unknown source occurred about 30 seconds after readout electronics was turned on at 15:12:42. This transient apparently generated a preset pulse which placed the PS in the solar eclipse mode, which in turn caused the readout electronics to turn off. In addition, both gain and focus counters were reset. As explained in the PS reference handbook, when power is interrupted in the final readout mode after "Bimat cut" and is then reapplied, an ambiguity in the film handling logic can occur. The film advance motor logic can come on in the wind-forward direction while the film supply motor and brake logic comes on in the reverse direction. When "solar eclipse off" is given, the film advance motor can then come on in the forward direction but cannot move film because the supply motor brake is on. It is apparent that this is what happened in this case. The logic to the film advance motor switched to the "wind forward" state while film supply motor logic and takeup motor logic remained in the final readout state. When "solar eclipse off" was given at 15:35:45, the film advance motor came on and stalled—as shown by the 2-amp increase in load current. At 16:08 the load current dropped by 1.2 amps. This is the probable time the film advance motor failed. All subsequent events can be explained assuming a film advance motor failure. The readout proceeded normally because the takeup

motor logic did not change during the power interruption. When readout was turned off, the readout looper did not empty because the film advance motor had failed and the supply motor did not have sufficient torque to pull film through the camera and turn the armature of the film advance motor. The film advance motor failure explains why film was not advanced following the "camera on" command. The shutters continued to operate because no "end of sequence" signal was received from the film advance encoder that controls the amount of film advanced per frame. The shutters stopped operating when the camera memory was turned off by the "V/H sensor off" command.

After photo subsystem status became apparent, considerable effort was devoted to further testing and to maximizing the readout looper contents. The minimum readout index reached was 79.00.

3.2 COMMUNICATIONS SUBSYSTEM PERFORMANCE

The Lunar Orbiter communications subsystem consists of the components shown in Figure 3-21. This subsystem basically serves to transmit telemetry and video data to Earth, to receive spacecraft commands from Earth, and to receive and transmit ranging signals.

The communications subsystem performed satisfactorily throughout the mission. All photo data presented to the communications subsystem was successfully processed and transmitted by the spacecraft throughout the mission. At the completion of the regular mission (Orbit 153-154), all components of this subsystem were functioning satisfactorily.

3.2.1 Launch Through Cislunar Injection

Launch vehicle liftoff occurred at 036:01:17:01.12 GMT with the subsystem performing

normally. Telemetry data received via the Agena interface provided real-time data at SFOF from liftoff to 22 minutes after launch with only 5 minutes of unusable data. Cislunar injection occurred at a TFL of 19.9 minutes and the communications subsystem was functioning normally in modulation Mode 3 when real-time data reception was lost at 22.3 minutes after launch.

3.2.2 Cislunar to Lunar Injection

Cislunar injection occurred 19.9 minutes after launch and 9.2 minutes prior to the first S-band acquisition by the DSN. Acquisition reports received from the DSN show that DSS-51 (Johannesburg) acquired the spacecraft 29.1 minutes after launch at a signal strength of -132.0 dbm on the "S"-band acquisition-aid radar. This acquisition occurred 6.5 minutes after Agena-spacecraft separation, 4.6 minutes after the start of spacecraft antenna deployment, and 2.9 minutes after the initiation of Sun acquisition. DSS-51 established two-way phase lock with the spacecraft 30.7 minutes after launch at a signal strength of -101.5 dbm and remained in contact for about 6.5 hours. (DSS-51 acquired the spacecraft prior to the stored-program Mode 4 switchover.)

DSS-41 (Woomera) acquired the spacecraft in three-way lock at a signal level of -145 dbm 50.5 minutes after launch and 2.2 minutes before Mode 4 switchover. No signal strength for either DSS-41 or -51 was reported at Mode 4 switchover (52.7 minutes after launch); however, at 67 minutes after launch DSS-41 reported -109.4 dbm. These signal levels correspond to the expected levels before and after Mode 4 switchover.

Real-time telemetry data became available again at SFOF at 036:02:23:30 GMT or 66.5 minutes after liftoff (two frames of good data were received 56.0 minutes after launch).

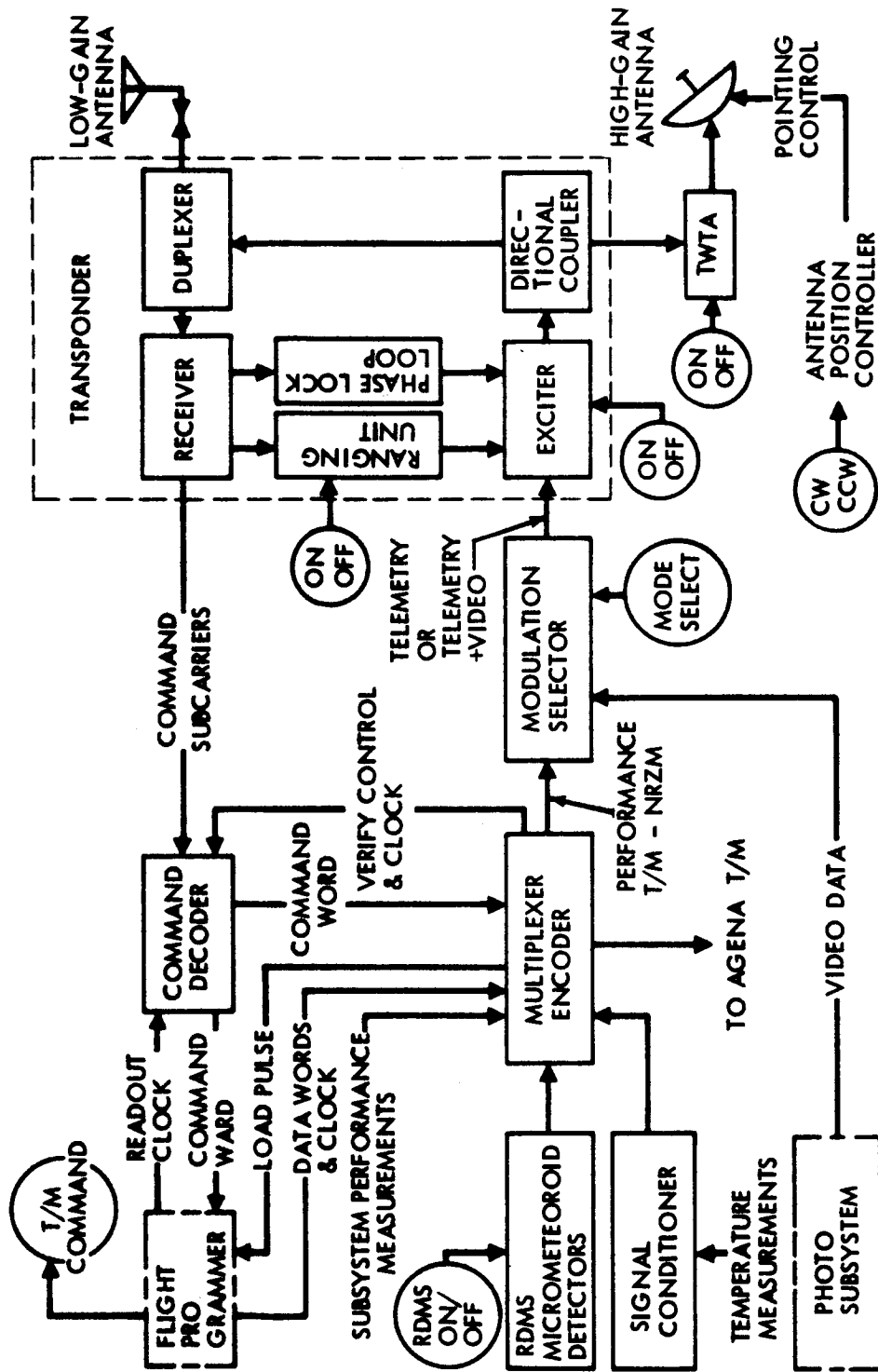


Figure 3-21: Communications Subsystem Block Diagram

The data was from DSS-41(three-way station) and the communications subsystem measurements indicated that the spacecraft signal strength (AGC) and static phase error (SPE) were within allowable command limits. The data also indicated that both antennas and all solar panels were deployed.

The spacecraft began a +360-degree roll maneuver 52.7 minutes after launch and completed the maneuver approximately 12 minutes later. Signal levels during the roll maneuver were not available; however, there were no problems reported in connection with the receivers maintaining rf lock. Handover from DSS-51 to DSS-41 occurred 73 minutes after liftoff and no problems were encountered. DSS-41 commanded Mode 4 off by RTC 90 minutes after launch, and a resulting signal strength decrease of approximately 7db occurred. Approximately 1 hour after handover, DSS-41 began ranging and continued to range for about 2.5 hours. Three hours 40 minutes after launch, handover back to DSS-51 was effected. (This was required because DSS-41 set before DSS-62 rose). DSS-62 acquired the spacecraft, three-way, 4 hours 3 minutes after launch and handover from DSS-51 was accomplished 33 minutes later without problems.

During the cislunar trajectory two high-gain antenna maps were obtained while 360-degree roll maneuvers were being performed for star mapping operations. The antenna maps show that the spacecraft roll position, as determined by the attitude control subsystem and antenna boresight, agree within 2 degrees.

3.2.3 Lunar Injection Through Final Readout

3.2.3.1 Telemetry Link

Downlink telemetry operation was satisfactory throughout the mission. It was noted, however, that after lunar injection the level

of signals received from the spacecraft during Mode 3 telemetry operations decreased considerably during sunset periods when the spacecraft temperatures decreased quite rapidly. Shortly after this situation was noticed, DSS signal levels were recorded every 10 minutes for ten orbits in an effort to correlate any factors that might be contributing to these signal level changes. The results of this investigation only showed that (1) the downlink power level did indeed decrease with decreasing temperatures and (2) the uplink signal level (transponder AGC) did not follow the variations of the downlink signal. During the same period, the Deep Space Stations made several measurements of telemetry modulation index, and the conclusion from these tests was that the modulation index remained essentially constant at 1.4 radians.

Figure 3-22 summarizes, to some extent, the variations in ground receiver signal levels throughout the orbital phase of the mission. It should be noted that the decreases in signal strength presented no problems with telemetry reception, and the signal strength margins for telemetering reception varied from 1.5 db below to 8 db above the nominal link design through the orbital phase of the mission.

3.2.3.2 Video Link

The performance of the video link was satisfactory throughout the mission. Signal levels recorded at the Deep Space Stations during readout varied from -98.5 to -91.5 dbm, which correspond, respectively, to video margins of 1.0 db below and 6.0 db above the nominal link design. Throughout the mission readout periods were not degraded or jeopardized by low signal levels from the spacecraft.

3.2.4 Component Performance

3.2.4.1 Transponder

Transponder performance was satisfactory

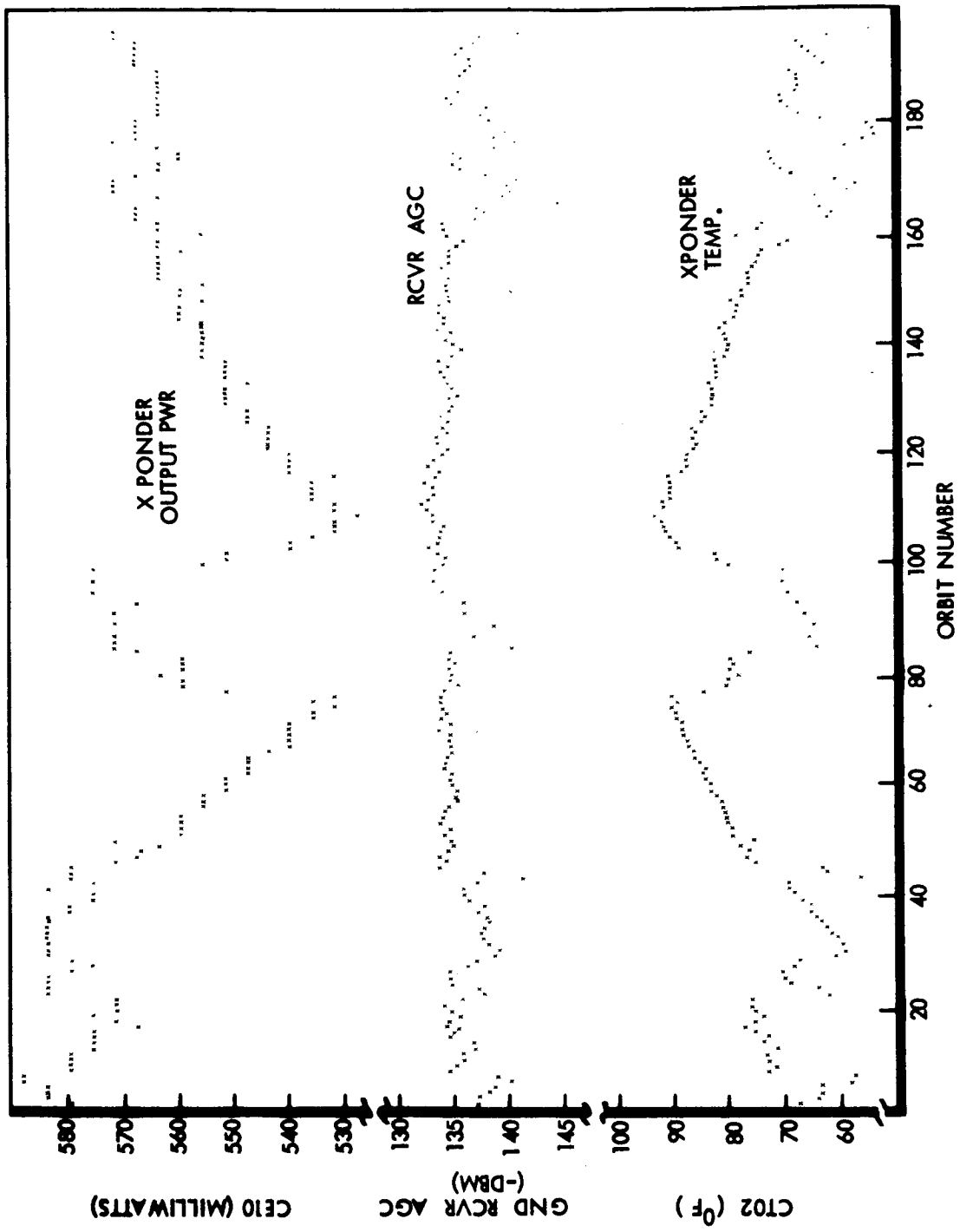


Figure 3-22: Typical Mode 3 Received Signal Strengths during Lunar Orbit

throughout the mission even though two anomalies were observed. The following discussion summarizes transponder performance.

The telemetered transponder output power indication telemetry channel (CELO) varied inversely with temperature with typical values of 584 mw at 61°F and 543 mw at 87°F. Shortly after lunar injection it was noted that the power output exhibited a pair of discontinuities in its power-versus-temperature

profile during each orbital period. One of the discontinuities appeared shortly before sunrise, when the power decreased approximately 4 mw during its normal increasing trend. The other discontinuity occurred shortly after sunrise, when the power increased approximately 8 mw during its normal decreasing trend (see Figure 3-23). The discontinuities and temperatures at which they occurred were quite consistent throughout most of the mission. A tabulation of a portion of

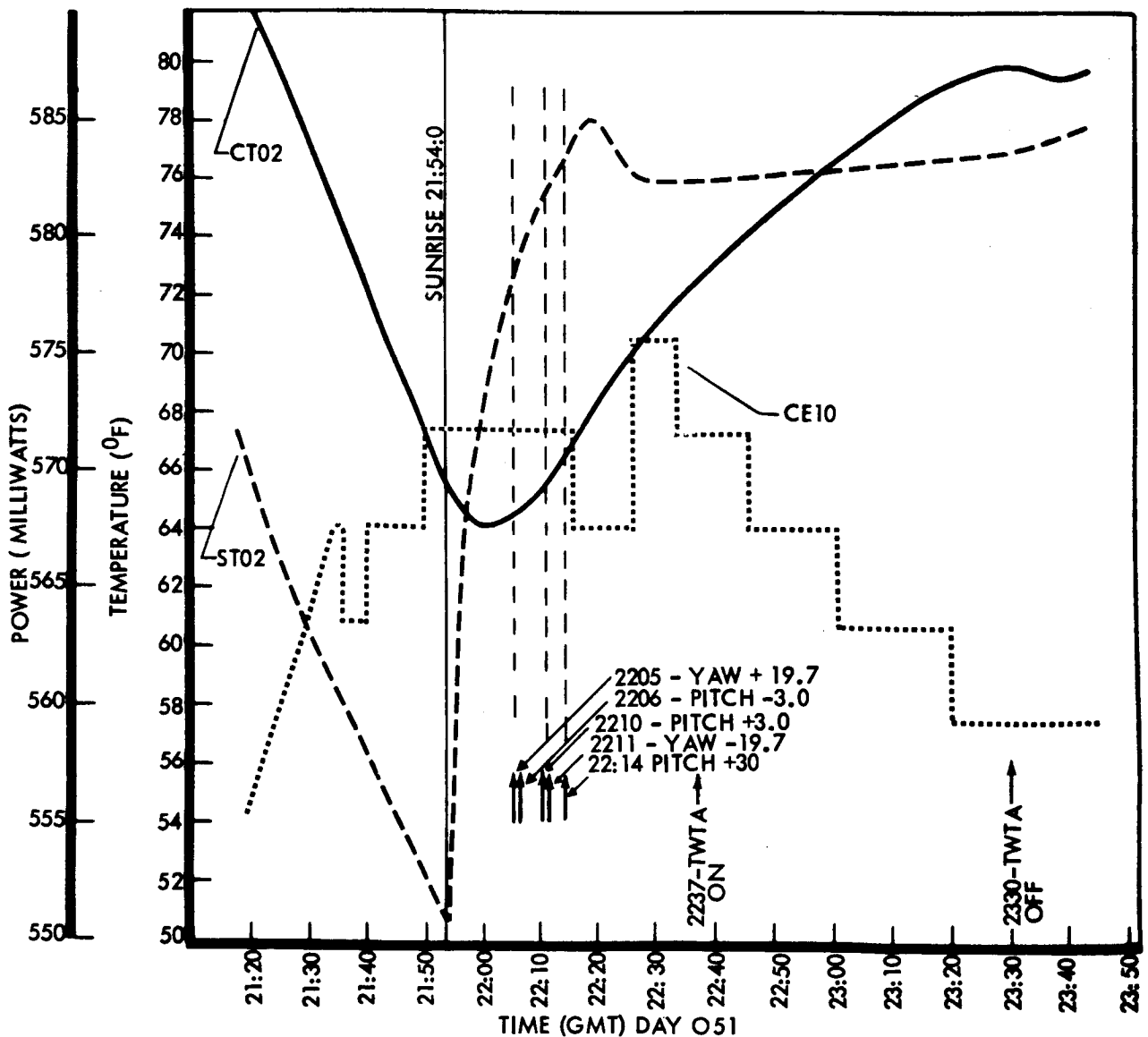


Figure 3-23: Transponder Temperature—RF Power and EMD Temperature

the above discontinuities is given in Table 3-3. The foregoing discontinuities presented no operational problems in connection with the transponder; however, the TWTA operation and performance appeared to be affected. A complete discussion of TWTA performance and constraints as related to transponder output power discontinuities will be found in the TWTA section of this report.

The transponder AGC, CEO8, reflected the effect of increasing range on the uplink signal strength during cislunar flight as well as changes in ground transmitter power levels. In most cases, CEO8 tracked the reported changes in ground transmitter power within 1 db. Command modulation was clearly evident on CEO8: one tone causing a decrease of about 2 db, and two tones causing a decrease of 3 to 4 db. Ranging modulation caused the uplink carrier power (CEO8) to decrease by approximately 8.5 db as expected. CEO8 was also found to vary with transponder temperature; during a typical orbital temperature cycle of approximately 20 degrees, changes of 3 to 4 db were noted for CEO8.

Throughout the orbital phase of the mission it was noted that the sensitivity of the transponder AGC measurement appeared to be slowly increasing (i.e., a particular DSS transmitter power and transponder temperature at the end of the mission produced an AGC value 8 to 10 db higher than comparable transmitter power and transponder temperature at lunar injection similar to previous missions). Figure 3-24 summarizes the change in AGC sensitivity over the orbital phase of the mission.

The transponder static phase error (SPE), CEO6, displayed an approximately sinusoidal variation (at one cycle per orbit) during

each orbit of the mission, with the average total excursions being equal to about 5.2 degrees. This variation was dependent on two factors; namely, doppler changes in spacecraft received frequency, and transponder temperature (CTO2) changes. Depending on the spacecraft's orbit configuration, these two factors can be either cumulative or subtractive in their effect on CEO6. During the mission, the amplitude of CEO6 was generally centered about 0 degree SPE with equal positive and negative excursions. No problems with SPE were encountered throughout the mission.

3.2.4.2 Signal Conditioner

Signal conditioner operation was satisfactory throughout the mission. CE09, the signal conditioner voltage measurement, varied from 4.68 to 4.76 volts—within the specified $\pm 1\%$ tolerance band.

3.2.4.3 High- and Low-Gain Antennas

Both the high- and low-gain antennas performed satisfactorily throughout the mission. The antennas were deployed by store program command after Agena separation. Confirmation of successful deployment was obtained from telemetry measurements, CCO4 and CCO5. These are discrete channels that indicate 0 when the antenna is in the stowed position and 1 when the antenna has deployed. At launch CCO4 (low gain) and CCO5 (high gain) indicated 0; after acquisition by Woomera, both indicated 1. The gain of each antenna was nominal, as expected. Based on DSS received signal levels and the communications system link analysis, the gain of the directional (high-gain) antenna was approximately 24.5 db and the omnidirectional (low-gain) antenna exhibited a gain pattern similar to that shown in Boeing Document D2-36355-1, Lunar Orbiter Low-Gain-Antenna Development.

Table 3-3: TRANSPONDER POWER DISCONTINUITIES

GMT	ORBIT	CE10(mw)	CT02	ST01
69	050:00:48:40	567.7 - 575.8	72.2	30.1
70	:04:15:38	567.7 - 575.8	72.2	27.1
71	:07:46:04	567.7 - 575.8	72.2	30.5
77	051:04:56:44	567.7 - 575.8	69.6	49.0
78	:08:35:14	567.7 - 575.8	70.9	60.8
79	:12:12:34	563.6 - 575.8	N/A	66.3
80	:15:31:06	567.7 - 575.8	70.5	66.2
81	:18:58:04	567.7 - 575.8	70.1	52.2
82	:22:26:58	567.7 - 575.8	70.5	50.8
83	052:01:55:29	567.7 - 575.8	70.5	49.9
84	:05:28:36	567.7 - 575.8	70.5	50.8
85	:08:49:03	567.7 - 575.8	69.2	50.4
86	:12:16:02	567.7 - 575.8	69.6	49.0
87	:15:52:13	567.7 - 575.8	70.5	50.8
88	:19:22:39	567.7 - 575.8	70.5	52.2
89	:22:41:11	567.7 - 575.8	69.2	49.5
90	053:02:08:55	567.7 - 575.8	69.6	49.9
91	:05:35:54	567.7 - 575.8	69.2	49.0
92	:09:04:25	567.7 - 575.8	69.2	47.2
93	:12:34:04	567.7 - 575.8	69.6	49.0
94	:15:59:31	567.7 - 575.8	69.2	49.9
95	:19:29:11	567.7 - 575.8	69.6	49.9
96	:22:56:55	567.7 - 575.8	69.2	48.6
97	054:02:25:26	567.7 - 575.8	68.4	47.7
98	:05:55:06	567.7 - 575.8	69.2	48.1
102	:19:37:14	567.7 - 575.8	70.1	41.3
103	:23:10:45	567.7 - 575.8	70.1	48.1
104	055:02:38:06	567.7 - 575.8	70.1	47.2
105	:06:04:42	567.7 - 575.8	70.5	45.4
106	:09:31:40	567.7 - 575.8	70.5	43.6
107	:12:59:02	567.7 - 575.8	70.9	42.7
108	:16:25:37	563.6 - 575.8	71.4	40.4
109	:19:51:27	563.6 - 571.7	71.8	37.6
110	:23:25:20	563.6 - 571.7	70.9	44.0
111	056:02:55:00	563.6 - 575.8	70.9	45.4
112	:06:26:12	567.7 - 575.8	70.5	48.6
113	:09:54:43	563.6 - 575.8	70.5	48.6
114	:13:22:27	563.6 - 575.8	70.9	47.7
115	:16:49:49	571.7 - 575.8	70.9	46.8
116	:20:17:11	563.6 - 575.8	70.9	44.9

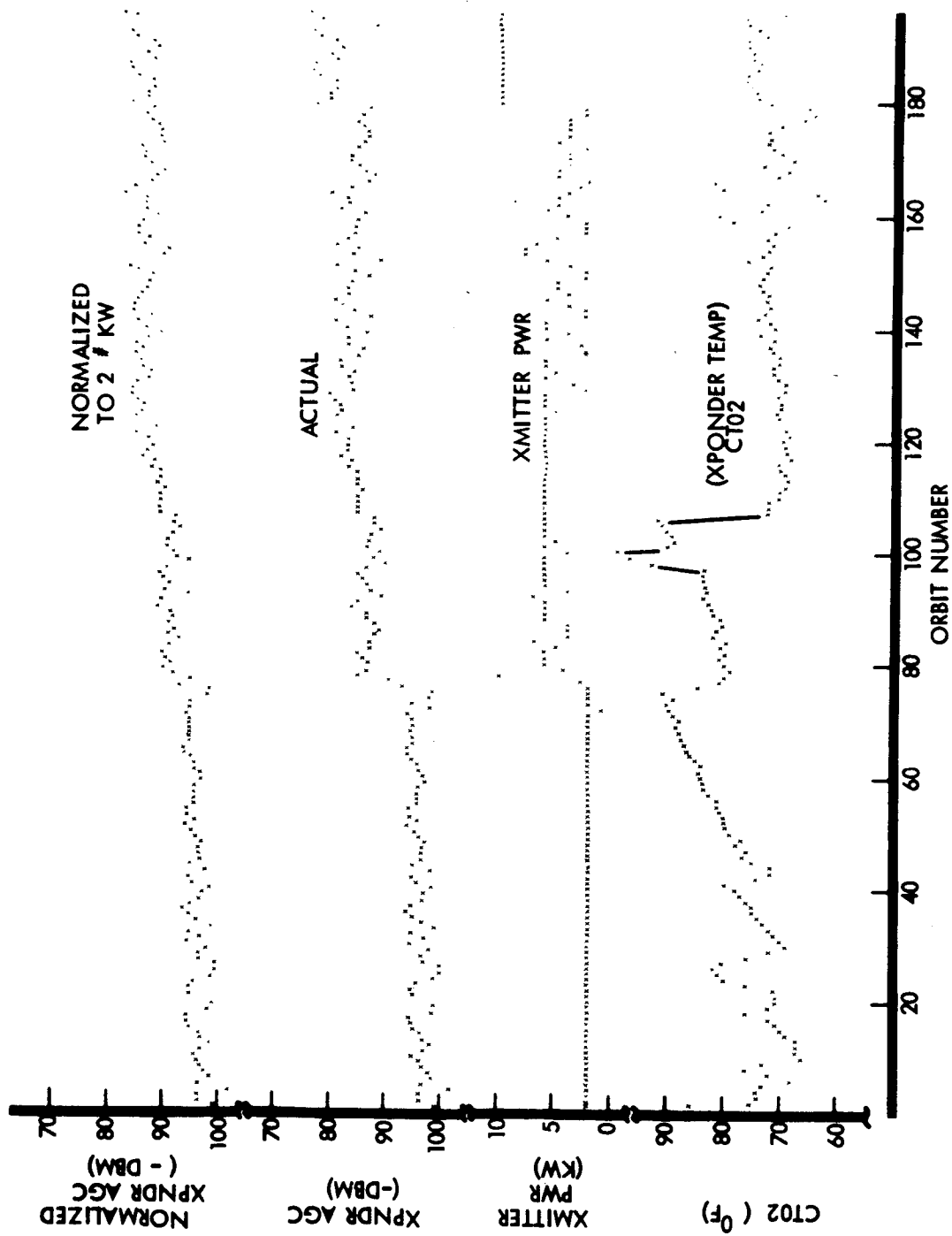


Figure 3-24: Transponder AGC Data

The high-gain antenna responded successfully to all rotation commands. The antenna rotated through a full 360 degrees during the course of the mission, in addition to several 30-degree rotations to compensate for pitching off the sunline. In all rotations the encoder that telemetered the rotation angle (CD 01) functioned correctly.

3.2.4.4 Traveling-Wave-Tube Amplifier

During the mission the TWTA was commanded on and off for 114 cycles with a total operating time of 155 hours.

3.2.4.5 Multiplexer Encoder

The multiplexer encoder performed satisfactorily throughout the mission. There was no indication of any failure or anomaly in the external/internal clock, and the telemetry properly indicating that all channel gates operated; CE01 signal conditioner zero reference and EE08 precision power supply voltage were constant at 0 M V and 20.00 V.D.C., respectively, indicating correct coding of analog channels; CC01 spacecraft identification, CC03 command verification word, CC06 telemetry. All telemetry channels performed frame marker were correct from start to finish, indicating correct programming in the multiplexer encoder. Occasional samples of these measurements indicated a switch to internal clock; however, closer examination reveals that this condition appeared generally in an area near a bad data frame and that the programmer did not enter the halt mode (indicating no clock switch occurred). It is concluded, therefore, that if any faults occurred they were transient in effect, that their occurrence was in no way progressive and that, considering the long-term performance of the multiplexer encoder, they did not in any way degrade the performance or affect the operation of the mission.

3.2.4.6 Command Decoder

The command decoder performed precisely

as planned throughout the mission. There were no errors in any of the verified words that were executed into the flight programmer. The threshold of command operation appeared to be approximately -123 dbm carrier signal at the spacecraft, which was within 2 dbm of the expected value.

3.2.4.7 Modulation Selector

Modulation selector operation was satisfactory throughout the mission. No problems or anomalies were experienced.

Average TWTA operating time during priority readout was 41.3 minutes per orbit. This time represents the total mission, including the two launch countdowns. After Bimat cut in Orbit 98 until Orbit 149, final readout was conducted with an average TWTA operating time of 129.3 minutes per orbit. From Orbit 149 to 154, the TWTA was operated occasionally with an average operating time of 77 minutes per turn-on. The following represents a summary of the TWTA telemetry data.

The TWTA collector temperature, CT01, rose exponentially during each cycle as expected. The maximum temperature attained during each orbit of priority readout was between 142.7 and 169.9°F, and during each final readout between 168.7 and 177.9°F. At TWTA turn-on, the temperature of the equipment mounting deck beneath the TWTA was between 46.8 and 72.9°F for both priority and final readout. Following the launch, the TWTA was never commanded on with a deck temperature below 45°F, as a result of Mission II experience.

The TWTA power output, CE02, was satisfactory for all TWTA operations up to the first readout (Goldstone test film in Orbit 39-40). At that time it was observed that the CE02 indicated power output was following the

trend of TWTA temperature (CT02). This condition, which was also present in ground testing, became progressively worse throughout the mission. In Orbit 154-155, turn-on power was indicated as 11.28 watts and turn-off power as 19.93 watts. This power increase was not reflected in the DSS received signal strength, which was essentially constant throughout each readout period. It is, therefore, concluded that the actual TWTA output power was not changing appreciably, and that there was evidently a malfunction in the CE02 telemetry circuitry.

The TWTA helix current, CE04, was satisfactory and normal until Orbit 78 readout. Prior to this time, the helix current measurement indicated approximately 5.1 ma and was quite stable throughout each readout period. From Orbit 78 on, however, the helix current turn-on values ranged from 5.2 to 6.97 ma, and the current decayed over the readout period to the normal value of 5.1 ma; also, the helix current was much more erratic than it had been earlier in the mission. The time required for CE04 to decrease to its normal value varied from 10 to 25 minutes, depending on the turn-on value and temperatures. From an examination of considerable data later in the mission, it appeared that the high helix current at turn-on was most dependent on transponder power (CE10) at turn-on, as well as transponder temperature (CT02). Specifically, it was found that if the TWTA were turned on before the occurrence of the transponder two-count discontinuity after sunrise, the helix turn-on current would be high (6.5 to 6.97 ma) and would remain at that high level until the CE-10 discontinuity occurred. After the transponder power "jumped," CE04 would begin to decrease until it reached its normal value of approximately 5.1 ma. After this correlation was discovered, TWTA turn-on was delayed,

throughout the remainder of the mission, until CE10 had decreased by one count following the two-count discontinuity (the one-count decrease was normally about 15 to 20 minutes after the two-count increase). The maximum helix turn-on current during readout was 6.97 ma, which occurred in Orbit 144-145.

The TWTA collector current, CE05, closely followed CE04 except that its variations were opposite those of CE04, as expected. The normal value of CE05 was 47.1 ma. (CE04 was 5.1 ma).

The TWTA collector voltage, CE03, was normal throughout the mission. This voltage had a tendency to increase very slowly over a readout period, with typical values being 1219 volts at turn-on and 1225 volts approximately 40 minutes after turn-on. Figure 3-25 shows TWTA parameters for a typical readout period.

3.2.5 Computer Program Performance

3.2.5.1 TRBL Program

TRBL is the computer program used, in part, by the communications subsystem analyst to determine the rotation angle (CD01) and corrective boresight maneuvers for the high-gain antenna when the spacecraft is pitched off the sunline. The program uses predicted vehicle attitude (i.e., roll, pitch, and yaw) and transforms the INTL/LIFL trajectory data in accordance with this attitude. The program then computes rotation angle and correction maneuvers from the transformed trajectory data.

The program ran successfully during the entire mission and no changes are planned prior to the next mission.

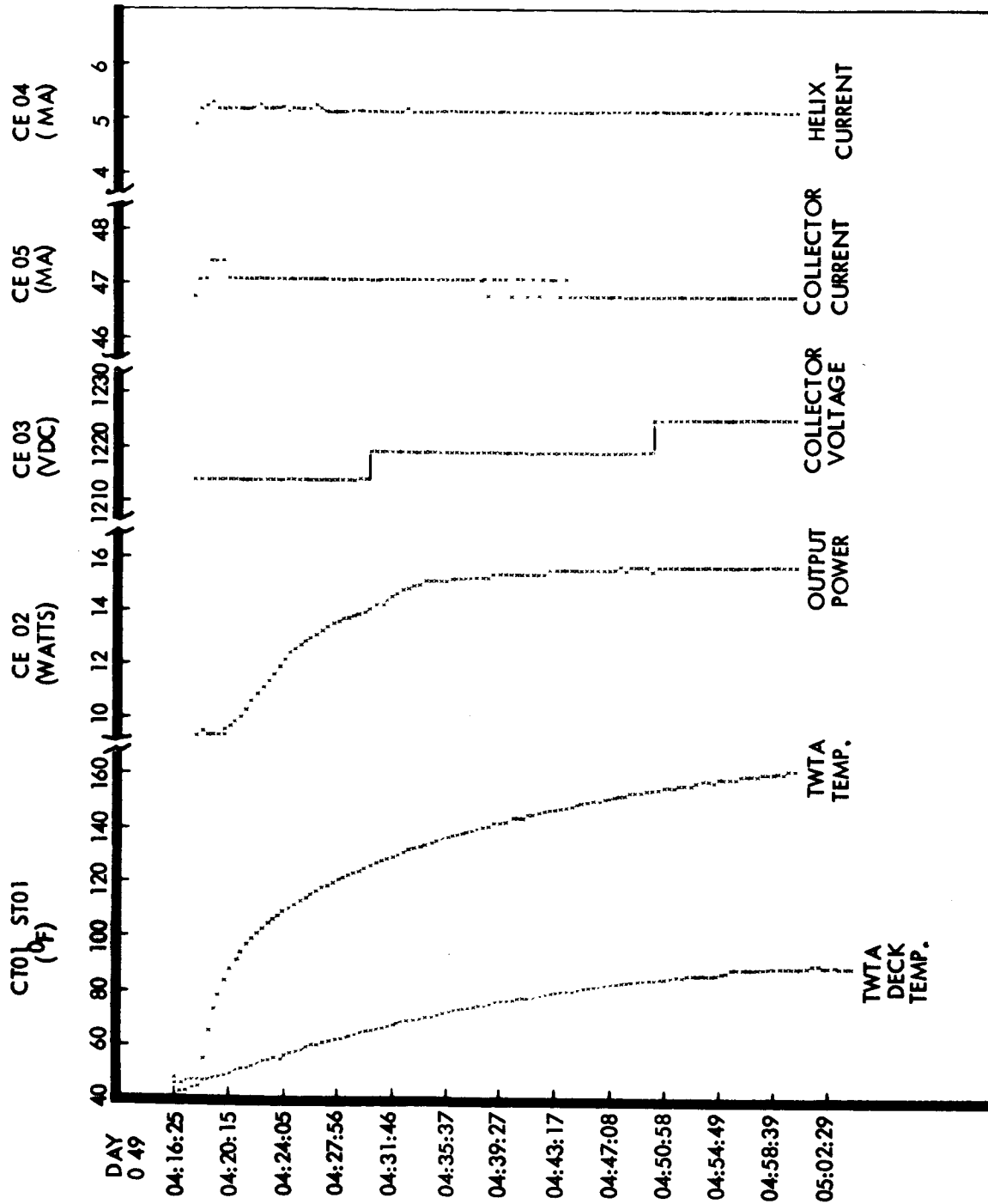


Figure 3-25: Priority Readout—Site III P-5B

3.2.5.2 SGNL Program

The SGNL program operated successfully throughout the mission. The calculations performed by the program yielded results that were well within the limits allowed. No changes to SGNL are planned prior to the next mission.

3.3 POWER SUBSYSTEM PERFORMANCE

The Lunar Orbiter spacecraft uses a solar cell battery power system consisting of four identical solar panels, a battery charger to control the charging current applied to a nickel-cadmium battery, and a shunt regulator to load the solar array and limit the array bus voltage. For further details on operation of the electrical power subsystem, refer to Mission I final report, (D2-100727-3, Volume III).

Mission Performance Summary—Power subsystem performance during Mission III was completely satisfactory. No constraints were imposed on flight operations beyond the requirement that array illumination be sufficient to meet the demands imposed by spacecraft electrical loads and energy balance requirements.

3.3.1 Launch to Sun Acquisition

External power was removed from the spacecraft 6 minutes before liftoff and from that time until Sun acquisition all electrical loads were supplied by the spacecraft battery. The array deployment and Sun acquisition sequences were not displayed on telemetry, but it is estimated that the batteries discharged approximately 3.1 ampere-hours for a 23.8% depth of discharge. Initial receipt of telemetry data via the Deep Space Network primary sites occurred 66 minutes after liftoff. The array was deployed and supplying 13.33 amps at 30.56 volts with an array temperature of approximately 100° F. The charge controller went into the constant potential

mode of operation 84 minutes after liftoff, and within another 26 minutes the charge current was down to 1.32 amps with the battery temperature at 60°F.

3.3.2 Cislunar through Lunar Injection

For the first 16 hours of cislunar flight, the spacecraft was flown with the array normal to the Sun-vehicle axis. The maximum array output was 13.40 amps at 30.56 volts with the array temperature approximately 100°F. During this time spacecraft loads accounted for about 107 watts of power and the shunt regulator had to dissipate approximately 250 watts.

To reduce spacecraft temperatures, the spacecraft was subsequently pitched 36 degrees off Sun and the array output was reduced to 10.7 amps at 30.56 volts with the array cooling to 75°F. The battery charging current fell to 1.02 amps with a corresponding battery temperature of 84°F.

The Sun was again acquired, 33 hours and 21 minutes after liftoff, in preparation for the midcourse maneuver. The midcourse maneuver required that the spacecraft be pitched 123.4 degrees off Sun so that spacecraft loads were supported by the battery for 14 minutes, until the reverse maneuver was performed and the spacecraft brought back on Sun. With the midcourse maneuver completed the spacecraft again was pitched 36 degrees off Sun. Spacecraft loads stabilized at 3.7 amps, except when the tank deck heaters were energized, causing the load current to increase to 5.6 amps.

The photo subsystem "heater inhibit" was removed approximately 1 hour before the orbit injection maneuver and the load current increased 0.6 amp. On February 8, (Day 039), at 21 hours and 31 minutes GMT, the spacecraft entered the Moon's shadow

for the first time and the injection maneuver was performed using the battery. During engine burn, the load current peaked at 7.93 amps while at other times during the occultation, the current varied from 4.0 to 4.25 amps. Total discharge capacity was estimated to be 3.28 ampere-hours for a 25.2% battery depth of discharge. Minimum bus voltage, which occurred during engine burn, was 23.36 volts.

3.3.3 Initial Ellipse through Orbit Transfer

Typical battery performance during the initial orbits (1 to 25) is shown in Figure 3-26. Battery depth of discharge was approximately 27% and the overcharge ratio was 1.8 to 2.0.

For the first three orbits the spacecraft was on Sun and maximum array output was 13.40 amps at 30.56 volts with an average panel temperature of 102°F. During Orbit 4, the spacecraft was pitched 28 degrees off Sun, thus reducing the array output to 11.95 amps and the average panel temperature to 89°F. The load current with tank deck heaters energized averaged 5.84 amps and with the battery charging current tapered to 1.83 amps; the shunt regulator was dissipating 124 watts at 30.56 volts.

The Sun was reacquired during Orbit 22 in preparation for the injection into the photo ellipse. Array output just prior to this injection maneuver was 13.27 amps at 30.56

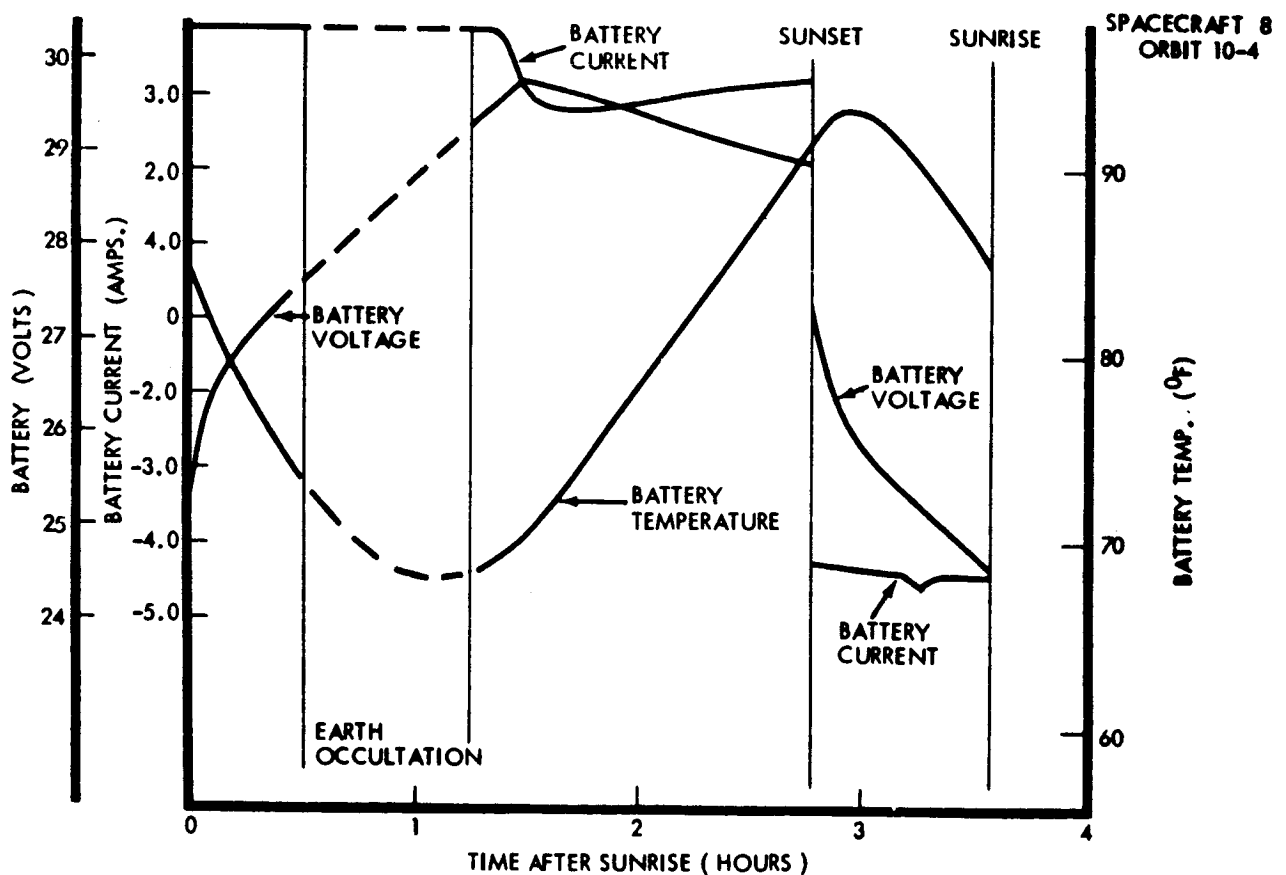


Figure 3-26: Array Current and Temperature vs Time

volts with an array temperature of 101°F. The injection maneuver required the spacecraft to be pitched 19.9 degrees off the sun-line, reducing the array output to 12.49 amps; this was still more than sufficient to supply all spacecraft loads and the bus voltage was maintained at 30.56 volts throughout the injection sequence.

3.3.4 Photo Ellipse through Photo Taking

After one orbit on Sun the spacecraft was pitched 30 degrees off Sun during Orbit 27. From then until the ten-frame film advance in Orbit 43, the spacecraft was

pitched from 17 to 35 degrees off Sun for temperature control. In Orbit 43, the Sun was reacquired with the attitude control system operating in a 0.2 degree deadband. Figure 3-27 shows the solar array performance during this orbit; the dotted portions of the curves indicate the period of Earth occultation where data from other orbits was used to determine the shape of the curves. Maximum array output was 13.27 amps at 30.56 volts with an array temperature of 100°F; minimum array current was 12.25 amps at 30.56 volts with the array temperature a maximum at 210°F.

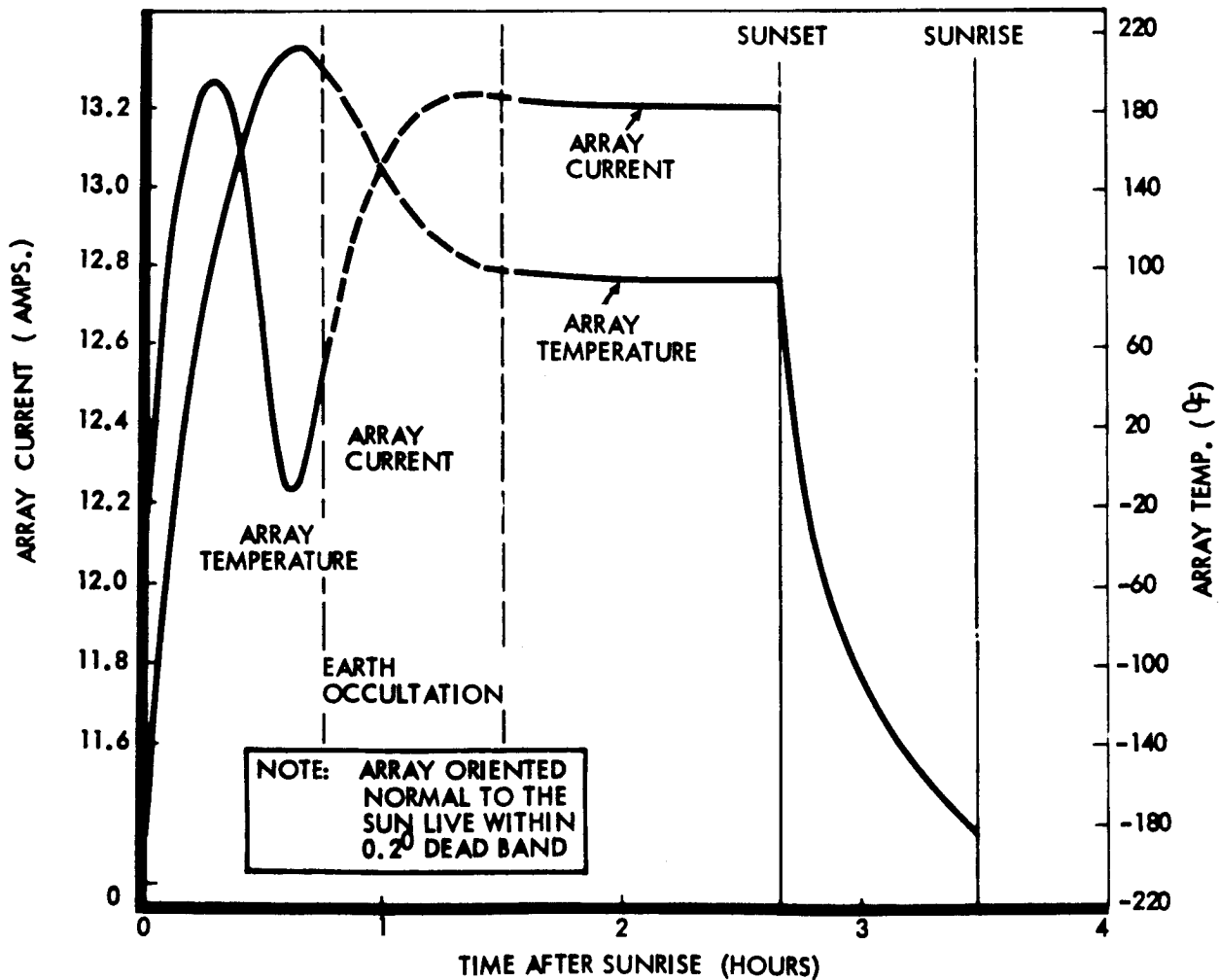


Figure 3-27: Array Current and Temperature vs Time

Battery operation is typified by the curve of voltage, current, and temperature obtained in Orbits 73-74, Figure 3-28. Maximum battery temperature during this phase of the mission was 119.2°F, with the peak temperature being reached about 8 minutes after sunset. Battery end-of-discharge voltage, which was 24.8 volts during the initial orbits, had fallen to 24.48 volts by Orbit 104.

The load currents at the spacecraft main bus during each mode of operation are tabulated in Table 3-4. Where thermostatically controlled heaters caused variations in the load current, maximum and minimum values are given.

3.3.5 Final Readout

Bimat cut occurred in Orbit 98; the spacecraft load current rose from 3.62 to 4.37 amps. The Sun had been reacquired at sunrise on this orbit and the spacecraft was then pitched 0.011 degree in preparation for the gyro drift test. Maximum array current during Orbit 98 was 13.03 amps at 30.56 volts with the array temperature approximately 100°F. On completion of the test, the spacecraft was pitched 30 degrees off Sun and the array output was reduced to 11.53 amps at 30.56 volts with the array temperature stabilized at 84°F. From this point until the end of readout in Orbit 154, the spacecraft was pitched from 23 to 35 degrees off Sun. Under these conditions

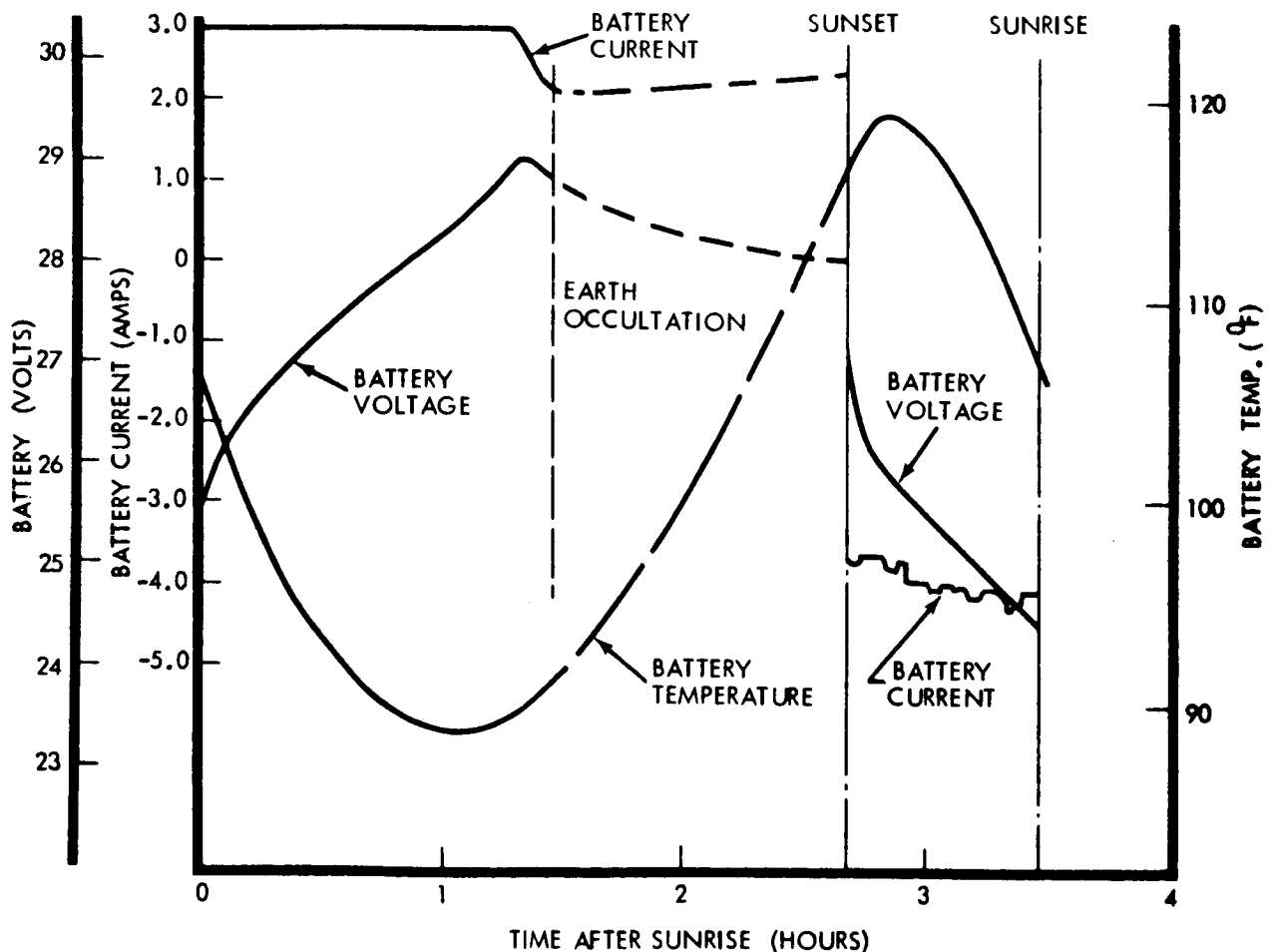


Figure 3-28: Array Current and Temperature vs Time

Table 3-4: SPACECRAFT LOAD CURRENTS

OPERATIONAL MODE	PHOTO HEATERS			SPACECRAFT LOAD EE07 (Amps)		
	DAY	NIGHT	INHIBITED	Min.	Nom.	Max.
DAYTIME						
Cruise			X	3.49	3.62	3.75
Photo Standby	X			3.37	3.49	3.81
Camera On			X	3.49	3.49	3.93
TWTA On	X			5.11	5.17	5.78
R/O Electronics On			X	6.20	6.32	6.56
R/O Drive On			X	6.26	6.56	6.68
Processing	X			4.18	5.84	6.26
NIGHTTIME						
Photo Standby		X		4.06	4.12	4.18
Canopus Tracker On		X		4.25	4.31	4.37

the power subsystem was able to supply all the normal spacecraft loads and maintain the bus voltage at 30.56 volts during daylight.

In Orbit 149 an anomaly occurred within the photo subsystem. During attempts to escalate the problems, the maximum load current was 8.05 amps, which caused the bus voltage to drop as low as 29.28 volts for one telemetry frame.

3.3.6 Component Performance

3.3.6.1 Solar Array

Mission III is the first of the Lunar Orbiter missions to be accomplished under a decreasing solar intensity. Solar array performance, when normalized to a standard solar intensity, would be a duplication of the preceding missions with similar normalization. Orbit 43, plotted

in Figure 3-27 as typical, shows the characteristic profiles of output current and panel temperature. But because the solar intensity decreased during the mission, the output was accordingly reduced by approximately 1% in addition to the decrease caused by the degradation from environmental exposure and thermal cycling. The decreasing output from all causes is illustrated by the four curves of array current versus temperature, Figure 3-29. To illustrate array output as a function of array degradation and solar intensity, Figure 3-30 was plotted with these parameters normalized in percent of their values at initial orbit injection. Array degradation is the difference between the decrease of array output and the decrease in solar intensity. From this figure it appears that the rate of solar array degradation becomes constant at slightly over 2% after approximately 100 orbits.

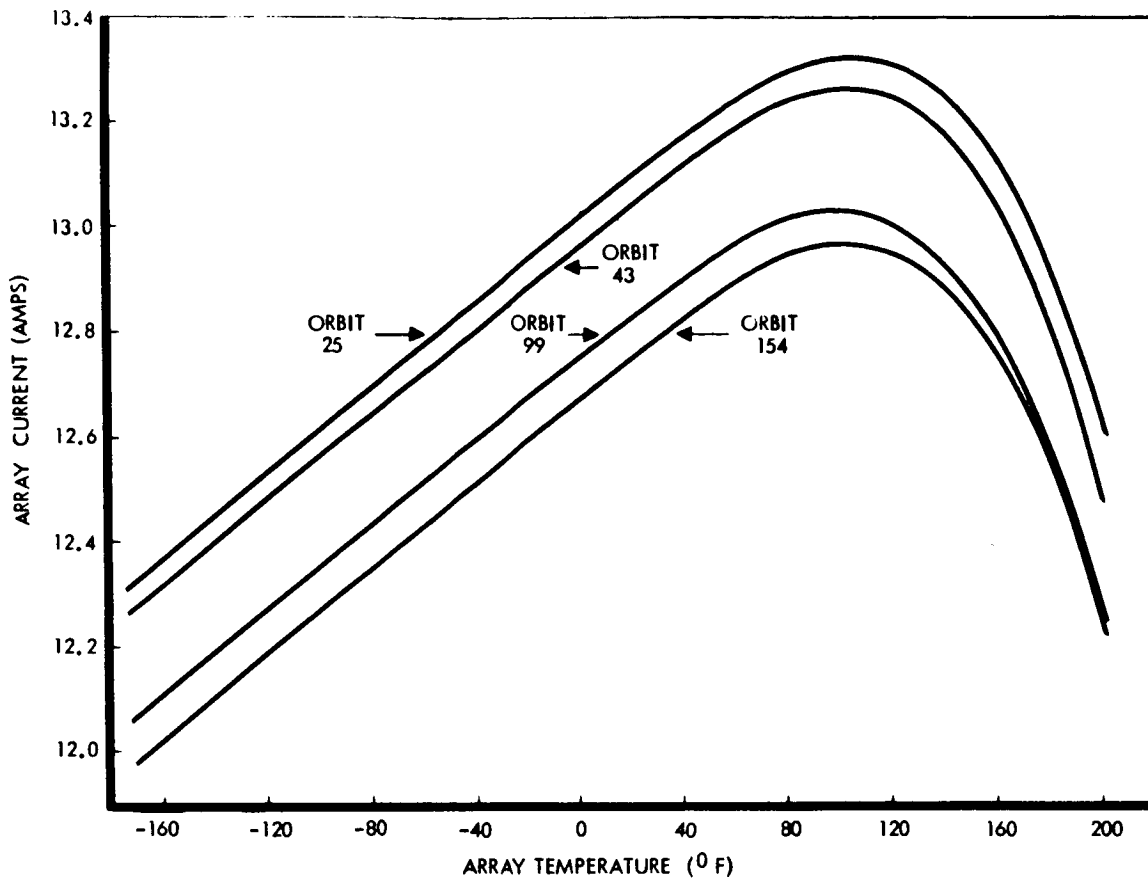


Figure 3-29: Array Current and Temperature vs Time

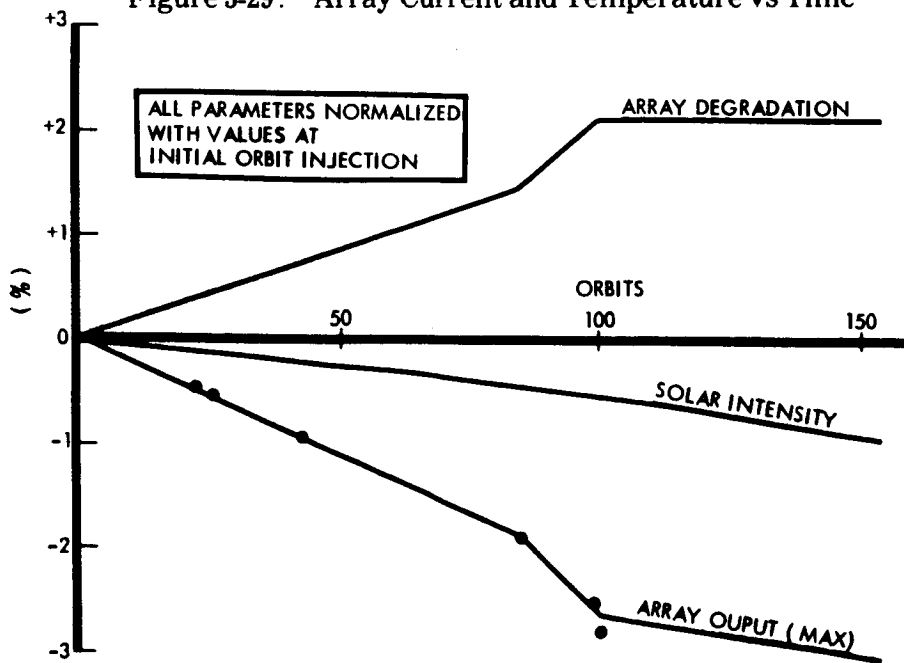


Figure 3-30: Solar-Array Degradation

Although the accuracy of solar array temperature and current telemetry is approximately $\pm 2.2\%$ and, thus, greater in magnitude than calculations of degradation, the calculations are considered valid because they are based on the ratio between two values of output current from the same panel at the same indicated temperature. Thus, the degradation calculation accuracy becomes a stronger function of the repeatability of the telemetry and a weaker function of the absolute accuracy of the telemetry.

3.3.6.2 Battery

Battery performance was satisfactory throughout Mission III although battery temperatures tended to be higher than in Mission II and were more comparable to those experienced in Mission I. In addition, during the cislunar phase of the mission the temperature differential between the two battery modules was varying from 3°F to as high as 11.4°F as the attitude of the spacecraft was changed. Later in the mission when the spacecraft was in lunar orbit the module temperatures were more in accordance with one another and the temperature difference was generally just 1 or 2 degrees. The maximum battery temperature of 122.2°F occurred 92 hours after launch during lunar orbit injection. The end of discharge voltage was 24.8 volts during the initial lunar orbits and had fallen to 24.48 volts when the end of discharge was last seen in Orbit 103.

The battery depth of discharge throughout the mission is shown in Figure 3-31. From Orbits 75 through 154, part or all of the battery discharge data was occulted, and predicted values of battery discharge current and temperature were used to calculate the depth of discharge. This accounts for the apparent greater variation in depth of discharge during this period. At other times, the vari-

ance is a function of the telemetry accuracy only.

3.3.6.3 Charge Controller

The charge controller on Lunar Orbiter III performed as expected, with the charge being limited to 2.877 amps during the constant current mode of operation. About 80 minutes after sunrise the battery voltage and temperature sensing circuits in the charge controller caused it to go into the constant potential mode of operation, decreasing the charge rate. As in previous missions, the cooler the battery at this time the more pronounced the effect of the taper charge. Minimum charge rates of 1.80 and 2.41 amps were obtained at battery temperatures of 74°F and 100°F , respectively.

3.3.6.4 Shunt Regulator

This unit operated properly throughout the mission. Dissipating as much as 250 watts at times, it limited the bus voltage to 30.56 volts whenever the array output exceeded the load demand.

3.4 ATTITUDE CONTROL SUBSYSTEM PERFORMANCE

The Lunar Orbiter III attitude control subsystem performed with accuracy satisfying all mission objectives. Any problems that occurred were accommodated by changes in operational procedures. Operational considerations to control temperatures required an off-Sun attitude for about two-thirds of the mission. Use of the Canopus star tracker was restricted to sunset periods except during cislunar flight. The revised operational procedures met performance requirements while maintaining an acceptable nitrogen consumption of 7.0 pounds for the photographic mission.

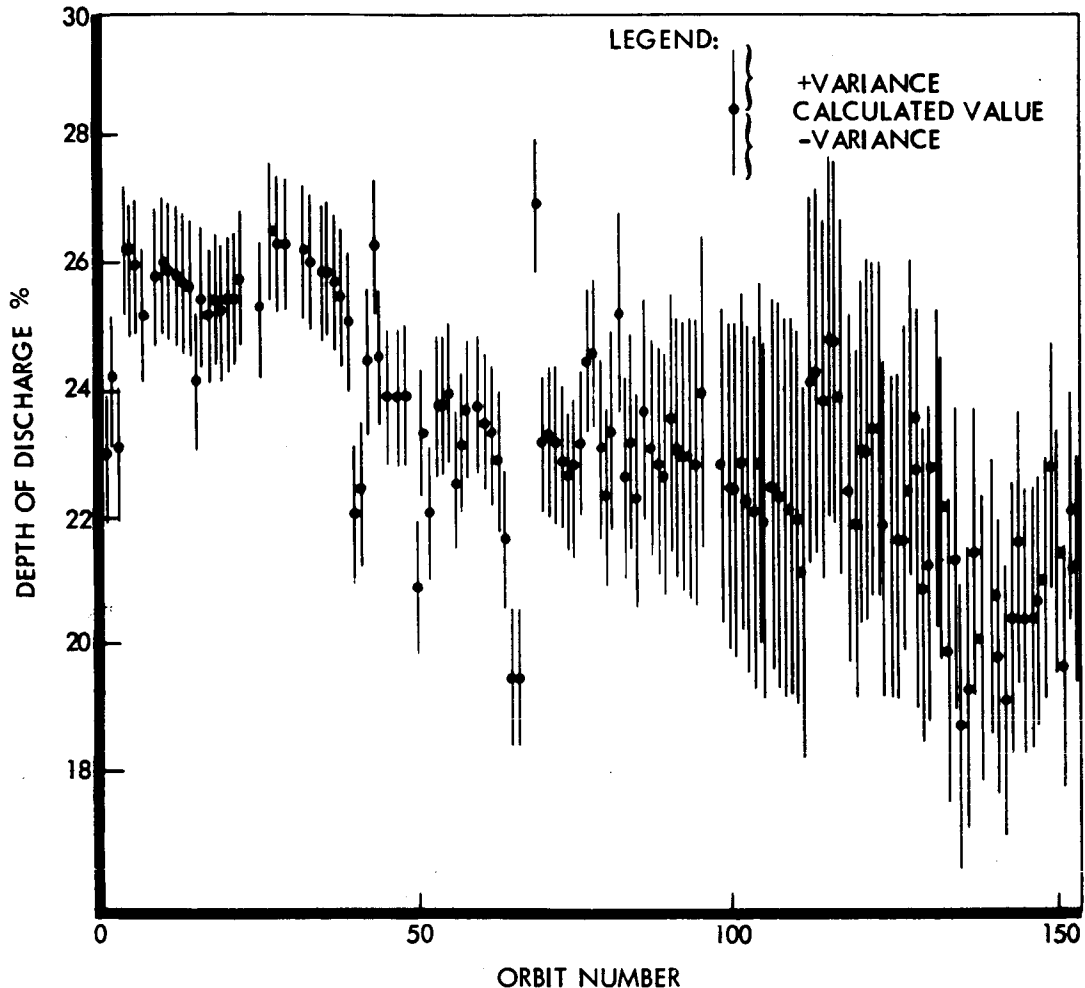


Figure 3-31: Spacecraft Battery Depth of Discharge

The attitude control subsystem maintains control of the attitude of the spacecraft with respect to inertial and celestial references. Control with respect to celestial references (conventional limit cycle) is accomplished using Sun sensors in the pitch and yaw axes and a Canopus tracker in the roll axes for position reference. Rate damping is provided by a single-axis floated gyro in the rate mode. Control of the spacecraft with respect to inertial reference (inertial hold) is by means of the gyros in the rate-integrating mode for all three axes. Lead-lag networks on the output of the gyros are used for rate damping. Ma-

neuver commands are relayed by the flight programmer and switching assembly to the closed-loop electronics. Maneuvers are performed with the gyros in the rate mode. Integration of rate-mode output is used to measure and control maneuver angles. Control torques are generated by nitrogen thrusters located on the engine-mount deck. Control of pitch and yaw attitude during engine burn is by means of actuators that vector the engine in response to rate-integrating-mode output of the gyros. Throughout the mission, the attitude control subsystem maintained stable operation for both reaction control and thrust vector control.

During Mission III, the attitude control subsystem performed its many design tasks within specification. It received commands through the flight programmer to perform 383 single-axis maneuvers during the mission. Maneuver accuracy of the subsystem was within the design tolerance. Attitude maneuver rates for all axes were within the design limits of 0.55 \pm 0.05 degree per second for maneuvers in narrow deadband. Maneuver rates in the wide deadzone ranged from 0.05 to 0.061 degree per second.

The attitude control subsystem maintained spacecraft orientation with respect to the Sun and Canopus on command within \pm 0.2 and 2.0 degrees, depending on the selected deadband. Deadband accuracies were within telemetry resolution for narrow and wide deadzones.

Attitude control was maintained with the spacecraft pitched from 15 to 45 degrees away from the Sun for approximately 56% of the mission. Drifts in the inertial reference were within design limits, which reduced the frequency of updating this reference.

Stable thrust vector control of the spacecraft attitude was maintained through three velocity control engine burns. Spacecraft-burn termination occurred within the design tolerances as far as could be determined from the telemetry resolution.

Operational methods used to control spacecraft attitudes by mission phases to circumvent problems and meet mission requirements are presented below.

3.4.1 Cislunar Coast

The cislunar portion of the mission required a 36-degree pitch off the Sun to reduce overheating and delay thermal paint degrada-

tion. A minus 36-degree pitch maneuver was performed after Canopus had been initially located. This attitude was maintained until the midcourse maneuver sequence. After the midcourse maneuver, a plus pitch 36-degree maneuver was performed; this attitude was maintained until the lunar orbit injection sequence. Both 36-degree pitch maneuvers were performed in wide deadzone to conserve nitrogen gas and at the same time calibrate the pitch coarse Sun sensors. To prevent possible loss of the reference star due to tracker "glint," Canopus was not acquired in a closed loop during the cislunar phase of the mission. Canopus reference was maintained by rolling the spacecraft to place Canopus in the tracker field of view after each pitch maneuver.

3.4.2 ΔV Maneuvers

The midcourse correction, lunar orbit injection, and orbit transfer maneuvers were performed based on a closed-loop Sun reference for the pitch and yaw axes. The roll-axis reference was established by an open-loop roll update maneuver from 2 to 5 hours prior to the start of the roll maneuver for the velocity correction. The roll axis drifted through a near zero-error condition at a predetermined gyro drift rate, at the time the roll maneuver for the velocity correction was initiated. Roll errors—with respect to Canopus—for midcourse, injection, and transfer were -0.12, -0.29, and -0.08 degree, respectively.

3.4.3 Photo Maneuvers

In general, each photo site required a three-axis maneuver, usually a roll, yaw, and pitch sequence. There were 41 three-axis, 8 two-axis, and one single-axis maneuvers to the photo attitude, and as many reverse maneuvers back to the celestial references.

All photo maneuvers were performed with the spacecraft in narrow deadzone. The

pitch and yaw axes were locked on the Sun prior to the photo sequence, thereby ensuring a reference point with a ± 0.2 -degree tolerance with respect to the Sun. Acquisition of Canopus at the start of the photo sequence could not be done because of the Canopus tracker glint problem. It was necessary, therefore, to turn the tracker on during the sunset period prior to the photo and acquire Canopus for 3 minutes to establish a roll reference. The tracker was turned off 4 minutes before sunrise.

The photo maneuver sequence was initiated 10 to 15 minutes after the Canopus reference update. Due to the Canopus update sequence, the following errors with respect to Canopus were incurred.

- 1) The roll gyro did not obtain a perfect update, i.e., zero-roll error when switched from the rate mode (Canopus tracked in a closed-loop mode) to the inertial-hold mode at the time the tracker was turned off. This error was always less than ± 0.2 degree (deadzone accuracy) but represents a normal spacecraft operational mode.
- 2) Roll gyro drift angle between tracker off and the start of the photo roll maneuver; this error amounted to approximately -0.03 degree.
- 3) Position of roll gyro relative to spacecraft deadzone at the start of the photo roll maneuver, i.e., when the roll gyro switches from the inertial-hold mode to the rate mode; this error was always less than ± 0.2 degree.

Table 3-5 contains a tabulation of the initial roll errors, with respect to Canopus, at the start of the photo roll maneuver. The highest initial roll error recorded was $+0.36$ degree for Site IIIS-13.

Table 3-5 also contains the deadzone during the photos. These data do not define camera pointing errors, but represent the position of the spacecraft in the deadzone while the shutter was opened.

Attitude maneuver rates during the photo taking sequence were well below the ± 0.01 degree per second design limit. These data are also tabulated in Table 3-5.

The crab-angle sensor was not used as an attitude reference at any time. This table also defines the average values of crab angle during the shutter-open sequence.

3.4.4 Readout

Off-Sun operation was required throughout readout to satisfy thermal requirements and retard thermal-paint degradation. A minus 30-degree pitch maneuver was performed while locked on Canopus at the beginning of readout. The minus 30-degree pitch maneuver was chosen to satisfy all constraints. Automatic updating of the roll axis by acquiring Canopus was continued. It was necessary to monitor the yaw axis to keep Canopus within the tracker yaw field of view and at the same time satisfy antenna pointing constraints. The pitch axis required periodic update maneuvers to maintain the spacecraft within readout limits.

Roll and yaw data were readily available during readout because the spacecraft position error did not exceed sensor telemetry saturation limits. The pitch axis, however, reached a Sun sensor telemetry saturation level at ± 29.0 degrees. It was therefore necessary to calibrate solar panel array current versus total angle off the Sun to determine pitch attitude. Knowing the total angle off-Sun and yaw angle, pitch angle could be determined. This procedure

Table 3-5: ATTITUDE CONTROL SUBSYSTEM DATA DURING PHOTO OPERATIONS

PHOTO SITE	NUMBER OF FRAMES	INITIAL ROLL ERROR (deg.)	MAX. RATE DURING PHOTO (deg/sec)			DEADZONE VARIATION DURING PHOTO (deg.)			AVERAGE CRAB ANGLE DURING PHOTO (deg.)
			ROLL	PITCH	YAW	ROLL	PITCH	YAW	
P1-S1	16-4	+0.026	+0.0040	+0.0014	+0.0019	.13	.11	.12	.35
P2a	8	+0.098	+0.0018	0	+0.0012	.18	.16	.16	.35
P2b	4	0.036	+0.0010	+0.0012	+0.0011	.15	.14	.14	.90
S2	1	0.148	—	—	—	—	—	—	—
S-3	1	0.076	0	.0014	+0.0011	.13	.15	.16	.53
S-4	1	+0.084	.0041	0	0	.12	.13	.14	.53
P-3	4	+0.079	0	+0.0024	.0011	.13	.04	.10	.25
P-4	8	0.075	+0.0018	+0.0020	.0013	.16	.02	.11	.20
P-5a	8	+0.117	0	+0.0018	+0.0023	.15	.17	.09	.20
P-5b	8	+0.108	+0.0010	+0.0010	-.0010	.16	.14	.12	.45
P-6	4	+0.016	.0021	0	0	.15	.14	.18	.22
S-5	1	-0.093	.0011	0	0	.08	.14	.16	.13
S-6	1	+0.137	0	.0009	0	.17	.12	.18	.80
S-7	4	-0.008	+0.0012	+0.0022	-.0011	.18	.10	.17	.40
S-8	1	0.137	0	+0.0012	0	.15	.13	.16	.53
S-9	1	+0.016	.0027	+0.0023	-.0013	.14	.12	.16	.14
S-10	4	-0.080	-.0020	-.0017	+0.0023	.12	.17	.04	.15
S-11	1	+0.113	-.0065	+0.0013	-.0020	0	.12	.11	.53
S-13	1	+0.093	-.0064	0	+0.0009	.08	.14	.13	.53
P-7a	8	-0.176	.0021	0	-.0012	.04	.16	.16	.90
P-7b	8	-0.052	+0.0010	+0.0020	0	.15	.06	.16	.35
S-14	1	-0.066	0	0	+0.0012	.12	.14	.12	.95
S-15	4	+0.050	-.0022	0	.0022	.11	.09	.16	.30
S-16	1	-0.028	-.0020	+0.0015	.0022	.14	.15	.16	.60
S-17	4	-0.259	0	0	+0.0009	.16	.12	.18	.53
S-18	4	-0.033	-.0018	0	+0.0010	0	.18	.08	.35
S-19	4	-0.042	+0.0093	0	+0.0010	.17	.16	.14	.30
S-21	1	-0.126	-.0016	-.0014	-.0017	.11	.16	.14	.53
S-21.5	1	-0.387	0	+0.0021	+0.0010	.16	.12	.16	.53
S-22	1	-0.042	0	+0.0016	0	.18	.04	.14	.05
S-20	1	0.074	+0.0020	0	0	.08	.12	.14	.53
P-8	8	-0.066	+0.0024	+0.0020	-.0014	.12	.06	.16	.25
S-23	4	+0.108	+0.0010	-.0010	+0.0024	.12	.10	.14	.25
S-24	1	+0.137	+0.0008	0	-.0023	.16	—	.18	.53
P-9a	8	+0.040	+0.0008	+0.0011	0	.15	.15	.15	.30
P-9b	8	+0.027	+0.0010	0	+0.0010	.16	.17	.08	.15
P-9c	8	-0.056	+0.0010	+0.0017	0	.14	.16	.13	.55
S-25	1	-0.157	0	0	-.0011	.16	.17	.16	.53
S-26	1	-0.032	+0.0012	+0.0010	0	.15	.16	.16	.53
P-10	8	—	+0.0020	+0.0007	-.0012	.05	.11	.15	1.05
S-27	1	-0.147	+0.0010	0	0	.16	.16	.16	.53
S-28	1	-0.340	-.0043	+0.0013	0	.08	.12	.16	.53
P-11	8	+0.141	-.0038	0	0	.17	.16	.13	.25
P-12b.2	4	+0.021	0	-.0012	+0.0011	.17	.08	.10	.30
P-12a	16	-0.046	0	-.0011	+0.0009	.17	.06	.12	.25
P-12b.1	4	+0.115	-.0022	0	0	.10	.14	.18	.25
P-12c	8	+0.006	+0.0014	+0.0014	-.0013	.15	.17	.16	.14
S-29	1	+0.209	-.0012	-.0020	+0.0008	.13	.12	.14	.53
S-30	1	0.104	+0.0026	+0.0006	-.0007	.08	.15	.14	.53
S-31	1	-0.172	—	—	—	—	—	—	—

proved to be accurate within ± 0.3 degree, averaging over a period of several days.

3.4.5 Component Performance

3.4.5.1 Canopus Star Tracker

The Canopus tracker was first turned on at 036:08:06, approximately 7 hours into cislunar flight. Result of the first star map, at 036:08:13, was uncertain because of data loss during the maneuver, however, a second roll of 360 degrees at 036:09:44 was successful in establishing a roll reference. At 036:11:52, the spacecraft was rolled +125 degrees to Canopus and a tracker off-on cycle was performed to observe and track the star.

Canopus was tracked without controlling the spacecraft in the closed-loop mode throughout cislunar. The tracker lost Canopus six times during this period: once when the squibs were fired, four times with no apparent spacecraft disturbance, and once just prior to injection when the Moon albedo caused a pronounced glint problem. Each time track was regained by performing an off-on cycle.

Star map signal was initially 3.7 volts, decayed to 2.6 volts through cislunar, and recovered to 3.25 volts by the end of the mission. Following injection the tracker was operated only in the dark.

During sunset of the fourth orbit, at 040:11:39, Canopus was acquired in the closed-loop mode. For the remainder of the mission the basic operational procedure was to operate the roll axis in the sensor mode (using celestial references) so that Canopus would be acquired each time the tracker was turned on.

A star map was performed at 041:02:08. Results of this map agreed well with the apriori maps.

Through GMT 061 the tracker had been on for a total of 79 hours, having gone through 158 on-off cycles.

3.4.5.2 Sun Sensors

The Sun sensors performed as expected for Mission III, providing a celestial reference for a variety of nonnominal situations.

The initial Sun acquisition took place automatically within the required 60 minutes from launch. During the initial Sun acquisition as soon as the telemetry data was good (56 minutes after launch), it was observed that the Sun had already been acquired in pitch and yaw. The exact time of acquisition could not be determined. Reacquisition of the Sun after Sun occultation of attitude maneuvers was performed approximately 126 times; 121 of these acquisitions were done in the narrow deadband and five were done in the wide deadband. Every acquisition went as expected.

The Sun sensor readings while occulted from the Sun are presented below.

SUN SENSOR OUTPUT DURING SUN OCCULTATION			
	MODE	PITCH (deg)	YAW (deg)
Fine	Observed T/M	+0.002	-0.044
	Ground Test	-0.093 to +0.097	-0.140 to +0.052
Coarse	Observed T/M	-0.11	+0.24
	Ground Test	-0.397 to +0.750	-0.343 to +0.814

*NOTE: Resolution of the telemetry for coarse mode is 0.3 degree.

These values are close to those observed during ground testing and are useful in ascertaining null shift in sensor position readings when viewing the Sun.

The capability of switching between fine, coarse and fine, and coarse only Sun sensors proved invaluable for "off Sun" operation. The ability to stay off Sun for extended periods using the coarse Sun sensors greatly reduced nitrogen consumption. Yaw Sun sensor degradation due to a large pitch attitude was approximately the same as observed for Missions I and II. This degradation at a pitch angle of 30 degrees is approximately 0.75. Moonlight on the coarse Sun sensors caused shifts in error output for various portions of the orbit as on previous missions with no effect on the mission.

Two Sun acquisitions were performed in the wide deadzone. Rates were observed to be 0.105 and 0.178 degree per second. The expected rate is 0.60 ± 0.50 or 0.10 to 1.1 degree per second.

3.4.5.3 Closed-Loop Electronics

The closed-loop electronics performed without incident throughout the mission. The closed-loop electronics successfully selected, on command from the programmer, the inertial reference unit, Sun sensors, and Canopus star tracker, closing the loop between sensor outputs and vehicle dynamics.

The minus pitch Sun sensor limiter had a very "hard" limit at 29 degrees, while the plus pitch Sun sensor limiter had a "soft" limit at 29 degrees.

The minimum impulse circuit or "one shot" appeared to be operating between 11 and 14 milliseconds throughout the mission (typical values for Missions I and II also). A value of 11 milliseconds is nominal. The minimum impulse circuit allowed "approximate single pulses" of 50, 50, and 20% of the time during limit cycle operation for the roll, pitch, and yaw axes, respectively. This type of operation was possible

in the inertial-hold and gyro-rate modes for both the 2.0 and 0.2-degree deadband.

3.4.5.4 Reaction Control System

The reaction control system thrusters performed satisfactorily during the mission. The thrusters operated approximately 17,000 times during the mission; 1654 operations were for attitude maneuvers and the remainder were for limit cycle operation. The individual thruster performance was evaluated for as many of the spacecraft maneuvers as possible. Actual, predict values, and specification values for each axis are tabulated below:

THRUSTER PERFORMANCE			
AXIS	ACTUAL THRUST (lb)	PREDICTED (lb)	SPECIFICATION VALUE (lb)
Roll	0.069 ± 0.004	0.063 ± 0.003	0.051 to 0.070
Pitch	0.065 ± 0.003	0.056 ± 0.003	0.045 to 0.062
Yaw	No data	0.058 ± 0.003	0.045 to 0.062

The observed thrusts are higher than the predict values. There were no yaw maneuvers that allowed a yaw thrust determination. However, the yaw thrust was probably approximately 0.065 pound. The roll and pitch thrust values are within specification tolerance but tend to be high. These slightly high thrust values in no way degraded the mission or the maneuver accuracy, and nitrogen consumption was not increased perceptibly.

Slight cross coupling was observed during maneuvers and limit cycle; however, in view of the data observed, it is impossible to estimate the magnitude of the cross coupling or

even to determine if it is caused by thruster misalignment or gyro cross coupling.

3.4.5.5 Thrust Vector Control System

Control of spacecraft attitude during the three engine burns were performed as required by the thrust vector control system. Residual rates after each burn were lower than predicted maximums for stable TVC limit cycle operation.

Travel of the center of gravity from nominal was small and compares closely with Mission II. Maximum excursion of the actuators for all of the burns were: pitch -0.2 to $+0.21$ degree and yaw $+0.02$ to $+0.35$ degree.

3.4.5.6 Inertial Reference Unit

The inertial reference unit performed satisfactorily throughout the mission. The gyro-rate-integrating-mode drifts were low and stable. Over the duration of the mission roll, pitch, and yaw were: -0.12 ± 0.01 , $+0.15 \pm 0.03$, 0.02 ± 0.03 degree per hour, respectively.

Spacecraft maneuver errors as determined from 360-degree maneuvers are tabulated below.

COMMANDED MAGNITUDE	ACTUAL MAGNITUDE (deg)	MANEUVER ERROR (deg)	ERROR (%)
Roll +360	360.19	+0.19	0.05
Roll -360	-359.74	+0.26	0.07
Pitch +360	360.45	+0.45	0.13
Yaw +360	360.56	+0.56	0.16
Yaw -360	-359.89	+0.11	0.03

These errors are partly attributable to gyro-rate-mode error and partly to voltage to frequency converter error, which are not separable in telemetry data.

Gyro-rate-integrating-mode output was found to agree with the tracker/Sun sensor position output within 0.03 degree, which is about the resolution of the measurement involved.

Gyro wheel currents were nominal and stable. Gyro thermal control was normal with no indication of heater saturation.

No direct method of evaluating accelerometer performance is available. At this writing computations have not been performed that will allow comparison of actual and commanded ΔV magnitude.

3.4.5.7 Flight Programmer And Switching Assembly

The command relay function of the flight programmer and switching assembly is essential for proper spacecraft attitude control. The flight programmer responded correctly to every command received from the command decoder during the mission. On March 2 (Day 061) 1266 real-time commands and 2349 stored program commands had been received as of 1530 GMT. Repetitive execution of stored program commands account for an estimated total of 14,000 commands executed correctly by the programmer. Total programmer clock drift was -0.16 second. The programmer breadboard was used satisfactorily at the SFOF to follow the mission sequence of commands and to maintain a check of flight programmer operations during spacecraft occultation periods. All stored-program commands that were to be transmitted to the spacecraft were first checked on the breadboard.

3.4.6 Nitrogen Consumption

Nitrogen consumption for the attitude control system for Mission III is presented in Figure 3-32. Missions I and II usage is also presented for comparison.

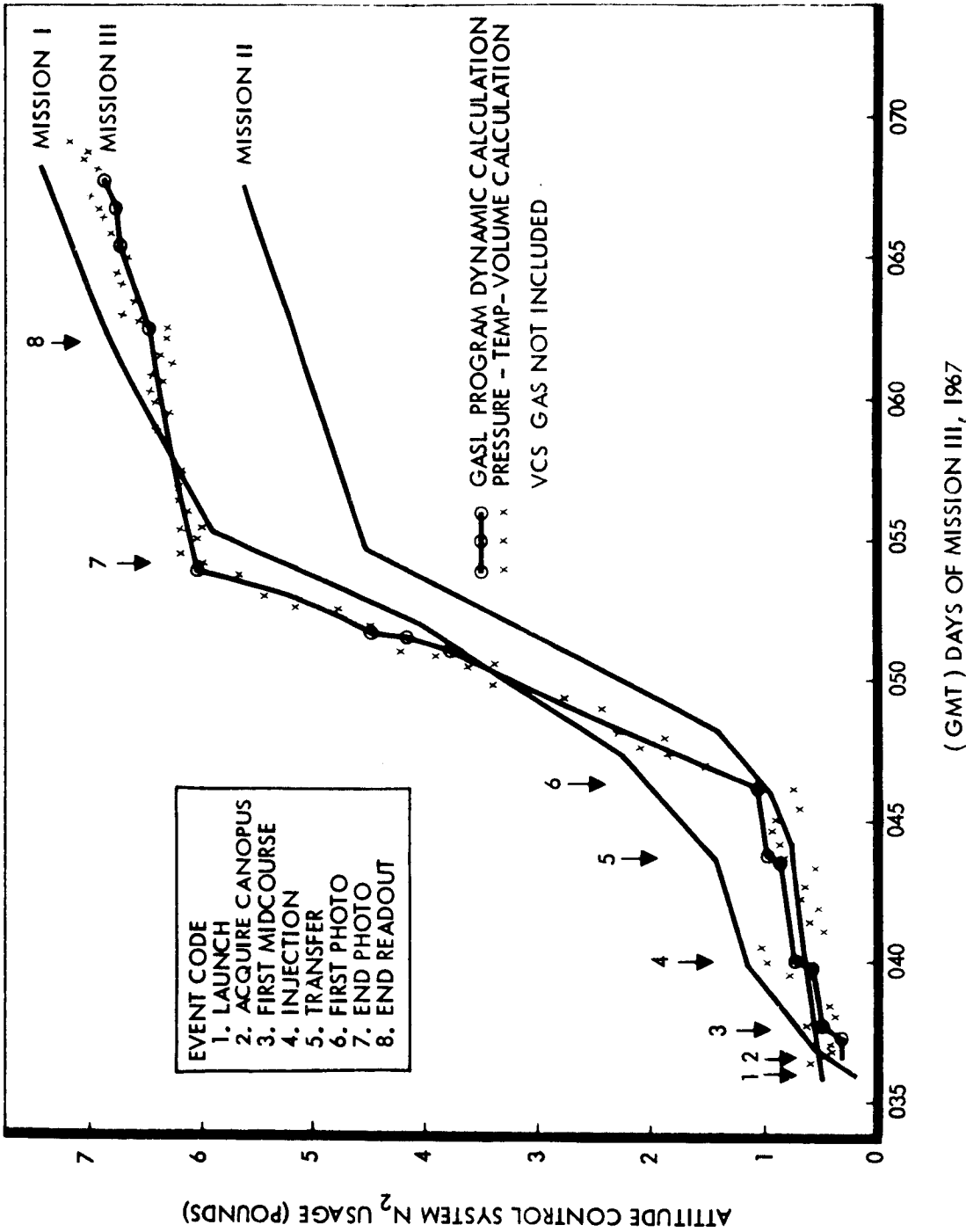


Figure 3-32: Attitude Control System Nitrogen Usage

Nitrogen usage for Mission III is substantially more (1.20 pounds) than for Mission II. Mission III did have 11 more photo maneuvers and 69 more pitch-off thermal maneuvers than Mission II. Other than those differences, Missions II and III were very similar in gas usage.

At Day 062, the amount of unaccounted nitrogen since launch at Day 036 was approximately 0.10 pound; this is 0.003 pound per day.

The slight disturbance (0.004 pound per day) that occurred in one to three axes whenever the tracker was turned on during Mission II did not occur during Mission III.

The total nitrogen quantities used for Lunar Orbiter photo missions follow.

	Nitrogen		
	MISSION I (lb)	MISSION II (lb)	MISSION III (lb)
Attitude Control System	7.80	5.50	7.00
Velocity Control System	3.38	3.14	2.70
Leakage	<u>1.13</u>	<u>0.0</u>	<u>0.0</u>
Total	12.31	8.64	9.70
Initial N ₂ at Launch	15.10	15.15	15.17
N ₂ for Extended Mission	2.79	6.51	5.47

The maneuvers performed on Mission III for launch through 062:07:17 GMT are given below:

MISSION III MANEUVERS						
Purpose of Maneuver	ROLL (WDZ)(NDZ)	PITCH+ (WDZ)(NDZ)	YAW (WDZ)(NDZ)	TOTALS (WDZ)(NDZ)	PREDICTED	
Star Map	0 4	0 0	0 0	0 3	3	
Attitude Update	5 4	0 1	0 1	5 6	30	
Thermal Pitch Off	0 0	10 57	0 0	10 57	10	
Velocity Change	0 6	0 6	0 0	0 12	12	
Photo Maneuver	0 104	0 94	0 82	0 280	286	
Other	2 3	0 5	0 0	2 8	17	
Subtotal	<u>7 120</u>	<u>10 163</u>	<u>0 3</u>	<u>17 66</u>	<u>358</u>	
Total	127	173	83	383	358	

Celestial Acquisitions	NARROW DEADBAND	WIDE DEADBAND	TOTAL
Canopus Acquisitions	108	19	127
Sun Acquisitions	116	5	127
Deadband Closures	9		

WDZ = Wide Deadzone
NDZ = Narrow Deadzone

3.4.7 Problem Areas

During Mission III, there were problems with equipment in or related to the attitude control system, or in other subsystems that resulted in a nonnominal operation of the attitude control system. Summarized below are the problems and their effects on the mission.

3.4.7.1 Thermal Problem

Again on Mission III, spacecraft overheating was encountered, resulting in operating the spacecraft in a pitch off-Sun attitude for approximately 65% of the mission. As a result, 73 maneuvers were required for pitch-off maneuvers and updates of the inertial reference as compared to 151 maneuvers during Mission I and 25 maneuvers during Mission II. There were a greater number of thermal maneuvers performed during this mission because of the pitch-off requirements during the photo mission that were not required on Mission II.

3.4.7.2 Tracker Glint Problem

Tracker glint continued to be present on Mission III as well as Missions I and II. During Mission III, Canopus track was lost six times (all of which were during the cislunar phase with the spacecraft in the Sun). Canopus track was regained each time by cycling the tracker off, then back on. The sixth loss of Canopus occurred about 5.5 hours prior to lunar orbit injection when reestablishment of the Sun/Canopus reference was performed. Severe glint continued for about 1.5 hours, making Canopus track impossible. The tracker regained lock on Canopus 1.5 hours after initial Canopus loss and a successful injection burn was obtained. If Canopus track could not be regained, a possible error of 1.5 degrees may have resulted in the orbit injection maneuver. Following orbit injection the tracker was used only in the shadow of the Moon without glint problems.

3.5 VELOCITY CONTROL SUBSYSTEM PERFORMANCE

The velocity control subsystem (VCS) is a liquid bipropellant, pressure-fed, expulsion-bladder propulsion system using a single 100-pound thrust, radiation-cooled, gimbal-mounted rocket engine for mid-

course, orbit-injection, and orbit-transfer maneuvers. The propellants are N₂O₄ and Aerozene 50 (a 50-50 mixture of hydrazine and UDMH). Nitrogen gas is the pressurizing medium.

Operation and performance of the VCS was well within specification throughout the mission. Three propulsive maneuvers were conducted in support of the primary mission; these were: 5.09-mps midcourse, 704.3-mps orbit injection, and 50.7-mps orbit transfer.

Prelaunch propellant and nitrogen servicing operations were accomplished without difficulty. There were 275.873 pounds of propellant and 15.17 pounds of nitrogen loaded; the spacecraft launch weight was 856.71 pounds. Based on this data, the nominal velocity increment capability of the VCS was determined to be 1010.6 mps with a 3-sigma tolerance of ± 43 mps.

Flight-data-performance analysis indicates that during the midcourse maneuver, the rocket engine average thrust was approximately 102.5 pounds; thrust determination was difficult because of the short (4.3 seconds) operating time. Delivered thrust during the orbit-injection maneuver was calculated to be 99.85 pounds. During the transfer maneuver, the delivered thrust was 100.3 pounds. The engine specific impulse was determined to be approximately 276.5 to 277.5 seconds during all three maneuvers. A total velocity change of 760.09 mps has been imparted to the spacecraft with a total engine operating time of 580.5 seconds.

The sections following present the various aspects of the velocity control subsystem's operation during the flight of Lunar Orbiter III as supported by the SPAC at the SFOF.

This includes discussion of the launch count-down and flight events. Emphasis is placed on flight operations and VCS performance during propulsive maneuvers. Before entering into the discussion of system operation and its characteristics, it is pertinent to briefly summarize, in tabular form (see Table 3-6), the results of the three propulsive maneuvers.

**Table 3-6:
VELOCITY CONTROL SUBSYSTEM
MANEUVER PERFORMANCE**

	Velocity Change (mps)	Burn Time (sec)	Thrust (lb)	Specific Impulse (sec)
Midcourse				
Predict	5.11	4.5 ± 0.5	99.6	273.2
Actual	5.09	4.3	≈ 102.5	≈ 276
Injection				
Predict	704.3	540.5 ± 10	100	276
Actual	704.3	542.5	99.85	277
Transfer				
Predict	50.7	33.4 ± 1.6	101.3	277
Actual	50.7	33.7	100.3	277

3.5.1. ESA Spacecraft Fueling Operations

After completing all Hanger S checkout tests, the Mission III spacecraft was transferred to the explosive safe area (ESA) for fueling and pressurization, further testing, and encapsulation into the nose shroud. The propellant and nitrogen servicing AGE functioned without incident. Table 3-7 summarizes the servicing quantities that were loaded on board January 18, 1967.

After completion of velocity control subsystem servicing, the complete flight-configuration spacecraft was weighed and balanced; launch weight was determined to be 856.71 pounds. Calculations were performed to ascertain the velocity increment capability

**Table 3-7:
PROPELLANT AND NITROGEN
SERVICING SUMMARY VELOCITY
CONTROL SUBSYSTEM**

	Fuel	Oxidizer	Nitrogen
On-Board, (lb)	94.123	181.75	15.17
Ullage Volume, (in ³)	63.0	118.89	-
Pressure, (psig)	45	45	3535
Temperature, (°F)	64	60	62

of the spacecraft based on the aforementioned weights and the rocket engine performance as determined from ground test. The Δv capability was found to be 1010.6 with a 3 sigma tolerance of ± 43 meters per second.

3.5.2 Launch and General Mission Events Through Midcourse Maneuver

The launch countdown was initiated on February 4, (Day 035) with power turn-on occurring at 17:13 GMT; all velocity control subsystem parameters were normal. The velocity control subsystem countdown test was successfully conducted at 20:28 GMT, resulting in pitch- and yaw-actuator deflections of -0.958 and +0.232 degree, respectively; maximum engine valve temperature was 70.6°F. Vehicle liftoff occurred at 0117:01.120 GMT on Day 036. Real-time telemetry loss occurred as expected until acquisition of the spacecraft by DSS-41; the spacecraft separated from the Agena at 0139:39.67 GMT.

Upon acquisition by DSS-41 at 0213 GMT (Day 036), it was verified that the propellant tanks had been pressurized to normal values of 193.6 and 193.8 psia, fuel and oxidizer, respectively. By 1708 GMT, the gradually increasing thermal environment had increased the pressure levels to 195 and 198 psia, fuel and oxidizer, respectively.

The next significant velocity control subsystem event concerned bleeding the propellant lines between the engine and the then closed propellant-squib valves. The bleed event occurred at 1708 GMT on February 5 (Day 036); the engine valves were open for 30 seconds, thereby increasing valve temperature by 11.3°F, as expected. This activity was followed by propellant-squib-valve actuation at 1720:31 GMT; propellant-tank-pressure decay down to 194 psia provided positive confirmation of valve actuation.

The midcourse maneuver for trajectory adjustment was designed for engine ignition to occur at 1500:00.0 GMT on February 6 (Day 037), thereby imparting a velocity change of 5.11 mps. The maneuver was conducted without incident; a velocity change of 5.09 mps was achieved with an approximate engine operating time of 4.3 seconds. The slight difference between desired and achieved velocity resulted from round-off techniques in the command generation programming; the flight programmer actually commanded the magnitude of 5.09 mps that was achieved.

3.5.3 Lunar-Orbit Injection through Final Readout

The orbit-injection maneuver was programmed for engine ignition to occur at 2154:19.0 GMT on February 8 (Day 039); the desired velocity change was 704.3 mps. The maneuver resulted in orbital elements that were well within the required tolerance. Engine operating time was determined to be 542.5 seconds; engine valve temperature was 70 to 77°F during engine operation, and reached a maximum value of 112.4°F approximately 1 hour following the maneuver.

The maneuver to transfer from the initial orbit to the photographic reconnaissance

orbit was performed with engine ignition occurring at 1813:26.6 GMT on February 12 (Day 043). The desired velocity change of 50.7 mps was achieved with an engine operating time of 33.7 seconds. Tracking data indicated that the desired perilune altitude was achieved with an error of approximately 0.1 km. This maneuver completed the propulsive requirements necessary to fulfill the primary objectives of Mission III. At the end of the photo mission operations on March 3 (Day 061), the spacecraft had a remaining velocity change capability of 250 to 260 mps, and approximately 60 pounds of nitrogen for attitude control purposes; the nitrogen shutoff-squib valve had not been actuated.

3.5.4 Subsystem Time—History Data

Figure 3-33 presents the quantity of nitrogen gas remaining in the storage vessel as a function of time throughout the primary phase of the mission. The gas weight data is calculated on the basis of the storage tank's known volume, pressure, temperature, and compressibility factor. The data points are plotted at 6-hour increments and represent a 6-hour average centered about the plotted time. For reference, a nominal mission budget and a significant-events code is included in the plot. The actual consumption rates are worthy of special mention. Note, for instance, the extremely small usage during the period between orbit injection and transfer. This results from two factors: (1) small gyro-drift rates, thereby requiring only six maneuvers for attitude update and thermal control; and (2) conducting those maneuvers in the wide deadzone. Consumption during site photography is observed to be greater than the nominal budget. This follows from the fact that the budget is predicated on photographing 11 sites; whereas, during Mission III there

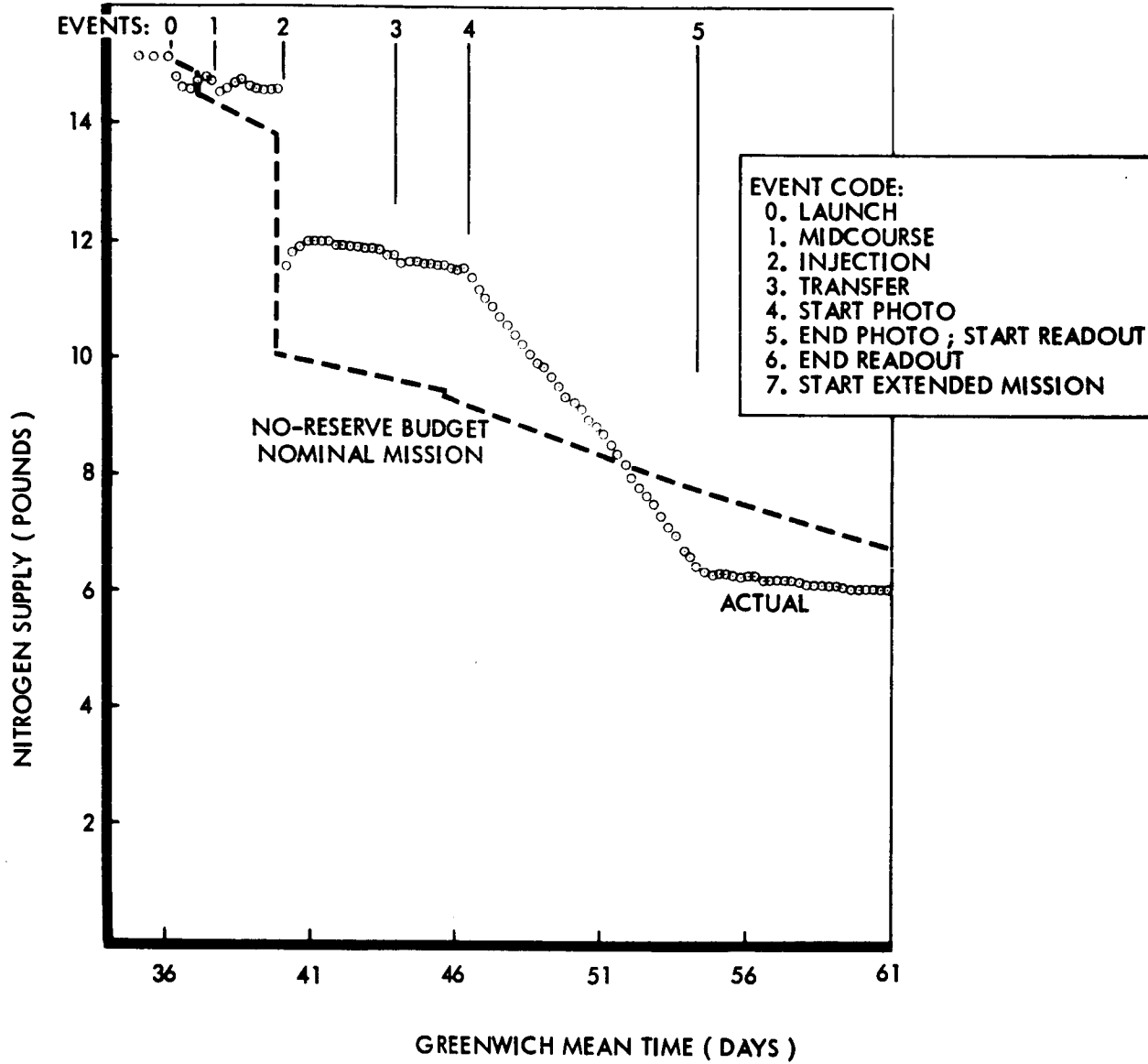


Figure 3-33: Velocity Control System Available Nitrogen History

were 51 sites photographed in 55 orbits. Nitrogen consumption during site photography is calculated to be 0.632 pound per day.

In Figure 3-33 note the increase in usage rate beginning at approximately Day 051; this results from the fact that, following the reverse attitude maneuvers away from a site, a fourth maneuver was included to pitch the spacecraft off the sunline. Low consumption rates are again apparent during final readout; (i.e., 0.049 pound per

day). Even though the ACS was in the narrow deadzone mode, gyro drift rates were minimal to the degree that only 12 maneuvers were required for attitude update.

Figure 3-34 shows the variations in subsystem pressures during the flight. The fluctuations in propellant tank pressures are essentially the result of whether the spacecraft was locked on the Sun, or pitched off the Sun. The pressure profiles throughout the mission are nominal.

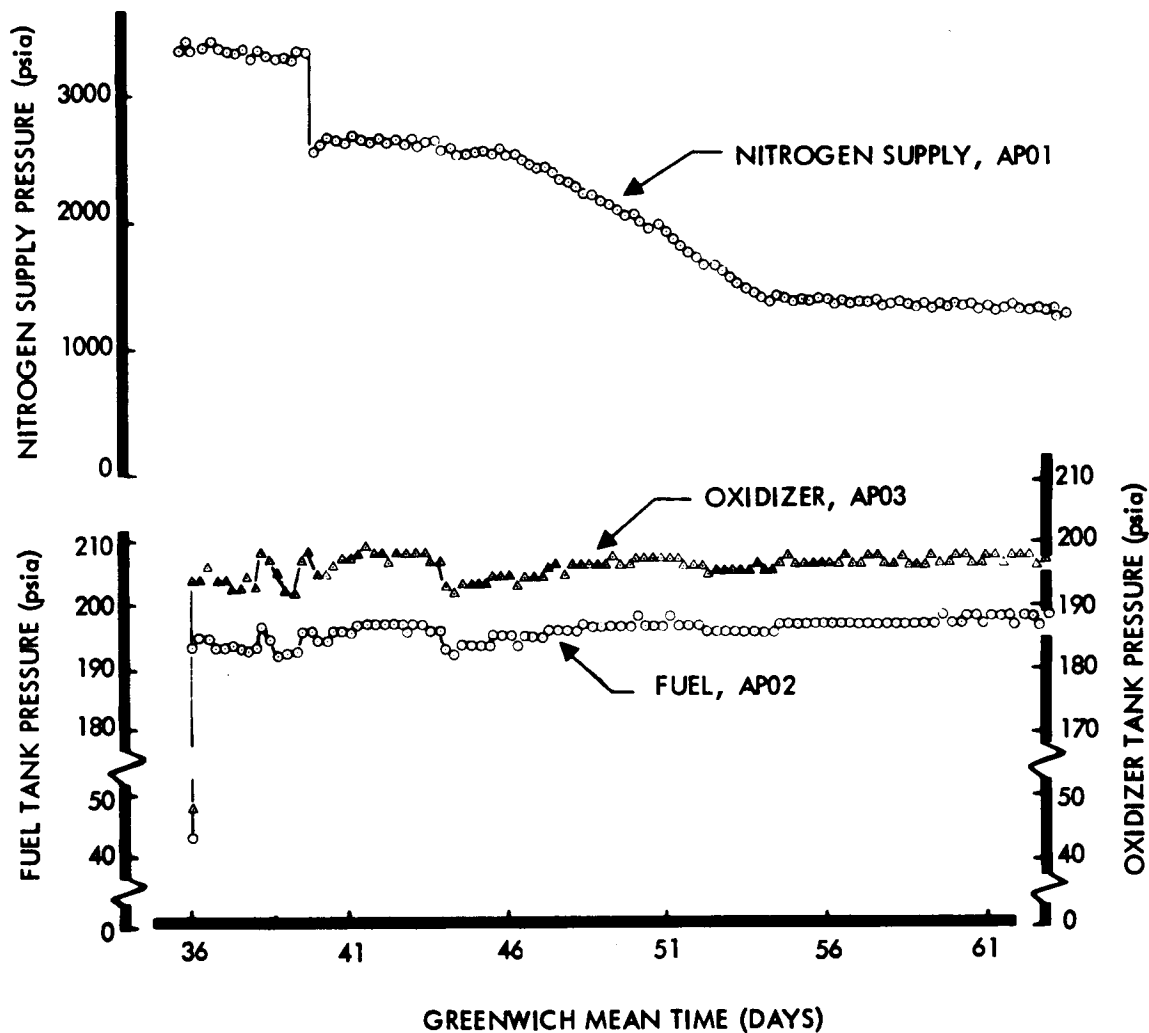


Figure 3-34: Velocity Control System Pressure-Time Histories

Figure 3-35 plots subsystem temperature/time histories in a similar manner (12-hour increments only). Local temperature values were generally in the region of 40 to 80°F during the flight, varying somewhat when the spacecraft was pitched on and off the sunline. Propellant tank heaters were used during the initial orbital phase of the mission to keep propellant-tank-deck temperature (ST04) above a value of 40°F. The heaters were activated on 21 occasions for a total on time of 1408 minutes; the average value of 67 minutes per cycle produced an average temperature increase of 4.7°F. All temperatures remained well within acceptable limits.

3.5.5 Maneuver Performance

During the primary photographic mission of Lunar Orbiter III, the velocity control subsystem provided three propulsive maneuvers for alteration of the spacecraft's trajectory or orbital elements. These consisted of midcourse, orbit-injection, and orbit-transfer maneuvers; 760.09 mps of an on-board nominal velocity increment capability of 1010.6 mps were expended. The subsystem performance summary is presented in Table 3-6.

The orbit-injection maneuver (the most representative) indicates that the system

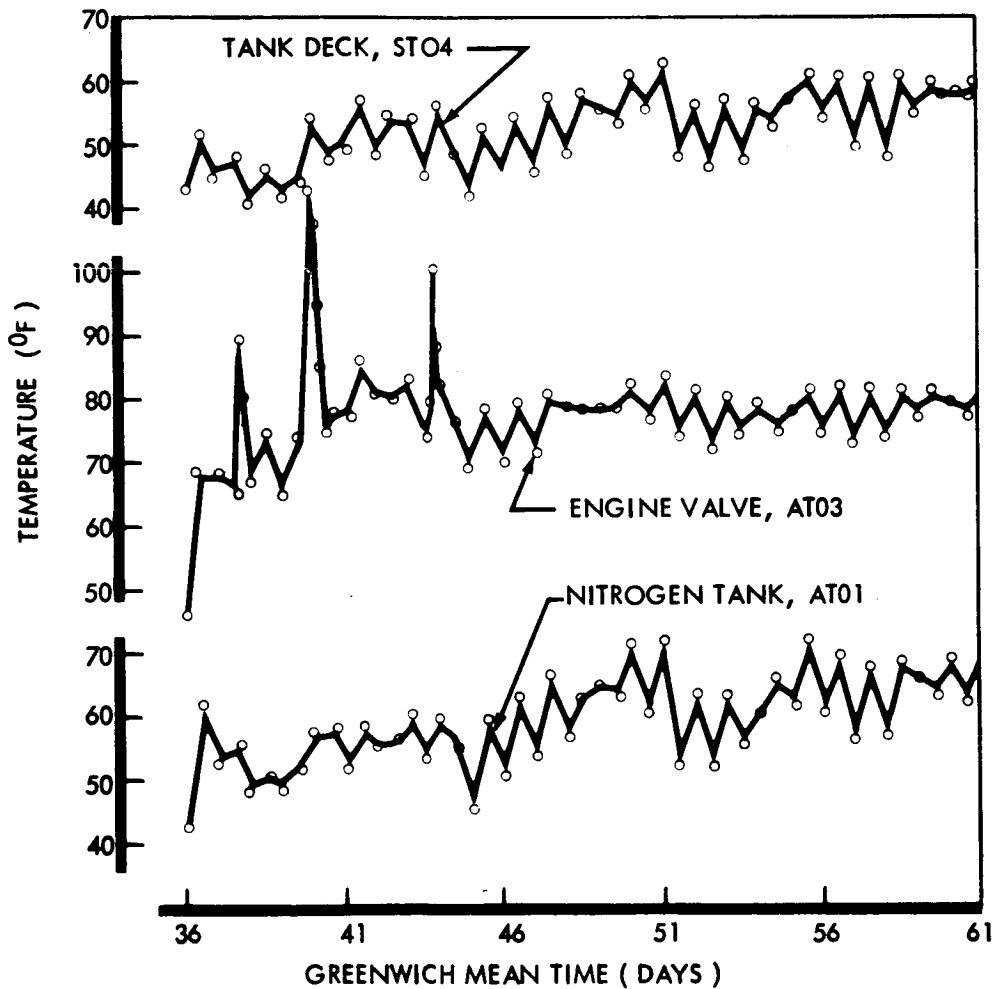


Figure 3-35: Velocity Control System Temperature-Time Histories

had a delivered thrust of 99.85 pounds at a specific impulse of approximately 277 seconds. For comparison, the engine on the spacecraft demonstrated the following performance characteristics during the acceptance test.

	Test Data	
	(5 sec)	(70 sec)
Thrust	99.6	99.7
Specific Impulse	279.3	278.8
Mixture Ratio	2.001	1.995

The engine acceptance test data is normalized to a standard propellant temperature of 70°F. An average value of propellant temperature (ST04) during flight, and specifically preceding the in-

jection maneuver, was approximately 53°F. Adjusting the acceptance test performance for actual temperatures indicates an anticipated flight specific impulse value of 276.1 seconds. The agreement between predicted and actual performance is well within the capability to evaluate flight telemetry results. It is possible to infer an average operating mixture ratio; this is accomplished by adjusting flight conditions with the proper influence coefficients, and then comparing with acceptance test data. For the orbit-injection maneuver, the estimated operating mixture ratio was found to be 1.99.

Figures 3-36 and -37 present velocity control subsystem telemetry data obtained during

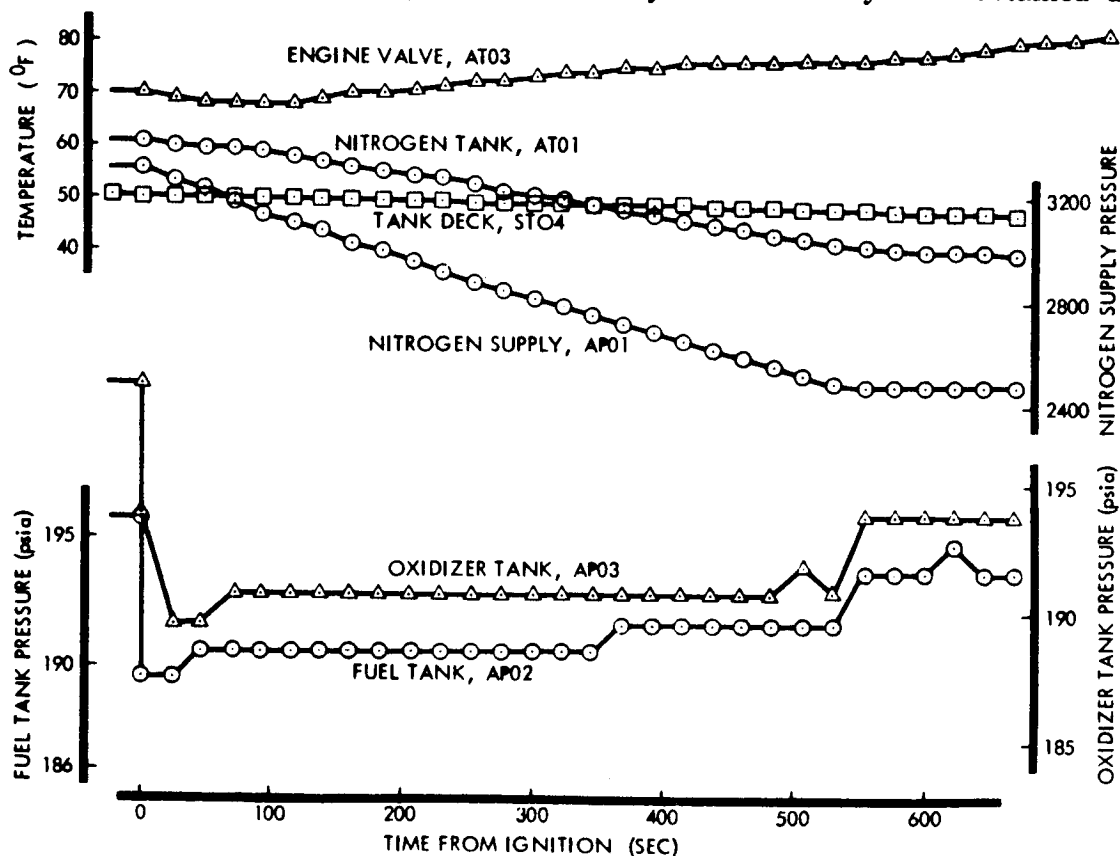


Figure 3-36: Velocity Control System Orbit Injection Maneuver—System Pressures and Temperatures

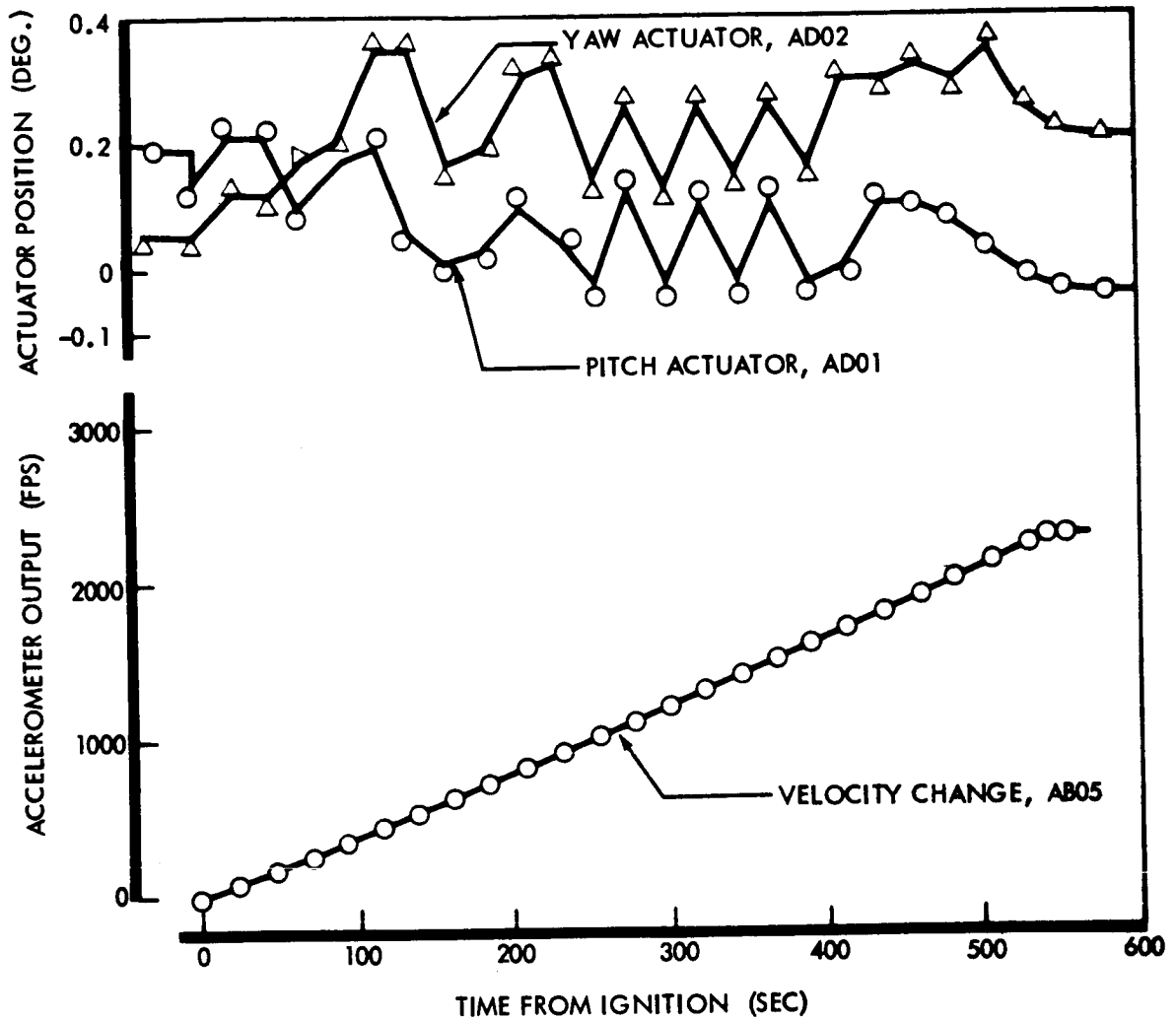


Figure 3-37: Velocity Control System Orbit Injection Maneuver—System Dynamics

the orbit-injection maneuver; Figure 3-36 shows pressure and temperature data, and Figure 3-37 plots dynamic data in the form of gimballed actuator positions and accelerometer output. It can be stated that the data, and their trends, are nominal and as expected.

Engine valve temperature during and following each maneuver was normal. A brief summation of maximum valve temperature (AT03), resulting from thermal conduction, is presented in Table 3-8.

Table 3-8:
ENGINE VALVE TEMPERATURE
MAXIMUM CONDUCTION

	°F
Midcourse	84.8
Injection	112.4
Transfer	100.1

The maximum value generally occurred 60 to 90 minutes after maneuver completion.

Table 3-9 summarizes gimbal actuator position before and after each maneuver.

Table 3-9:
GIMBAL ACTUATOR POSITION

	Pitch, (deg.)		Yaw, (deg.)	
	Pre-	Post-	Pre	Post
Launch	-0.040	-0.040	0.053	0.053
Midcourse	-0.063	0.191	0.009	0.053
Injection	0.191	-0.040	0.053	0.210
Transfer	-0.017	0.115	0.254	0.187

The slight discrepancies between the conclusion of one maneuver and the beginning of the next are reflections of the resolution characteristics of the data.

3.6 STRUCTURES AND MECHANISMS

A brief discussion of factors relating to the structures and mechanisms of Lunar Orbiter III follows. This involves a presentation of vibration data observed during launch, the deployment and squib-actuation sequencing, and camera-thermal-door operational history. No micrometeoroid impacts were recorded; one detector (DM-17) was punctured before emplacement of the spacecraft on the launch vehicle.

3.6.1 Launch Vibration Environment

Figures 3-38 through -53 present vibration data (as recorded from Agena telemetry) from liftoff at 01:17:01.120 GMT to Agena second cutoff at 01:36:55.5 GMT. For comparison, the upper envelope of spacecraft sinusoidal FAT vibration is included. The flight data peaks fall well below the peaks of the FAT envelope. These data are comparable to that observed during Missions I and II.

3.6.2 Deployment and Squib Actuation

Following spacecraft separation from the

Agena at 01:39 GMT, the deployment sequence was initiated. Based on the stored-program commands, antenna deployment was initiated at 01:41:30.4 GMT, solar panel deployment commenced at 01:41:56.2 GMT, and the nitrogen isolation-squib valve was actuated at 01:42:47.8 GMT. On receipt of first good data from DSS-41 at 02:13 GMT, it was verified that all deployment events had been successfully accomplished. The VCS propellant isolation-squib valves were successfully actuated at 1720:31 GMT. As of the conclusion of the primary mission, the nitrogen shutoff-squib valve had not been actuated.

3.6.3 Camera Thermal Door

No abnormalities were observed in actuation of the camera thermal door. The unit cycled satisfactorily on each of the 51 photographic sites.

3.6.4 Thermal Control

The thermal control subsystem of the Lunar Orbiter spacecraft is a passive system with the equipment mounted on a Sun-oriented equipment mounting deck (EMD). Heat generated by equipment is conducted to the EMD, where it is radiated to the space environment. The EMD is coated with a low-solar-absorptance paint. Thermal control is achieved by varying the attitude of the EMD with respect to the Sun. The equipment is enclosed in multilayer blanket insulation and supplemental heating is supplied, as needed, to the propellant tanks and photo subsystem by electric heaters.

Spacecraft temperatures were maintained within prescribed temperature limits throughout the mission - with the exception of Orbit 149, during which the film-drive-motor failure occurred. During this period, from 061:16:00 to 061:18:00 GMT, the

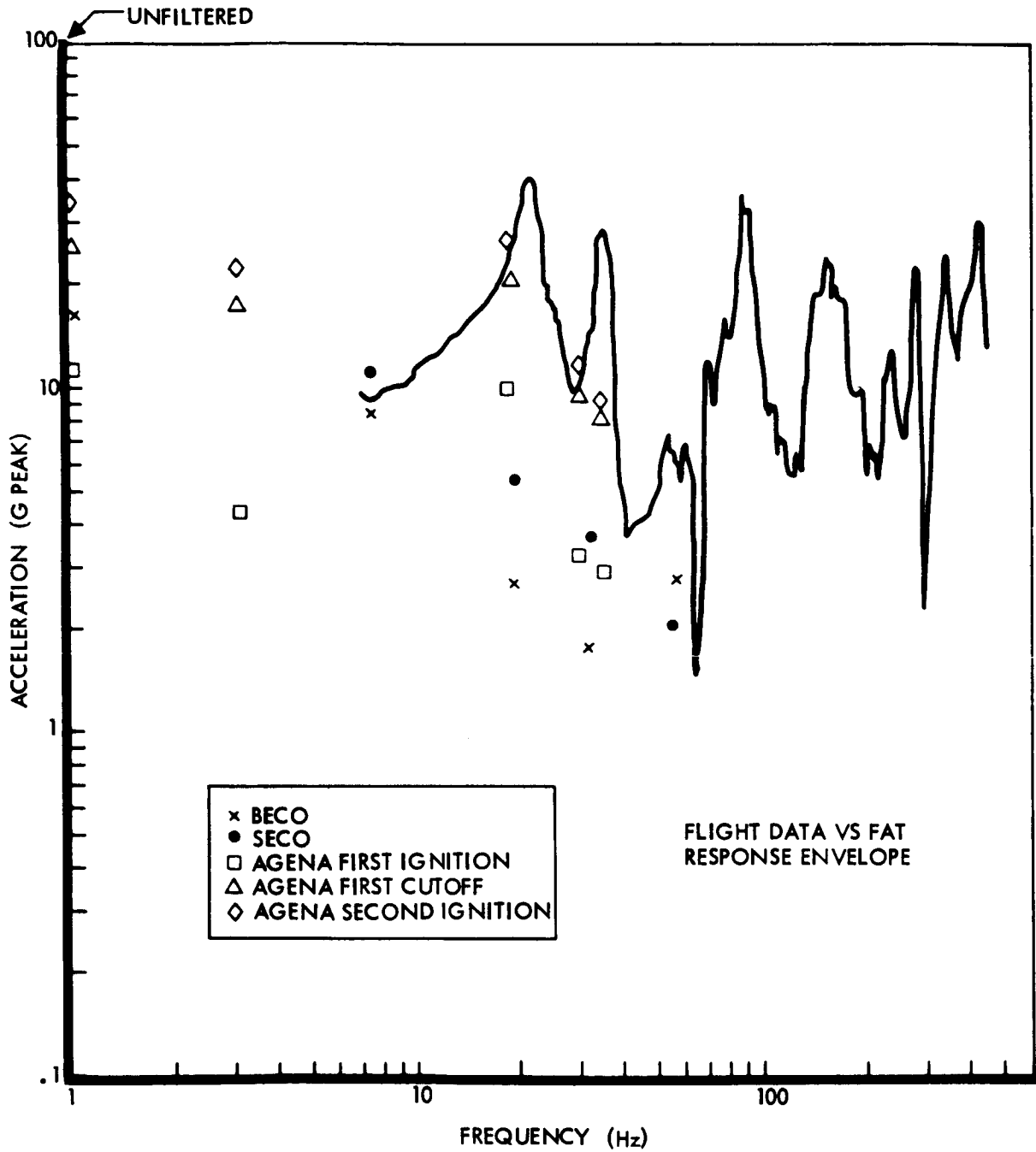


Figure 3-38: Spacecraft Vibration—Peak Longitudinal Response (214 x)

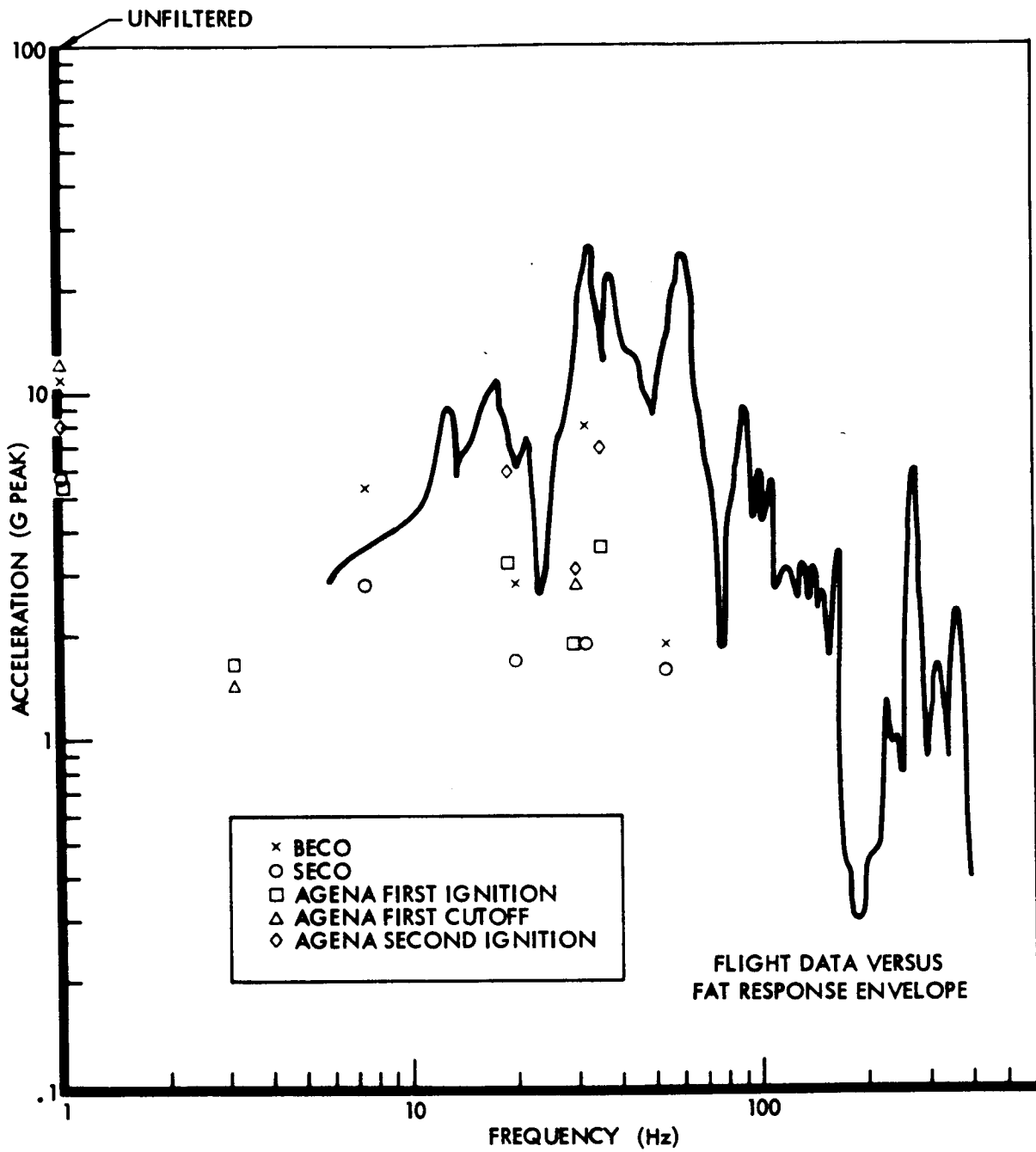


Figure 3-39: Spacecraft Vibration—Peak Lateral Response (210 z)

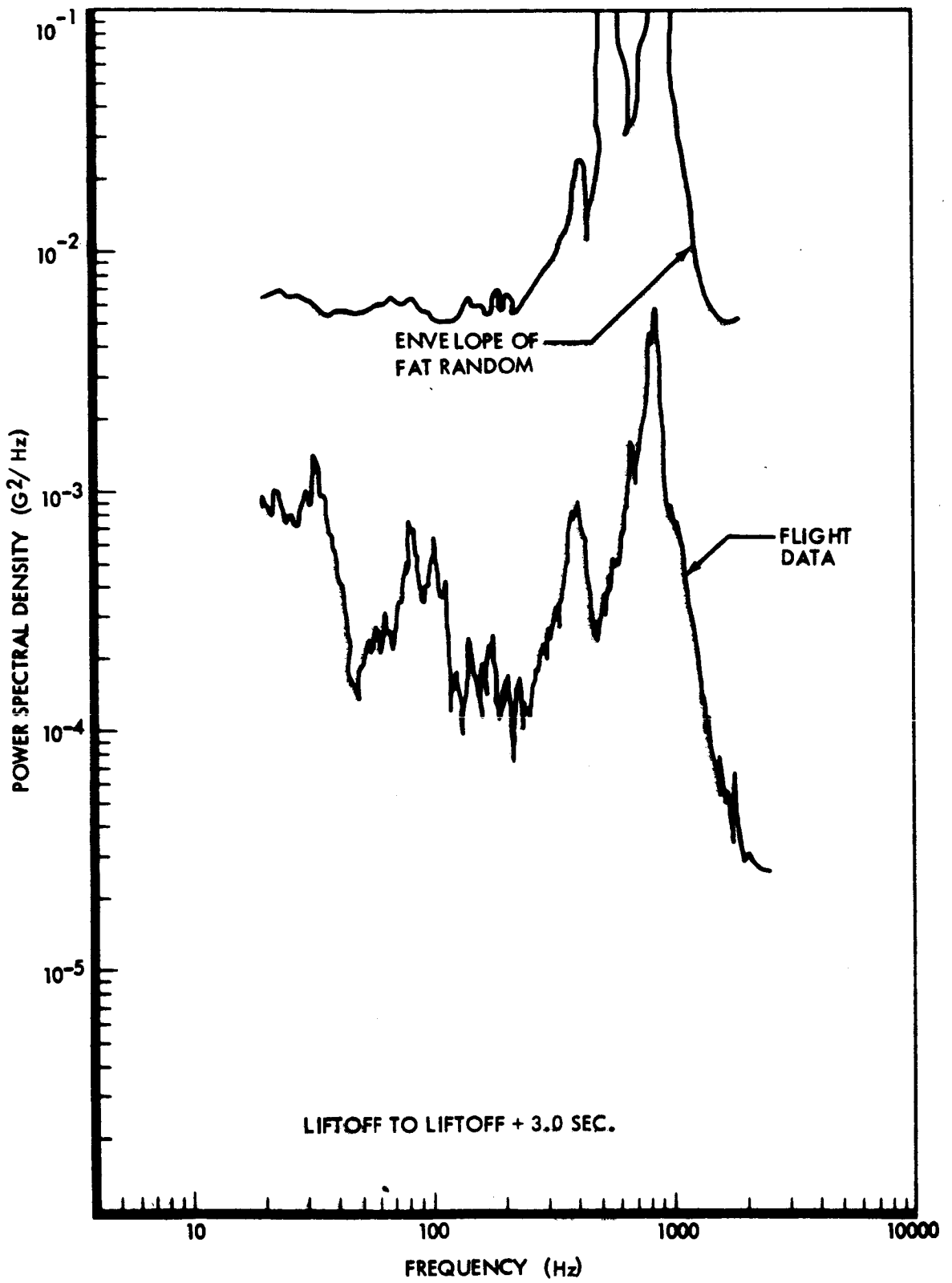


Figure 3-40: Random Response at Liftoff—Longitudinal Pickup (214 x)

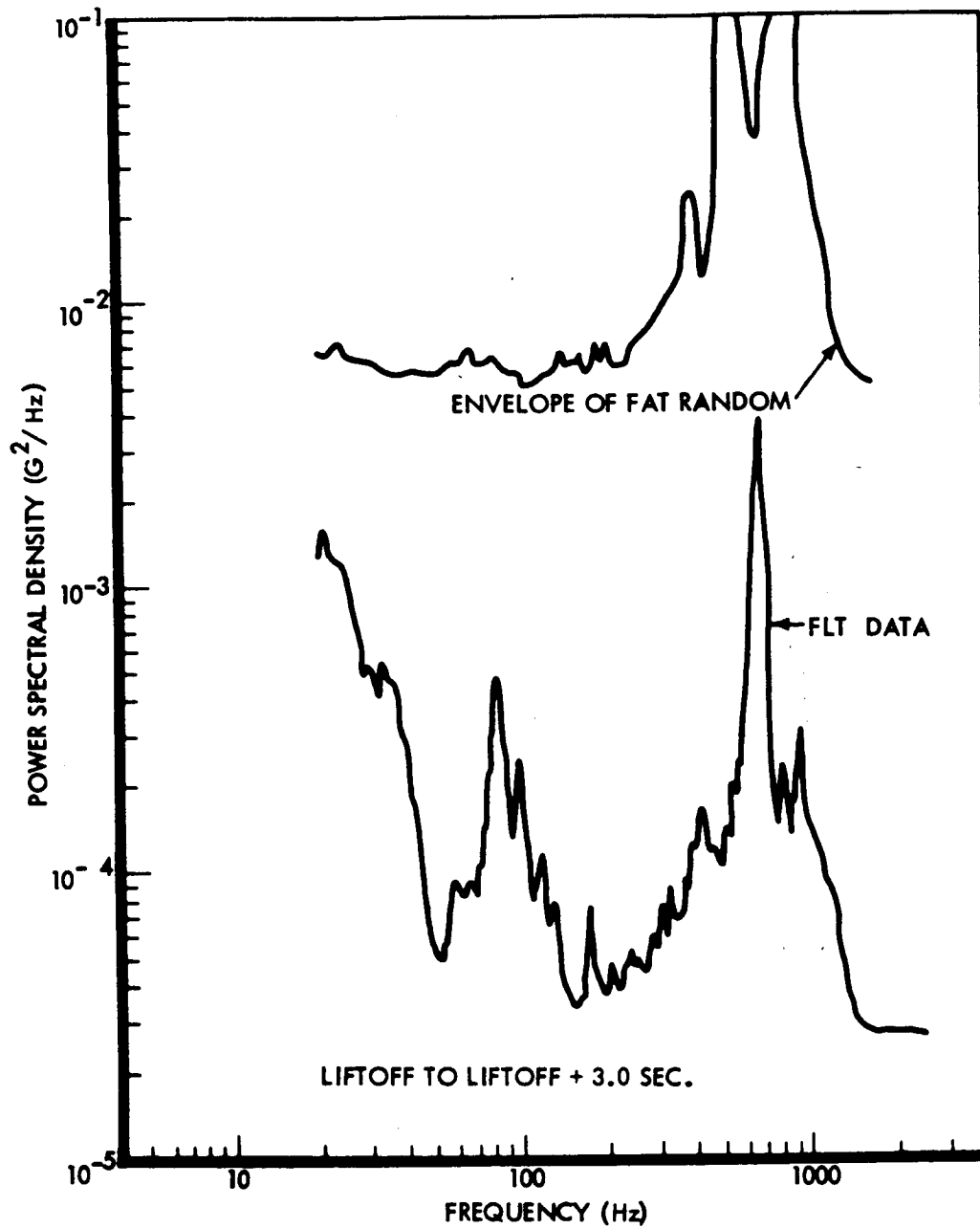


Figure 3-41: Random Response at Liftoff—Lateral Pickup (210 z)

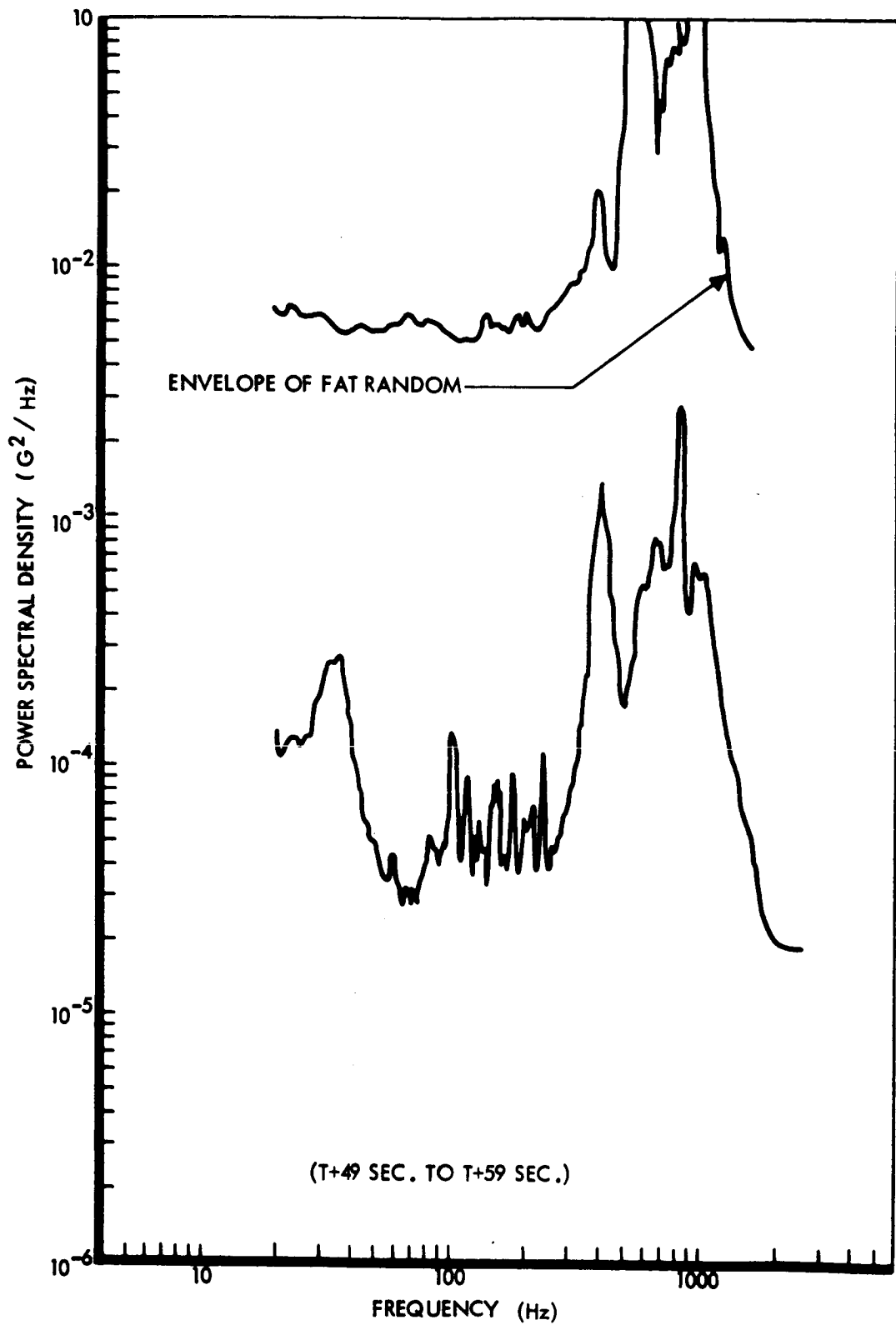


Figure 3-42: Random Response at Transonic Longitudinal Pickup (214 x)

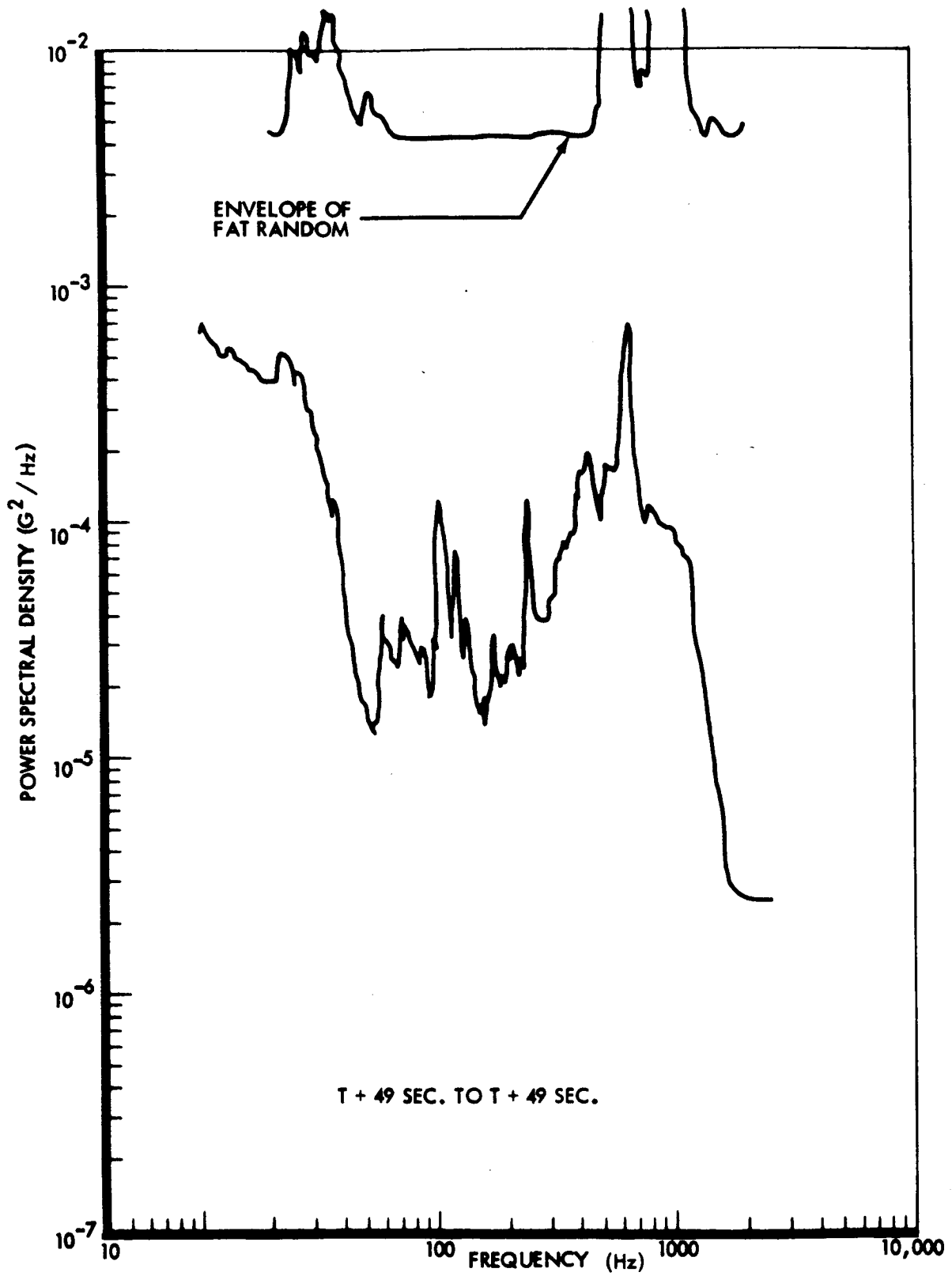


Figure 3-43: Random Response at Transonic Lateral Pickup (210 z)

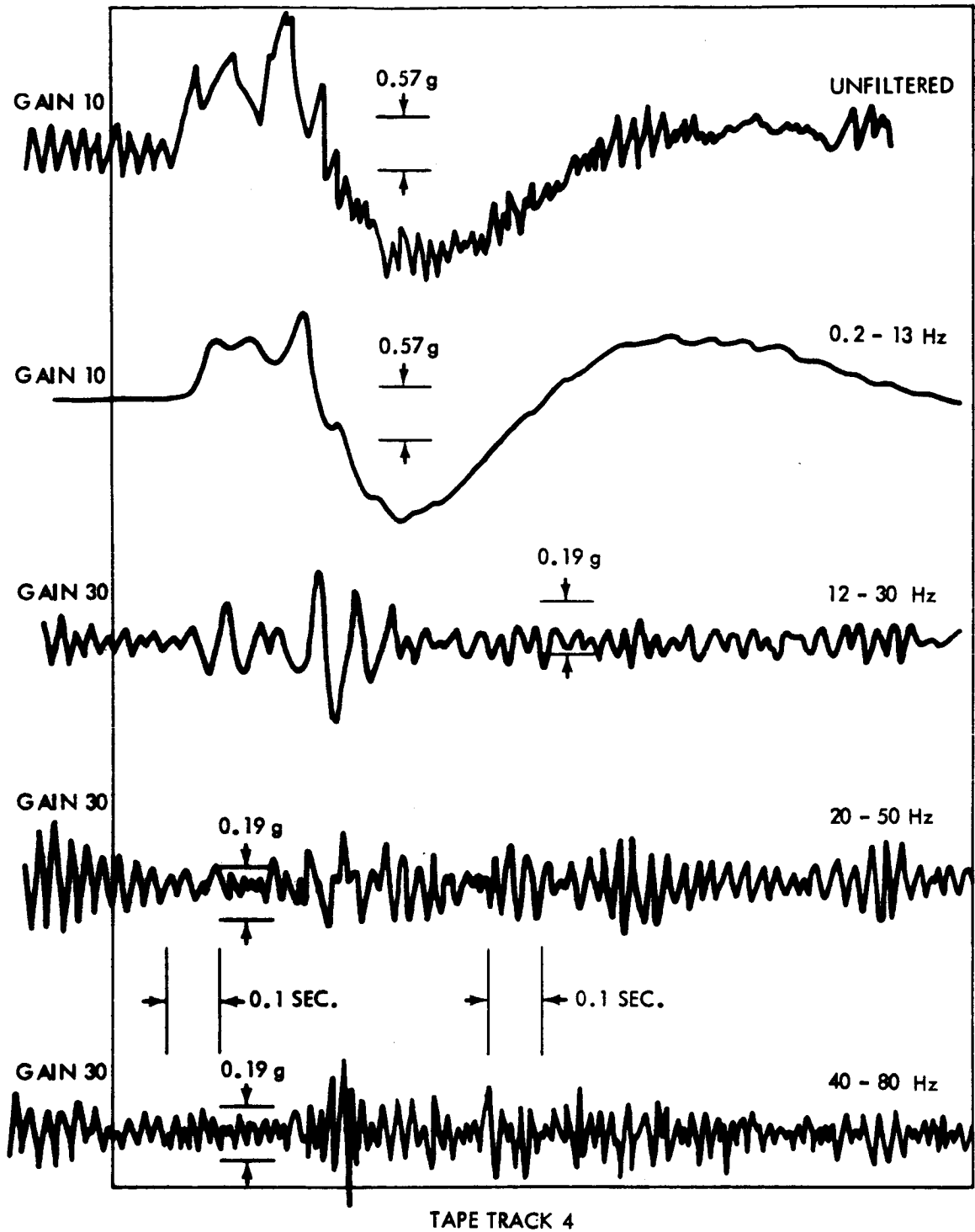
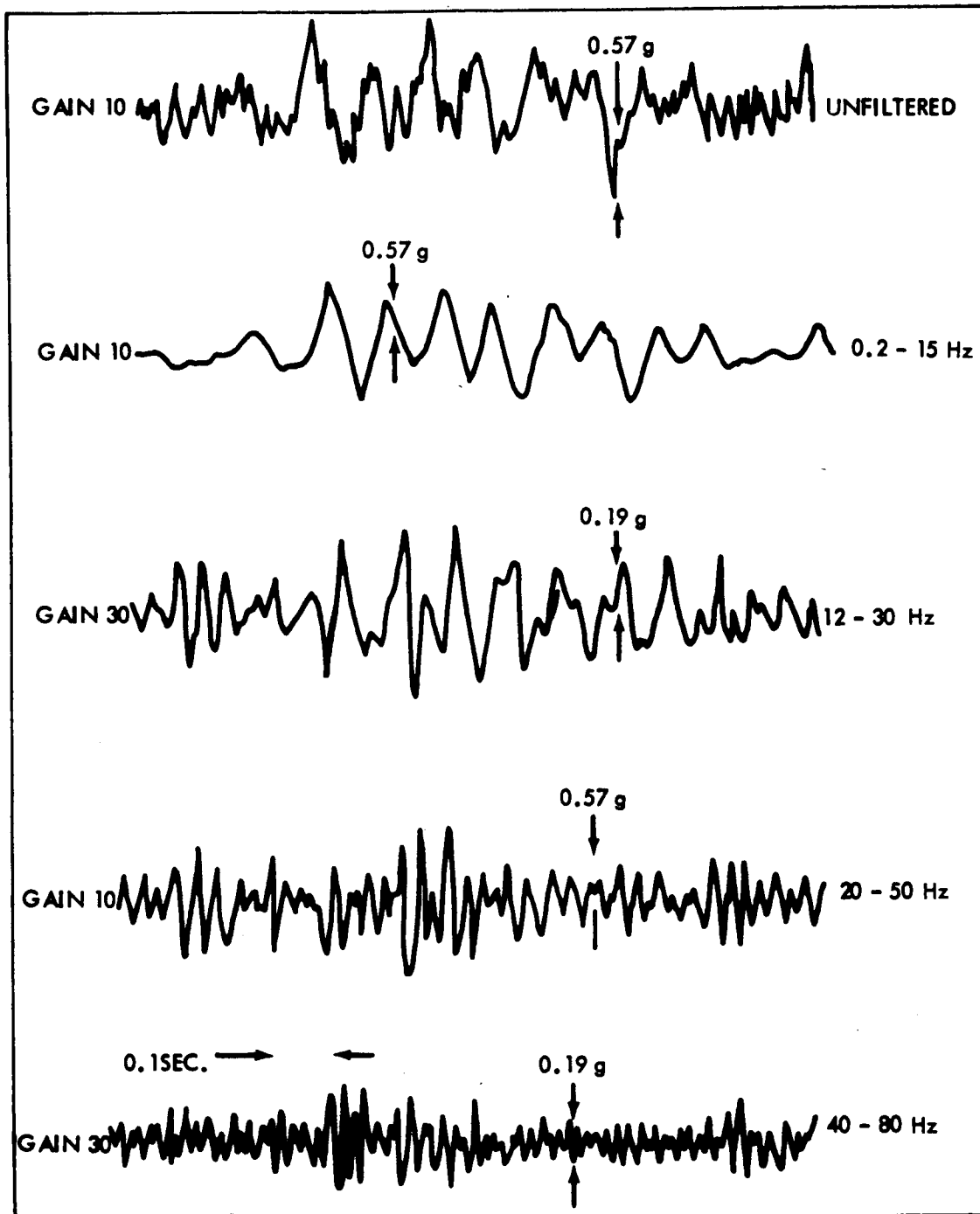


Figure 3-44: BECO Longitudinal Vibration (214x)



BECO LATERAL VIBRATION (210z)

TAPE TRACK 2

Figure 3-45: BECO Lateral Vibration (210z)

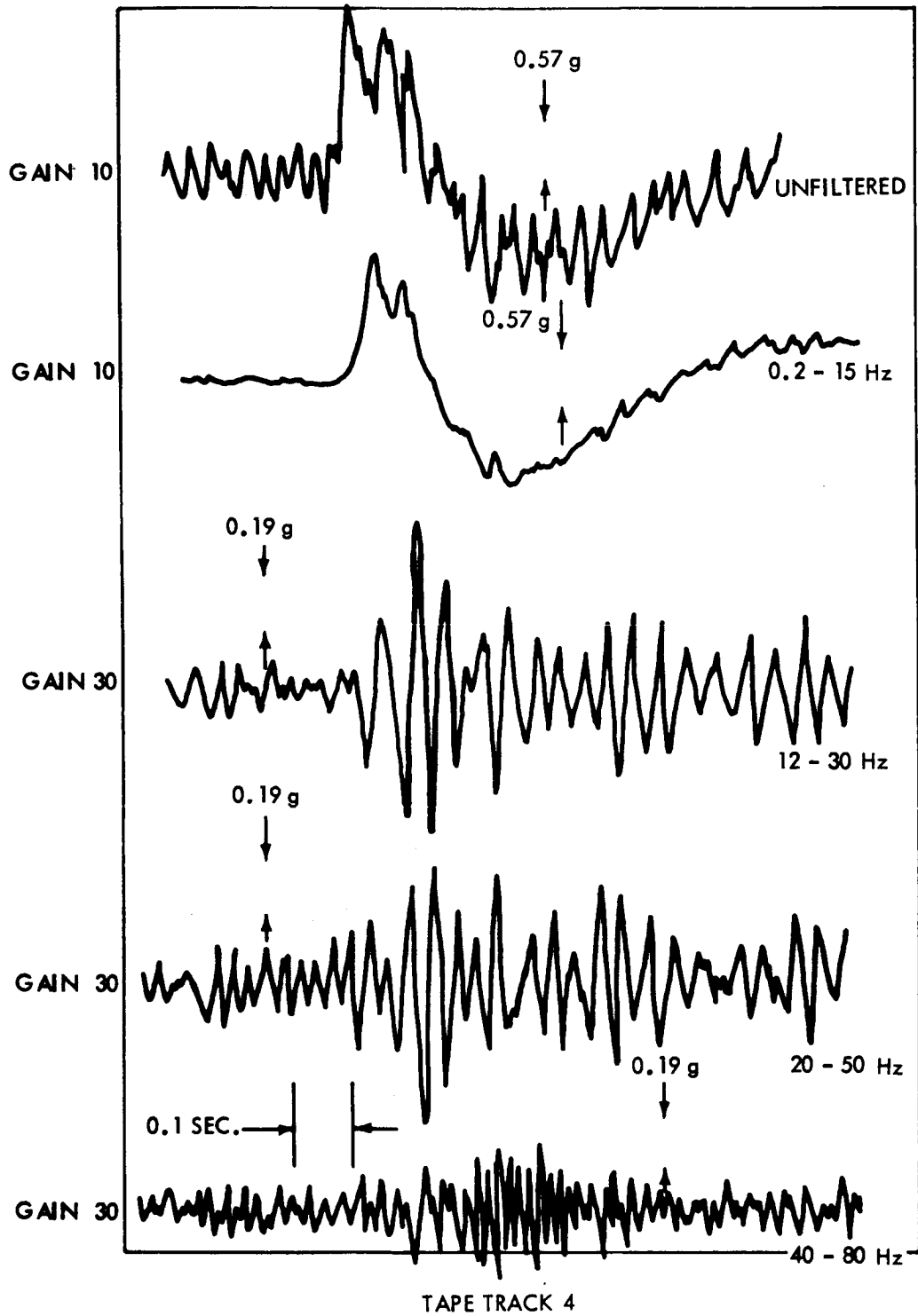
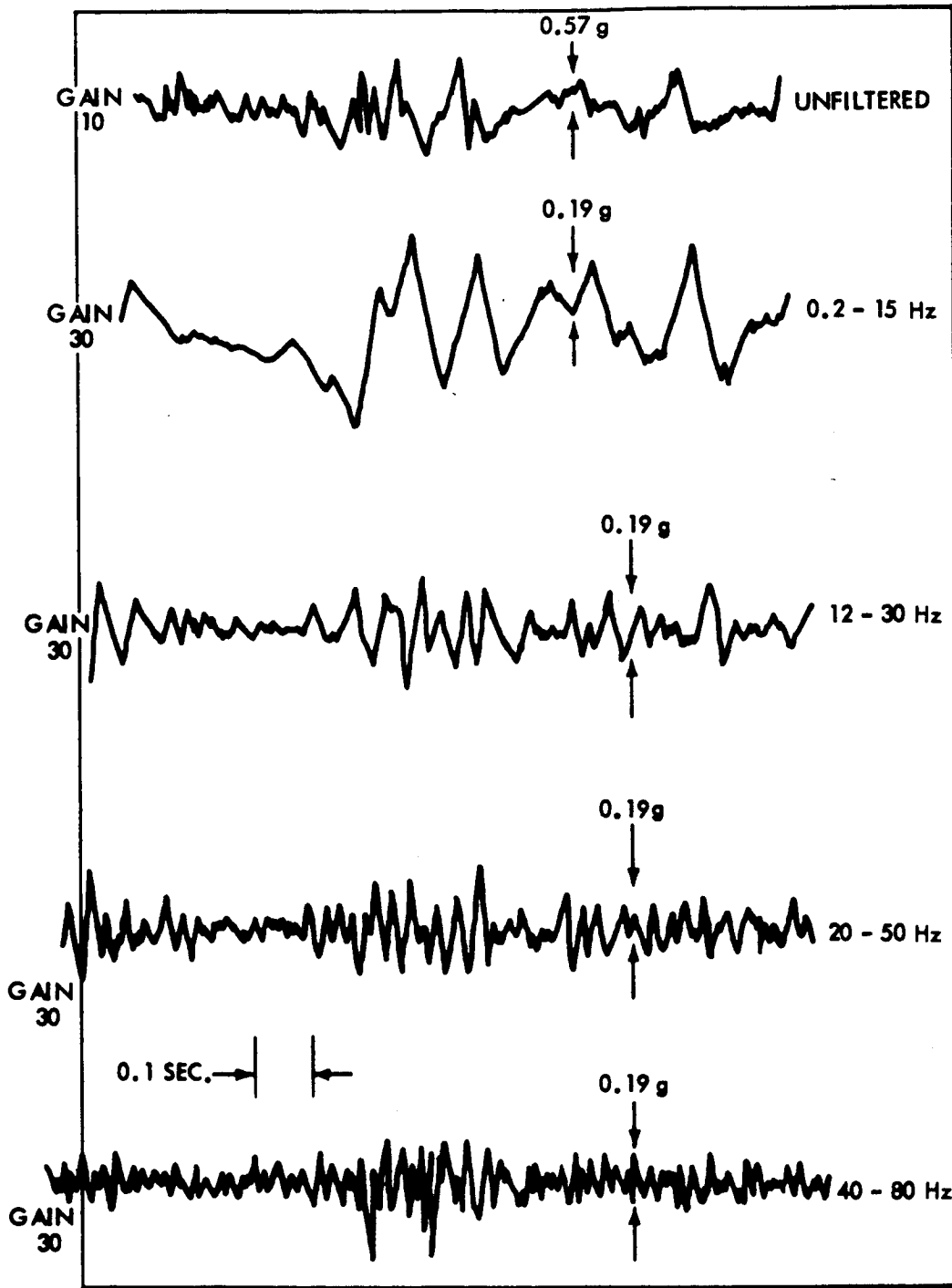


Figure 3-46: SECO Longitudinal Vibration (214x)



TAPE TRACK 2

Figure 3-47: SECO Lateral Vibration (210z)

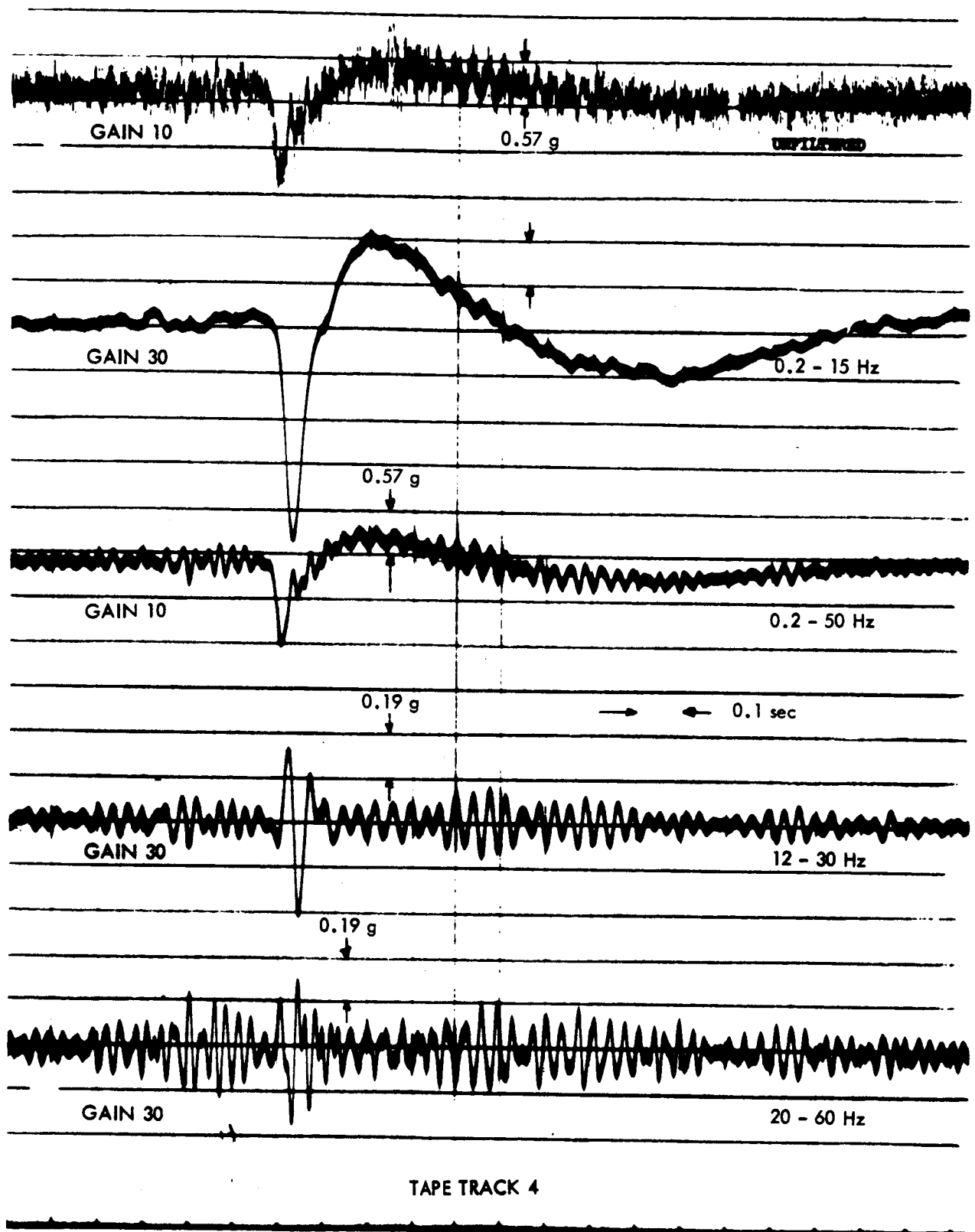


Figure 3-48: Longitudinal Vibration (214x)—Agena First Ignition

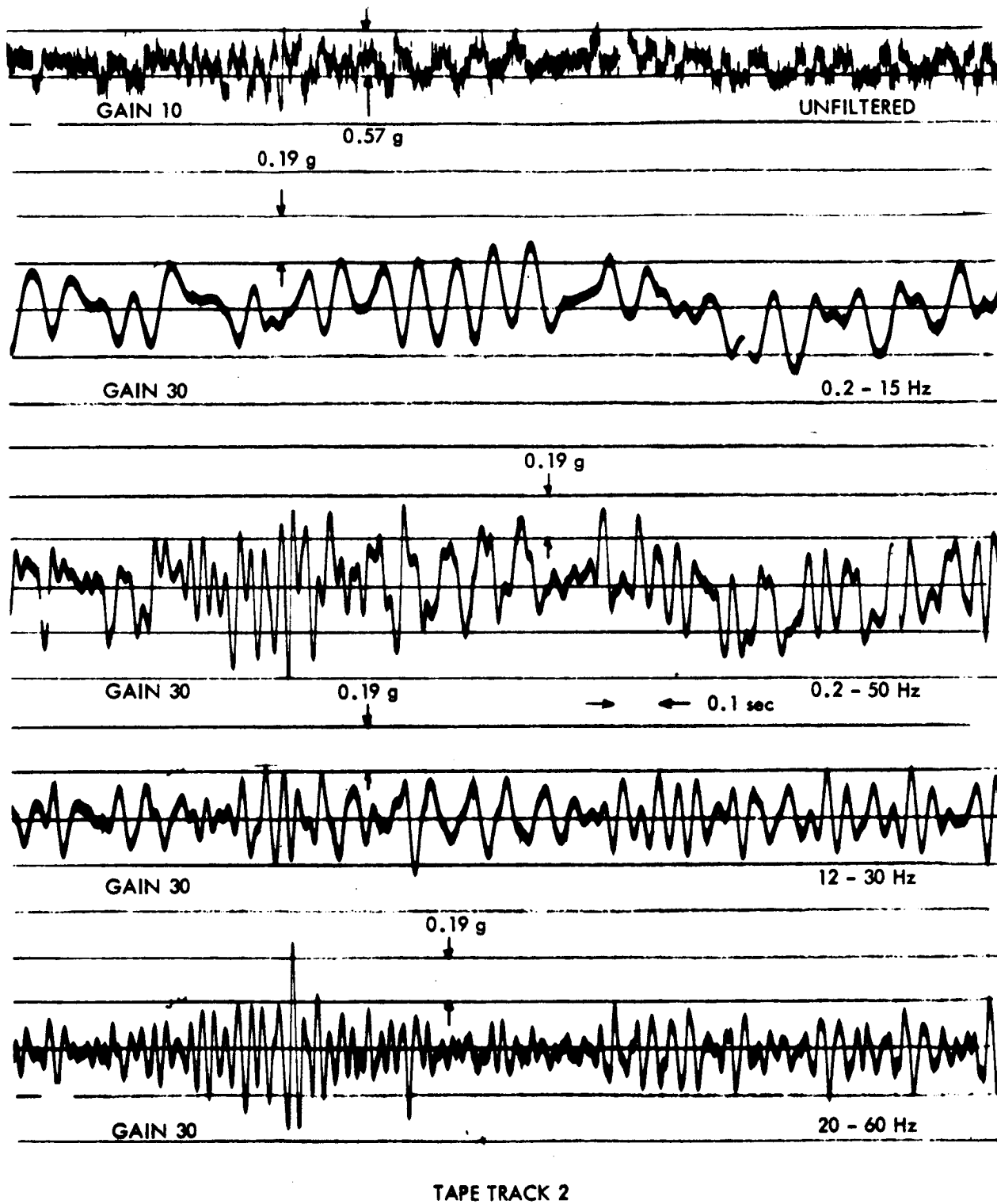


Figure 3-49: Lateral Vibration (210z)—Agena First Ignition

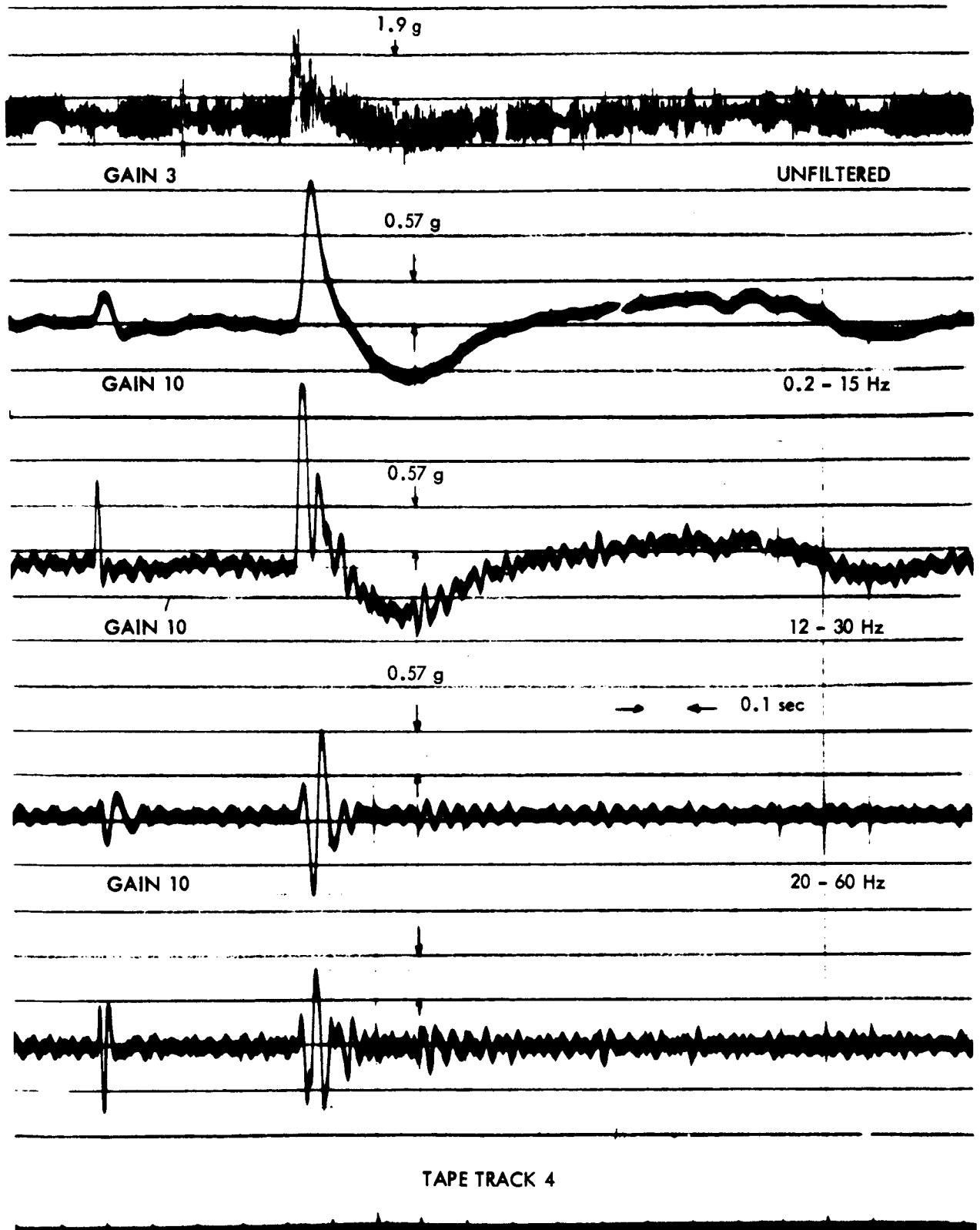


Figure 3-50: Longitudinal Vibration (214X)—Agena First Cutoff

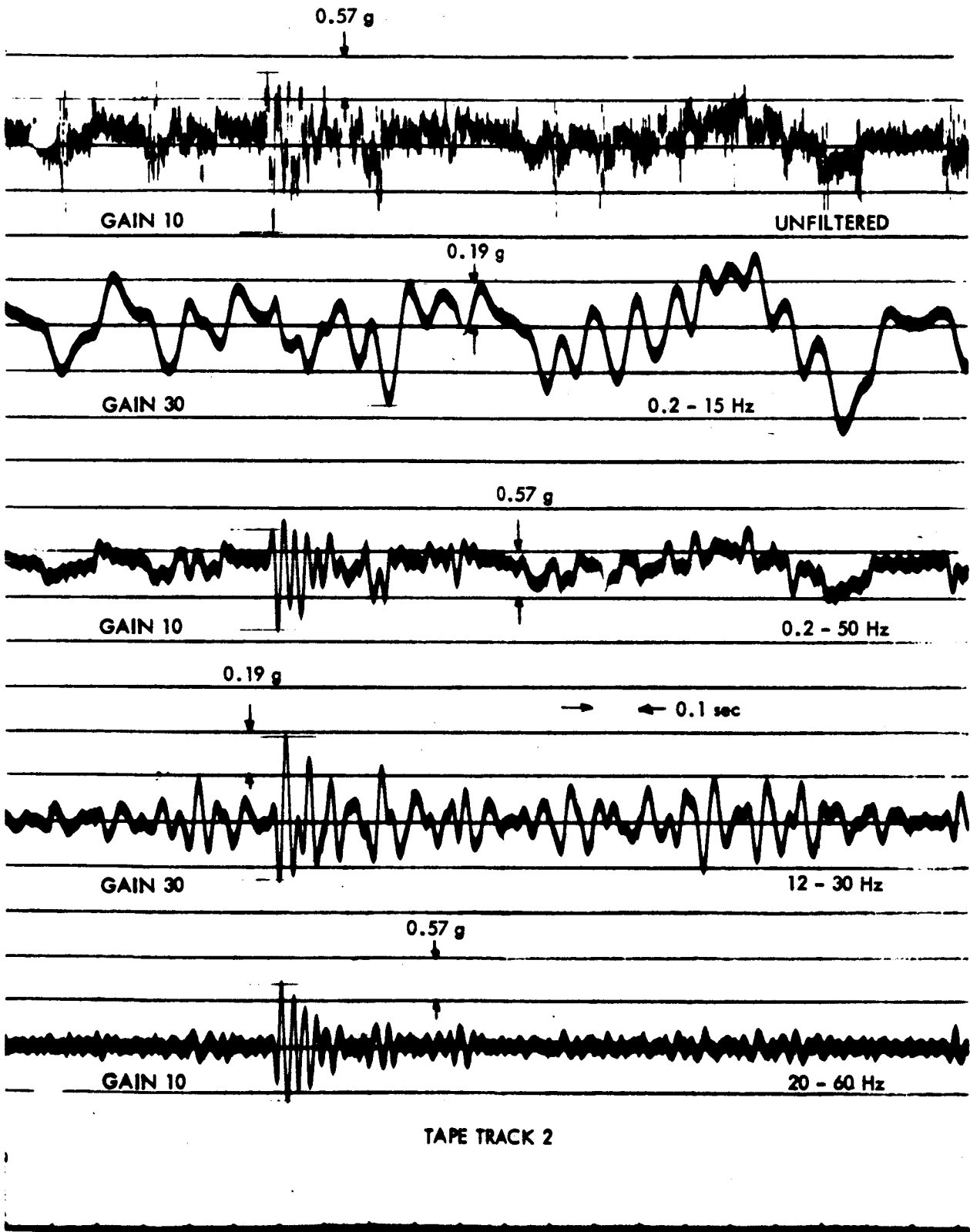


Figure 3-51: Lateral Vibration (210z)—Agena First Cutoff

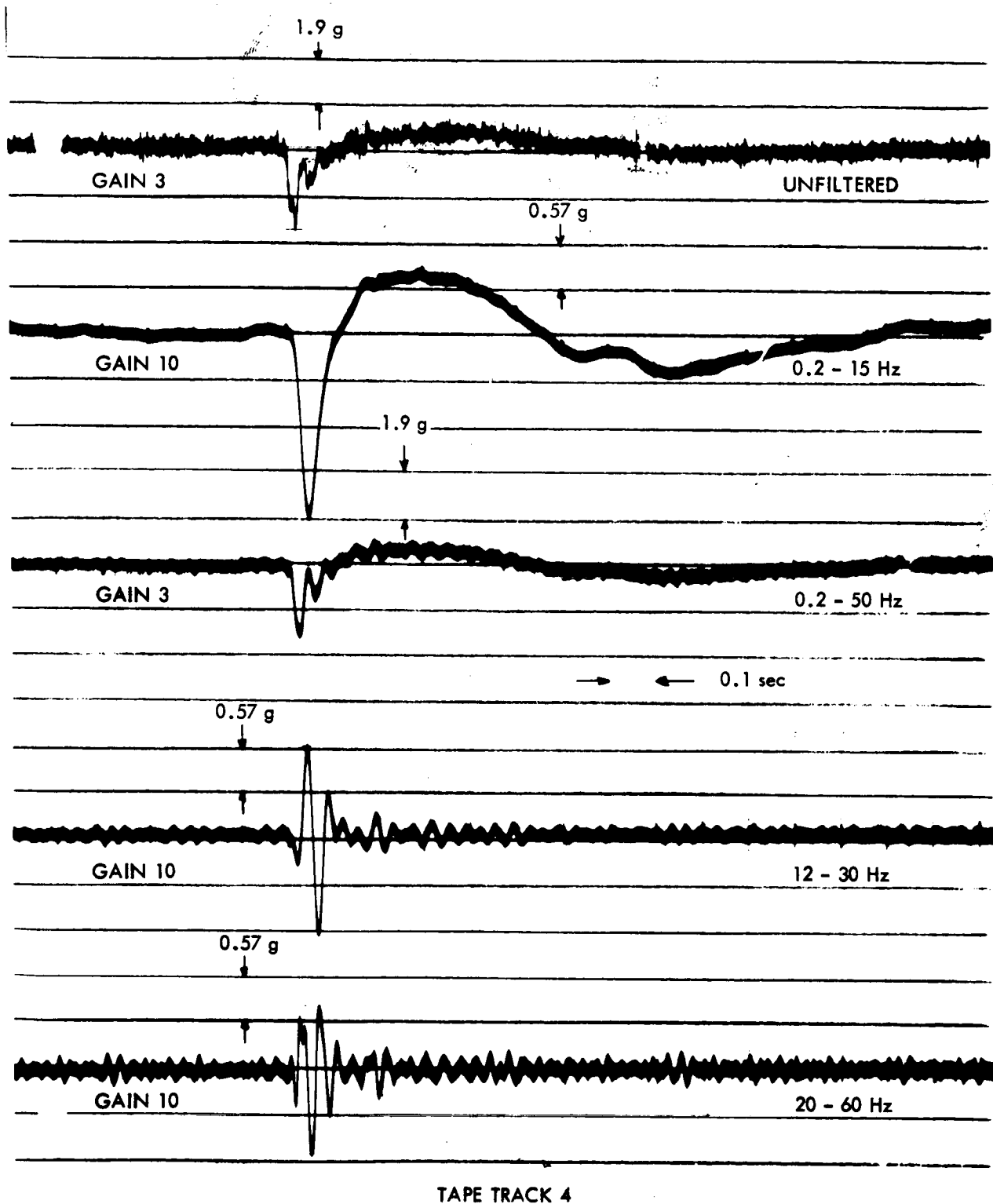


Figure 3-52: Longitudinal Vibration (214x) - Agena Second Ignition

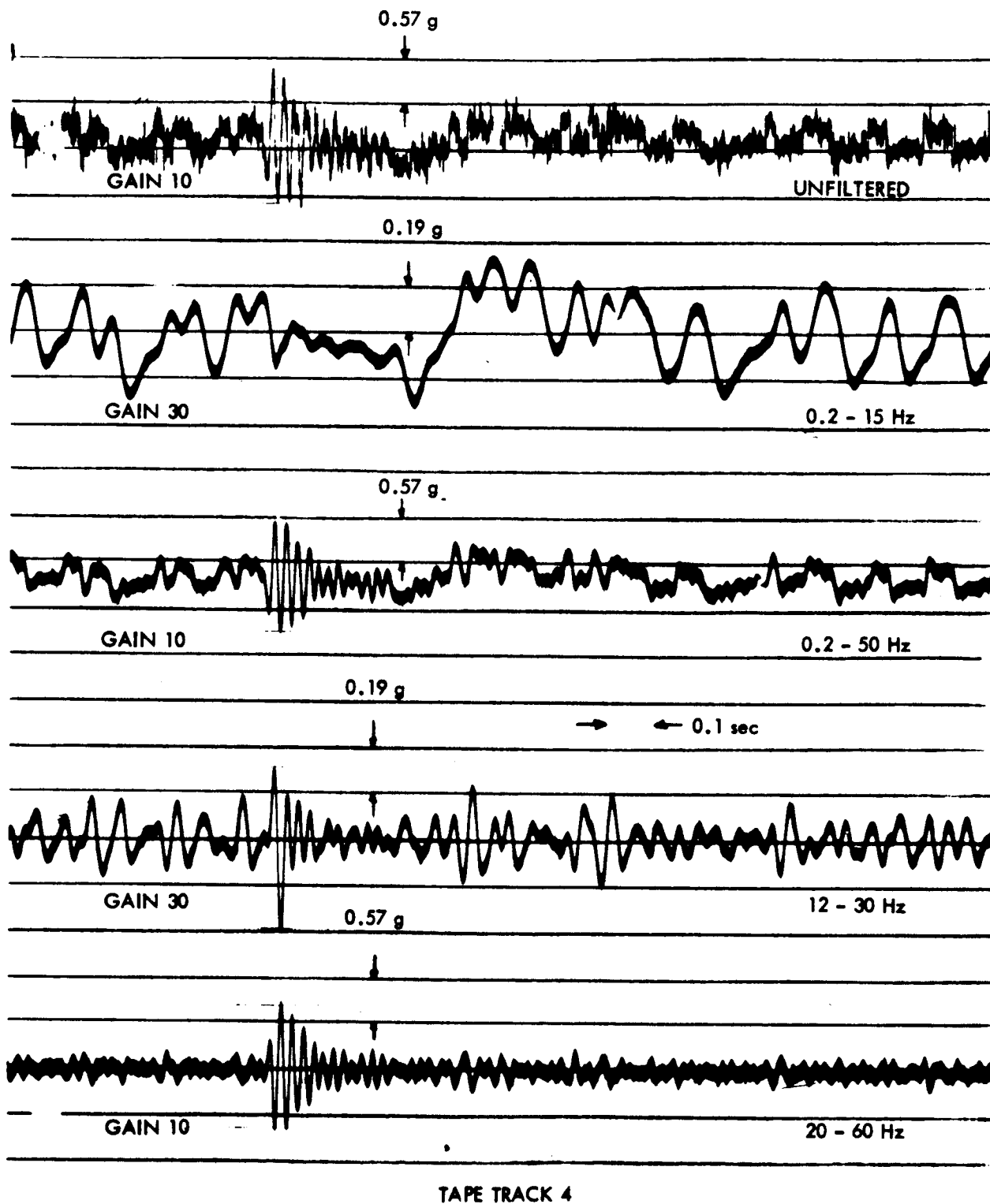


Figure 3-53: Lateral Vibration (210z)—Agena Second Ignition

temperatures of PT01 and PT02 increased to a maximum of 88.8 and 93.9°F, respectively. The normal temperature levels for these channels during preceding orbits, with approximately the same spacecraft attitude (31 to 34 degrees off Sun) were in the 73 to 78°F range.

Excessive EMD thermal-coating degradation occurred similar to that experienced during missions II and III. However, this degradation caused no impairment of the spacecraft mission objectives because its effect on the spacecraft was offset by pitching the spacecraft off the sunline to a pre-determined angle. This attitude maintained temperatures at the desired level.

3.6.4.1 Battery Temperature Variation

Battery temperatures of the S/C spacecraft were consistently higher than previous missions. Peak battery temperatures for Module I on Mission II varied from 70 to 114°F compared with 82 to 129°F for Mission III. The reason for this difference in peak temperatures may, in part, be due to the reduction in conversion efficiency during battery charging at the higher temperatures. This caused a greater portion of the energy to be converted into heat, which tended to perpetuate the high temperatures.

Another interesting phenomenon is shown in Figure 3-54. The battery temperatures during Mission II were nearly equal, whereas, during Mission III, Battery 1 (ET02) was approximately 6 to 10°F higher than Battery 2 (ET03). This difference persisted until sometime after Orbit 76 when the temperature difference between ET03 and ST02 increased to a value nearly equal to that between ET02 and ST02, bringing ET03 up to within 1 to 2°F of ET02. It is noted that this change occurred when

the spacecraft was pitched 30 degrees off Sun after being on Sun for more than 30 orbits. This temperature differential may be attributed to an EMD gradient. During the early orbits, Module 2 was the coolest; it was also closest to the TWTA that was off. Following Orbit 110 the TWTA was on almost continuously, raising the temperature of that portion of the EMD. This caused the temperature of Module 2 to rise to within 2 degrees of Module 1.

3.6.4.2 Lower TWTA Temperatures

TWTA temperatures were substantially lower for Mission III than for Mission II. Typical data for these missions during Orbit 109-116 are presented in Table 3-10 for comparison. It may be seen that the TWTA temperatures (CT01) were consistently above 180°F for Mission II compared with only 171 to 174°F for Mission III. The readout times, spacecraft attitude, and deck-coating degradation were approximately the same in each case. The TWTA temperatures for Mission III were lower, due to a better thermal bond between the TWT and the case of the TWTA. The TWTA used during Mission III was chosen for its low collector temperature (CT01).

3.6.4.3 Thermal Problems

Spacecraft thermal problems are discussed below with regard to their effect on spacecraft operational procedures.

The principal thermal problem was high temperature with the spacecraft normal to the Sun and was caused by degradation of the EMD thermal coating.

3.6.4.4 EMD Thermal Coating Degradation

The extent of thermal-coating degradation on Mission III was larger than anticipated from laboratory tests of thermal-coating

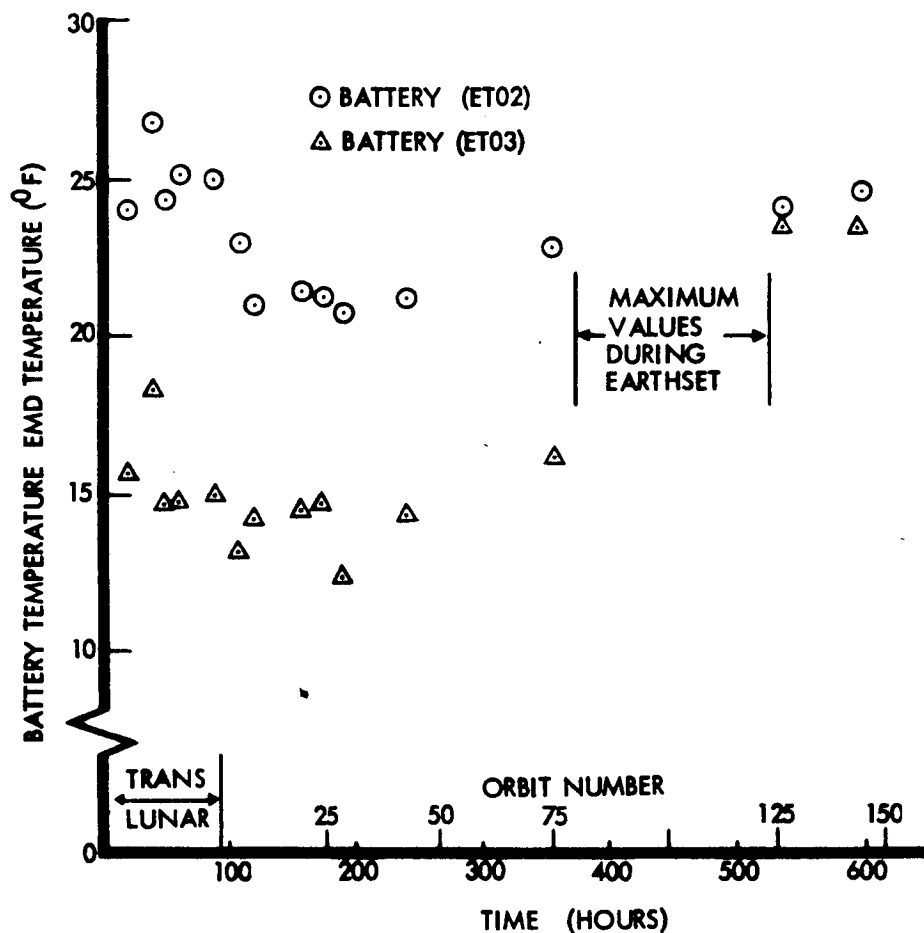


Figure 3-54: Spacecraft Battery Temperature Difference

Table 3-10 SPACECRAFT TWTA TEMPERATURES

ORBIT	CT01 (°F)		ST01 (°F)		CT01 & ST01 TEMP. DIFF. (°F)		TWTA OPERATING TIME (min.)		ATTITUDE (deg.)	
	II	Mission III	II	III	II	III	II	III	II	III
109	180.8	173.8	92.6	99.1	88.2	74.7	127	146	28	27.1
110	180.8	173.8	93.9	99.8	86.9	74.0	128	131	28	26.5
111	180.8	173.8	93.9	99.8	86.9	74.0	135	136	28	30.0
112	180.8	171.2	93.9	97.8	86.9	73.4	136	132	28	29.7
113	180.8	171.2	93.9	97.8	86.9	73.4	137	132	28	29.1
114	180.8	171.2	93.3	98.4	87.5	72.8	138	130	31	28.5
115	180.8	172.5	93.3	99.1	87.5	73.4	139	131	31	27.8
116	180.8	173.8	92.6	99.8	88.2	74.0	138	134	31	27.2

CT01=TWTA Temperature
ST01=Equipment-Mounting-Deck Temperature

samples. A similar discrepancy between laboratory and flight data was experienced on Missions I and II.

0.004 higher than the absorptivity based on ST01.

Figure 3-55 compares the absorptivity of the thermal-control coating of Mission II with that of Mission III. Absorptivity values, calculated for two cislunar, one initial orbit, and two photo orbit conditions are plotted on the curve. In general, the Mission III data points are very similar to Mission II for the same period. The absorptivity based on ST03 is approximately

The thermal coatings used on the EMD surface facing the Sun were different for Missions II and III than for Mission I. Because of the excessively large EMD thermal-coating degradation experienced with Mission I, a new coating was applied for Missions II and III that laboratory results indicated would be superior to the Mission I thermal coating. The Mission I coating was designated B-1056 and the

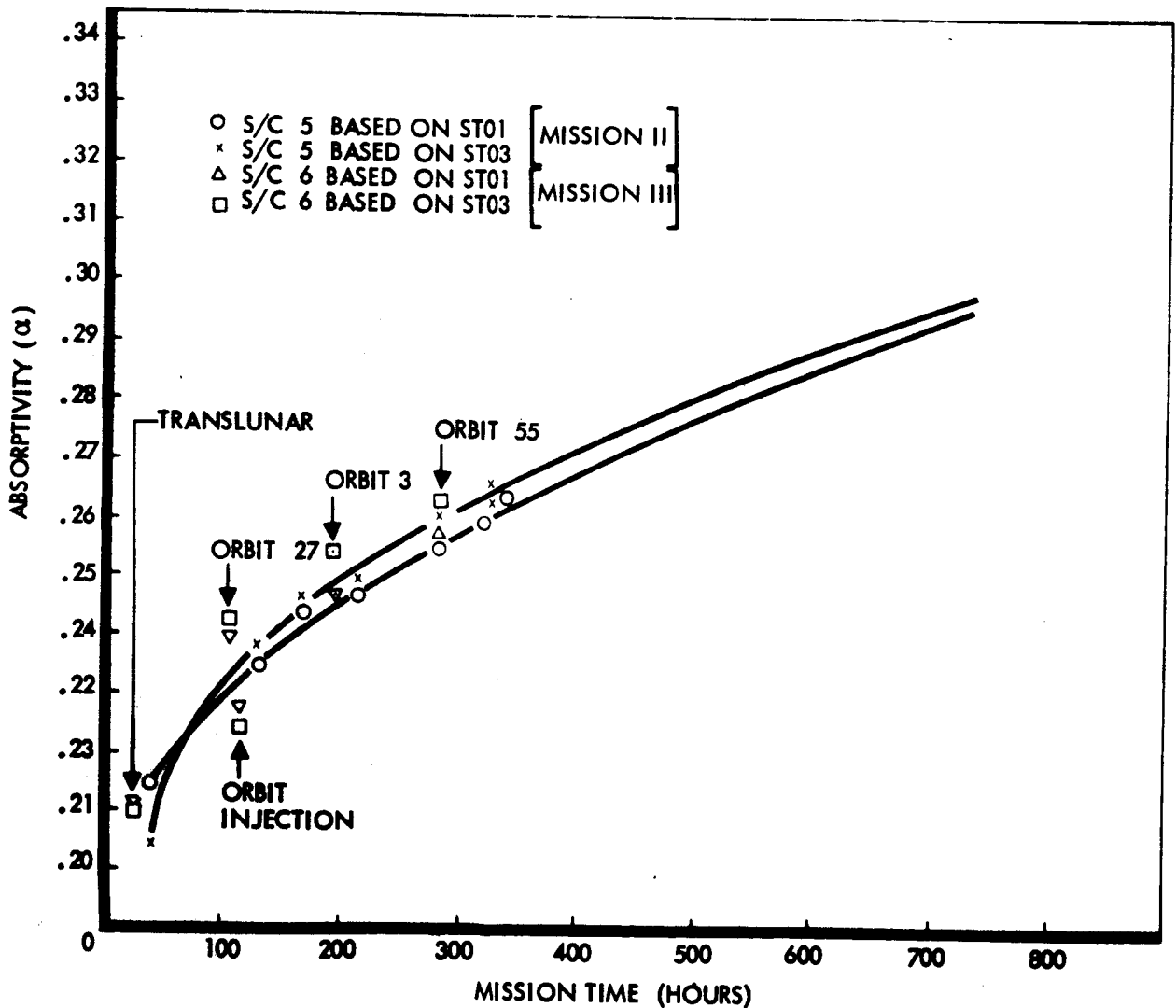


Figure 3-55: Spacecrafts 5 and 6 Solar Absorptivity History

Missions II and III coating was designated B-1056 with an overcoat of S-13G. The actual performance of the Missions II and III coating was superior to that of Mission I.

Although these degradation rates are sufficiently low and do not become a major problem during a 30-day mission, the degradation rates would impose a severe limitation on the spacecraft during an extended mission lasting up to 1 year. The primary interface for the spacecraft thermal-coating system is with the electrical power subsystem. This limitation is imposed by the requirement that the spacecraft be oriented off the sunline at a sufficient angle to maintain satisfactory temperature levels. The electrical power subsystem is then marginal due to reduced incident solar energy on the fixed solar panels.

Paint Sample Degradation—Lunar Orbiters II and III have carried coupons of several candidate thermal-control paints in an effort to determine their performance in the space environment. In general,

the results of these evaluations have been unrewarding because all paints tested have exhibited similar characteristics. The change in temperature, which is a function of solar absorbance, has been at variance with results obtained during ground test where many of the tested paints appeared to offer significant improvements over the original B-1056.

A review of flight test data indicates that heat additions, from sources other than the EMD, are responsible for coupon temperatures running approximately 12°F higher than the EMD itself. This explains why all of the paint samples ran at nearly the same temperature. Radiation from the solar panels appears to be a principal source of this energy.

3.6.5 Thermal-Design Differences Between Missions II and III

There were no significant thermal-design differences between Missions II and III. A minor difference, which would have no effect on the spacecraft thermal performance, was a recessed mounting of the paint samples to reduce thermal-edge effects.

4.0 GROUND DATA SYSTEM PERFORMANCE

The Lunar Orbiter ground data system provides the facilities and equipment required to receive, record, process, and transmit data and commands between the Space Flight Operations Facility (SFOF) and the spacecraft. In addition, all facilities necessary to sustain mission operations were provided by a complex consisting of three primary DSS's, the SFOF, and the ground communications system. Separate facilities were provided at Eastman Kodak, Rochester, New York, and at Langley Research Center, Hampton, Virginia, to process and evaluate the photo data obtained.

All of these facilities provided the required support. A few failures occurred; however, there were no serious consequences because they happened during noncritical times and adequate backup was available. Each area is discussed separately in the following sections.

4.1 SPACE FLIGHT OPERATIONS FACILITY

The SFOF provided the mission control center and the facilities to process and display data to support operational mission control. Facilities were provided for the ground reconstruction equipment and for analysis of the reconstructed lunar photographs; there were also facilities for reproduction and distribution of operational data and for micro-filming all computer program output. The performance of the entire data system at the SFOF was satisfactory.

4.1.1 Computer and Communications Complex

The telemetry processing station (TPS) and the internal communications system at the SFOF provided tracking and telemetry data from teletype and the high-speed data line

to the SFOF computers, and teletype data to the operations areas. The computer complex provided telemetry data processing, tracking data processing, command generation, and command verification. The central computer complex consists of three computer strings, each containing an IBM 7094 computer coupled to an IBM 7044 input-output (I/O) processor through an IBM 1301 disk file memory and a direct data connection (DDC). The entire system performed exceptionally well, losing only a few frames of data that were not detrimental to the flight.

All three computer strings (X, Y, and W) were used to support Mission III. All strings and associated equipment performed adequately with no particular hardware problems.

The computer strings were used as follows.

	Mode 2 (hr)
X-String	344
Y-String	383.5
W-String	37.5

The total amount of Mode 2 time used was 765 hours. Of this total, 253 hours were used in dual Mode 2; 1 hour in triple Mode 2.

Dual Mode 2 was used only during critical mission phases. Only the normal amount of support equipment failures were experienced and were corrected as they occurred.

4.1.2 SFOF Software

The software system for Mission III contained changes from the Mission II software. The system was demonstrated successfully and frozen prior to the Mission III training exercises. The software system worked exceptionally well. One minor problem caused the common environment in the seal area to be scrambled; this occurred twice during the

mission. There was no explanation although considerable analysis was done.

4.1.2.1 System Software

The SFOF mission-independent software system performed satisfactorily throughout Mission III. There were considerably fewer communication errors than during the previous two missions due to a correction in the IBM 7044 software system. This minimized the computer downtime and data loss.

4.1.2.2 SPAC Software

SPAC software consists of the IBM 7094 computer programs that monitor the status from and predict the performance of the spacecraft subsystems. It includes a program that prepares and simulates command sequences to be transmitted to the spacecraft computer; a program that coordinates mission planning; and a program that updates the IBM 7044 calibration coefficients. There were no major program changes between missions resulting from Mission III performance due to their satisfactory and acceptable performance.

Table 4-1 shows a tabulation of all SPAC program executions. Unsuccessful executions are divided into two groups: input and system errors. Input errors include incorrect messages and option switches entered from the input console and misspunched input cards. System errors are the system hardware and software failures. There were no unsuccessful executions due to SPAC software failure during the mission.

4.1.3 FPAC Software System Performance

Several modifications were made to the FPAC software system between Missions II and III to correct some computational inaccuracies and increase the usefulness and convenience of the programs. The performance of all FPAC computer programs during Mission III was satisfactory. A de-

Table 4-1: LUNAR ORBITER SPAC PROGRAM EXECUTION

PROGRAM	EXECUTIONS	INPUT UNSUCCESSFUL EXECUTIONS	SYSTEM ERRORS	TOTAL
CEUL	789	11	5	805
DATL	550	18	4	572
TIML	441	19	2	462
COGL	274	3	3	280
TRBL	204	13	2	219
SEAL	130	3	1	134
QUAL	113	4	0	117
GASL	103	8	1	112
HUBL	88	9	0	97
UTAB	44	1	0	45
SIDL	35	3	0	38
SGNL	35	0	0	35
CORL	16	6	0	22
COOL	9	4	0	13
TOTALS	2831	102	18	2951
% of TOTALS	95.93	3.46	0.61	100.

scription of the changes that were made are discussed below.

4.1.3.1 Flight Path Control Programs

During Mission II it was found that two of the targeting subprograms, post-midcourse guidance (PMG) and pre-injection guidance (PIG), require different conversions for input argument of perilune. A program change was made before Mission III to correct this confusing situation. Performance of user programs using these revised subprograms during Mission III was satisfactory.

A thorough check on the midcourse command programs indicated an error present in both MC1L and GCML. Although the effects of this error were small, the correction was made and the programs performed satisfactorily for Mission III.

User program GCTL was modified to print out a description of the orbit prior to and following the maneuver. These data, contained in the end condition (ENDCO) array, were of great assistance to the guidance and maneuver analysts.

4.1.3.2 Orbit Determination Programs

The DSN provided the project with new links for the tracking data edited programs, TDPX and ODGX. The result was a net loss in capability because the new TDPX links prevented use of the rejected data file. This was not a serious problem but was an inconvenience that was worked around during the mission. ODGX worked as in previous missions and, thus, the same difficulty in processing ranging data when bad angle was being received was present. A successful workaround was developed for this problem also.

Several changes were made to the orbit determination program, ODPL, for Mission III. These changes fell into two categories: (1) correction of minor computational errors and (2) operating convenience features. The program errors corrected involved five quantities in the Boeing special output of Moon encounter parameters and their statistics. Convenience features primarily involved orbital parameters with other FPAC programs. All changes worked successfully and the convenience features particularly aided orbit determination analysts to adhere to the tight computer schedule imposed by the mission design.

A new version of the orbit determination

starter program, LFDL, was received at the SFOF prior to flight (too late to be included in the flight software system but available for an off-line operation). This program was not needed during the flight but tests before the flight indicated that all significant changes worked as planned. These changes involved primarily a special print-out feature that allows manual editing of the tracking data to eliminate blunder points. The blunder points, if not eliminated, prevent LFDL from fulfilling its purpose.

4.1.4 Ground Reconstruction Equipment (GRE)

GRE performance was satisfactory; there were no major problems encountered during the mission. The GRE was only manned during the priority readout portion of the mission. The primary function of the GRE was the reconstruction of video data for early photo and site analysis and for publicity releases. In addition, the video signal was analyzed using a density averaging technique to determine the exposure value. The exposure value was used by the photo analysts for exposure and readout control. The video signal was also routed from the ground-reconstruction interface equipment to the Surveyor scan converter to be compatible with the SFOF television monitors and commercial television.

Before Mission III, the GRE was relocated and the film processor was plumbed for tap water (distilled water was used in Mission II). There were no problems resulting from the move.

4.2 GROUND COMMUNICATIONS SYSTEM

The ground communications system provides for the transmission of voice, teletype, and high-speed data between DSIF sites and the SFOF. One high-speed data line (HSDL), one voice line, and three teletype lines are

provided between each station and the SFOF. The primary source of spacecraft performance telemetry data is the HSDL. One or two teletype lines are provided as a backup for the HSDL depending on the priority assigned to the second teletype line. The remaining TTY lines are used for tracking data, command transmission and verification, and administrative data.

Overall performance of the ground communications system was good. Little data was lost with the backup capability that was provided. Table 4-2 shows the percentage of down time of the ground communications elements.

Table 4-2:

COMMUNICATIONS DOWN TIME - (%)

	HSDL	TTY	VOICE
DSS-12	0.1	0.06	0.06
DSS-41	1.8	0.9	0.5
DSS-62	2.2	1.1	0.5

Ground communications between DSS-12 and the SFOF were excellent. The maximum time of HSDL outage was 9 minutes. At no time was the HSDL and TTY lines down simultaneously.

Ground communications between DSS-41 and the SFOF were good. The HSDL was down for periods ranging from 1 to 42 minutes. On three occasions the HSDL was down in excess of 30 minutes. The TTY lines provided backup coverage on all occasions. All communications lines were down three times for a total of 18 minutes over the entire mission. This does not include 44 minutes when the 85-foot antenna was inoperative. Total line outages did not occur during critical periods.

Ground communications between DSS-62 and the SFOF were satisfactory. HSDL outages

ranged from 1 to 50 minutes. There were four outages of more than 30 minutes, three between 20 and 30 minutes, and nine between 10 and 20 minutes; TTY backup was available for all but one 10-minute interval. There were four periods totaling 30 minutes when all TTY lines and the HSDL were down. The total line outages did not occur during critical mission periods.

4.3 DEEP SPACE STATIONS

Lunar Orbiter operations were transferred from DSS-61 to DSS-62 between Missions II and III. This resulted in a greater than normal effort in checking the ground equipment and bringing it up to operational readiness before Mission IV.

Performance of the ground equipment at the Deep Space Stations was satisfactory. The mission-dependent equipment, including the GRE, operated nominally with a normal number of minor problems that were corrected as they occurred. There was one exception in which a power failure at DSS-62 caused the loss of approximately 20 feet of GRE film in the film processor at the time. Only one GRE film was affected; the second film was not damaged. Subsequently the film processor was rewired to critical power rather than utility power. There were no recurring equipment failures and only a few significant operational problems associated with mission-independent equipment. The maser amplifier was used on all passes by all stations, with the exception of one pass over DSS-41 when the PARAMP was used.

The only significant problems at DSS-12 occurred when the 85-foot antenna had to be shut down due to high winds and when the FR 900 capstan drive motor failed. The antenna was stowed for approximately 90 minutes until the wind decreased while tracking continued with the 35-foot antenna; no data

was lost during the shutdown. The FR 900 capstan drive failed near the end of a video readout. Repairs were not completed before the next pass the following day and the unit did not have playback capability. However, due to overlapping coverage, DSS-41 and DSS-62 were able to provide sufficient recording capability so that no FR 900 data were lost.

There was only one significant failure at DSS-41. This occurred when the 85-foot antenna was unable to move due to the loss of the main input hydraulic feed. Approximately 25 minutes of telemetry data were lost before DSS-62 rose and acquired the spacecraft. DSS-41 reacquired the spacecraft on the same pass after bleeding the hydraulic lines.

DSS-62 had several significant difficulties. Telemetry data were lost on two occasions

for 12 and 10 minutes, respectively, when a fuse was blown in the antenna declination drive and a station power overload occurred, causing a circuit breaker to trip and shut off power. The video readout following the power failure was delayed 6 minutes. An apparent SDS 920 computer failure prevented transmission of a sequence of Mode 1 commands to the spacecraft; the commands were, however, successfully transmitted in the backup transmission (Mode 3). During one pass a power meter was broken and the station was unable to determine their transmitter power; this required adjusting the uplink transmitter power by monitoring the spacecraft AGC reading. During the same pass the station was unable to calibrate their PARAMP because of a test transmitter problem. The PARAMP would have been usable in an emergency but was not needed.

5.0 LUNAR ENVIRONMENTAL DATA

5.1 RADIATION DATA

During Mission III, the radiation dosimetry measurement system functioned normally and provided data on the Earth's trapped radiation belts and on the radiation environment encountered by the spacecraft in transit to and near the moon. Data obtained from the dosimeters is shown in table 5-1.

Initial Dosimeter 1, (DF04), readings indicated that the spacecraft received a total dose of 0.75 rad while penetrating the inner Van Allen belt. The outer belt resulted in no additional increments in DF04. Dosimeter 2 (DF05) was not turned on until after the Earth's trapped belts were passed.

For the next few days, the DF05 dosimeter indicated that a residual flux of low-energy protons from the solar particle event of January 28 was still present near the Earth-Moon system. This flux declined below the RDMS threshold by about February 8. From that time until March 31, only the normal cosmic-ray dose and dosimeter noise have been recorded.

On February 13 (Day 44, 17:43 GMT), a very large optical flare, Class 4, was observed by Sacramento Peak. This flare, which was unexpected because it did not develop from a sizable sunspot group, resulted in enhanced

Table 5-1: RADIATION DATA - RECORD - MISSION III

GMT	Detector	Reading
36:02:00	DF04	0.75
36:07:35:41	DF05	Turn On
37:01:03:37	DF05	0.5
37:10:29:39	DF04	1.0
37:17:33:35	DF05	1.0
38:13:30:08	DF05	1.5
39:17:50:29	DF05	2.0
41:04:49:49	DF04	1.25
45:11:23:48	DF04	1.50
48:12:55:12	DF05	2.5
49:10:30:12	DF04	1.75
53:12:21:47	DF04	2.00
57:08:10	DF04	2.25
59:12:22:10	DF05	3.00
60:07:49:09	DF04	2.5
63:22:49:16	DF04	2.75
68:00:21	DF04	3.00

low-energy proton fluxes in the vicinity of Pioneer VII, but the particle energies were not adequate to affect Lunar Orbiter dosimetry or film.

5.2 MICROMETEOROID DATA

No micrometeoroid hits were recorded during Mission III. One detector, number 17, was punctured prior to launch.

SUMMARY OF LUNAR ORBITER III ANOMALIES

The following paragraphs discuss the three principal malfunctions that occurred during Mission III:

- 1) **Traveling-wave-tube amplifier**
 - a) **High TWTA current at first turn-on;**
 - b) **TWTA power output variations;**
 - c) **High TWTA helix current during orbits 141 and 143;**
- 2) **Faulty film advance during priority readout;**
- 3) **Final-readout malfunction.**

TWTA MALFUNCTIONS

High TWTA Helix Current at First Turn-On

On Day 036 (February 5) of Mission III, the TWTA was commanded on for the first time 6 hours and 53 minutes after launch. The telemetry indication of TWTA helix current indicated 8.8 milliamps and decayed after 1.5 minutes to 5.1 milliamps and remained at this level throughout an on-time of 35 minutes. The second time the TWTA was commanded on was at 8 hours and 24 minutes after launch; the helix current, at turn-on, was between 6.1 and 6.9 milliamps. The normal value at turn-on should be 5.75 milliamps, gradually stabilizing at approximately 5.3 milliamps. A detailed analysis of this anomaly, which involved research of test records from Lunar Orbiter thermal vacuum testing, indicates that the cause was either the result of mechanical stresses induced by the launch environment and were subsequently relieved by operating temperature cycles, or the result of slow internal pressure decay (outgassing) after launch.

As a result of this anomaly, a constraint dictating the turn-on time for the TWTA will be developed. The constraint will be dependent on time from launch, allowing ample time for the TWT to properly outgas.

TWTA Power Output Variations

Telemetry indication (CE02) of TWTA output power was excessively temperature sensitive. During photo readout in early orbits, the telemetry power output indication varied from approximately 10 watts at turn-on to 16 watts at turn-off. This variation gradually increased with the number of orbits. At the time of the last photo readout, telemetry power output was 9.45 watts at turn-on and 20.4 watts at turn-off.

Telemetry voltage is obtained from the diode power monitor in the filter/monitor assembly located within the TWTA proper. An adjustable probe extracts a small amount of the S-band energy present at the filter input. The rf signal is rectified by two Type IN831A point-contact diodes connected in series across the probe to ground.

Although the diode monitor indicates total power and would be affected by an increase in TWT harmonic content, it is believed that the variation in telemetry power output results from a gradual shift in the diode rectification characteristics with temperature.

Research of spacecraft test records indicates that the above phenomenon is unique to this TWTA and was exhibited during thermal/vacuum testing. The power output varied from 10.5 watts at turn-on to 16.9 watts at turn-off in this case.

High TWTA Helix Current During Orbits 141 and 143

When the TWTA was commanded on during Orbit 141, the helix current at turn-on was 6.75 milliamps. Normal value, about 5.75 milliamps at turn-on, will gradually stabilize at 5.3 milliamps. After the Orbit 141 turn-on, the helix current gradually decreased for the

next 29 minutes to 5.84 milliamps, then abruptly decreased to 5.41 milliamps. The same pattern was followed in Orbits 143 and 144, but not Orbit 142, although there was essentially no difference in turn-on procedures. At the time the abrupt 0.4-milliamps decrease occurred, TWTA temperature was 150.6°F in all three cases.

The changes in helix current described above are possible due to corresponding change in rf drive from the spacecraft transponder. It should also be noted that there are many factors that can cause helix current variations. However, based on tests and analysis conducted to date, it is concluded that variations of this magnitude do not affect the life of the tube.

FAULTY FILM ADVANCE DURING PRIORITY READOUT

During priority readout and also during the final readout sequence, the film movement through the photo subsystem optical mechanical scanner would stop. The stoppage events were irregular and did not establish a pattern throughout the mission. It was always possible to resume readout by executing commands to terminate readout, which emptied the readout looper assembly. Once the looper was empty, readout was again initiated and would continue.

Extensive testing was conducted to determine the cause of film stoppage; the most plausible was that of an overlength mounting screw on the readout looper assembly. The long screw caused the teflon separators to press against the film and act as a brake.

A test was conducted on a readout looper assembly with the long screw installed, and the film tension was found to be 0.25 to 0.5 pound below the specified value. It is presumed that this reduced the drive-friction

level to a marginal value, so small changes in some other factor could cause slippage.

Following this malfunction the remaining photo subsystems were inspected and found to have short screws installed throughout.

FINAL READOUT MALFUNCTION

On Day 061 (March 2) at 15:12:40.4 (the beginning of the normal readout sequence in Orbit 149), the camera readout electronics turned on momentarily and then turned off without a command being sent to the spacecraft. Video came on momentarily (approximately 1.4 seconds), following a delay of approximately 22 seconds after readout electronics turned on. A second attempt to command "readout electronics on" had negative results. A "solar eclipse off" command was sent. The readout electronics were enabled and the third attempt to turn electronics on was successful. Optimization of the video signal was unusual in that one "focus increase" and five gain commands were required before active scanning was started (15:56:50). With readout in progress, a load current 1.25 amps in excess of that usually experienced during readout was noted. Readout progressed normally until 16:47:31.2, when readout was turned off to dump the readout looper. When readout was terminated, the readout looper did not dump. Readout was restarted and a second attempt was made to dump the looper by terminating readout. The looper again failed to empty. All subsequent attempts to empty the readout looper failed.

The telemetry data indicated the "R/O electronics on" was commanded at 15:12:40.4 during Orbit 149. An analysis of the signal strength data indicated the readout electronics turned on at approximately 15:12:42 and the high-voltage power supply came on at 15:13:8.6. The video remained on for 1.4

seconds and then turned off without being commanded.

Subsequently readout was successfully accomplished; however, when "R/O drive off" was commanded the readout looper failed to empty.

Further analysis of the telemetry data indicated that several logic circuits changed state, concurrent with the loss of video, as a result of an apparent voltage transient. Because of excessive spacecraft current for approximately 33 minutes, following the transient (during successful readout), and the subsequent inability to empty the readout looper it was assumed the film-advance motor was burned out.

Tests performed on Spacecraft 2 with PS-3 installed eliminated the possibility of the transient having occurred external to the photo subsystem. Details of this test were reported to NASA by Boeing Letter 2-1553-70-040, March 22, 1967.

The following analyses were performed to isolate the source of the failure in the photo subsystem:

- 1) DC. to - DC converter—All circuits and components were analyzed. Any one of six components (one Zener diode and five transistors) could have been in a temporary failure mode, which would result in the transient on the +6.5 volt output necessary to trigger the logic circuits that were inadvertently reset during Mission III.
- 2) Command Control Programmer (CCP)
—The preset pulse, platen count, and

film-advance circuits could have been triggered by the transient on the +6.5 volt line.

3) Thermal Analysis—

- a) Calculations based on spacecraft telemetry and parts reliability data indicate the insulation in the film-advance motor would fail at 380°C after 30 minutes. Telemetry data indicates the motor failed "open" after approximately 33 minutes.
- b) Calculations based on data from a simulated flight configured film-supply motor indicate the stabilization temperature reached was approximately 112°C. Since the insulation in this motor is the same as in the film-advance motor, the film-supply motor could operate in a stalled condition indefinitely without damage to the windings.

Additional details of the photo subsystem analysis may be found in the minutes of the NASA/Boeing/EK meeting, EK L-025044, March 30, 1967.

Because the analysis did not yield a specific cause of failure, and because no design or hardware deficiency was discovered, modification of the remaining photo subsystem is not recommended. SPAC personnel have been alerted to the need for recognition of excessive load current should a similar situation arise. Prompt return to "solar eclipse on" will ensure no motor damage. The logic can be reset by established procedures.